REPEATED LOADING OF FINE GRAINED SOILS FOR PAVEMENT DESIGN

by

SIMON C. LOACH, M.A. (Cantab)

Thesis submitted to the University of Nottingham for the degree of Doctor of Philosophy

FEBRUARY 1987

ABSTRACT

The primary aim of this research was to investigate the behaviour of a clay subjected to a loading regime similar to that experienced by a road subgrade under traffic loading in Great Britain. The material used was Keuper Marl. The samples were anisotropically consolidated in a triaxial apparatus from a slurry which allowed careful control over the stress history and produced uniform samples. The samples were fully instrumented and the apparatus was capable of applying repeated axial and radial stresses. The test programme was designed to investigate the resilient and permanent response of the samples to a variety of stress pulse magnitudes and time periods.

The main conclusions were:

i) The material exhibited a marked stress softening.
ii) The mean normal effective stress remained constant under a variety of total stress paths over the range of frequencies tested.
iii) The resilient response was found to depend on the magnitude of the applied stress pulse and the mean normal effective pressure, and to be independent of the preconsolidation pressure.
iv) The material exhibited significant thixotropy.

A smaller parallel series of tests was carried out on compacted triaxial samples of three clays (Keuper Marl, Gault clay and London clay) in a simple pneumatic repeated load triaxial rig. The test programme was designed to investigate the resilient response of the samples over a range of repeated deviator stresses. The suction moisture content relationship for each clay was established, and the resilient response of the clay was found to be controlled by the magnitude of the stress pulse and the suction.

A series of California Bearing Ratio tests was carried out on compacted samples of the three clays, and on anisotropically

consolidated samples of Keuper Marl, to allow a comparison to be made between the resilient modulus and CBR.

A review of previous work is presented.

ACKNOWLEDGEMENTS

The author would like to thank the following people for their help in this research project:

Professor R C Coates and Professor P S Pell for making available the facilities of the Department of Civil Engineering. Professor S F Brown for his helpful supervision throughout the work. Mr B V Brodrick for his help and advice on running and maintaining the equipment. Mr J Moody for his help, advice and workmanship in the construction and maintenance of the apparatus. Mr G Hanley for his help, advice and workmanship in the modification and repair of the electrical equipment. Mrs P Elliott for typing the thesis. Miss C Brayley for tracing the figures.

This research project would not have been possible without the generous financial support of the Transport and Road Research Laboratory and this is gratefully acknowledged.

CONTENTS

Page

LIST OF SYMBOLS

S	Soil Suction
B	pore pressure coefficient
G_s	specific gravity
H_z	Hertz (1/seconds)
k	bulk modulus
K	stress ratio during consolidation
K_o	stress ratio during consolidation giving no radial strain
LVDT	linear variable differential transformer
M_r	resilient modulus of elasticity
N	number of load cycles
OCR	overconsolidation ratio
V	specific volume (1 + e)
V_λ	specific volume of λ line at p'=1
V_k	specific volume of k line at p'=1
cs	centistokes
c_v	coefficient of consolidation
e	voids ratio
k	coefficient of permeability
m_v	coefficient of volume compressibility
u	pore pressure
Γ	specific volume of critical state line at p'=1
Δ	small increment
μ	10^{-6}
M	ratio of q/p' at failure
k	slope of overconsolidated line in V - ln p' space
λ	slope of normally consolidated line in V - ln p' space
ν	Poisson's ratio
τ	shear stress
ϕ'	angle of internal friction
σ_a	axisymmmetric axial stress - triaxial axial stress
σ_r	axisymmetric radial stress - triaxial radial stress
ε_a	axisymmetric axial strain - triaxial axial strain
ε_r	axisymmetric radial strain - triaxial radial strain

		triaxial stresses
p	normal stress	$\frac{\sigma_a + 2\sigma_r}{3}$
q	deviator stress	$\sigma_a - \sigma_r$
ϵ_v	volumetric strain	$\epsilon_a + 2\epsilon_r$
ϵ_s	shear strain	$\frac{2}{3}(\epsilon_a - \epsilon_r)$

Superscripts

p	permanent
r	resilient

Stresses listed are total stresses. Effective stresses are denoted by the use of primes.

Compressive stresses and strains are taken as positive. Other symbols are defined and used in restricted conditions as the need arises.

CHAPTER ONE

INTRODUCTION

The rapid growth in road traffic over the last few years, especially in the numbers and gross weights of commercial vehicles has led to premature failures of trunk roads and motorways. This is expensive not only because of the cost of repair but also because of the extensive delays to private and commercial road users. These failures and the need to design roads for greater and greater volumes of traffic has highlighted the need for a fuller understanding of the behaviour of the different materials in a road, both individually and collectively as a road structure. Once this has been achieved pavements can be designed analytically, rather than empirically as is the case at present where the results from existing pavements are extrapolated to design roads to carry ten or more times the traffic flow of the original pavements.

Much research has been done on the properties of bituminous materials, unbound aggregates and concrete, but less relevant data is available on cohesive soils under the stress conditions occurring in road subgrades. Hight and Stevens (1982) using the Nottingham design charts, Brown (1980), have demonstrated the sensitivity of the life of a pavement to changes in the value of the modulus of the subgrade, as shown in Figure 1.1, and hence the necessity of accurately estimating the value of the modulus of the subgrade at the design stage. The elastic properties of soil are needed for computing the response of a pavement to a single wheel load as this controls the magnitude of the tensile stresses in the upper layers and hence the ability of a pavement to resist fatigue failure. However the most common form of failure of a road pavement in this country is by rutting, which is due to the excessive build up of irrecoverable deformation caused by large numbers of load repetitions. Therefore an understanding of how plastic strains accumulate under repeated loading is also required.

ASSUMED PAVEMENT DESIGN		SUBGRADE VERTICAL STRAIN	PAVEMENT LIFE
ASPHALT THICKNESS	220mm		10^7
STIFFNESS	7 GPa	237 με	STANDARD
SUBGRADE STIFFNESS	50 MPa		AXLES

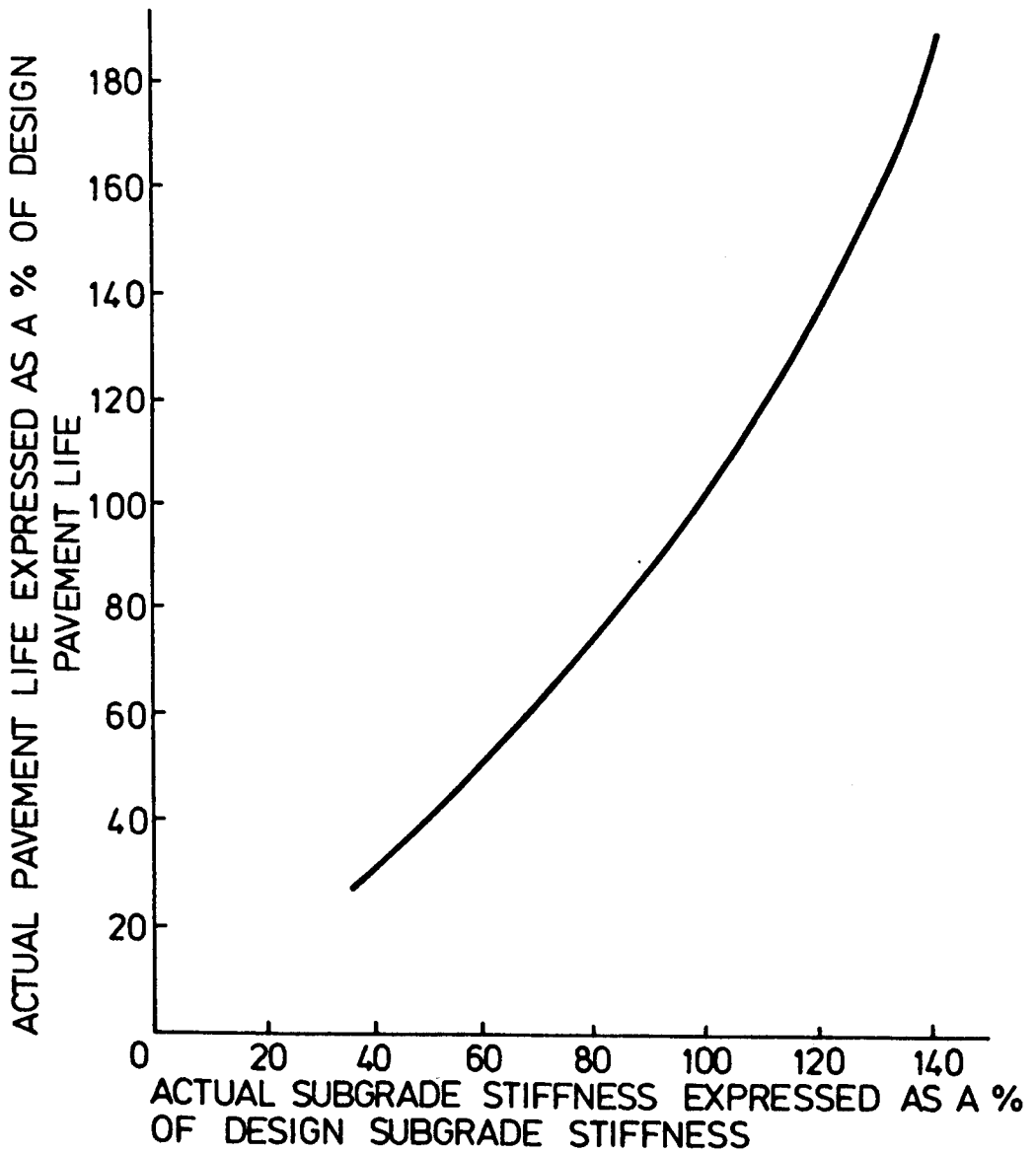

FIGURE 1.1 THE INFLUENCE OF SUBGRADE STIFFNESS ON PAVEMENT LIFE

Conventionally, subgrades are characterised by a California Bearing Ratio (CBR), either determined insitu or in the laboratory. This is an empirical penetration test which has been related to stiffness but it is not of direct use in an analytical design method which requires a stress strain model. However, as the CBR test is so widely used, correlations with elastic stiffness have been proposed and are used at present in design computations in the absence of more accurate data. The correlations with CBR include:

$$E = 10 \times CBR \text{ MPa} \qquad 1.1$$

proposed by Heukelom and Klomp (1962) and

$$E = 17.6\ CBR^{0.64} \text{ MPa} \qquad 1.2$$

developed by Powell et al (1984) at TRRL. The permanent deformation of the subgrade is limited by a resilient strain criterion without any consideration of the type of soil or the insitu conditions.

Previous work on soils, although not under the conditions applicable to road pavements, have indicated that the actual stiffness of soil is influenced by a number of variables. These include not only the physical conditions such as the stress state, moisture content, and preconsolidation pressure but also such variables as the rate of loading. The stress strain response of soils is known to be non linear.

Soil, whether it is undisturbed or compacted as fill is very variable and a very extensive and expensive site investigation would be required to provide sufficient undisturbed samples for laboratory testing to determine the variations of the stiffness of the subgrade along the length of the road. What is required then is a simple and inexpensive test, which ideally can be performed insitu, which allows the subgrade to be characterised such that its stress strain response can be predicted sufficiently accurately to allow a proper analytical design of a

road pavement. To be able to design such a test requires a detailed knowledge of the response of soils to traffic loading and how this is influenced by the various insitu parameters.

The aim of the research described in this thesis was to reconstitute samples of a clay under laboratory conditions to a stress state similar to that found at the top of road subgrades and to subject them to a comprehensive test programme. The samples were fully instrumented and subjected to stress pulses of a similar magnitude and frequency to those acting on road subgrades and the resilient response was recorded per load pulse and the permanent deformation recorded per number of load pulses. The test programme was extended to cover the application of a variety of lower stress level, lower frequency total stress paths to investigate the effective stress response of the soil. A servo hydraulic loading rig was used for the test programme and the samples were overconsolidated anisotropically from a slurry in the laboratory. The results from this series of tests are reported in Chapter 6. The equipment had been developed over a number of years at Nottingham during earlier research projects and is described more fully in Chapter 4. In order to verify that the samples were consolidated to representative stresses some undisturbed samples were obtained from road subgrades and the preconsolidation pressures of these samples were determined. These results are described in Chapter 9.

In view of the importance of the CBR test in current pavement design practice some CBR samples of the same clay were anisotropically consolidated to similar stress states and the CBR values determined.

A smaller less time consuming test series was performed on hand compacted triaxial samples in a simple repeated load pneumatic triaxial rig to investigate the response of samples which were not necessarily saturated. The same clay was used in this test series and the samples were manufactured to moisture contents similar to those achieved by the consolidated samples. The test series was repeated on two other clays compacted to similar

liquidity indices as the first clay. These results are presented in Chapter 7.

A parallel series of CBR test on compacted samples of the same three clays was also carried out together with suction measurements. This enabled the responses of the compacted samples to be analysed in effective stress terms. These tests are detailed in Chapter 8.

The objective of this work therefore, was to determine the stress strain response of soil samples with a known and controlled stress history and to determine which parameters had the most significant effect on the resilient and permanent response. This research therefore provides a source of experimental data on the behaviour of a particular soil under this type of loading which is the first stage in identifying a much simpler and cheaper test than the repeated load triaxial test which would give a better estimation of soil stiffness than the standard CBR test, and which can be used in analytical design methods.

CHAPTER TWO

LITERATURE REVIEW

2.1 EQUILIBRIUM STATES UNDER CYCLIC LOADING

Most researchers reporting on the behaviour of clay under cyclic loading have found a threshold value of repeated deviator stress magnitude, above which the sample eventually fails and below which an equilibrium state is reached regardless of the number of further cycles. Sangrey et al (1969) reported that if the peak deviator stresses at equilibrium for all their tests were plotted in stress space then they fall on straight lines, the lines for different overconsolidation ratios being at different angles as shown in Figure 2.1a. This was found to be valid for both isotropic and anisotropic normally consolidated specimens, and isotropically overconsolidated specimens. Anisotropically overconsolidated specimens were not tested. Further work reported by France and Sangrey (1977) on a different clay and at higher overconsolidation ratios confirmed their earlier findings, though the work was not extended to cover anisotropic overconsolidation.

Sangrey et al (1977) proposed that all cyclically loaded samples at equilibrium would show this relationship if the pore pressure change due to creep was eliminated. They proposed that the total change in pore pressure (Δu_T) was the sum of Δu_p, the creep component, (dependent on time and p'), Δu_q, which is dependent solely on q, and Δu_y which is the pore pressure change generated by cyclic loading. Therefore, if Δu_T was corrected for the creep dependent part, Δu_p, in each case, then the equilibrium points would move in effective stress space, as shown in Figure 2.1b, to form straight lines.

2.2 PORE PRESSURE-STRAIN RELATIONSHIP

Lo (1969) showed, mathematically, that the excess pore pressure induced by shear may be expressed as a sole function of the major principal strain. He carried out slow strain controlled cyclic

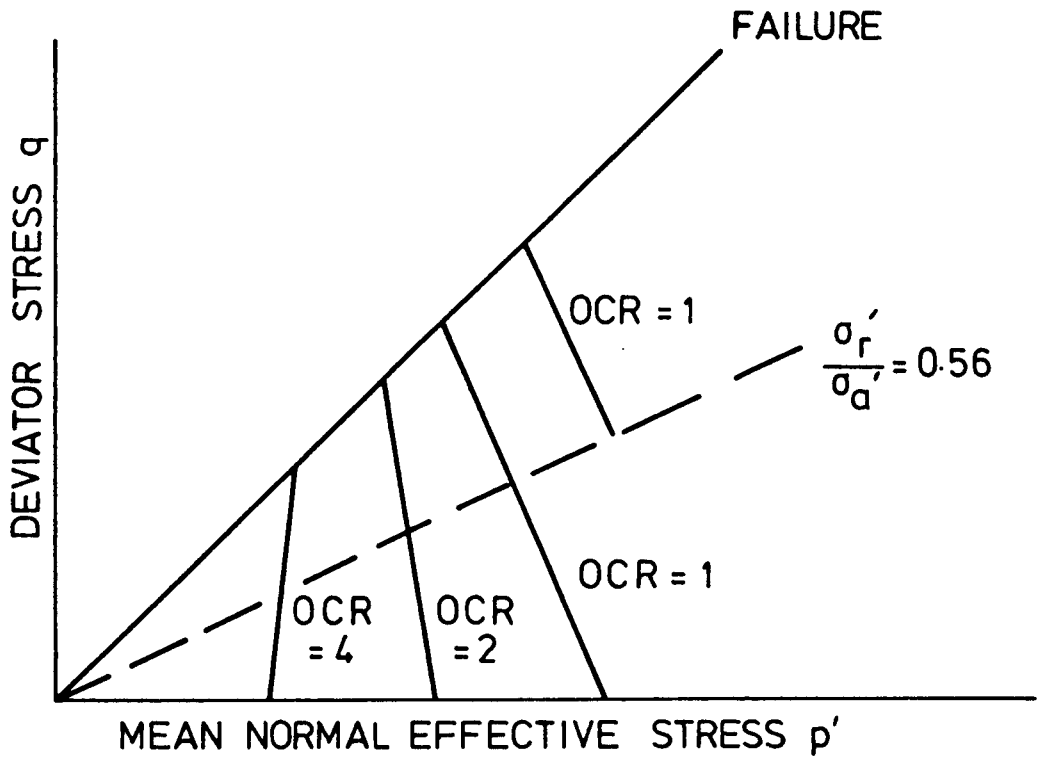

FIGURE 2·1a EQUILIBRIUM STATES DURING CYCLIC LOADING (AFTER SANGREY et al 1969)

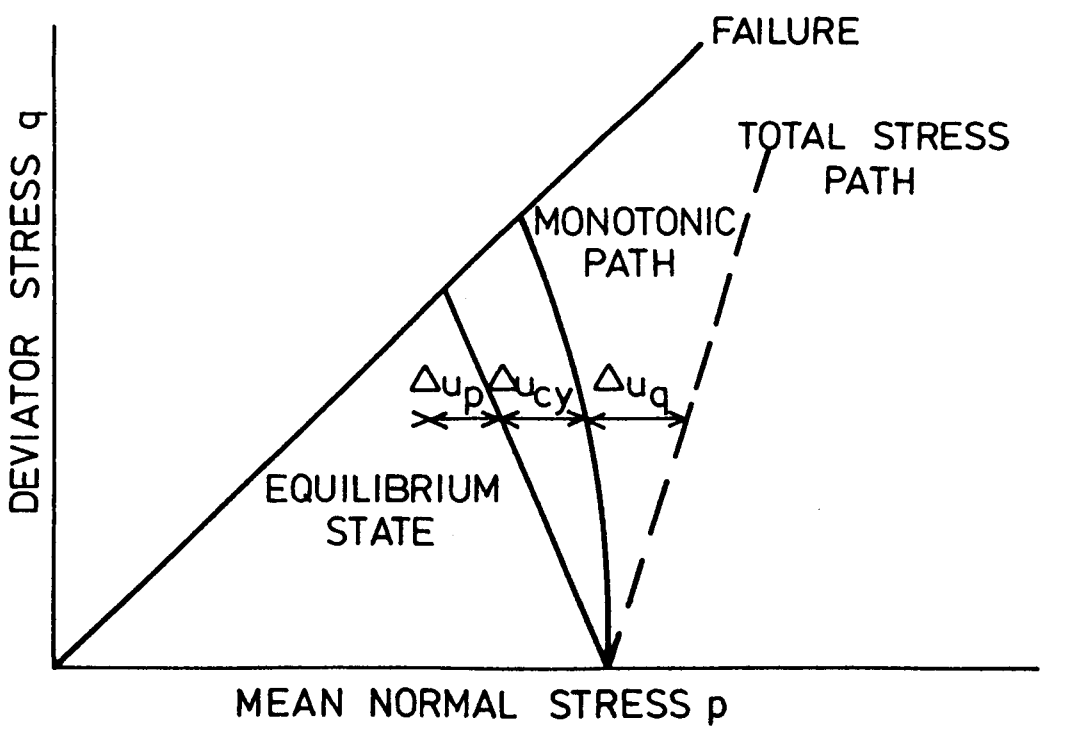

FIGURE 2·1b EFFECT OF CREEP CORRECTION ON EQUILIBRIUM STATES (AFTER SANGREY et al 1977)

triaxial tests on isotropic and anisotropic normally consolidated samples, the results of which confirmed his theory. He showed that the pore pressure-strain relationship varied for different modes of consolidation, but was independent of time of sustained stress, magnitude of consolidation pressure or time of consolidation. Lo used a parameter called the pore pressure ratio defined as $1 - k + \Delta u_s / \sigma'_{vc}$ where k is the principal stress ratio, Δu_s the pore pressure increment due to shear stress and σ_{vc}, the vertical effective stress at preconsolidation.

Yasuhara et al (1982) working with isotropic and anisotropic normally consolidated clay found that $\Delta u/\sigma_c$, where Δu is the excess pore pressure and σ_c the cell pressure, was related to the axial strain by a unique hyperbolic function independent of the loading method, i.e. either static or repeated. However, Mitchell and King (1977) working with isotropically normally consolidated clay found no apparent relationship between distortional or axial strain and the development of pore pressures.

Wilson and Greenwood (1974), testing normally consolidated clay, found that the permanent pore pressure developed was linearly related to the plastic axial strain, for small strains, and that the cyclic pore pressure was linearly related to the elastic or resilient axial strains. The frequency they used was 0.017 Hz, which should have allowed the pore water transducer to follow the pore pressure response, though no positive evidence was presented.

Matsui et al (1980), testing normally consolidated and over-consolidated clay, found that plots of u_r/σ'_c, where u_r is the residual excess pore pressure and σ_c, the radial or minor principal effective stress, against $\ln\gamma_c$, where γ_c is the maximum single amplitude cyclic shear strain, produced straight parallel lines for each value of over-consolidation ratio tested (see Figure 2.2). Koutsoftas (1978) produced results similar to Matsui et al but these were presented as $\Delta u/\sigma_c$, against γ_r (the peak to peak shear strain), so the relationship may not be quite the same if $\ln\gamma_r$ is plotted.

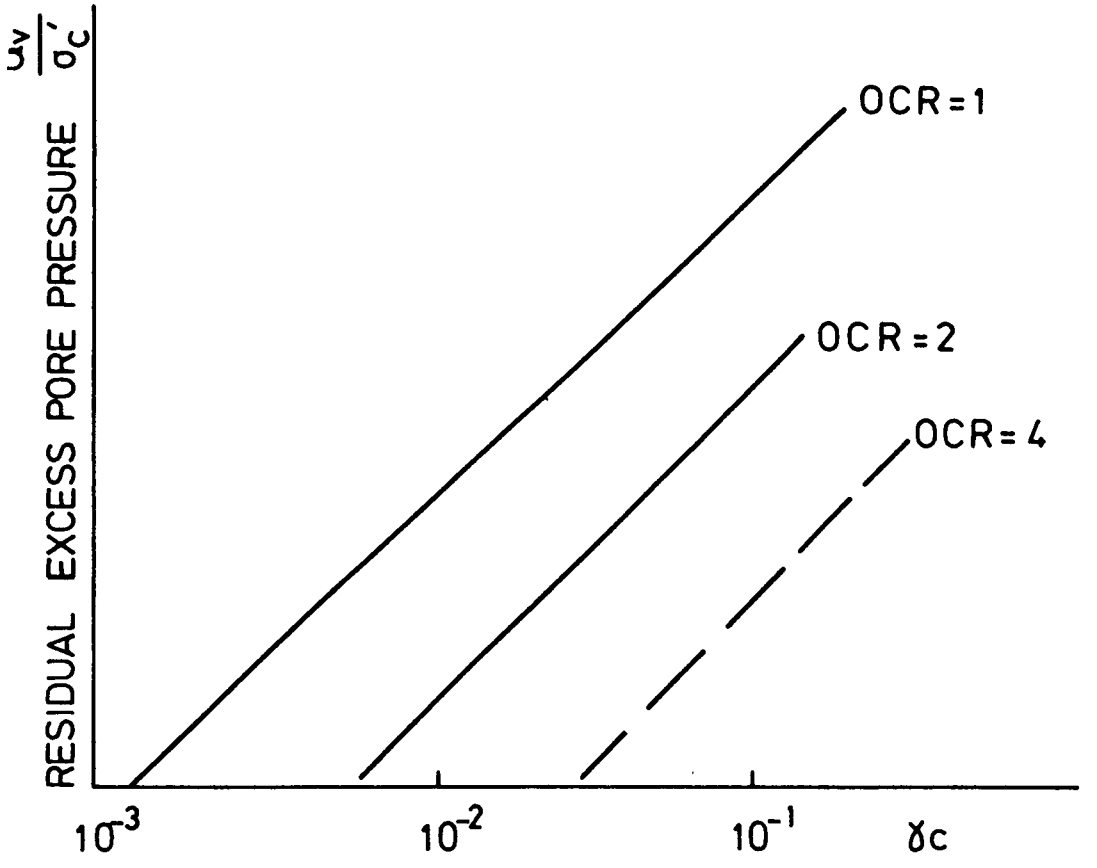

FIGURE 2.2 RESIDUAL EXCESS PORE PRESSURE AGAINST MAXIMUM SINGLE AMPLITUDE CYCLIC SHEAR STRAIN (AFTER MATSUI et al 1980)

2.3 EFFECT OF FREQUENCY OF LOADING

Brown et al (1975) found that there was no apparent effect on resilient strains for a loading frequency range between 0.01 Hz and 10 Hz. Yasuhara et al (1982) reported little effect on undrained strength for loading frequencies between 0.1 Hz and 1 Hz, and Sherif et al (1977), working with a hollow cylinder apparatus, reported little change in cyclic strength over the frequency range 0.025 Hz to 10 Hz.

Matsui et al (1980) found that as the frequency increased over the range 0.02 Hz to 0.5 Hz, there was less excess pore pressure generated for the same number of cycles and that the axial strain amplitude decreased. Wood (1980) states that it seems more likely that the effect of frequency is greater for more plastic clays. The plasticity index of the silty clay tested by Brown et al was 18%, which supports Wood's assertion, but the remaining soils all had plasticity indexes in the range 55 to 60.

The only way to subject a specimen to a large number of cycles in a feasible time, is to use frequencies of the order of 10 Hz, which, in the case of road subgrades, models the loading rates correctly (Croney, 1977). The majority of pore pressure transducers will then only record the mean or permanent pore pressure reliably. Therefore to monitor the pore pressure response to an individual cycle would mean reducing the frequency. Matsui and Abe (1981) report a fully saturated response from a miniature pore pressure transducer in the sample up to frequencies of 3 Hz. Hight (1983) reported a response time of 0.5 seconds for a small transducer placed against the side of the specimen, while Overy (1982) reported a loss in response at about 0.1 Hz for a miniature pore pressure transducer in the centre of the sample and 0.005 Hz for the base pore pressure transducer.

2.4 EFFECT OF OVERCONSOLIDATION RATIO

The overconsolidation ratio reflects the type of behaviour

exhibited by a soil when it is sheared. Those samples on the wet side of the critical state have low overconsolidation ratios and tend to behave uniformly, while those on the dry side with higher overconsolidation ratios tend to develop discrete failure planes. Under monotonic loading samples on the wet side of critical state develop positive pore pressures, while those on the dry side develop negative pore pressures.

Brown et al (1975), testing a silty clay under cyclic loading, report similar results to the monotonic tests for overconsolidation ratios of 2 and 10, namely positive pore pressure development for OCR 2 and negative for OCR 10. Hyde (1974), testing the same clay, reported that initially positive pore pressures were developed up to 10^4 cycles for samples at high overconsolidation ratios. Anderson et al (1980), working on Drammen clay, reported that all cyclic loading compression tests showed initial positive pore pressure development except at an overconsolidation ratio of 10. Togrol et al (1979) also reported positive pore pressure development when testing a clay at an OCR of 4.

France and Sangrey (1977) reported negative pore pressure development when testing a clay at an OCR of 8 and Koutsoftas (1978) and Knight and Blight (1965) also reported negative pore pressure development for samples on the dry side of critical i.e. at OCR's of about 4 or more. Matsui et al (1980) and Taylor and Bacchus (1969) reported their findings more fully and obtained negative pore pressure development initially, which increased in magnitude as the overconsolidation ratio increased. They both also report that, as the number of cycles increases, the negative pore pressure peaks and then starts going positive, even for an overconsolidation ratio of 16.

Ladd et al (1977) presents results from monotonic loading tests which indicate that the stiffness of a soil under a set value of deviator stress increases as the overconsolidation ratio increases from 1 to approximately 3 and then decreases quite

rapidly as the overconsolidation ratio increases further. However, the results of Brown et al (1975) show that the resilient modulus of samples of silty clay after reaching equilibrium under 10^5 cycles seems to be independent of overconsolidation ratio. The results of Ogawa et al (1977) support this and they conclude, generally, that the effects of overconsolidation ratio decrease with increasing numbers of cycles.

2.5 EFFECT OF DRAINAGE PERIOD

Knight and Blight (1965) point out that, even on heavily trafficked roads, the total time actually under load is quite small and it is therefore reasonable to assume that there is some drainage although individual load pulses themselves are undrained. France and Sangrey (1977) allowed some continuous drainage during their cyclic tests, but not sufficient to inhibit the build up of pore pressures. Brown et al (1977), Anderson et al (1976), and Overy (1982) have all considered this problem and the general conclusion is that samples on the wet side of critical with positive excess pore pressures expel water and become stiffer while those on the dry side, with negative residual pore pressures will tend to imbibe water and soften. The amount of water imbibed will depend on the slope of the swell back line, and if this is shallow, the effects of allowing drainage will only have a small effect as reported by Brown et al (1977). There seems to be a tendency for the failure plane of overconsolidated samples to be at a water content some 3% higher than the main bulk of the sample as reported by Togrol et al (1979) and France and Sangrey (1977).

2.6 STRESS-STRAIN RESPONSE

Ogawa et al (1977) presented some results of cyclic loading tests in the form of stress-strain hysteresis loops and they show that for small resilient axial strains the loops are symmetrical and elliptical in shape. For larger strains the loops degenerate into S shapes. They also state that there is a much more marked

change of shape for the samples with higher overconsolidation ratios. Sherif et al (1977) also reported symmetrical elliptical hysteresis loops from their low strain cyclic tests using a hollow cylinder apparatus. Anderson et al (1980) obtained similar findings from their work on Dramman clay. They also show that, for two way cyclic loading, the loops are not symmetrical between the extension and compression zones. Taylor and Bacchus (1969), using strain controlled cyclic loading tests, also report a degeneration of elliptical hysteresis loops into S shapes with increasing numbers of cycles. Macky and Saada (1984) also report a similar finding from their tests on isotropically consolidated and overconsolidated clay samples in a hollow cylinder apparatus. Overy (1982) did not report any change in the stress strain hysteresis loops with numbers of cycles from his work on repeated triaxial loading of Keuper Marl.

Sanchez and Sagaseta (1981) reported discontinuities in the effective stress paths of triaxial specimens subjected to slow undrained strength tests. They occurred at strains of less than 0.5% for normally consolidated samples, up to strains of about 9% for samples with an overconsolidation ratio of 3. This discontinuity was exhibited by both isotropically and anisotropically consolidated samples. Bjerrum (1973) reported that when a cohesive soil is loaded the cohesive component of the strength is mobilised and this reaches a peak at a low strain and then tails off to a residual value, meanwhile as the strain increases, more friction is mobilised but, by then, the particle structure has started to change. This effect will lead to change in stress-strain behaviour under monotonic strength tests and some similar mechanism may well be acting in samples under low strain amplitude cyclic loading.

2.7 ANISOTROPY

Most work on anisotropically consolidated samples has been on normally consolidated material in the repeated load triaxial test. The results which have been reported indicate some differences in behaviour caused by anisotropy. For example,

Yasuhara et al (1982) found that smaller excess pore pressures were developed with increasing axial strain for anisotropic samples. France and Sangrey (1977) reported that strength tests on samples which had reached equilibrium under repeated loading showed a gain in strength of 30% for isotropic and only 15% for anisotropically consolidated samples.

Saada and Bianchini (1975) investigated the effects of different stress paths to failure for anisotropically consolidated samples using a hollow cylinder apparatus. Their results show that there is no unique c-$\emptyset'$, relation for an anisotropic sample. Saada et al (1978), again using a hollow cylinder apparatus, report that under low frequency, low strain cyclic loading the behaviour of anisotropic samples was totally different from isotropic ones, even after severe cyclic straining.

Graham and Houlsby (1983) reported a theoretical analysis and a series of experimental results which demonstrate that some of the effects of anisotropy can be observed in the triaxial cell, though the work was limited to a vertical axis of symmetry of the sample coinciding with that of the triaxial cell. The work was concerned with small amplitude stress paths within the yield surface and demonstrates that the elastic response of an isotropic soil to various total stress paths was unique, as for isotropic material, but that p' was not constant during the load cycles. This is because, unlike isotropic material, there is a cross dependence of shear strain on the mean pressure p', and of volumetric strain on the deviator stress q.

2.8 LOADING REGIMES

A large number of the cyclic load triaxial tests reported in the literature are isotropically normally consolidated or overconsolidated, and the pulsed loading starts from zero deviator stress. Most tests involve one way loading (compression) while some are two way loading with equal positive and negative peaks of deviator stress (compression - extension).

Anderson et al (1980) reported that much larger shear strains developed under two way loading than one way loading. They reported that, in triaxial samples, the behaviour is different in compression and extension and that a mean plastic strain will develop even if the loading is symmetrical. At large cyclic strains, some dilatancy occurs and affects the cyclic pore pressure changes. One way cyclic loading causes a change in both pore pressure and strain. In general, though, cyclic pore pressures in triaxial tests are caused by mean normal stress changes, a fact which has been recognised by Matsui et al (1980) who report a series of tests where the cell pressure is pulsed 180° out of phase to the deviator stress at such an amplitude as to keep the total mean normal stress constant. They do not, however, report tests results where the mean normal stress changed for comparison purposes.

Most researchers have reported threshold values separating failure and equilibrium conditions for cyclic load triaxial tests. Most of these are pulses from isotropic conditions. However, Mitchell and King (1977) report that, for their normally consolidated clay, a repeated deviator stress pulse of 0-50% of undrained strength was sufficient to cause failure, but if the soil was allowed to reach equilibrium under a static deviator stress of 20% of the undrained strength, then a cyclic deviator stress of 50% was still required to fail the sample. Houston and Herman (1980), working mainly with normally anisotropically consolidated soil demonstrated that soils under a static deviator stress of about 30% of undrained failure require a larger cyclic deviator stress to cause failure than when starting under isotropic conditions.

2.9 YIELD SURFACES

The yield surface for normally isotropically consolidated samples under slow monotonic loading has generally been found to be equivalent to the Roscoe surface, as predicted by the critical state theory, Schofield & Wroth (1968). Mitchell (1969) demonstrated that the yield surfaces were different for normally

consolidated isotropic and anisotropic samples. Crooks and Graham (1976) testing reconsolidated undisturbed site samples demonstrated that the yield envelope for anisotropic samples was centred approximately on the K_0 consolidation line in q-p' space. Tavernas et al (1979), testing three different naturally occurring clays, reported similar findings and concluded that their yield surface approximated to a surface of constant strain energy. Later work by Folkes and Crooks (1985) working with two different clays confirmed the above findings. The work covered low overconsolidation ratios, though still remaining on the wet side of the critical state.

Graham et al (1983) tested a natural clay, reconsolidated to the insitu stresses, in a triaxial rig under a variety of effective stress paths. They reported a nest of yield surfaces, depending on the overconsolidation ratio and mean normal effective stress, which were not symmetrical about the K_0 line, the critical state line or the isotropic consolidation line. Normalising the q-p' axes by dividing by the preconsolidation pressure resulted in a single yield locus. Graham et al pointed out that the position of the yield locus would depend on the loading rates.

Banerjee and Stipho (1979) proposed a yield surface for heavily overconsolidated clays which involved adapting the Hvorslev surface and using it as a yield surface. The model they proposed was for isotropically overconsolidated samples where the original yield surface, consisting of the Roscoe and Hvorslev surfaces, was set by the preconsolidation pressure. Subsequent loading beyond this surface caused plastic straining and reset the yield surface to pass through the peak of the effective stress path. The intercept of the surface on the deviator stress axis also changed. The model was developed for monotonically loaded samples and test data was presented which showed that the model gave reasonable results.

Hyde and Ward (1985) reported the results of a series of repeated load triaxial tests on Keuper Marl and concluded that the Hvorslev surface forms a yield and consequent failure surface for

cyclic effective stress paths of samples of all stress histories. They found that normally consolidated samples eventually failed by stress path migration caused by a build up of pore pressure in the same way as heavily overconsolidated samples.

2.10 THIXOTROPY

It has been found by most researchers that the response of clays subject to repeated loading differs with different rates of loading. Indeed one of the original assumptions in the critical state theory, Schofield and Wroth (1968), was that the rates of loading were sufficiently slow for viscous effects to be ignored. The continual deformation of clays under a constant load, i.e. creep, is also well documented and some researchers have had some success relating the behaviour of clays under repeated loading to that under creep loading, Hyde (1974), Hyde and Brown (1976).

Thixotropy is another aspect of the time dependent behaviour of clays but reference to it in the literature is less common. Thixotropy is the stiffening of the soil sample with time under constant stress conditions with no change in state. Seed et al (1962) carried out a large number of repeated load triaxial tests on subgrade soils compacted by different methods to various dry densities and moisture contents. They found that the length of time after compacting a sample before testing it caused significant changes in behaviour. Samples left for 50 days before testing showed a much reduced permanent strain after 50,000 stress pulses, and the samples were found to be stiffer for up to about 4000 stress applications. In fact the initial stiffness could be as much as 4 times that of a sample tested almost immediately after compaction. The repeated loading was found to have effectively destroyed the thixotropic strength gain after approximately 4,000 applications, and this was considered likely to have been caused by the deformations induced by the cyclic loading.

Pusch (1982) working with natural undisturbed clays and saturated

laboratory prepared clay samples also demonstrated that there was a stiffening effect with time, present in clay samples stored undrained under constant stress conditions after disturbance of the clay structure by loading. Kim and Novak (1981) measured the stiffness of normally and overconsolidated, naturally occurring clay samples in a resonant column apparatus and demonstrated that the low strain amplitude shear modulus measured immediately after higher amplitude shear straining was lower than if it was measured prior to the high amplitude shear straining. They noted that the reduced stiffness was only temporary and not due to changes in stress or state brought about by excess pore pressure or drainage.

Mitchell (1960) postulated that the interparticulate force balance between soil particles is such that soil will tend to flocculate and become stiffer. He stated that the energy of interaction between soil particles is at a level commensurate with externally applied forces, and that therefore shearing the soil is capable of disrupting the thixotropic bonds and reorganising the platey clay minerals into a uniform parallel structure. When shearing stops the interparticulate forces become dominant again and the structure readjusts itself. Since these structural changes are dependent on actual physical movement of particles and ions they are time dependent.

Osipov et al (1984) examined the structural arrangements of various clays under different loading regimes using an electron microscope and confirmed Mitchell's hypothesis about the structural changes caused by externally applied forces. They measured the torque of a knurled cylinder continuously rotating in wet clays with and without an externally applied vibration to the clay. The torque required was considerably less when the soil was vibrated, but soon regained the original level when the external vibration was removed. The clay structure was examined by freezing the samples under various loading conditions using liquid nitrogen, and was found to become much more uniform under the vibrating load, but to revert to its more disorganised state when the vibration was removed.

2.11 END RESTRAINT

Perloff and Pambo (1969) used a finite element method to analyse the triaxial test to determine the effect of end restraint. They considered the case with total fixity at the ends and compared it with the results obtained using smooth end platens. They found considerable non-uniformities in the stresses and hence the pore pressures and strains at the ends of the samples. However, the middle section was relatively uniform even with total fixity at the ends. Carter (1982) used a finite element programme to examine constant strain rate triaxial strength tests, which showed non uniformity in stress at the edges of the sample as well as at the ends. Kimura and Saitoh (1983) carried out a series of undrained shear tests on saturated clay samples with pore pressure transducers in the centre, at the end and on the periphery of the samples and demonstrated that each section of the sample followed a different effective stress path. The paths became more similar at low strain rates of approximately 4%/hour or less. Balasubramanian (1976) consolidated lead shot in triaxial samples of kaolin. X ray photographs were then taken of the samples during shearing. The axial strain was found to be reasonably uniform up to 2% for fixed ends, and up to 8% for free ends. The material tended to form rigid cones on the platens at approximately $\emptyset'$ to the platen

Lee (1976) reported on the various methods to reduce end friction and concluded that the most satisfactory way was to use silicone grease on polished steel end platens with a rubber membrane separating the soil and grease. Brown (1974) reported the results obtained from an investigation into end restraint during the research programme on Drammen clay, and reached the same conclusion as Lee provided high vacuum grease was used. Lee reported that if the greased end platens were left under load for as little as 10 hours then some effectiveness was lost and a peak friction angle developed which reduced once radial movement commenced and resmeared the grease. Overy (1982) reported a similar effect and stated that a modified system with a grease reservoir consisting of two membranes stuck together at the

edges, with bleed holes to allow the grease onto the platen, proved to be effective for at least seven days. The technique was originally developed by Austin (1975). However, Overy reported practical difficulties in assembling and using the reservoir, and found that the extra grease could clog the side filter paper drains.

Lee raised another point concerned with the effect of the viscosity of the grease. He demonstrated that, assuming free ends, the shear stress developed at the circumference of the sample under a 1 Hz loading was quite significant. He stated that this effect could be reduced by using more than one greased membrane, but this would cause more uncertainty in axial measurement for those researchers still measuring axial strains between the end platens.

Most triaxial testing equipment measures pore pressures at the base of the sample, and because some end restraint will always be present, the measured pore pressure will not be representative. Some researchers, such as Sangrey et al (1969), used very low frequencies of loading to allow time for pore pressure equalisation, while others, Koutsoftas (1978), allowed time after faster cyclic loading for the pore pressure to equalise. In either case the recorded pore pressure will still be distorted by the end effects but the second method has the advantage of testing at representative frequencies or rates of loading. It seems likely that the most accurate pore pressure measurements will be from a centre probe in the relatively uniform central section of the sample before pore pressure equalisation has taken place (Hight 1983), assuming that the transducer itself does not cause any significant effects.

2.12 SUCTION

Water is held in the soil matrix by absorption and surface tension forces at a pressure less than atmospheric (Croney 1977). Soil moisture suction, or suction, is a measure of the pressure required to abstract water from a sample of soil which is free

from external loading. Suction is expressed on the pF scale, which is the common logarithm of the height in centimetres of an equivalent column of water.

Krahn and Fredlund (1972) define the total suction as the negative gauge pressure relative to the external gas pressure on the soil water to which a pool of pore water must be subjected in order to be in equilibrium through a semi permeable membrane with the soil water. The total suction was proposed as the sum of the osmotic suction and the matrix suction and the relationship was proved by measurements of all three parameters on a variety of soils. The osmotic suction is due to the different salts which may be dissolved in the pore water and which affect the surface tension. The matrix suction is due to the size and shape of pores in the soil skeleton and the clay particle surface absorption.

The total suction of a soil sample is measured using a psychrometer which measures the humidity of the air surrounding, and in equilibrium with, the soil sample by using thermocouples. The osmotic suction can be computed from electrical conductivity measurements. All types of suction apparatus which involve allowing the sample to reach moisture equilibrium across a porous stone or membrane measure the matrix suction as the stones are permeable to salts dissolved in the pore water.

Krahn and Fredlund found that the variation in total suction with moisture content of the sample was almost entirely due to variations in the matrix suction as the osmotic suction remained virtually constant. Krahn and Fredlund concluded that for remoulded compacted soils the matrix suction and hence the total suction, was dependent on the moisture content of the sample but essentially independent of the dry density. Shackel (1973) concluded that the suction was slightly influenced by the dry density but primarily depended on the degree of saturation of the sample. Croney et al (1958) found that the dry density has little effect on the suction moisture content relationship for heavy clays, but that dry density affects the suction moisture content relationship for sandy or silty clays below a pF of

approximately 2.

Snethen and Johnson (1977) state that the matrix suction is both water content and surcharge dependent, and that the osmotic suction is independent of water content and surcharge pressure.

Russell and Mickle (1970) demonstrated that the suction moisture content relationship for clays has three distinct regions with points of inflection at approximately the liquid limit and the plastic limit. The suction at the plastic limit was found to be approximately pF 3.7 for heavier clays reducing to approximately pF 3.2 for silty clays. A vacuum is equivalent to approximately pF 3.0.

Croney et al (1958), using a pressure plate apparatus, demonstrated that the suction moisture content relationship exhibits some hysteresis in that the measured suction at a particular moisture content depends on whether the sample has been wetter and allowed to dry or is being wetted up from a drier state. This was put down to the fact that pores may empty at different suctions from that at which they fill. Croney also found that there was a unique suction moisture content curve for continuously disturbed soil.

However, Snethen and Johnson (1977) determined the suction moisture content relationship for four soils with plasticity indices varying between 13 and 68 using a psychrometer and found that there was no hysteresis between the wetting and drying curves. They were of the opinion that the pressure plate type apparatus caused the hysteresis found by other researchers.

Shackel (1973) proposed that suction (in pF) was linearly proportional to the logarithm of the moisture content, for the range pF 0.6 to pF 1.8, although the constants depended on the degree of saturation and the dry density. Croney (1977) demonstrated that a plot of moisture content against plasticity index gave approximate linear contours of suction for the range pF2 to pF3. Snethen and Johnson (1977) found that there was a

linear relationship between suction (in pF) and the moisture content over the range pF2 to pF4.7.

Mou and Cha (1981) working with a clay with a plasticity index of 19 demonstrated that static and kneading compaction resulted in different suction moisture content curves, with a greater suction for the statically compacted samples in each case.

2.13 RELATIONSHIP BETWEEN SUCTION AND RESILIENT MODULUS

Croney (1977) states that soil moisture suction is an overriding factor in determining the elastic modulus for saturated clays. An analysis of the results presented by Brown et al (1975) in terms of suction show a linear relationship between resilient modulus and suction at constant deviator stress. A similar relationship is reported by Finn et al (1972) determined with data from a test road subgrade. Dehlen (1969), working with silty clay, showed a measured suction decreasing with increasing depth below a road surface and a corresponding linear decrease in resilient modulus with suction.

Fredlund et al (1975) measured the resilient modulus and suction of a till and a clay and found that the modulus increased with increasing suction, but at a decreasing rate. Most of their work concentrated on samples much drier than the plastic limit with quite high suctions.

Richards and Gordon (1972), working with a clay subgrade, determined the resilient modulus in repeated load triaxial tests and subsequently measured the suction of each sample. They concluded that the resilient modulus is very sensitive to changes in soil moisture suction and that there is a linear relationship if the logarithms of each are plotted. However, Edris and Lytton (1977) found that resilient modulus increased with suction until a moisture content about 2% less than the optimum, and that there was little change in resilient modulus as the suction increased further. Sauer and Monismith (1968), working on a glacial till, determined resilient modulus from repeated load triaxial tests

and also measured the soil suction of the specimens. They reported that the resilient modulus increased rapidly with increasing soil suction until a moisture content equivalent to optimum, thereafter the curve reached a steady value of resilient modulus as the suction increased. Edil et al (1980) found that their was little change in the resilient modulus with suction up to 100 kPa from their test results.

2.14 PREDICTION OF RESILIENT MODULUS FROM SOIL PROPERTIES

Kirwan and Snaith (1976) published a chart showing contours of resilient modulus on a graph of relative compaction against relative moisture content. This chart was based on experimental results on Irish glacial tills (P.I. range 14-20%) and showed that there was an optimum moisture level for maximum resilient modulus at any particular degree of compaction.

Later work by Kirwan et al (1982) showed that the resilient modulus increased gradually with increasing load applications and reached a steady value after 10,000 cycles. At higher values of deviator stress the modulus decreases with increasing number of cycles and did not reach a steady value after 80,000 cycles.

The variations in steady state resilient modulus and permanent deformation (after 40,000 cycles) with dry density and moisture content showed these parameters to be more sensitive to changes in moisture content than dry density. Kirwan et al concluded that for their soil a reasonable estimate of resilient modulus could be obtained from the dry density and moisture content.

Edris and Lytton (1977) tested three soils in a repeated load triaxial rig and monitored the elastic and plastic deformation, the vertical load and the soil suction. The soils had a wide range of clay content and plasticity indices. Expressions were developed for resilient modulus and plastic strain from their results showing that it is possible to predict these parameters for any soil with a clay content between 20% and 70% using their equation. They found that the resilient modulus was dependent on

temperature, increasing as the temperature decreased, and provided temperature correction factors for their expressions.

CHAPTER THREE

THE TEST PROGRAMME

3.1 INTRODUCTION

The main body of the research concentrated on repeated load tests on a reconstituted anisotropically consolidated clay (Keuper Marl) under triaxial conditions. The initial stress conditions and the loading magnitude and frequencies were chosen to simulate actual road subgrade conditions as closely as possible. A servo hydraulic testing rig which had been developed at Nottingham over a number of years was modified and used for the research. Chapter 4 gives details of the equipment and modifications. In view of the importance attached to the California Bearing Ratio (CBR) in the design of roads, Road Res. Lab (1970) and Powell et al (1984) a subsidiary test programme on consolidated CBR samples was carried out.

A smaller parallel investigation into the behaviour of compacted (i.e. not necessarily saturated) clay samples was carried out using a much simpler repeated loading triaxial rig. A parallel series of tests on compacted CBR samples was also carried out. Three different clays were used in this part of the research and the suction moisture content relationship of each clay was determined over the range of moisture contents used in the triaxial and CBR test programmes. The following sections detail the range of stress conditions chosen for each of the test programmes.

3.2 CONSOLIDATED TRIAXIAL SAMPLES

3.2.1 Initial stress conditions

There is little data available on the insitu stress conditions in road subgrades under roads in serviceable condition in this country, as only roads that have failed are investigated in detail. The range of stress conditions used in the test

programme was based on a survey of the literature and some assumptions and calculations which are detailed below.

Croney (1977) states that it is reasonable to assume that the majority of road subgrades in this country are saturated or nearly saturated, and therefore the use of fully saturated samples, which allow analysis in effective stress terms, can be justified.

Roads in Britain are generally provided with a drainage system designed to maintain the water table a metre or so below the formation level. It is recognised though, Russam (1967), that this is not always feasible for plastic clays where the permeability may be less than that of the surfacing material. However, in practice the water table can be found as high as the top of the subbase. Early research at TRRL into the seasonal variation of moisture content in the ground beneath an extensive paved area showed that, provided there were no cracks, there was little variation in moisture content with change in season (Black et al 1958). Therefore it can be assumed that there will be little water flow in the subgrade under a road in good condition and consequently there will be an approximately linear increase in pore pressure with depth. Water held above the water table by capillary action will cause a linear increase in negative pore pressure with height above the water table until desaturation occurs. Croney (1977) states that this is unlikely to occur unless the water table is greater than 5m deep. A range of pore pressures at the top of the subgrade of between 0 and -70 kPa was chosen to give a reasonable range of effective stresses for the test programme.

The total vertical stress on the subgrade can be calculated from the overburden pressure due to the road construction. The horizontal stress though cannot be calculated without assuming a value for K_o, which in turn depends on the overconsolidation ratio. It is reasonable to assume that most natural clays in this country are overconsolidated to some degree, and there is some evidence to suggest that compacted clays also behave as if

they were overconsolidated (Croney, 1977). Naturally overconsolidated clays would be anisotropic as they were consolidated one dimensionally. As there were no values of typical overconsolidation ratios available it was decided to use values of 6, 12 and 18 as defined by the mean normal effective stress, as this covered a reasonable range. Some undisturbed U4 sample tubes of road subgrades were obtained part way through the research project and the preconsolidation pressures determined. The results are presented in Chapter 9 and show that the range of overconsolidation ratios chosen was reasonable.

Assuming an overburden pressure of approximately 20 kPa from about 1 m thickness of road construction, and a value of K_o of between 1.5 and 2.0 at an overconsolidation ratio of 12 for clays with a Plasticity Index in the range 10 to 40 approximately, Lambe and Whitman (1979), gives, for a water table at the top of the subgrade, a mean normal effective pressure of about 30 kPa. Lowering the water table to give a negative pore pressure of about -70kPa increases the mean normal effective stress to approximately 100 kPa.

It was decided therefore to test samples at mean normal effective stresses of 33 kPa, 65 kPa and 100 kPa at overconsolidation ratios of 6, 12 and 18. Figure 3.1 shows the sample numbering system.

3.2.2 Loading conditions

The test programme was designed to investigate the elastic response of the samples to low level stress pulses, and the resilient and permanent responses of the samples to loading sequences typically undergone by road subgrades.

The range of test frequencies and pulse amplitudes was limited to some extent by what it was feasible to measure and control. This was especially true for any analysis in terms of effective stress which required accurate pore pressure measurement. The main limitation in the equipment was the X-Y plotter which was unable

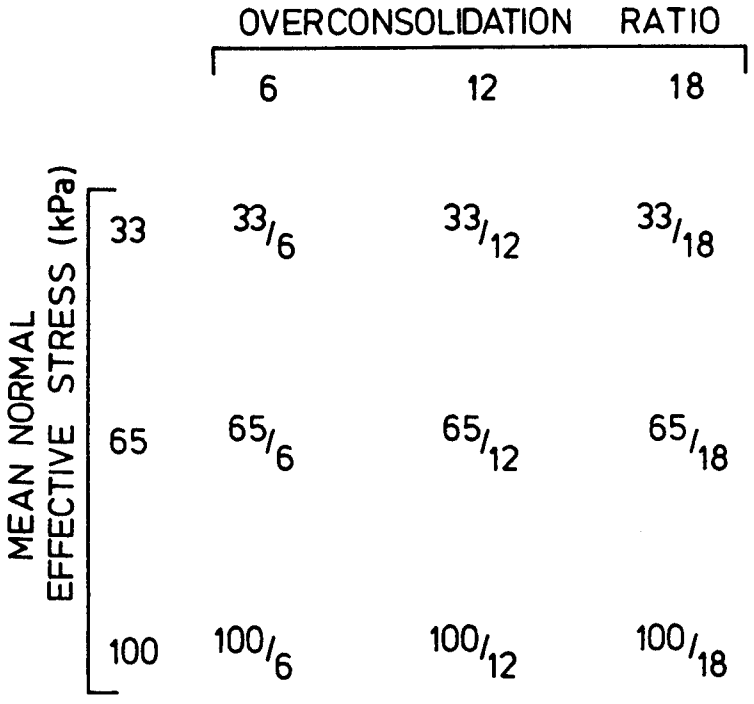

FIGURE 3.1 NUMBERING SYSTEM FOR CONSOLIDATED SAMPLES OF KEUPER MARL

to follow an input signal accurately above approximately 0.3Hz. The introduction of the computer data recording system part of the way through the test programme allowed the stress and strain parameters to be plotted against each other at higher frequencies.

In order to investigate the elastic response of the samples the stress paths had to be recorded to allow a full effective stress analysis. Therefore the samples were tested at as low a frequency as possible (approximately 0.05Hz) to allow accurate recording of the pore pressure and low stress levels generally in the range ±2.5kPa to ±10 kPa were used to limit any permanent deformation.

To establish a realistic range of test frequencies and stress pulse magnitudes to simulate traffic loading two different pavements were analysed using a finite element computer program called SENOL. Full details of the program and the results of the analyses are presented in Chapter 10. The results suggested that a deviator stress pulse magnitude of between 10 and 20 kPa with a period of 0.15 seconds would be suitable. This was equivalent to a vehicle speed of 50 km/hr. Croney (1977) and Barksdale (1971) suggest that periods of about 0.1 second would be applicable, and Croney (1977) suggests deviator stress pulses of between 20 and 50 kPa would be typical.

To simulate traffic loading more accurately the load was applied as a number of individual pulses of constant magnitude rather than continuously.

Hyde (1974) suggested that rest periods between pulses or groups of pulses could be important as it allowed for what he termed delayed elastic recovery. However too many long rest periods would make it impractical to apply the large numbers of stress pulses required. It was decided that these tests would be carried out with a deviator stress pulse of 0.1 second duration followed by a rest period of approximately 0.25 seconds. The stress pulses were derived from a single cycle of a sine wave as this is the closest easily derivable waveform to the pulse shape produced by the computations using SENOL. The arrangement of the

triaxial cell does not allow the direction of the principal axes of stress to rotate, except by 90°, and consequently it is impossible to simulate fully the stress conditions caused by a wheel load rolling over the subgrade.

Single pulses of 0.1 second duration can be considered undrained when applied to clays, but there will be some dissipation of excess pore pressure caused by repeated loading in road subgrades. It was decided to run the tests undrained and to monitor the development of pore pressure, and if necessary to allow some drainage if required.

The initial deviator stress pulse magnitude for these tests was chosen as 20kPa and the test was continued until the sample either reached equilibrium or failed. If the sample reached equilibrium the test was terminated and the sample left for at least 24 hours to recover with the drainage tap open. The test was then repeated with a deviator stress pulse magnitude of between 15kPa to 20kPa greater than the previous repeated stress level. This process was continued generally until the repeated deviator stress level was high enough to cause failure.

In order to determine the effect that this type of test had on the resilient properties of the sample a simple test consisting of a few cycles at each of a range of pulsed deviator stresses up to about 75% of the test level was applied to the sample just prior to and immediately following the main test. These tests were also undrained but used a pulse length of 1 second.

Figure 3.2 shows diagrammatically the type and sequence of the tests applied to each sample.

Cyclic load data is presented on nine anisotropically overconsolidated samples. There was only a one in three success rate at consolidating the samples due to the length of time required (about 8 weeks on average) and the number of equipment failures which occurred and caused excessive sample disturbance or

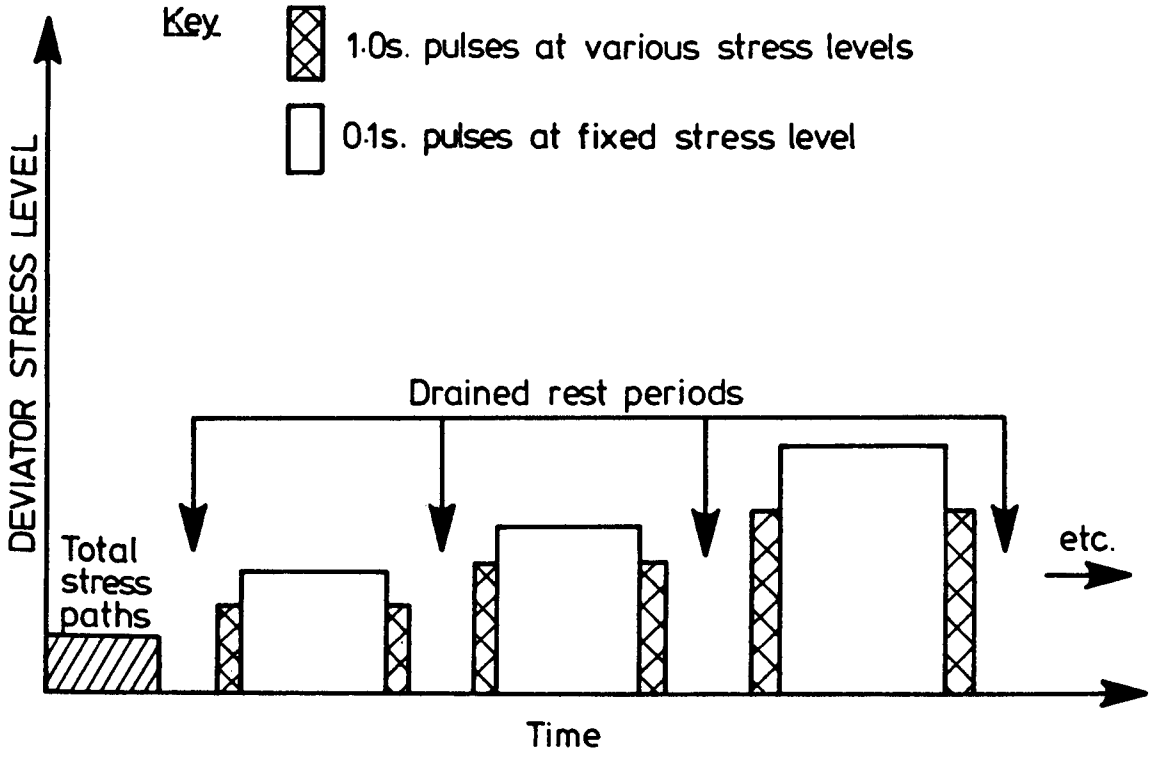

FIGURE 3·2 SEQUENCE OF REPEATED LOAD TESTS ON SATURATED TRIAXIAL SAMPLES

failure. The results of all tests on the consolidated triaxial samples are presented in Chapter 6.

3.3 COMPACTED TRIAXIAL SAMPLES

A number of much simpler repeated load triaxial tests were performed on compacted samples of three different clays. The aim was solely to determine the variation of resilient modulus with moisture content and no attempt was made to measure the pore pressure or the development of permanent strain with the number of cycles applied. The tests on the Keuper Marl samples were designed to provide a comparison between compacted and reconstituted samples, and those on the Gault clay and London clay to determine if different clays showed similar behaviour under similar loading conditions. The test programme on each clay included suction measurements which would give an indication of the effective stress state of the compacted samples and enable the results to be compared more easily with those from the consolidated samples.

The range of moisture contents for the compacted Keuper Marl samples was chosen to cover that of the reconstituted samples at the end of consolidation. The samples were compacted by hand to as dense a state as possible at each moisture content. It was considered to be too difficult to produce uniform samples with lower dry densities using this method of compaction. The range of moisture contents of the test samples of the London and Gault clays was chosen by ensuring that the same liquidity index was achieved as that used for Keuper Marl tests. This method was chosen to try and take into account the different plasticity indices and ensure that the samples were tested under similar conditions.

The frequency of loading could not be varied and was set at 1Hz, which was similar in frequency to some of the tests performed on the reconstituted samples. The samples were tested for 100 pulses at each of a series of increasing deviator stress magnitudes. The axial and radial deformations were monitored

during the first and one hundredth pulse. The deviator stress was not increased beyond that causing a resilient axial strain of about 3500 microstrain, and the resilient response was then monitored for decreasing deviator stress pulse magnitudes. All samples were pulsed with a positive deviator stress pulse from the initial isotropic state.

The Keuper Marl tests were divided into three sets at different cell pressures, namely 0kPa, 15kPa and 30kPa. The London clay and Gault clay samples were tested with a cell pressure of 0kPa only, as this allowed the results to be interpreted in terms of the measured suction, and because further development of the apparatus would be required to allow accurate control of the cell pressure.

The test details for the Keuper Marl, Gault clay and London clays and the test results are presented in Chapter 7. The equipment is described in Chapter 4 and the sample preparation procedure in Chapter 5.

3.4 CALIFORNIA BEARING RATIO TESTS

As the elastic stiffness of subgrades for use in analytical design is at present obtained from the CBR value of the subgrade, either by using the empirical expression $E = 10 \times CBR$, Heukelom and Klomp (1962), or a more complicated relationship $E = 17.6 \times CBR^{0.64}$, Powell et al (1984), it was decided to try and measure CBR values for the clays used in this research at the moisture and stress conditions used for triaxial samples.

A CBR mould was adapted to enable overconsolidated samples of Keuper Marl to be prepared from a slurry. The same range of overconsolidation ratios as the triaxial samples was used. However, it was found to be too difficult to control the final mean normal effective stress precisely enough so all samples were allowed to swell back to the same final vertical effective stress.

The compacted CBR samples of London clay, Gault clay, and Keuper Marl were manufactured in the same manner as the triaxial samples and covered approximately the same range of moisture contents.

The tests were carried out at the standard rate of loading of 1mm/minute, although some tests were unloaded and reloaded at the same rate after 1mm, 2.5mm and 5mm deflection. This was in an attempt to obtain more information from the standard CBR test.

The results and test details of all the CBR tests are presented in Chapter 8.

CHAPTER FOUR

THE EQUIPMENT

4.1 THE SERVO HYDRAULIC TRIAXIAL TEST FACILITY

The servo controlled hydraulic triaxial testing facility at Nottingham was first developed by Lashine (1971). The original development is described in detail by Lashine (1971) and modifications to the system are described by Cullingford et al (1972), Parr (1972), Hyde (1974), Austin (1979) and Overy (1982). The equipment as it existed at the start of this project is described below, followed by a description of the changes and improvements made by the author.

4.2 EXISTING TRIAXIAL EQUIPMENT

4.2.1 The test equipment

The equipment was contained in an air conditioned laboratory and consisted of a loading frame with two hydraulic actuators, the electronic control system and the data monitoring and recording systems. Hydraulic power was supplied by a pump at a normal operating pressure of 14MPa. Figure 4.1 shows a schematic layout of the load and control systems. The control systems compared the output of the relevant transducer with the input command signal, and the difference was amplified and fed to the servo valve which adjusted the oil flow to the actuator to reduce the difference between the input and output signals. The summing junction allowed a signal from a signal generator to be superimposed on the command signal which caused the load on the sample to cycle. A high frequency (400Hz) dither signal was applied to the servo valve to prevent the shuttle sticking.

Axial load was applied to the sample by connecting the load ram in the triaxial cell directly to the hydraulic actuator. The load ram was designed by Austin (1979) and incorporated a strain gauge bridge located within the triaxial cell to avoid errors

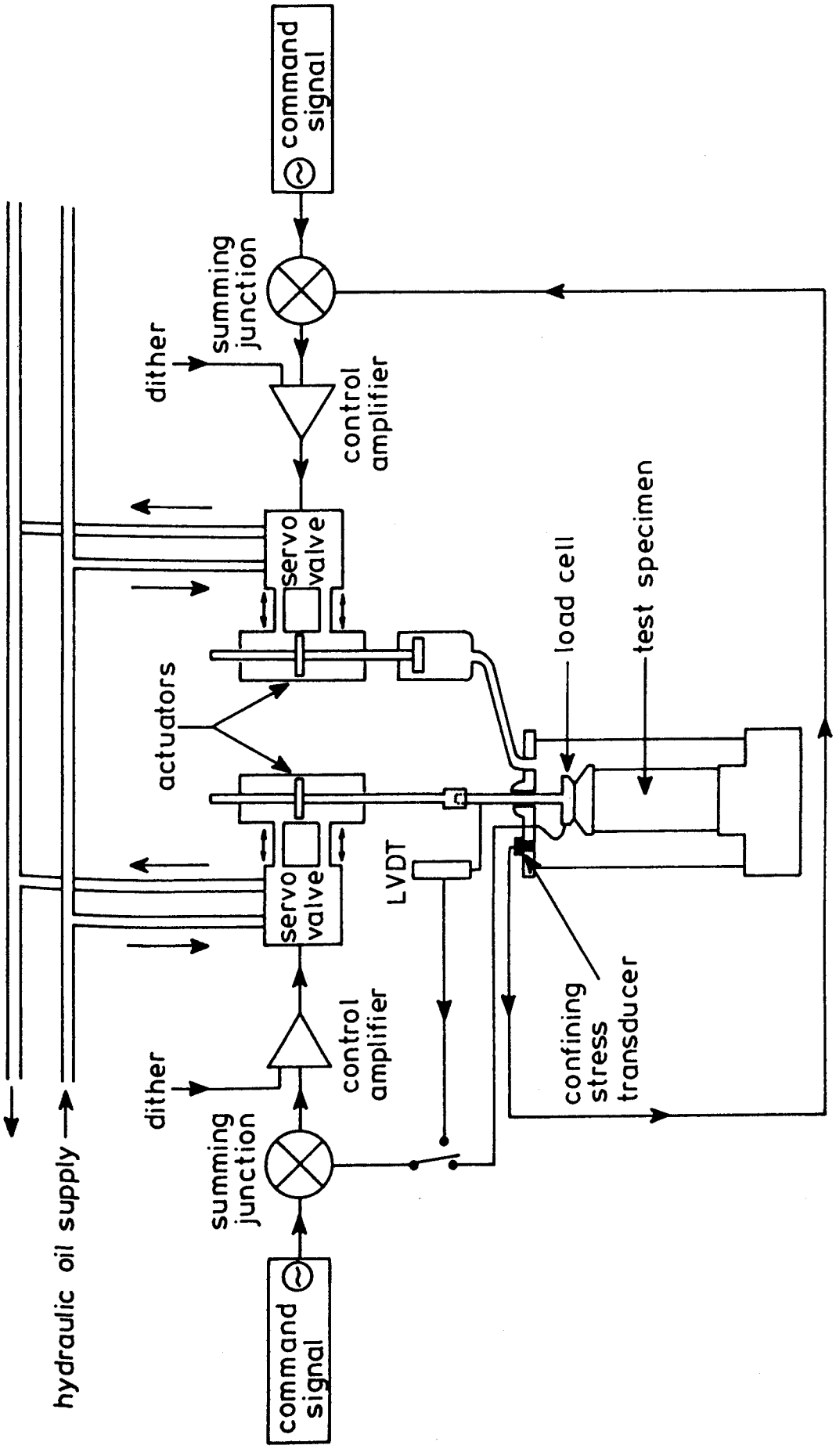

FIGURE 4.1 SERVO - HYDRAULIC CONTROL

caused by friction in the cell bearing. The load cell provided the feedback signal required for the control system. There was an option of position control instead of load control which used a large linear variable differential transformer (LVDT) connected to the load ram to provide the feedback signal.

The confining fluid used in the triaxial cells was silicone oil (Dow Corning 200/20 cs) and pressure was applied by connecting the hydraulic actuator to a piston which acted on the silicone oil. The feedback transducer was a strain gauged diaphragm pressure transducer located in the cell top.

The triaxial cells were designed by Austin (1979) and consisted of an epoxy resin base, perspex side walls and an aluminium cell top. The specimen size was 150mm high by 78mm in diameter. The samples were encased in latex rubber membranes. The bases were made of resin to eliminate any bi-metallic corrosion caused by different metals on contact under water, which was the original cell fluid. Pore pressure was measured at the base of the sample through a porous stone secured to the cell base, with a tapping connecting to a pressure transducer which was screwed into the base.

Overy (1982) modified the triaxial cells to allow additional instrumentation to be added to the sample. The top platen and cell base were modified to allow the pore pressure to be measured in the centre of the sample using a miniature pore pressure transducer which had been consolidated into position in the slurry moulds. Overy (1982) added a metal support system to the cell base which carried four linear variable differential transformers (LVDTs) and two proximity transducers (PTs). The instrument layout is shown on Figure 4.2 and provided a measure of the axial deformation over the centre third of the sample and the radial deformation across a diameter.

Back pressure could be applied to the samples from an air pressure regulator via an air water interface. Volume change of the sample could be measured using either a 100ml or a 5ml burette

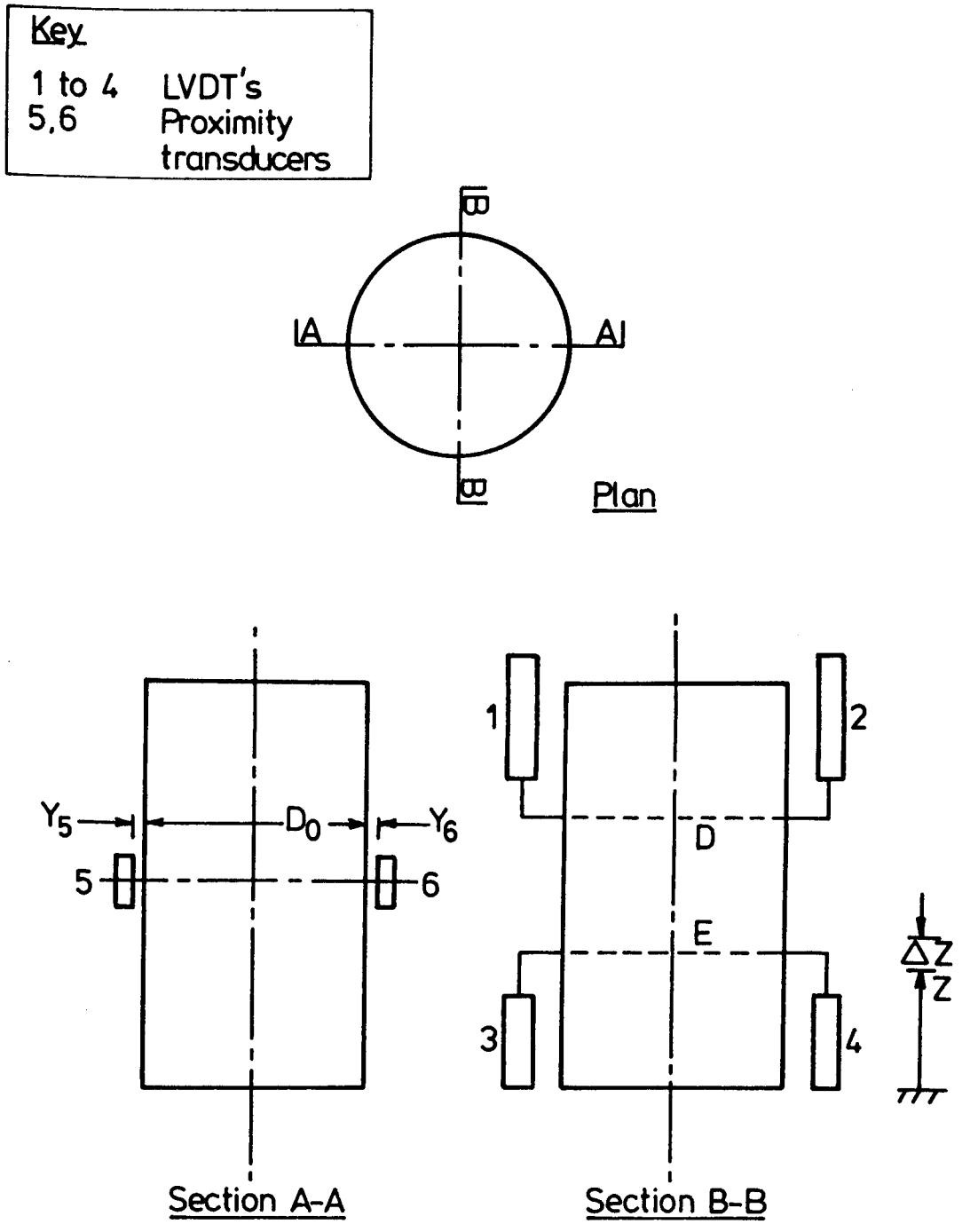

$$\text{Radial strain} = \frac{\Delta Y_5 + \Delta Y_6}{D_0}$$

$$\text{Axial strain} = \frac{\frac{\Delta Z_1 + \Delta Z_2}{2} - \frac{\Delta Z_3 + \Delta Z_4}{2}}{Z_D - Z_E}$$

FIGURE 4.2 TRIAXIAL APPARATUS INSTRUMENTATION

plumbed into the back pressure system. There were two complete cells with the full instrumentation.

Overy (1982) incorporated a bellofram piston unit into the cell tops which could be clamped to the load ram and was used to apply a deviator stress to the samples during consolidation.

4.2.2 The consolidation equipment

Overy (1982) developed a system to allow anisotropic consolidation of the samples in the triaxial cell. A schematic layout of the system is shown in Figure 4.3. The system consisted of a servo control unit which detected a change in the sample diameter measured using the proximity transducers and adjusted the deviator stress to correct the change by adjusting the air pressure in the bellofram unit connected to the load ram. The air pressure was adjusted by a motor driven air regulator. The system was used in conjunction with another motor driven air regulator which was connected to the cell pressure system and was used to increase the cell pressure at a constant rate during the consolidation phase.

The equipment was arranged to allow control over one cell only and only allowed consolidation without extensive rearrangement of the drive system.

4.3 MODIFICATIONS TO THE TRIAXIAL TEST FACILITY

4.3.1 Modifications to the control system and loading frame

Plate 4.1 shows loading frame, control unit and signal conditioning equipment used in this project. A Wykeham Farrance constant strain rate machine was incorporated in the loading frame to allow undrained strain controlled strength tests to be carried out on samples after cyclic loading without relieving the stress on the sample by disconnecting the hydraulic loading systems. The triaxial cells were fitted with castors and an oil proof preparation area which connected directly to the load frame

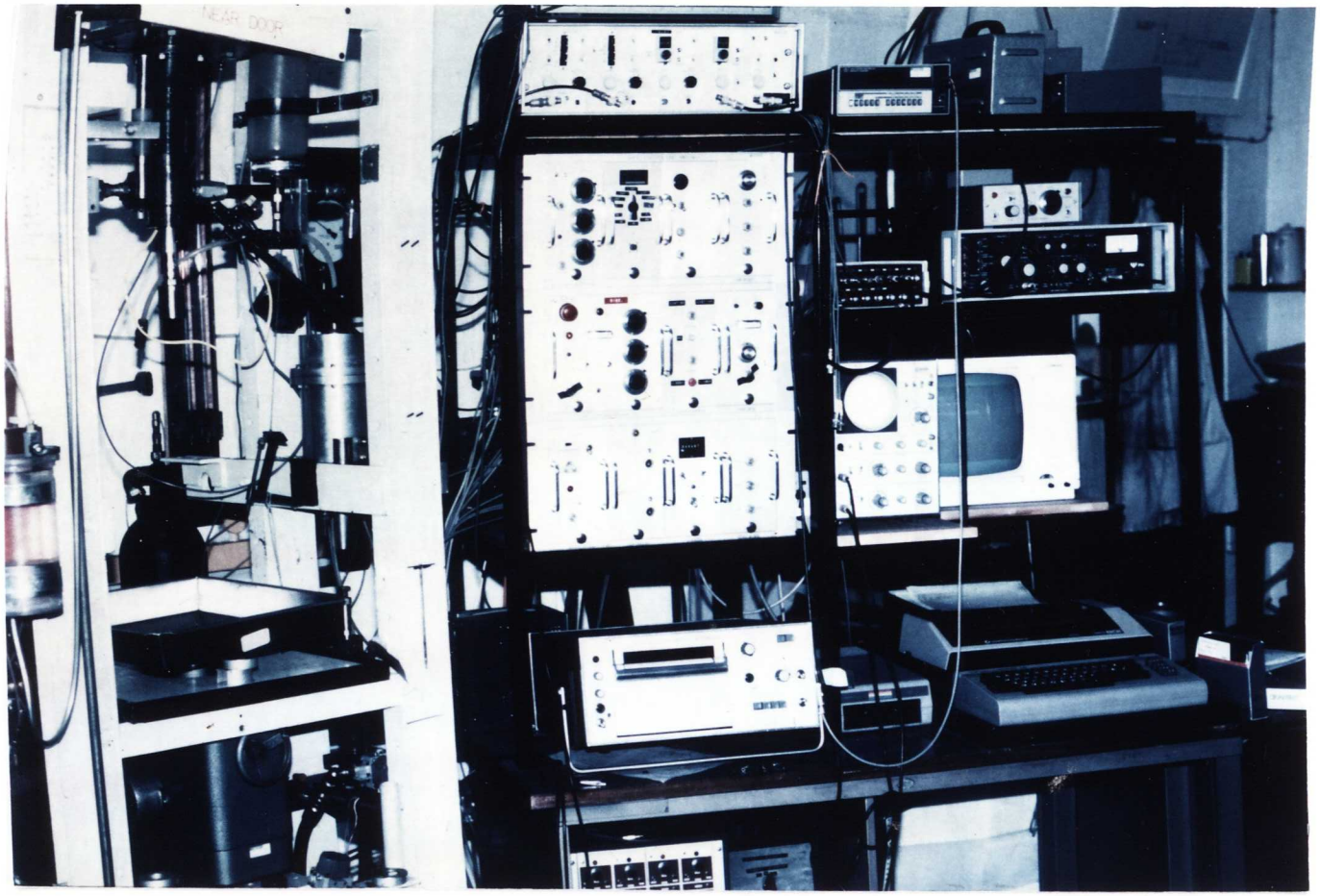

PLATE 4.1 GENERAL VIEW OF THE LOADING FRAME AND CONTROL SYSTEM

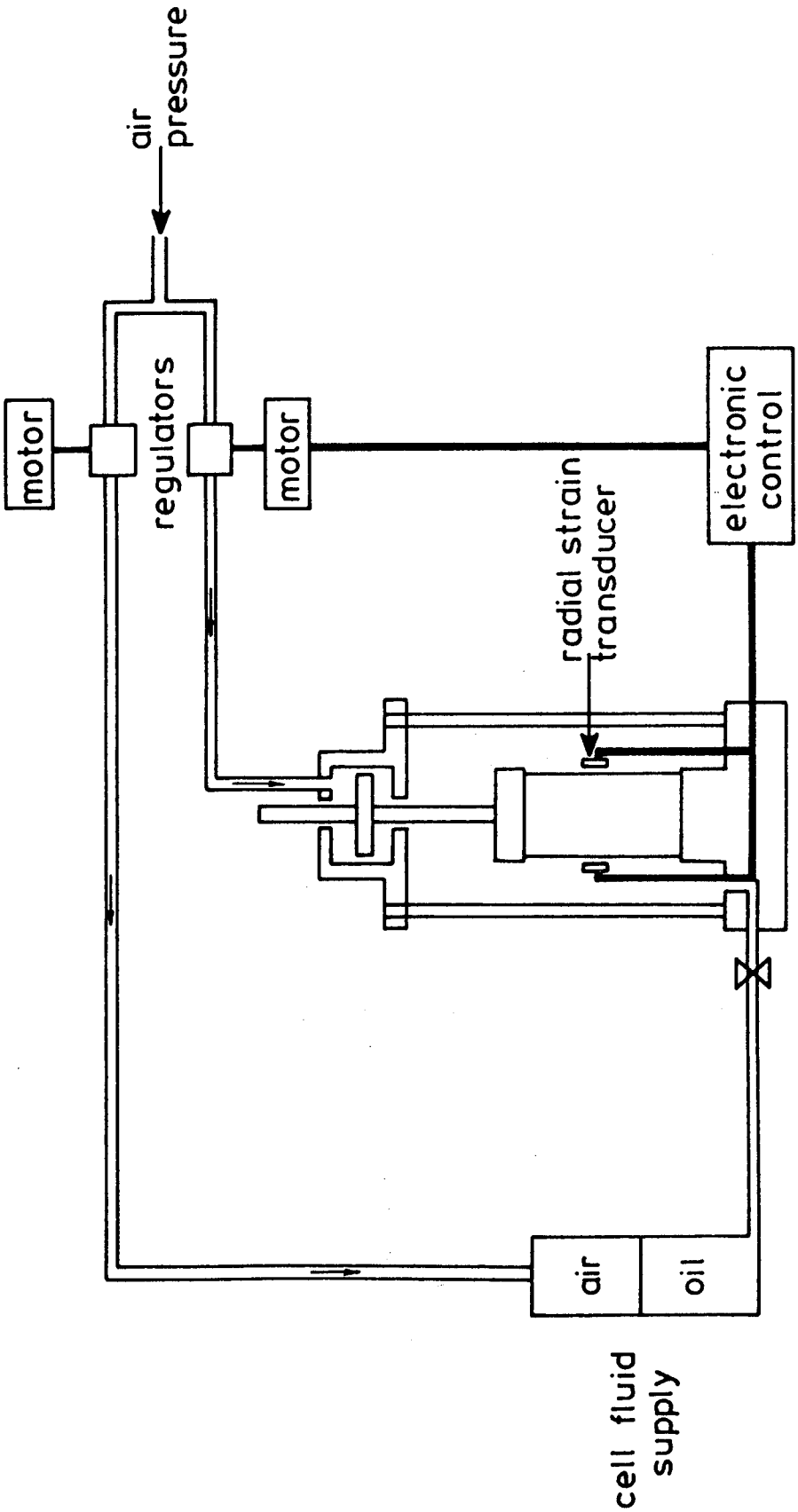

FIGURE 4.3 ANISOTROPIC CONSOLIDATION CONTROL SYSTEM

was constructed. This eliminated the need to carry the triaxial cells and limited sample disturbance.

As the equipment was going to be used for long term tests a cut out switch was fitted which limited the travel of the ram into the cell and therefore prevented damage to the instrumentation in the event of the sample failing. A safety cut out switch was not required for the cell pressure system as the travel of the piston unit exceeded that of the hydraulic actuator.

The original piston unit on the cell pressure system was sealed by O rings and was rigidly attached to the hydraulic actuator. A combination of friction and binding caused by these two factors prevented low magnitude (± 5 KPa) and low frequency (± 0.05 Hz) stress pulses from being applied to the sample. A new piston unit was constructed which incorporated a bellofram seal and which was not rigidly attached to the hydraulic actuator, but relied on the cell pressure for the return stroke. This system was found to work well.

The control system was found to be very susceptible to interference which was caused mainly by the air conditioning system in the laboratory switching on and off. Rewiring the earth system of the control unit and installing supressors on the air conditioning system unit removed some but not all of the interference.

4.3.2 **Modifications to the consolidation control unit**

The consolidation phase of the test programme required fairly heavily anisotropically overconsolidated samples to be produced. This was time consuming and required independent control of each triaxial cell to eliminate any time delays in the sample preparation procedure.

The control system was rebuilt with new motors to allow three completely independent consolidation control systems. Plate 4.2 shows the layout of the consolidation system and two samples

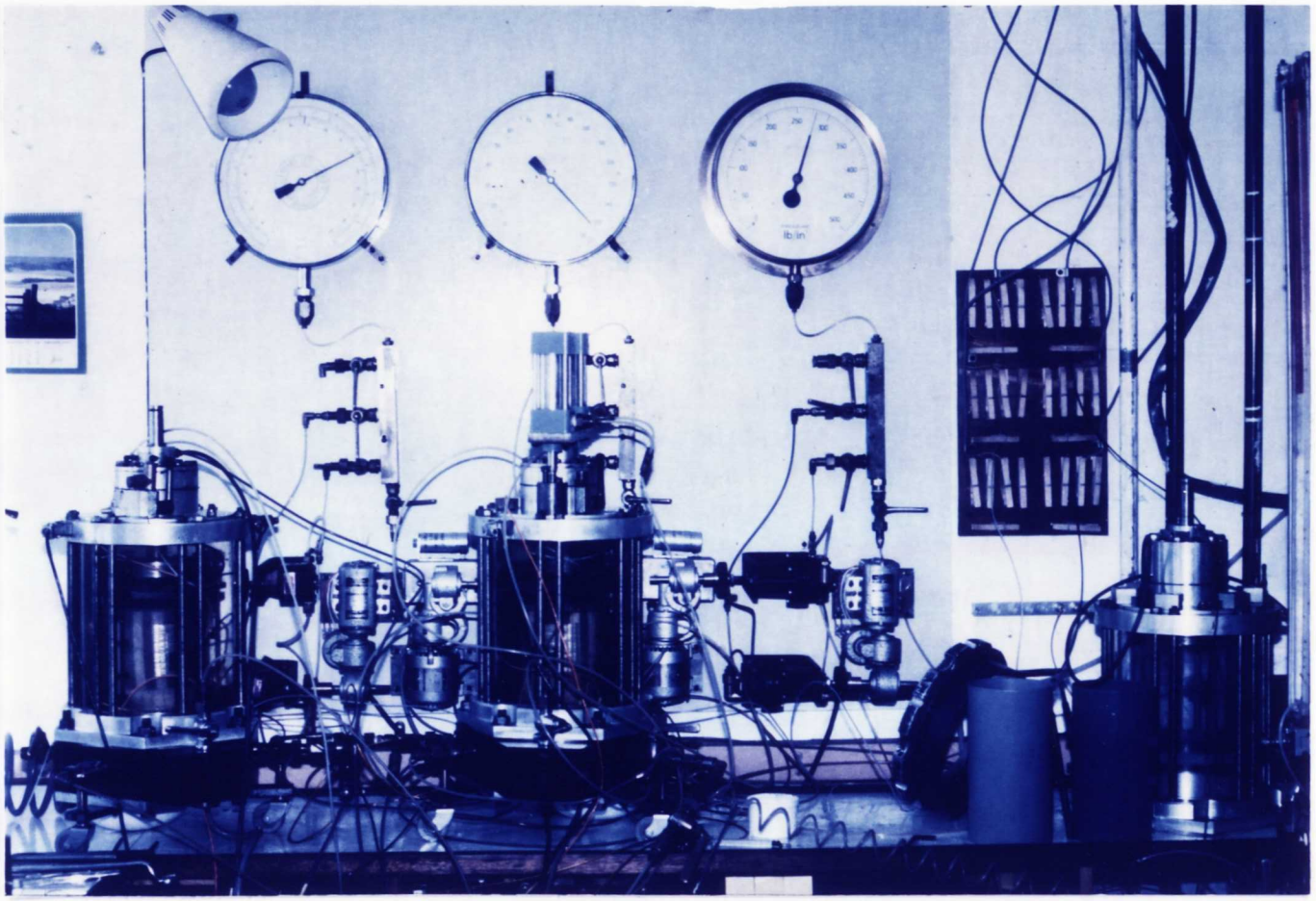

PLATE 4·2 THE CONSOLIDATION EQUIPMENT

consolidating. A high pressure air line (2.5MPa) was installed in the laboratory to supply one of the consolidation systems. This allowed the high consolidation pressures required to be achieved. The anisotropic consolidation control box had to be extensively rewired to eliminate crosstalk between the channels, and to provide additional power to supply the extra motors controlling the regulators.

The clamping arrangement between the bellofram piston on the cell top and the load ram was improved to cater for the higher pressure required from the standard airline by changing from clamp type A to clamp type B, as shown in Figure 4.4. To cater for the high pressure airline another bellofram piston unit was built which acted directly on the load ram, rather than through a clamp, as shown in Figure 4.5. To produce anisotropically overconsolidated samples requires negative deviator stresses as K_o exceeds 1.0. Some uplift was supplied to the load ram by the cell pressure acting on the lower bellofram in the case of the low pressure cells, and this was supplemented by small additional air cylinders which were clamped to the load ram. These acted against the cell top. A special bellofram piston unit was incorporated in the high pressure cell to provide the required negative deviator stresses. All the triaxial cells were equipped with a vacuum connection between the load ram and the top platen. This was installed by Overy (1982) although the system was first developed by Boyce (1976).

4.3.3 Modifications to the measuring and recording systems

The Transport and Road Research Laboratory generously provided sufficient funds to fully instrument a third cell. Identical instrumentation was chosen to ensure compatibility with the existing triaxial cells.

4.3.3.1 Axial load

The existing load rams, which were designed by Austin (1979), were found to be unsuitable for the relatively high loads

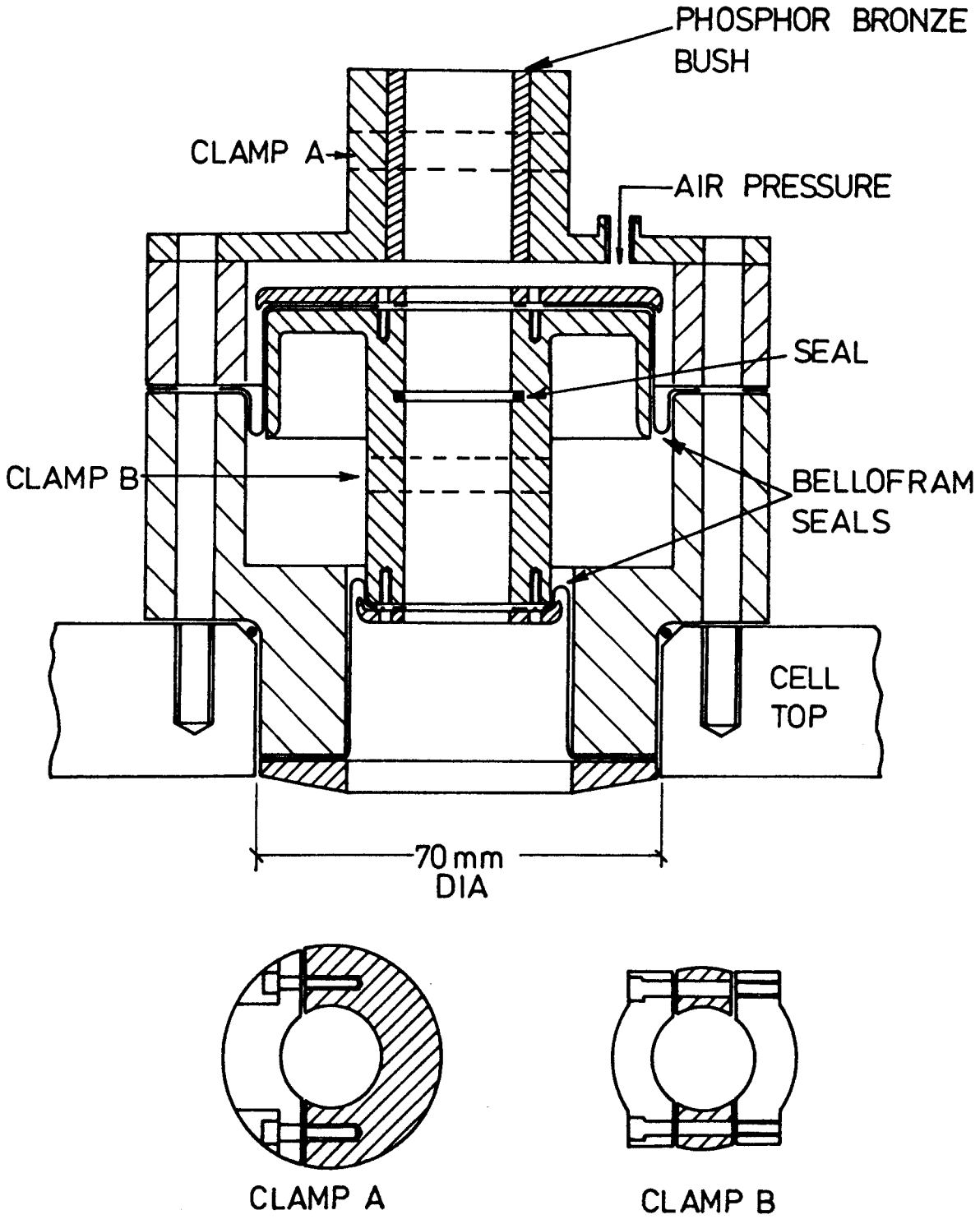

FIGURE 4.4 ANISOTROPIC CONSOLIDATION CELL TOP

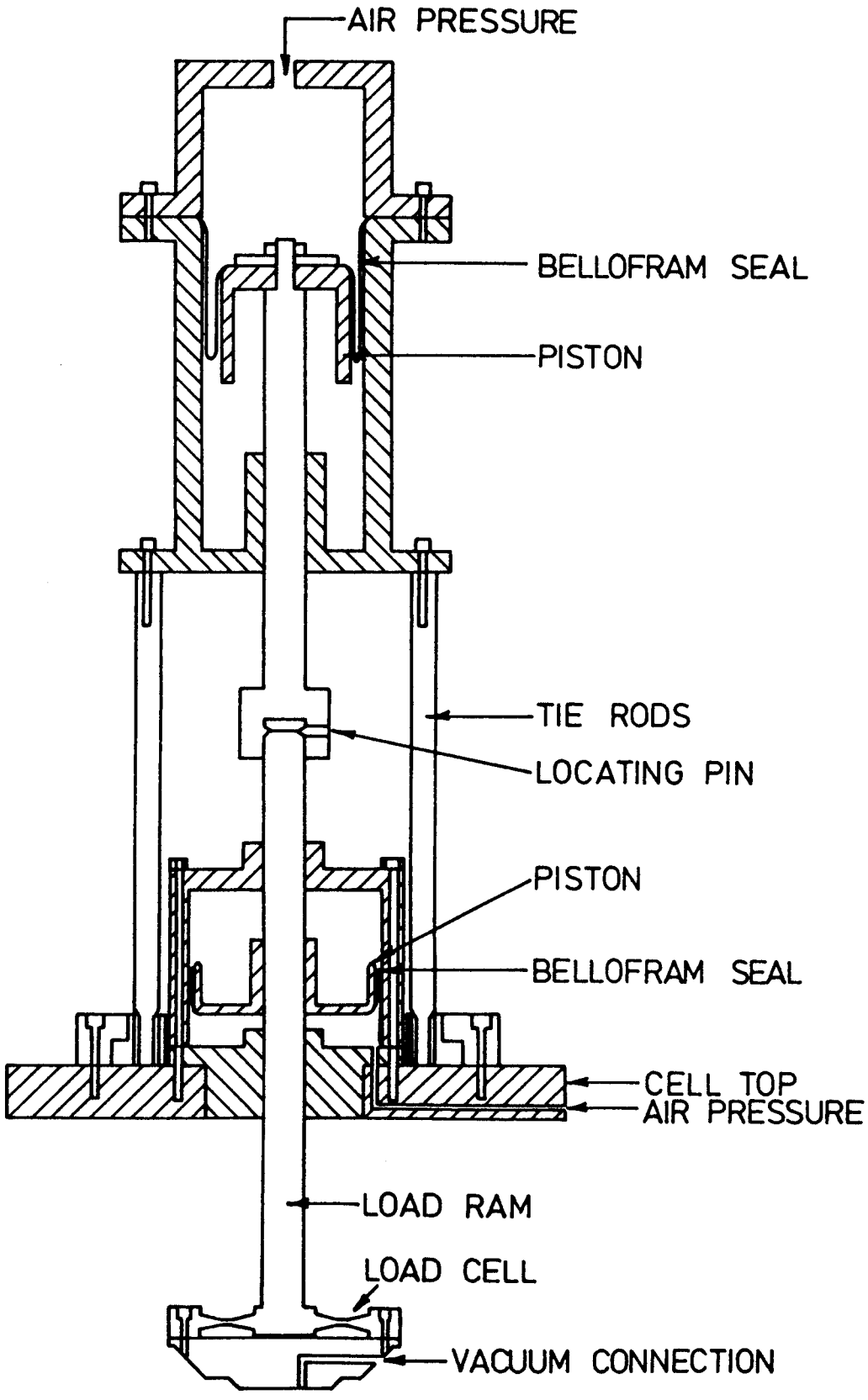

FIGURE 4.5 BELLOFRAM LOAD UNIT FOR ANISOTROPIC CONSOLIDATION AT HIGH CELL PRESSURES

required during consolidation. It is thought that this was due to their age and past overstressing. The Transport and Road Research Laboratory generously provided additional funds and three small commercial tension/compression load cells were purchased and installed in the triaxial cells. These were found to suffer from zero drift in the long term and were replaced by load cells designed in the Civil Engineering Department at Nottingham. These were disc load cells and consisted of a loaded web, which was shaped to give an approximately linear strain profile with radius. This allowed load cells with similar outputs to be constructed. They were found to work very well.

4.3.3.2 Pressure transducers

The cell pressure, base pore pressure and centre pore pressure transducers were from a range of strain gauged silicone transducers made by Druck Ltd and worked well. The transducer lead for the centre pore pressure transducers had to be sealed as it passed through the top platen and the cell base and consequently could not be fitted with a proper electrical connection. It was found that clothes pegs with metal faced jaws provided a good electrical connection with the bared transducer leads.

4.3.3.3 Deformation transducers

The arrangement of LVDTs and PTs was found to work satisfactorily and could only be improved upon by adding additional instrumentation measuring across diameters at right angles to the original instrumentation. This would be very expensive and the improvement was thought not to be large enough to justify the additional cost.

4.3.3.4 Volume change

The original system used by Overy (1982) consisted of four separate back pressure/drainage lines, two with 100ml capacity burettes and two with 5ml capacity burettes. The back pressure

was applied to the sample using air pressure, controlled by an air regulator, acting on an air water interface. The direction of flow through the burettes could be reversed by operating two valves simultaneously. The 100ml burette was used during consolidation while the 5ml burette was found to be sufficient for drainage periods during cyclic load testing. However to change burettes required changing back pressure lines.

The system was rebuilt and incorporated both 100ml and 5ml burettes in the same back pressure line either of which could be selected by a valve. The direction of flow could be reversed by using a single four way ball valve which proved much more satisfactory than the original system. The original system using air pressure was retained for two of the cells but a system using mercury in two pots, one fixed and one adjustable, was provided for the third cell. The aim was to be able to apply negative back pressures or suctions to the samples but the time scale of the test programme did not allow any experiments with negative back pressures to be carried out.

4.3.3.5 **Data Processing Equipment**

The outputs from all the transducers were taken through a signal conditioning unit with variable gain amplifiers as described by Overy (1982). The outputs were recorded on ultra violet sensitive paper by an oscillograph. Each circuit could be monitored by a voltmeter or oscilloscope for instantaneous readings. A further summing unit was provided which accepted outputs for all the transducers, scaled them and output the results to an X - Y plotter. This allowed total and effective stress strain paths to be plotted.

The deformation and pore pressure measuring circuits were fitted with offset generators with outputs to the oscillograph. These circuits enabled the small cyclic component of a large input signal to be separated from the d.c. level and amplified further.

There was a lot of electrical noise on the traces and the

equipment was very susceptible to electrical interference from various other pieces of equipment in the laboratory. This was cured by rewiring the earthing system within the signal conditioning system.

The amplification of the deformation measuring transducers was increased and d.c. offset controls fitted to all the amplifiers. This allowed the maximum gain of the amplifier to be used whatever the output signal of the transducer. Appendix D gives the calibrations for all the transducers.

The original system incorporated only one bridge balance control for the load, cell and pore pressure systems, which made operating more than one cell at a time rather difficult. The system was extended to give separate bridge balance controls for each circuit for each cell. These were all switchable through the main amplifiers and allowed all three cells to be operated simultaneously.

4.3.3.6 **Digital Data Recording System**

An analogue to digital converter, computer, disk drive and printer were purchased. The A-D converter was made by CIL Microsystems Ltd and the computer system by Commodore Business Machines. A Hewlett Packard X-Y plotter was used for direct plotting of the results. The A-D converter had its own memory sufficient for 16000 readings and could be programmed to take x scans with a y millisecond time delay and store the data for retrieval later by the computer. The machine was 16 bit and accepted inputs in the range ± 10 volts giving an effective resolution of 15 bits, the 16th bit being used for the sign. Sufficient resolution from the load, cell and pore pressure transducers could be obtained using the minimum gain available from the signal conditioning unit. Therefore inputs for the A-D converter were taken before the gain switch, enabling the gains to be adjusted without affecting the computer calibrations. However the signals from the deformation transducers had to be amplified further to get sufficient resolution and involved extra

software to keep track of the permanent strain as the gains and d.c. offsets were set at the start of each test.

At present the system is limited by the time taken to retrieve, process and store the data using Commodore basic, rather than by the amount of available memory. This could be overcome by programming, at least in part, in machine code which can speed up repetitive processes by a considerable amount.

4.4 PNEUMATIC TRIAXIAL RIG

4.4.1 Existing Equipment

This rig was originally constructed by Pappin (1979) for determining the resilient modulus of aggregate samples. It consisted of a triaxial cell similar to those used in the main servo hydraulic rig with a bellofram loading piston acting on the load ram. This was supplied with air under pressure from an air regulator acting through a solenoid valve, which was switched by a motor driven cam. This provided an approximation to a square wave with a frequency of about 1Hz. The load was measured inside the triaxial cell by using a strain gauged load cell. The cell pressure was supplied directly from an air regulator and measured using a pressure gauge. Axial deformation only was measured between the end caps using a wire wound linear potentiometer.

4.4.2 Modifications to the equipment

The deformation measuring system was improved by adding two LVDTs working as a pair over a gauge length in the centre third of the sample. The signals were summed electronically, amplified and output to an ultra violet oscillograph through an offset generator. Appendix D gives the calibrations.

An attempt was made to measure the radial deformation, initially by using strain coils, then subsequently by a strain gauged araldite hoop. The strain coils were made by Bison Instruments Inc and consisted of two 2 inch diameter coils, placed one each

side of the sample across a diameter. One coil acted as the emitter and the other as the receiver. The output from the balancing box was taken directly to an ultra violet recorder. The strain hoop was a scaled down version of those developed by Boyce (1976) and consisted of a ring attached concentrically to the sample across a diameter as shown in Figure 4.6. The strain gauges were mounted 90° around from the attachment points and the output taken to the U.V. oscillograph via an amplifier and offset generator.

It was found that the solenoid operating the air valve controlling the load interfered with the offset generator signals. The load system was modified to use mechanically operated air valves running directly from a cam. Air bleeds were incorporated into the system to provide some adjustment of the shape of the waveform and the facility for supplying an ambient deviator stress and pulsing from that level was added.

4.5 SLURRY MOULD FOR CBR SAMPLES

A mould was constructed to allow overconsolidated CBR samples to be produced in a similar manner to the consolidated triaxial samples. The mould, shown in Figure 4.7, was constructed as a tube which was split into three sections. The middle section was the same height as a standard CBR mould. The pistons were faced with porous stones which allowed end drainage. The weight of the mould was counterbalanced by two weights connected to the mould by a pulley arrangement. The consolidation pressure was applied by a bellofram piston unit which was connected to the high pressure air line through an air regulator.

There was appreciable friction between the pistons and the mould which made it impossible to swell back to very low pressures in the complete mould. To avoid this the mould was dismantled after consolidation to the maximum pressure and the sample trimmed to size in the centre section. The bottom plate was attached to the centre section of the mould and the sample loaded at the swell back pressure through the top piston. The piston

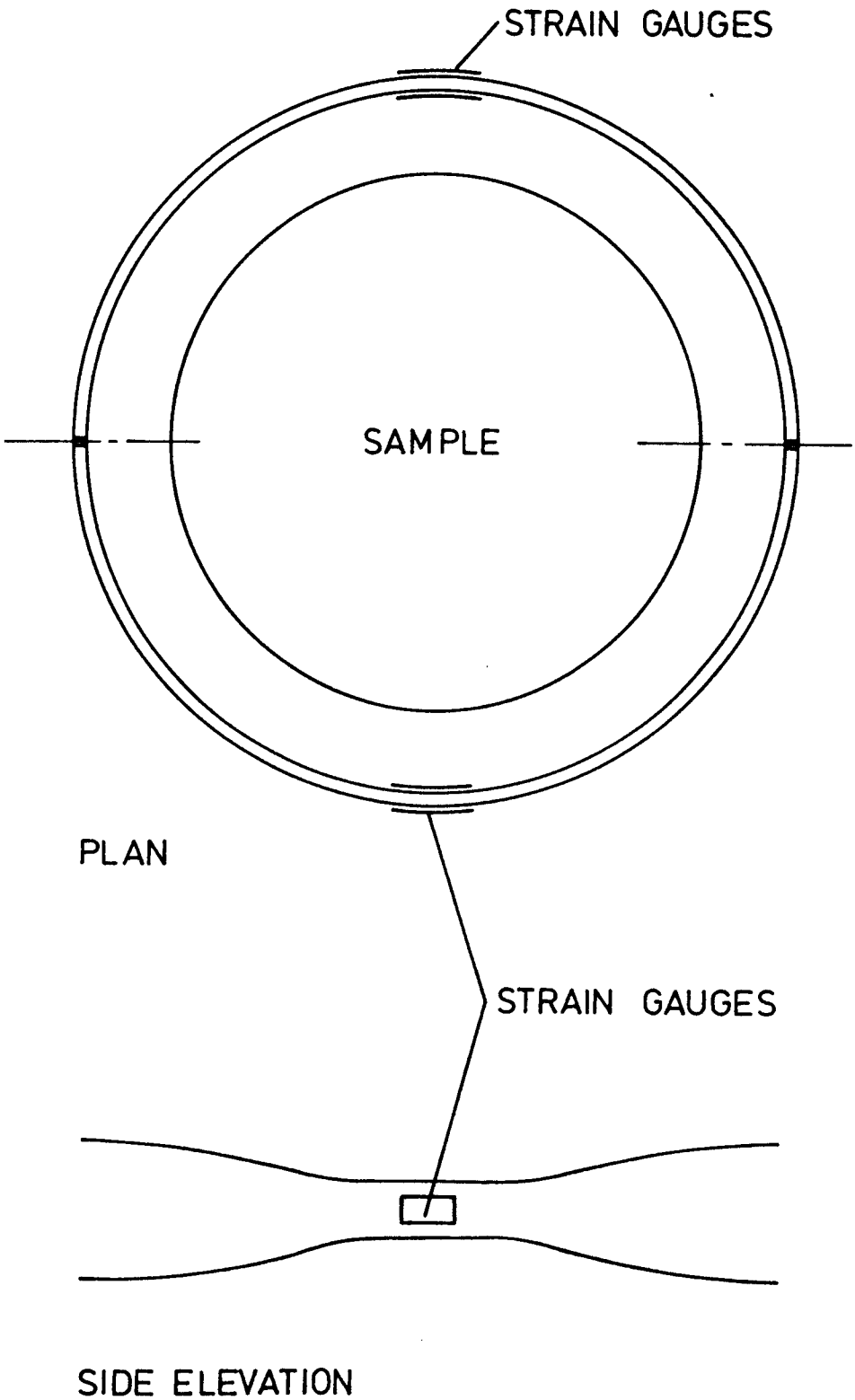

FIGURE 4.6 STRAIN HOOP FOR MEASURING RADIAL DEFORMATION OF COMPACTED SAMPLES

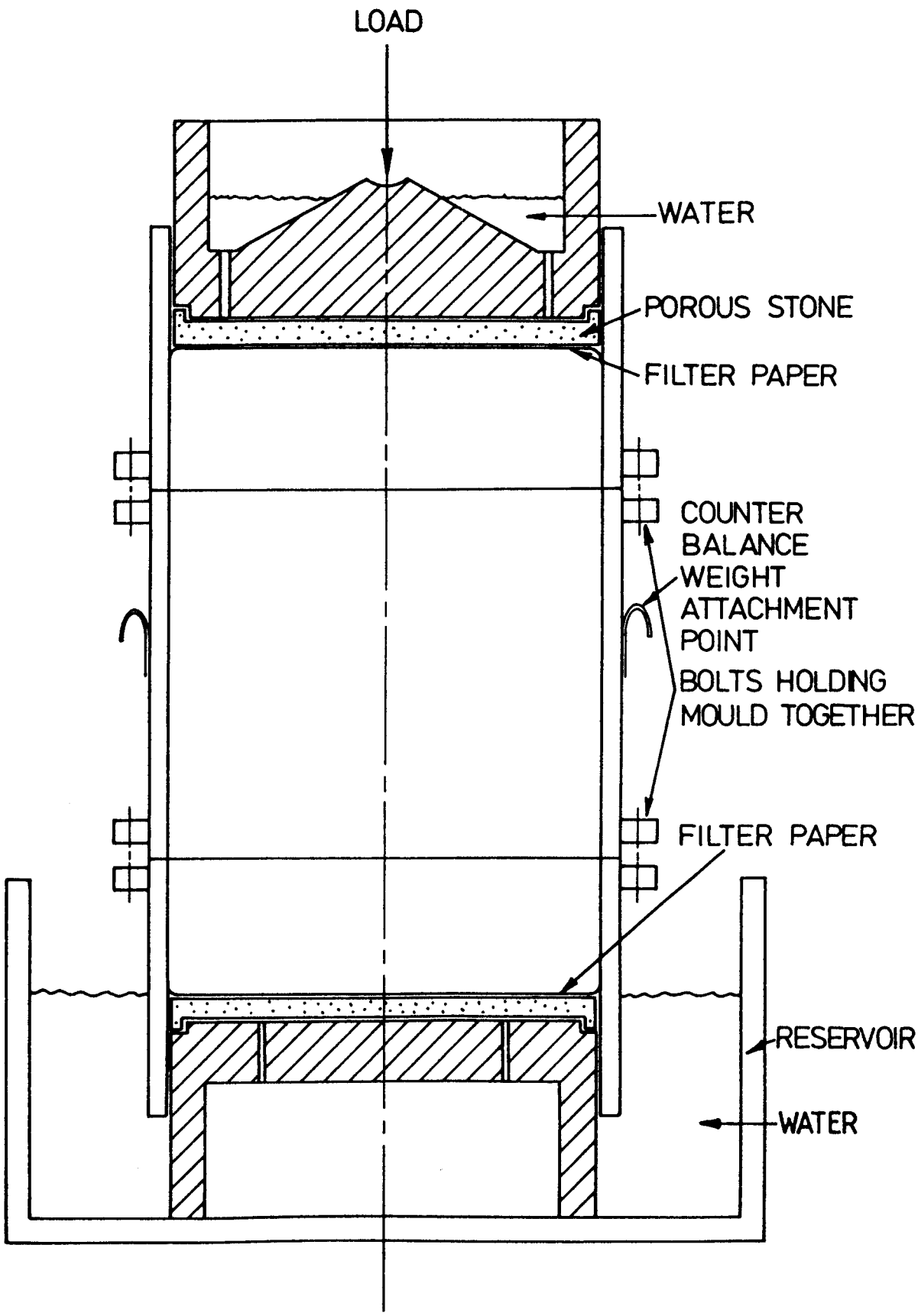

FIGURE 4.7 CBR SLURRY MOULD

was placed free on top of the sample and therefore ensured that the correct pressure was applied to the top of the sample. The sample was kept under water to ensure saturation.

4.6 SUCTION MEASURING APPARATUS

Two types of apparatus were used to measure the suctions of the samples. The first measured the suctions of the sample at its original moisture content using a piece of apparatus called the Rapid Suction Apparatus which was developed at the Transport and Road Research Laboratory and is described by Dumbleton and West (1968). Figure 4.8 shows a diagrammatic layout of the apparatus. The apparatus consists of a high air entry porous stone 12mm in diameter connected to a hand operated suction pump via a capilliary tube. The sample was placed on the stone and the pump operated until the suction was sufficient to balance that in the sample. This was indicated by no movement of the meniscus in the capillary tube. The range of the apparatus could be increased by applying an external pressure to the sample. Both pressures were measured by pressure gauges.

The second method allowed samples to reach an equilibrium moisture content under a set value of suction. The layout of the apparatus is shown on Figure 4.8 and consisted of 40mm diameter high air entry porous stones. These were saturated and a constant value of suction was applied to them from a vacuum pump via a regulator. The samples were placed on the stones and allowed to reach the equilibrium moisture content for that suction. The vacuum regulators worked on the controlled air bleed principle, and once set were found to be very stable. The porous stones tended to dry out after three or four days and then leak air, but this time scale was found to be sufficient for the Keuper Marl samples to reach equilibrium provided that they were mixed to a moisture content reasonably close to the equilibrium value for that suction.

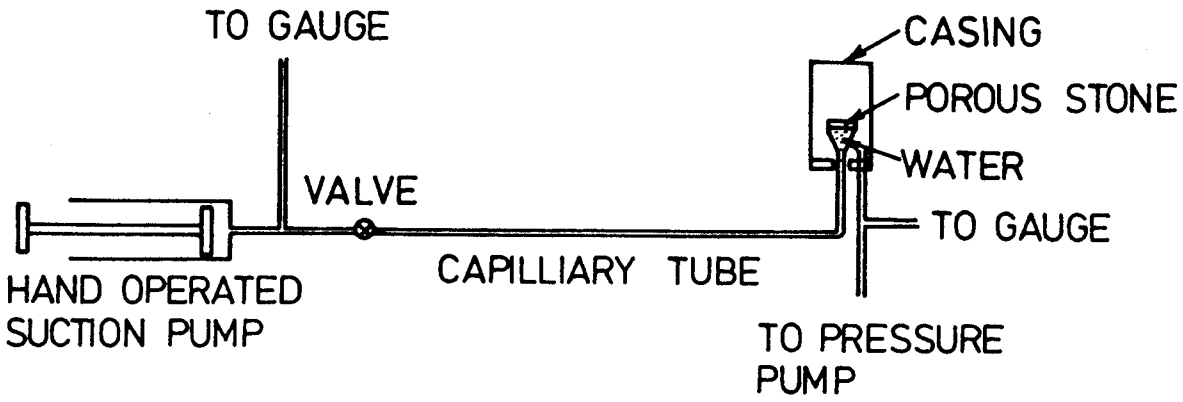

RAPID SUCTION APPARATUS

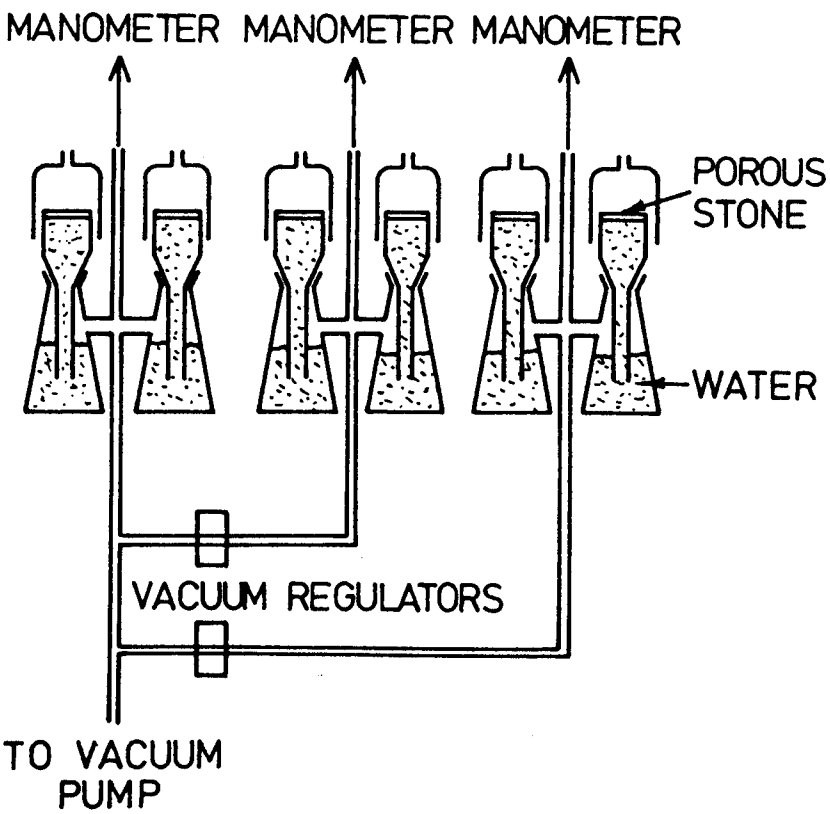

EQUILIBRIUM SUCTION APPARATUS

FIGURE 4.8 DIAGRAM OF SUCTION MEASURING EQUIPMENT

4.7 DETERMINATION OF PRE-CONSOLIDATION PRESSURE

Some undisturbed site samples were obtained and the preconsolidation pressure determined, using Rowe cells. These are described more fully by Rowe and Barden (1966). By assuming values of in situ stresses and the level of the water table an estimation of the natural overconsolidation ratio could be made. The samples were supplied in U4 tubes and had to be trimmed to fit in the Rowe cells. A cutter was manufactured which fitted over the end of the U4 tube and cut the sample as it was extruded. The tip of the cutter was positioned level with the end of the tube to try and limit sample disturbance, and the cutter body was the correct length for the Rowe cell samples.

The Rowe cell is shown in Figure 4.9 and consisted of a base with a tapping, cell walls, and a cell top with a rubber diaphragm and two further tappings. The axial load was applied to the sample by hydraulic pressure acting on the sample through the rubber diaphragm. Various drainage options and pore pressure measurement points are available using the tapping in the cell base and the second tapping in the cell top. Top and bottom drainage was used in this research to minimise the drainage path and speed up testing. No attempt was made to measure pore pressure.

The back pressure and load pressure were controlled by air regulators acting through air water interfaces. The pressures were monitored using pressure cells which consisted of a strain gauged diaphragm rigidly clamped at its edges. These were developed by Parr (1972), and were capable of resolving to 1kPa. The axial deformation was recorded by a dial gauge.

The Rowe cells were paired up to operate off one loading system to increase the rate of testing. The pressure to the diaphragm, the axial deformation and the volume change were recorded. The analysis was based on the axial effective pressure and deformation results as the volume change readings were found to be unsatisfactory.

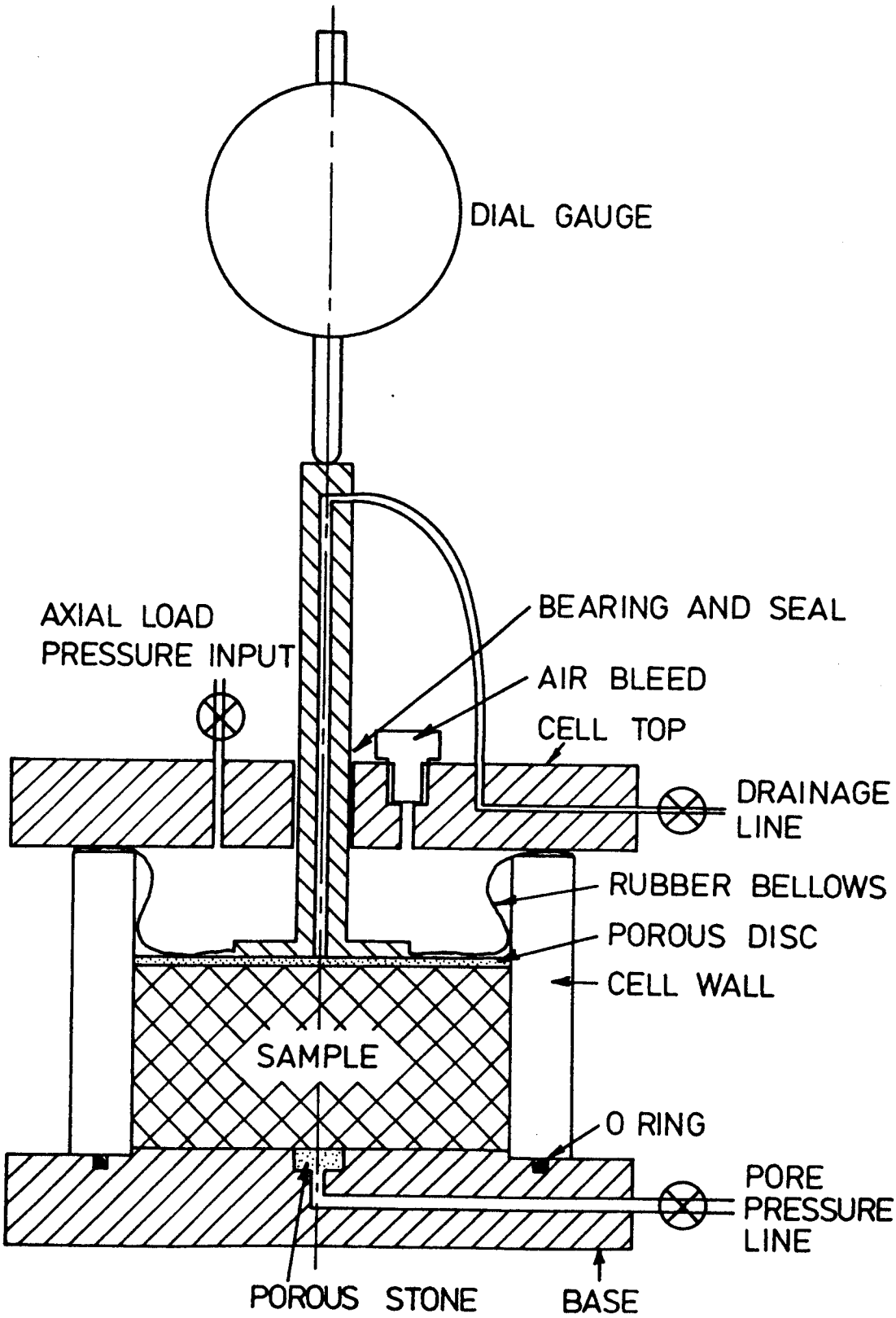

FIGURE 4.9 ROWE CELL

CHAPTER FIVE

EXPERIMENTAL PROCEDURE

5.1 THE MATERIALS

The main research programme was carried out on Keuper Marl, and some further simpler tests were performed on London clay and on Gault clay. Standard soil classification tests were carried out on all three clays and the results are presented in Appendix A.

Extensive use has been made of Keuper Marl at Nottingham in earlier research projects on repeated load triaxial testing (Lashine 1971, Hyde 1974, Austin 1979 and Overy 1982) and as the subgrade in the pavement test facility (Bell 1978, Brown et al 1980). The Keuper Marl used in this research was taken from existing stocks in the laboratory. The material was originally obtained from a local brickworks as tailings from unfired bricks. These were dried and then broken down in a mixer. The material passing through a BS 52 (150 micron) sieve was retained and used in the research programme.

The Gault and London clays were provided by the Transport and Road Research Laboratory from stocks held by them for their research projects.

5.2 CONSOLIDATED TRIAXIAL SPECIMENS

5.2.1 Initial Soil Preparation

Dry Keuper Marl was placed in the bowl of a Hobart mixer together with sufficient de-aired water to give a moisture content of about 50%. The Marl was left to slurry for at least three days with any water loss through evaporation made good by adding de-aired distilled water to maintain a constant slurry level.

5.2.2 First Stage Consolidation - Slurry Moulds

The moulds were designed by Overy (1982) to produce 78mm diameter samples and are shown in Figure 5.1. The porous stones in the pistons were de-aired under water in a vacuum vessel for at least 24 hours before use. The tips to the miniature pore pressure transducers were sintered bronze to ensure rapid response of the transducer and hence were easier to de-air. Applying a vacuum to the transducer and then releasing it under de-aired water three times just before use was found to be sufficient provided that the transducer was then kept immersed in water.

The bottom piston was placed in a container of de-aired water and the mould placed over it. The mould rested on a spacer which prevented it from completely covering the piston. The spacer was removed just prior to applying the consolidation load. The bottom piston was covered with a disc of filter paper, which, when wet, swelled sufficiently to close off the clearance gap between the piston and the tube. It also prevented the porous stone from clogging. The container and mould was placed on a vibrating table and the tube slowly filled with slurry using a long handled pot. The slurry was stirred to aid removal of any air bubbles which may have been trapped when the tube was filled.

The top cap, and filter paper, complete with pore pressure transducer, was then placed in position and the complete mould installed in the loading frame. A vertical load of 70kPa was applied and the sample left to consolidate. It was found that handleable samples could be produced in approximately 10 days.

5.2.3 Cell Base Preparation

The most important aspect of preparing the cell base was ensuring that the drainage system and base pore pressure probe were saturated. To achieve this, a metal collar was clamped to the cell base, see Figure 5.2, and carefully filled with de-aired water. The tappings were flushed through with a hypodermic syringe, which was found to be very effective at removing bubbles

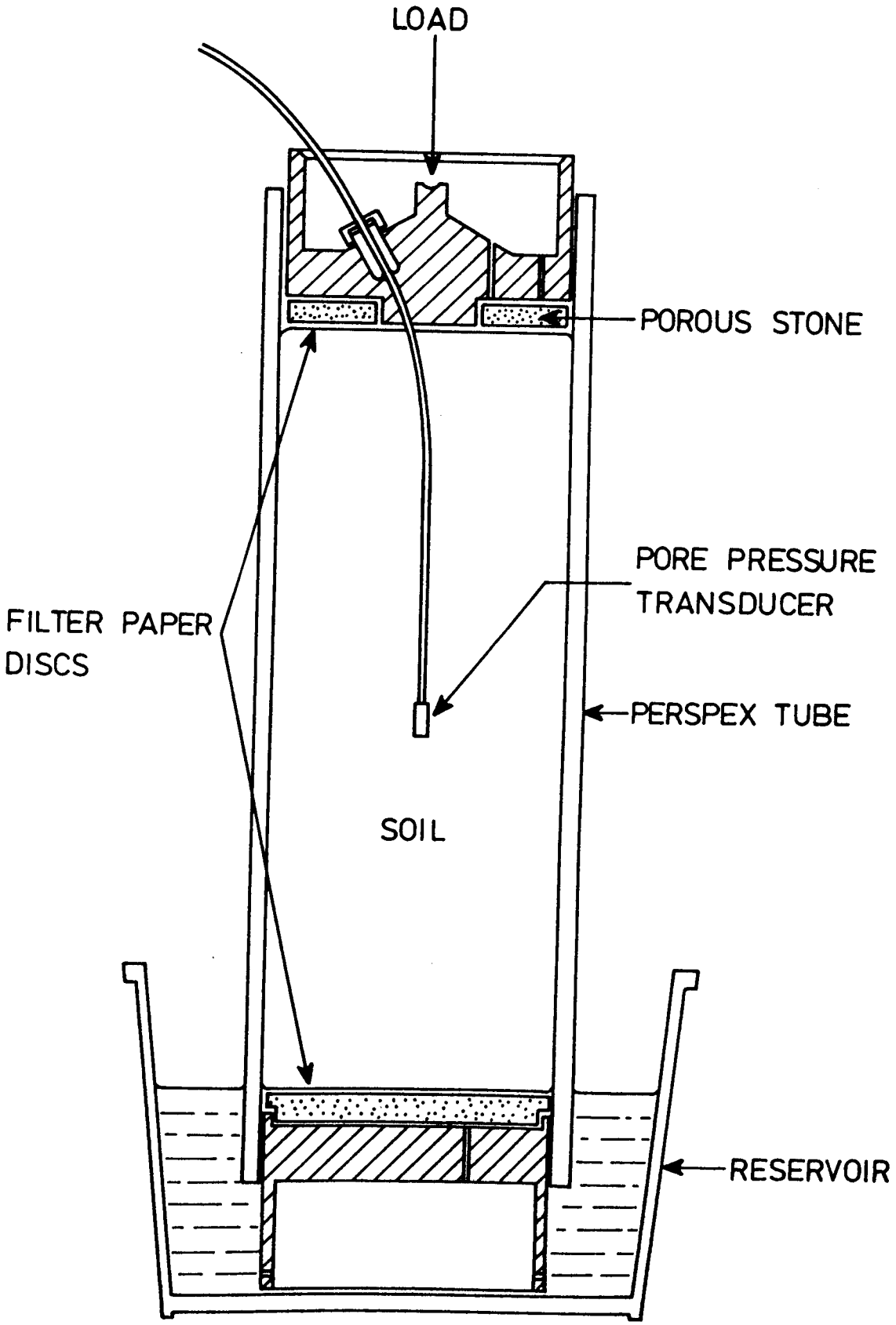

FIGURE 5.1 SLURRY CONSOLIDATION MOULD

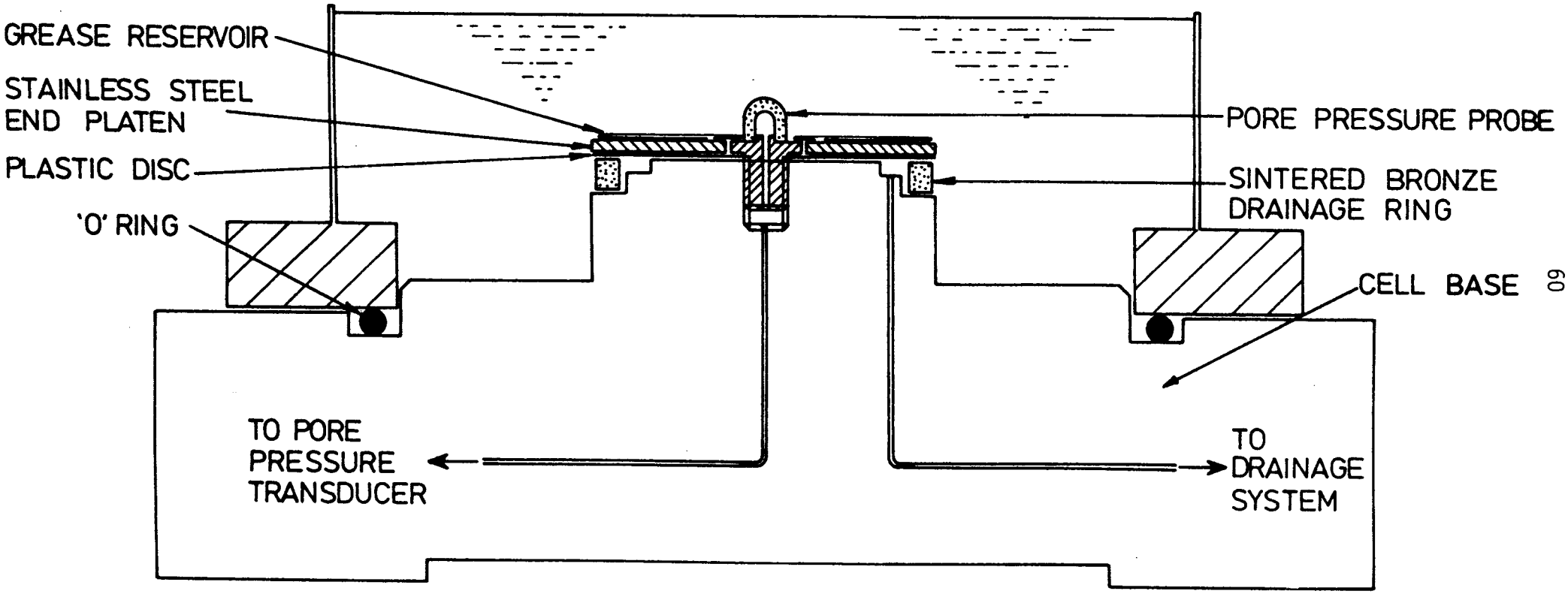

FIGURE 5.2 DETAIL OF CELL BASE

adhering to the base.

The drainage ring and porous stone had been de-aired by boiling in distilled water for some time and then storing under distilled water in a vacuum vessel for at least 24 hours. The drainage ring was placed in position in the cell base and then covered by a thin disc of PTFE sheet. The porous stone was then screwed into place clamping the plastic in position. The PTFE sheet separated the sintered bronze drainage ring from the stainless steel bottom platen and prevented any possibility of bimetallic action.

The top and bottom platens were prepared by first greasing the stainless steel surfaces with high vacuum silicone grease. They were then covered by a disc of polythene sheet. This was cut in a series of concentric overlapping arcs which would allow radial expansion of the sample to take place. A further layer of grease was applied and then finally covered with an offcut of latex membrane. The sides of the pedestal were greased to ensure a good seal with the membrane, and then the bottom platen was placed in position.

5.2.4 **Sample Installation**

The consolidation load was removed from the sample and the sample extruded from the slurry mould. The sample was trimmed to 150mm length, weighed and placed on the pedestal. The trimmings were used for moisture content determinations. The samples were very soft and could only be handled using two 120° longitudinal sections of tube of the same diameter as the sample which acted as load spreaders.

A piece of latex rubber membrane, 25mm long, was positioned at the base of the sample such that it just covered the bottom platen. This was to ensure that there was no possibility of any grease from the bottom platen contaminating the filter paper drains, and to improve the response of the base pore pressure probe during consolidation by removing any possibility of a

drainage path forming between the sample and the bottom platen.

The studs which provided the attachment points for the LVDT cores were then carefully embedded in the sample using a jig. This positioned the bottom studs 50mm up from the base of the sample and positioned the top studs to give a gauge length of 50mm over the centre section of the sample. The studs were designed by Overy (1982) and are shown in Figure 5.3.

The radial drainage system was then fitted. This consisted of two sets of filter paper drains cut to form a solid band around the base of the sample with eight vertical fingers of paper along the length of the sample. Sandwiched between the two sets of filter paper were individual wicks, eight in all, consisting of lengths of unravelled string. The radial drains were cut in the form of fingers to allow clearance for the instrumentation mounting points and to eliminate any restriction to radial deformation of the sample. A rubber band was used to secure the bottom end of the filter paper to the drainage ring and, once the paper was wet, it was found to stick to the sample and required no additional support.

The targets for the proximity transducers were cut from aluminium foil and placed up against the sample across a diameter 90° around from the LVDT studs. It was found that they also adhered well to the sample and remained in place while the membrane was positioned.

The membrane, supported by a membrane stretcher, was placed over the sample and the bottom O-ring rolled off. The top cap was then threaded over the pore pressure lead and placed in position. The membrane was then finally rolled off the stretcher and sealed at the top and bottom by three additional O-rings, after ensuring that there were no air bubbles trapped by the top cap. The transducer lead exit from the top cap was sealed using two small O-rings, one inside the other, and clamped up tightly with a metal collar.

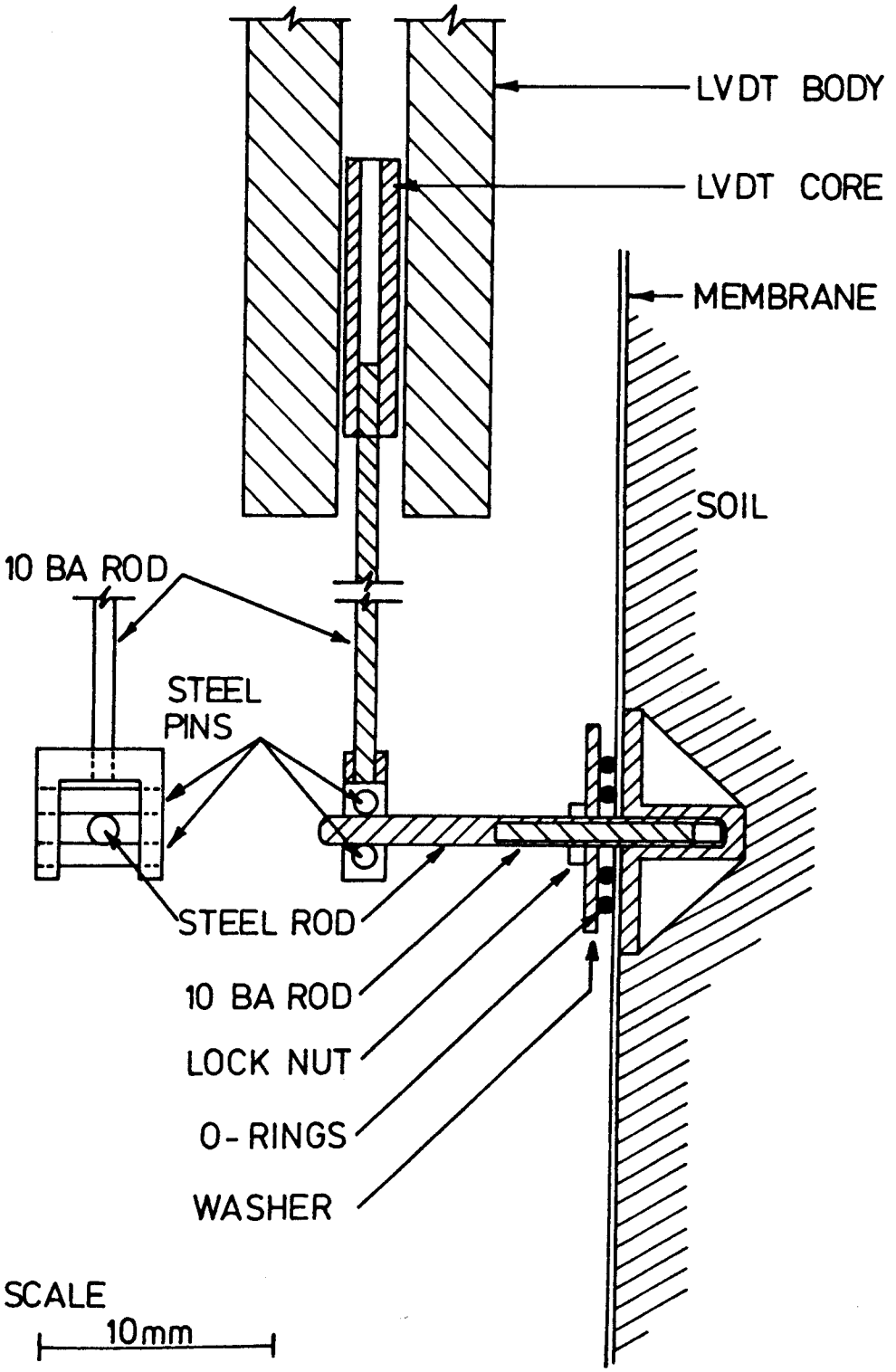

FIGURE 5.3 LOCATION STUD FOR LVDTS

At this stage the metal collar on the cell base was removed, and the cell base and specimen wiped clear of excess water.

5.2.5 Installing the Instrumentation

The instrumentation was supported by a metal framework which had been developed by Overy (1982). The framework was placed in position and bolted to the cell base. The membrane was carefully punctured over the LVDT mounting studs using a soldering iron and the supports for the LVDT cores screwed in. The holes in the membrane were sealed using two small O rings, see Figure 5.3. The proximity transducers were placed in position. Plate 5.1 shows the sample complete with the instrumentation just prior to fitting the cell top. The cell top, complete with load ram, was then fitted and filled with silicone oil. The back pressure line was attached and the sample was allowed to consolidate overnight under approximately the same pressures as in the slurry mould. This allowed the sample to reconsolidate and expel any excess water trapped behind the membrane before the LVDTs and PTs were zeroed.

The sample was then checked for saturation by increasing the cell pressure and monitoring the change in pore pressure with the sample drainage off. Generally the pore pressure increments equalled the cell pressure increment giving the B value of 1. If this was not the case the back pressure was increased and the sample left to stand for twenty four hours before rechecking the saturation. Any sample with a B value of less than 0.97 was rejected.

The cell was then drained of oil and the cell top removed. The instrumentation was then set up accurately. The LVDTs were set at the end of their range to allow for the movement of the sample during consolidation and the proximity transducers were set near the outermost limit of their range to allow for sample expansion during testing. The cell top was then replaced and refilled with oil and pressurised to the original pressure.

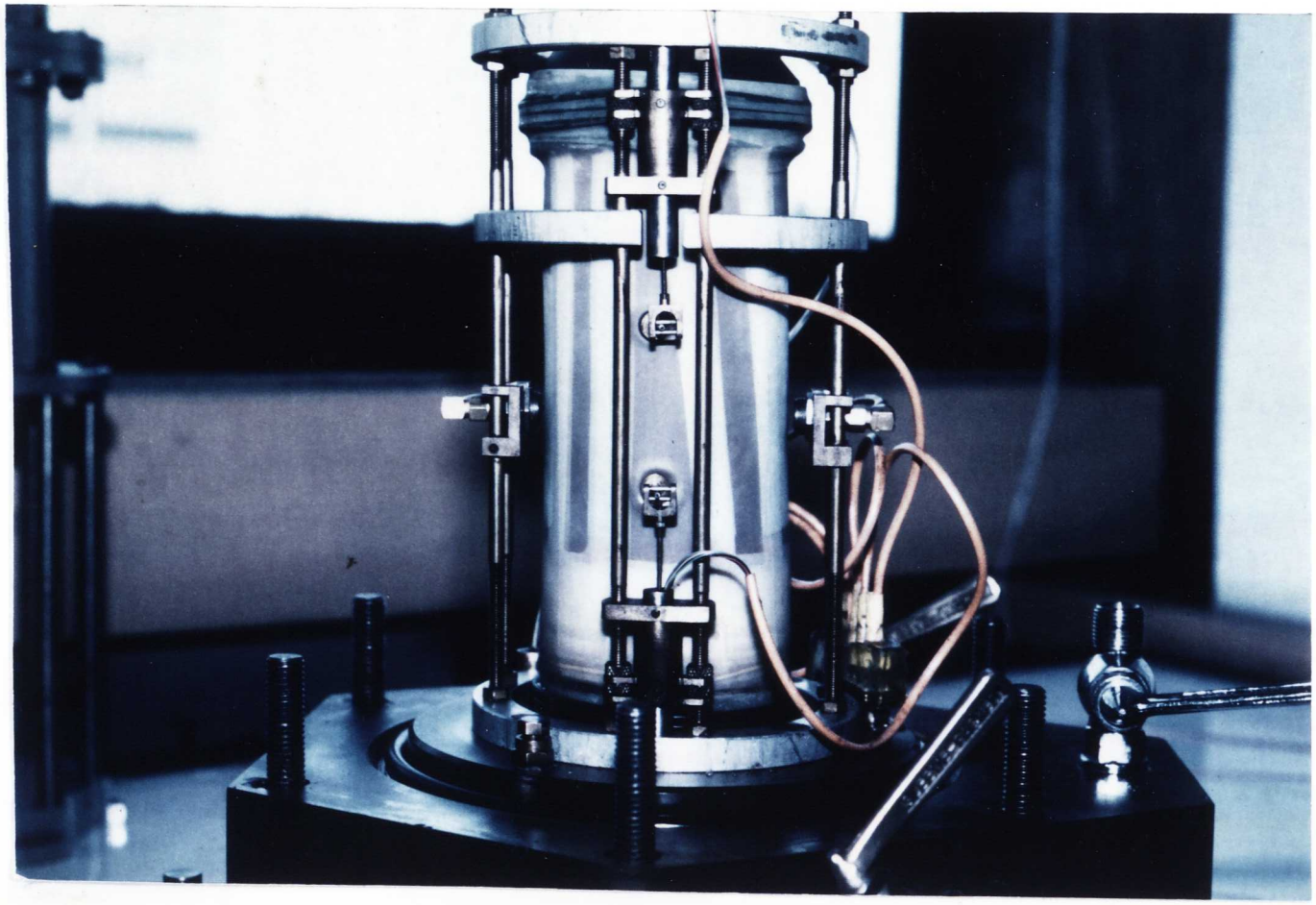

PLATE 5.1 SAMPLE COMPLETE WITH INSTRUMENTATION PRIOR TO FITTING THE CELL TOP

5.2.6 Consolidation Procedure

The servo unit controlling the anisotropic consolidation was set at the null position and the system switched on. The motor controlling the cell pressure was switched on and the sample allowed to consolidate. A minimum of two readings a day were taken from all transducers during the consolidation phase.

The sample was allowed to remain under the maximum cell pressure and deviator stress until the pore pressure had stabilised and no further drainage took place. This usually took about four days after which the cell motor was reversed and the sample allowed to swell back. When the sample reached the required final mean normal effective stress it was left to reach equilibrium before testing. This again took four to five days.

5.2.7 Test Procedure

Before the hydraulic actuators were connected to the sample the drainage taps were closed and the signal conditioning amplifiers were set at the required level. The cell pressure was connected to the hydraulic loading system first, and then the load ram was carefully connected to the hydraulic actuator. With care the sample could be transferred to hydraulic control with a maximum change in the deviator stress or cell pressure of approximately ±2kPa.

Following a period of cyclic load testing the sample was returned to pneumatic loading at the pressures achieved at the end of consolidation by carefully disconnecting the hydraulic actuators.

The results from the overconsolidated triaxial samples are presented in Chapter 6.

5.3 CONSOLIDATED CBR SAMPLES

The mould for these samples was a much larger version of the mould for the triaxial samples described in section 5.2.2 and was

prepared in the same manner. The mould was placed on the vibrating table, with the bottom piston under water in a container, and filled with slurry. The spacers supporting the mould above the container base could not be removed until the sample was installed in the loading frame and mould counter balance weights attached. This prevented the mould from falling under its own weight and allowed the consolidation load to be applied directly to the sample through the bottom piston as well as the top piston.

The sample was left for approximately three weeks to consolidate under the maximum load. The sample was then removed from the loading frame and the mould split into the three sections. The sample was cut with a cheese wire. The bottom plate was clamped in place to the centre section forming the CBR sized mould which was then returned to the loading frame. The final load was applied to the sample through the top piston. The sample was kept under water by a rubber sheath sealing the gap between the piston and the mould walls as shown in Figure 5.4. The sample was left for two to three weeks to swell back before testing.

When equilibrium was judged to have been attained the sample was removed from the loading frame and the top trimmed off level. A standard constant strain rate machine was used for the CBR test. The sample was tested with no surcharge weights.

After the CBR test the bottom plate of the mould was removed and two standard oedometer samples were carefully cut as the CBR sample was extruded. These were used to determine the maximum pressure applied to the sample during consolidation. The undrained shear strength was measured at the top and bottom of the sample using a 19mm shear vane and also a pocket penetrometer. The sample was sectioned and the moisture content at the top and bottom of the sample was determined. The results from the consolidated CBR samples are presented in Chapter 8.

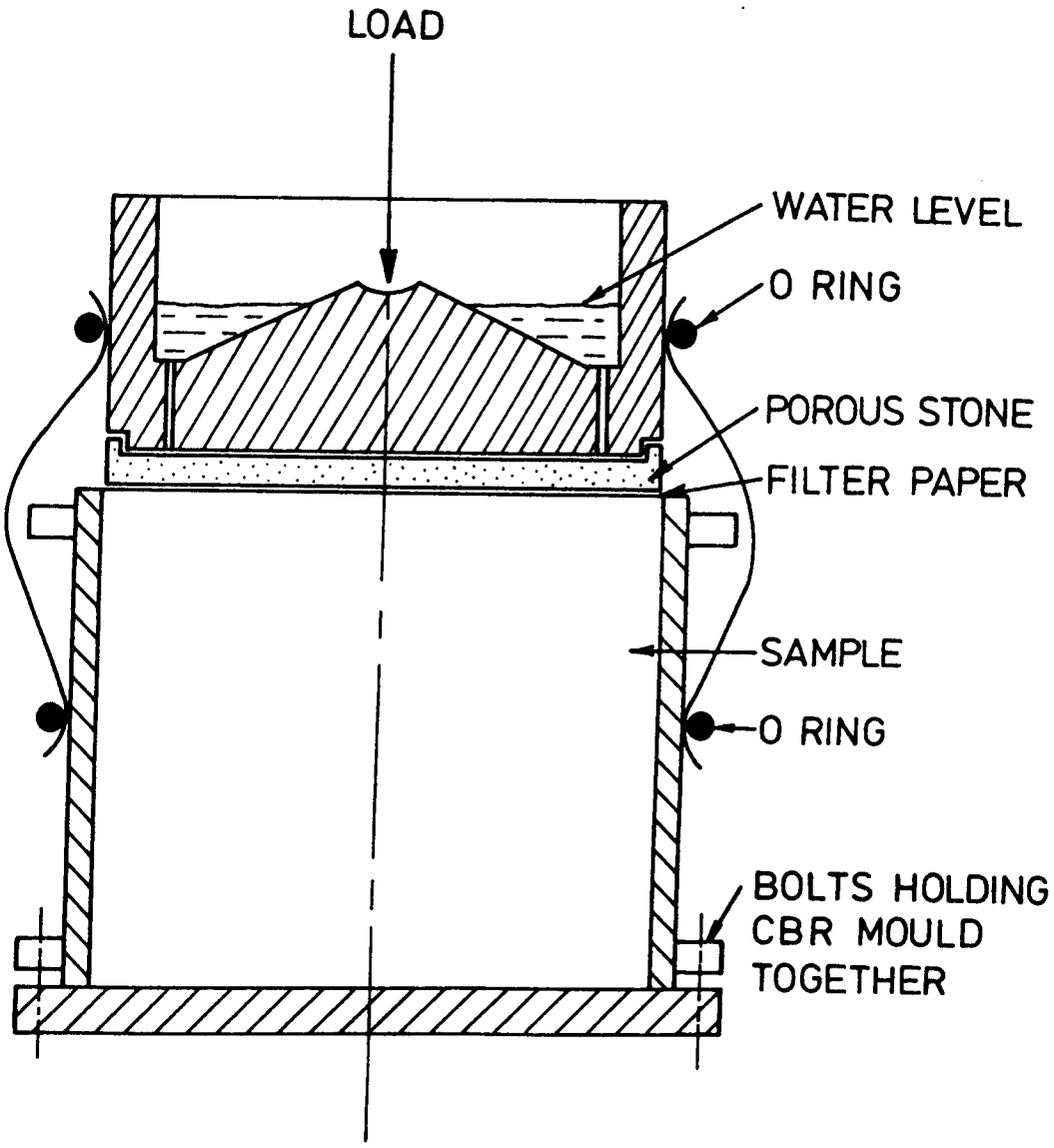

FIGURE 5.4 ARRANGEMENT FOR ALLOWING SAMPLES TO OVERCONSOLIDATE IN THE CBR MOULD

5.4 COMPACTED TRIAXIAL SAMPLES

The compacted triaxial specimens were 78mm in diameter and 148mm long. The dry powdered clay was weighed out into the bowl of a Hobart Mixer and sufficient distilled water added to give the required moisture content. It was found that approximately fifteen minutes mixing time was sufficient to give a consistent uniform mix.

The mould in which the samples were compacted consisted of three equal longitudinal sections which were clamped together with jubilee clips to form a cylinder. The inside of the mould was prepared by inserting a liner made of polythene sheet. This was easy to separate from the sample and prevented the sample from adhering to the mould. The mould was clamped to a base plate and the soil placed in thin layers and compacted by hand using a tamping rod approximately 12mm in diameter.

The mould was dismantled, the sample weighed and placed on the cell base. The top and bottom platens were prepared as for the consolidated samples, see section 5.2.3. A jig was used to place the LVDT and strain hoop studs in the correct locations and the membrane was then positioned using a standard membrane stretcher and sealed in place with O-rings. Neoprene membranes were used as they are impermeable to air which was used as the confining medium. No provision was made for drainage or for the measurement of pore water pressure.

The membrane was punctured over the mounting studs using a soldering iron and the instrumentation fitted and zeroed. The LVDT details were the same as for the consolidated samples, as shown in Figure 5.3, and the radial deformation transducers were attached to similar studs and sealed in the same manner.

The cell top was fitted and the sample was left for twenty four hours before testing. This was to allow for any variation in moisture content or suction caused during sample assembly to equalise. The test programme is detailed in Chapter 3. After

testing the cell was dismantled, the sample weighed, and the centre third of the sample used for moisture content determinations. The results of the tests on the compacted triaxial samples are presented in Chapter 7.

5.5 COMPACTED CBR SAMPLES

The soil was prepared in the same manner as for the compacted triaxial specimens, section 5.4, and compacted into a standard CBR mould (BS 1377). The soil was placed in thin layers and compacted to refusal using the same hand tamper. The weight of the soil was determined by subtracting the weight of the mould from the total weight after compaction. The top of the mould was screwed into position and the sample left for twenty four hours before testing, again to allow any pore pressure or moisture content variations to equalise.

The CBR was determined at the top and bottom of the sample using a standard CBR testing machine. The undrained strength of the soil was determined using a 19mm shear vane and also a pocket penetrometer. The moisture content profile with thickness was also determined.

The results are presented in Chapter 8.

5.6 MEASUREMENT OF SOIL SUCTION

5.6.1 Rapid Suction Apparatus

The apparatus is described in Chapter 4, section 4.6 and shown in Figure 4.8. The apparatus was prepared by applying a suction to the porous stone while it was immersed in de-aired distilled water. This saturated the porous stone and allowed the meniscus to be set at a suitable place in the capillary tube.

The porous stone was approximately 12mm diameter and a small mould and tamper were manufactured to make samples of a suitable size. The mould produced samples 12mm in diameter and 10mm long.

Sufficient dry soil for a number of tests was mixed to the highest water content desired for the initial suction measurement. A sample was compacted in the mould, weighed, and then extruded on to the porous stone. The suction was recorded and the moisture content of the sample determined. A little dry soil was added to the remaining mixture to decrease the moisture content and the process was repeated.

5.6.2 Equilibrium Method

The apparatus is described in Chapter 4, section 4.6 and shown in Figure 4.8. It consists of a number of high air entry porous stones 40mm in diameter on to which each sample was placed. A known constant value of suction was applied to the stone and the sample allowed to reach equilibrium. The moisture content of the sample was then determined.

The porous stones were de-aired by leaving them under water in a vacuum vessel. It was found that the stones de-aired much more quickly if the vacuum vessel was placed on a vibrating table. A cylindrical mould was manufactured and used to produce suitably sized samples. The soil was mixed to a moisture content which was estimated as being close to the equilibrium moisture content at the value of suction chosen and then compacted in the mould. The sample was extruded and placed on the porous stone and left to reach equilibrium. After a few days the moisture content of the sample was determined and the suction, as measured by a mercury manometer, recorded.

The results from both types of test are detailed in Chapter 7.

CHAPTER SIX

BEHAVIOUR OF OVERCONSOLIDATED SATURATED SAMPLES OF KEUPER MARL

6.1 INTRODUCTION

The objective of this section of the work was to produce and then test triaxial samples with a known, carefully controlled stress history which resulted in final stress conditions similar to those found in road subgrades in the U.K. The test programme was designed to investigate the resilient and permanent response of the samples subjected to loading conditions similar to those applied to a road subgrade by traffic loading. The range of initial stress conditions and the test programme is described in Chapter 3. The test equipment is detailed in Chapter 4 and the sample preparation procedure in Chapter 5.

6.2 TRIAXIAL CONSOLIDATION RESULTS

6.2.1 Consolidation Paths

The consolidation phase of each sample was monitored regularly to ensure that it attained the correct consolidation history. Figure 6.1 shows the results for the samples in mean normal effective stress-specific volume space and shows quite clearly that there is a unique virgin consolidation curve for this material. In this case the curve is the K_o consolidation curve as the samples are all anisotropically consolidated. The individual swell back lines for each sample are shown and are all of a similar shape. These curves have a very shallow initial gradient which tends to get progressively steeper as the mean normal effective stress decreases further and the overconsolidation ratio increases. This result was as expected and is typical behaviour for overconsolidated samples. The critical state parameters determined from this Figure are given in Appendix A.

The consolidation results for all samples plotted in mean normal

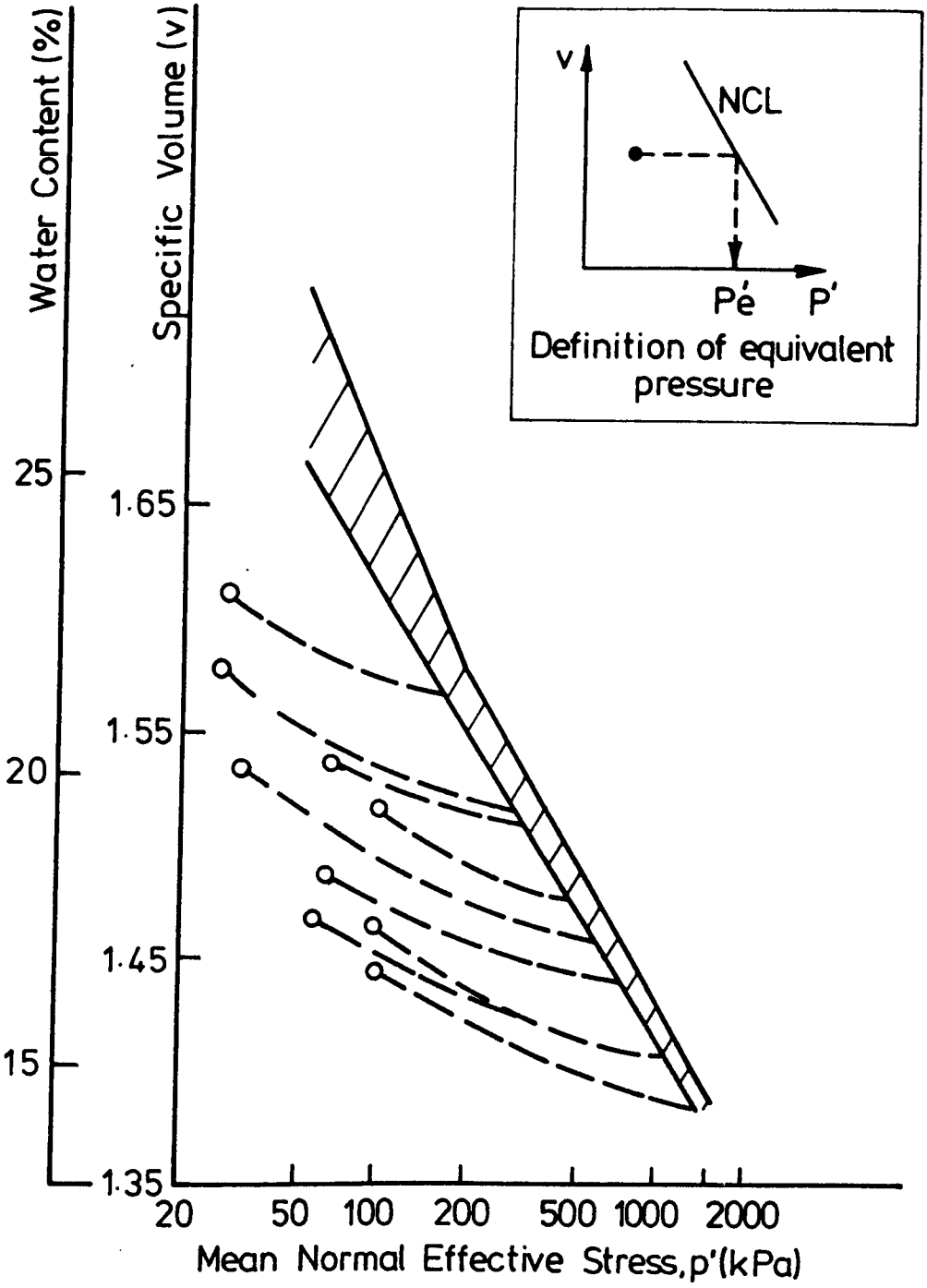

FIGURE 6.1 COMPRESSION AND SWELL - BACK DATA FROM TESTS ON KEUPER MARL

effective stress - deviator stress space again show a scatter around a unique curve for the consolidation phase, the gradient of which gives the value of K_o. However, the overconsolidated sections of the curves tend to oscillate about a mean curve and Figure 6.2 shows a typical test result only for clarity. This effect was noticed by Overy (1982) and is due to the way in which the servo system maintains anisotropic conditions. The system uses the proximity transducers to detect any change in the sample diameter during consolidation and adjusts the deviator stress accordingly to maintain a constant sample diameter. During virgin consolidation there is an appreciable volume change as the effective stress changes, i.e. the gradient of the consolidation curve, λ ; in lnp'-v space is relatively large. This means that the servo system is activated frequently and consequently produces small increases in deviator stress which results in a smooth curve in p'-q space.

The swell back curves in lnp'-v space though, have a much lower gradient than the virgin consolidation curve and consequently there is a large change in stress for a small change in volume. The samples are effectively a lot stiffer. This means that the servo system operates relatively infrequently and hence causes large deviator stress changes, which result in the overconsolidation path in p'-q space oscillating around the mean curve.

Mayne and Kilhaney (1982) suggested that the value of K_o was a function of the overconsolidation ratio such that

$$K_o = (1 - \sin \phi') \times OCR^{\sin\phi'} \qquad 6.1$$

This relationship is shown plotted in Figure 6.2 and fits the mean curve drawn through the data quite accurately.

6.2.2 Response of the radial drainage system

Overy (1982) tested normally consolidated samples of Keuper Marl prepared using this test equipment. The samples were

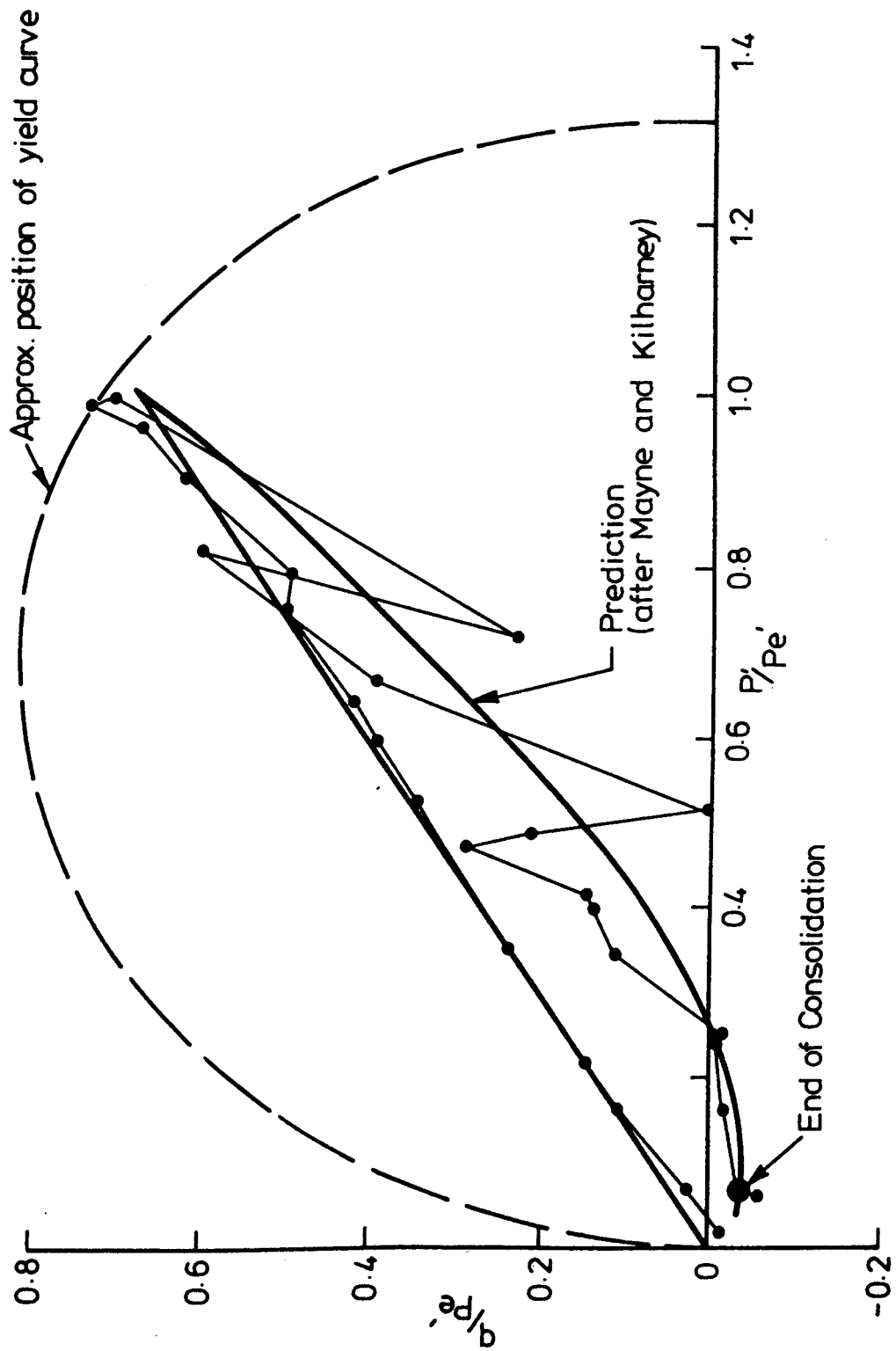

FIGURE 6.2 COMPRESSION AND SWELL - BACK DATA FROM TESTS ON KEUPER MARL

consolidated from a slurry initially, and then transferred to the triaxial cell for the main consolidation phase. In order to minimise the effects of sample disturbance when the sample was unloaded and transferred from the slurry moulds to the triaxial cell Overy used the lowest consolidation pressure in the slurry mould that would give handleable samples.

As this research concentrated on producing overconsolidated samples the first few samples were consolidated to higher stresses in the slurry mould to reduce the consolidation time in the triaxial cells, although the samples were all consolidated in the triaxial cell to at least three times the effective stress achieved in the slurry mould. This factor was suggested by Loudon (1967) to eliminate the effects caused by stress relief.

The preliminary tests highlighted deficiencies in the radial drainage system with large excess pore pressures developing during consolidation, which took a week or more to dissipate. It proved impossible to overconsolidate some samples to any real degree as they seemed to reach an 'equilibrium' state with a negative excess pore pressure of up to -60 kPa without absorbing any more water.

This was thought to be caused by constrictions in the filter paper drain either by pinching between the bottom platen and the membrane or general restrictions caused by the cell pressure as this was higher than had been used previously. Another possibility was that the sample surface had been 'smeared' when it had been extruded from the mould. Smear is defined as the localised remoulding and 'sealing' of a clay surface causing a barrier of lower permeability than that of undisturbed clay.

The permeability of the filter paper drains in the triaxial cell was measured as a function of the cell pressure, and was found to be higher than that quoted for Keuper Marl by Overy (1982) by a factor of approximately 6000. Appendix B contains the test details.

The possibility that the filter paper drains had become clogged during the consolidation phase was also considered. However the permeability of a used filter paper drain could not be measured in the same manner as they were impossible to remove intact from the samples.

The flow path of the drainage system was improved by reducing the diameter of the bottom platens to approximately 3mm greater than the sample diameter, and rounding off the edges. Two filter paper drains were used with a small wick sandwiched between them, as discussed in Chapter 5. Samples consolidated to lower effective stresses in the slurry mould seemed to suffer less drainage problems, and the author considers that the 'smear' effect is more apparent on the more heavily consolidated samples. The samples tested in the main test programme were all consolidated to low effective stresses in the slurry mould before transfer to the triaxial cell.

One sample was consolidated under end drainage by modifying the top and bottom platens to allow porous stones and drainage lines to be fitted. This system proved to be more efficient than the original radial drainage arrangement, but less efficient than the modified radial drainage system used in this research.

Excess pore pressures generated during consolidation were generally dissipated within twenty four hours. The time calculated for 95% consolidation using values for the permeability and for the coefficient of volume compressibility from Overy (1982) ($k = 2.5 \times 10^{-7}$mm/sec., $m_{iv} = 3.53 \times 10^{-4}$ m^2/kN), and the consolidation curve for radial drainage from Lambe and Whitman (1979), is of the order of 6 hrs. The radial drains could therefore be improved further, but were judged to be sufficiently good for this research and no further modification was attempted.

Atkinson et al (1985) carried out a series of tests on triaxial samples to investigate the distribution of moisture in samples of kaolin consolidated with radial drainage under various rates of

consolidation, and compared these with samples consolidated with end drainage under the same conditions. The samples consolidated with radial drainage in one step were found to be as much as 1.5% wetter in the centre than at the periphery. As the samples were saturated this led to quite considerable non uniformities in effective stress across the sample. Atkinson et al reported that the outer part of the sample started to consolidate first, and as it consolidated it became stiffer. This relieved some of the total stress on the inner part of the sample which led to the final uneven distribution of water content at the end of consolidation. Atkinson et al demonstrated that at rates of loading as low as p' = 10 kPa/hr then a difference in moisture content of about 0.4% between the centre and the periphery would be expected for triaxial samples of Kaolin consolidated with radial drainage.

At the end of the test series on each sample the centre third of the sample was sectioned and the moisture content determined at the centre, at an average radius of approximately 27mm, and at an average radius of approximately 35.5mm. The overall radius of the samples varied but was generally about 40mm. Table 6.1 gives the moisture contents determined for each sample.

There is little significant variation in moisture content across the radius for each sample although the centre sections do appear to be slightly wetter in most cases. The loading rate p' in all cases was constant at approximately 3kPa/hr, which is considered to be sufficiently low to minimise the non uniformities demonstrated by Atkinson et al. It may be that the problem is less marked for anisotropically consolidated specimens as the sample is being sheared during the consolidation process. However further work would be required to investigate any difference in behaviour between isotropic and anisotropic consolidation.

6.3 EFFECTIVE STRESS RESPONSE

The effective stress response of the samples to a variety of total stress paths over the range of frequencies used is discussed below. The main series of such tests were the low

Table 6.1 Moisture content of consolidated samples

Sample Number	Outer Annulus r = 35.5mm %	Inner Annulus r = 27mm %	Centre %
33/6	22.29	22.45	22.49
33/12	21.47	21.37	21.36
33/18	19.14	19.33	19.49
65/6	20.29	20.21	20.18
65/12	17.90	17.95	17.98
65/18	17.51	17.68	17.70
100/6	19.51	19.74	19.84
100/12	16.92	17.09	16.97
100/18	17.07	17.01	17.17

frequency stress path tests performed initially on each sample, see Figure 3.2, but the effective stress response has been determined from the results of the 1 second and 0.1 second deviator stress pulse tests.

6.3.1 Total stress path tests

A series of undrained total stress paths of low magnitude (in the range ± 2.5 kPa to ±10 kPa) and low frequency (0.05Hz and below) was applied to each sample to allow investigation of the elastic response at sufficiently low loading rates to allow the pore pressure to be monitored accurately. The stress paths are shown diagrammatically on Figure 6.3. The stress level and frequency were at the limits of the control system in its present state. Five samples were tested in this manner and all showed that the change in total stress caused the pore pressure to alter such that the mean normal effective stress remained constant. The resilient shear strain-deviator stress plots were similar for each sample at any particular stress level, and showed a slight hysteresis although the area enclosed by the loop and hence the energy absorbed by the sample, was small in all cases. The resilient volumetric strain recorded in all cases was negligible, and indicates that Poisson's ratio was 0.5. The calibrations of the proximity transducers and LVDTs were shown to be valid over such small strains by a comparative test detailed in Appendix C. Overy (1982) demonstrated similar behaviour for normally anisotropically consolidated samples of Keuper Marl at repeated stress levels of the order of 50kPa or more. Overy carried out these stress path tests after cyclic loading tests and therefore the yield locus had been extended from its position at the end of consolidation by the cyclic loading, and his stress paths were within the new yield locus.

Figure 6.4 shows the effective stress and strain response of samples 100/18 and 33/6 to a variety of total stress paths. In both cases the cyclic total stress level applied was ± 2.5kPa. The fact that the mean normal effective stress remained constant during the loading sequences and that Poisson's ratio was 0.5

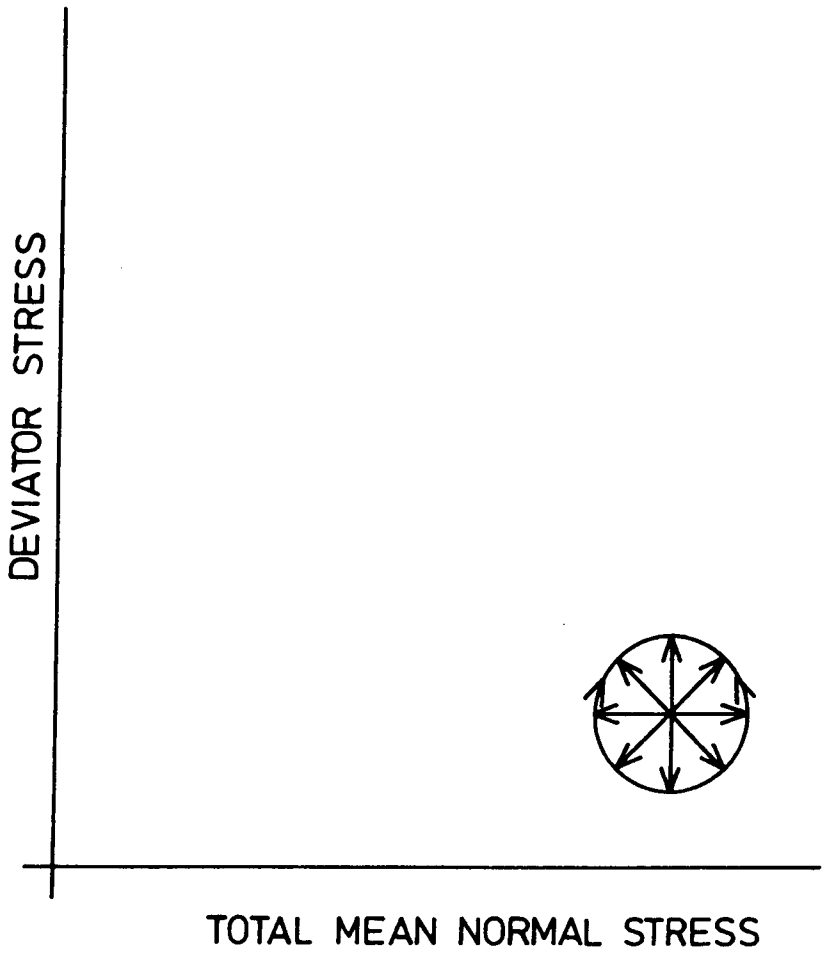

NOTE

1 All stress paths are centred on the final stresses at the end of consolidation.

2 Six different stress paths were applied to each sample.

FIGURE 6.3 DIAGRAMMATIC REPRESENTATION OF TOTAL STRESS PATHS FOR UNDRAINED TESTS AT ~0.05Hz

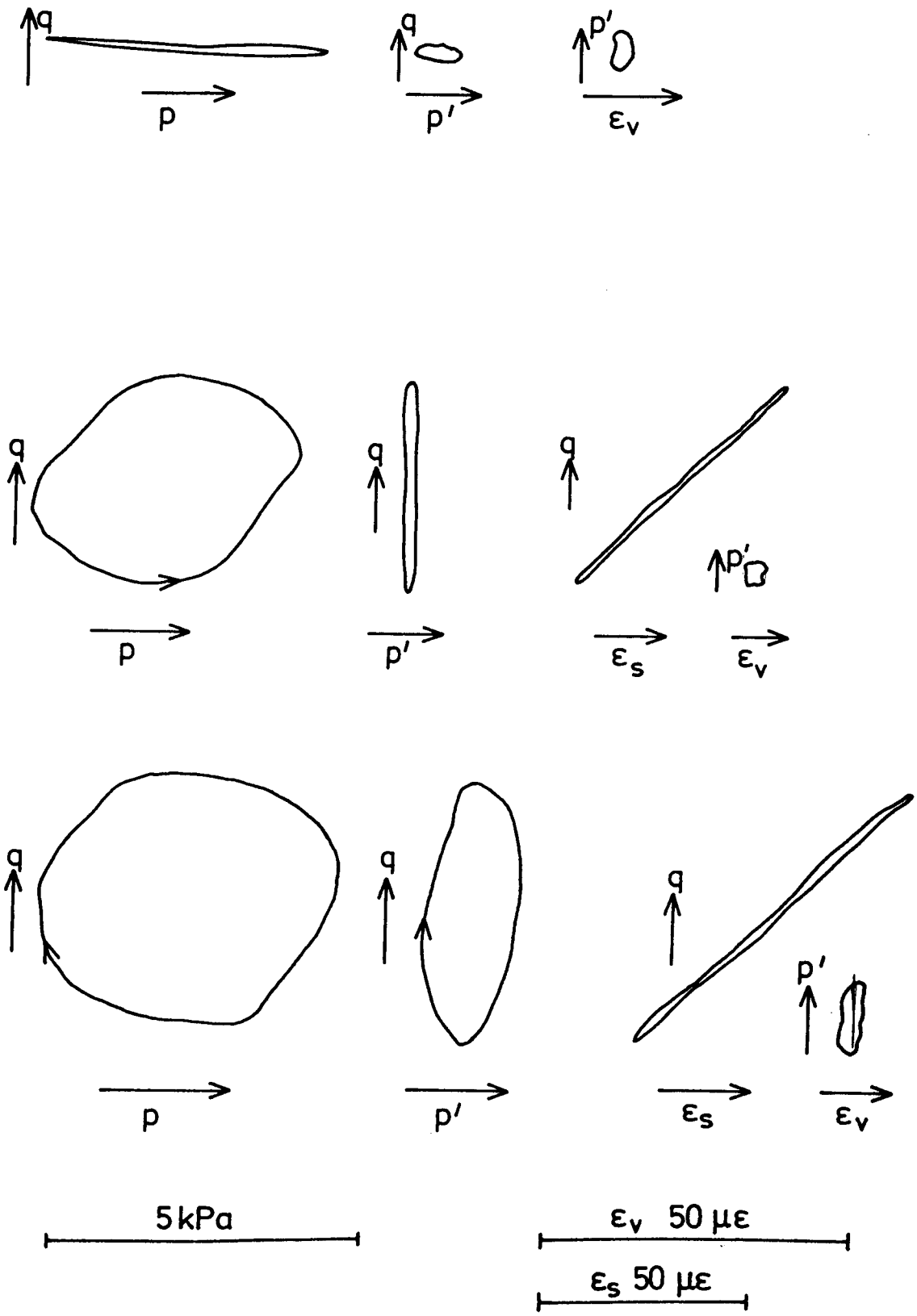

FIGURE 6.4a SOME STRESS PATH TEST RESULTS FROM SAMPLE 100/18

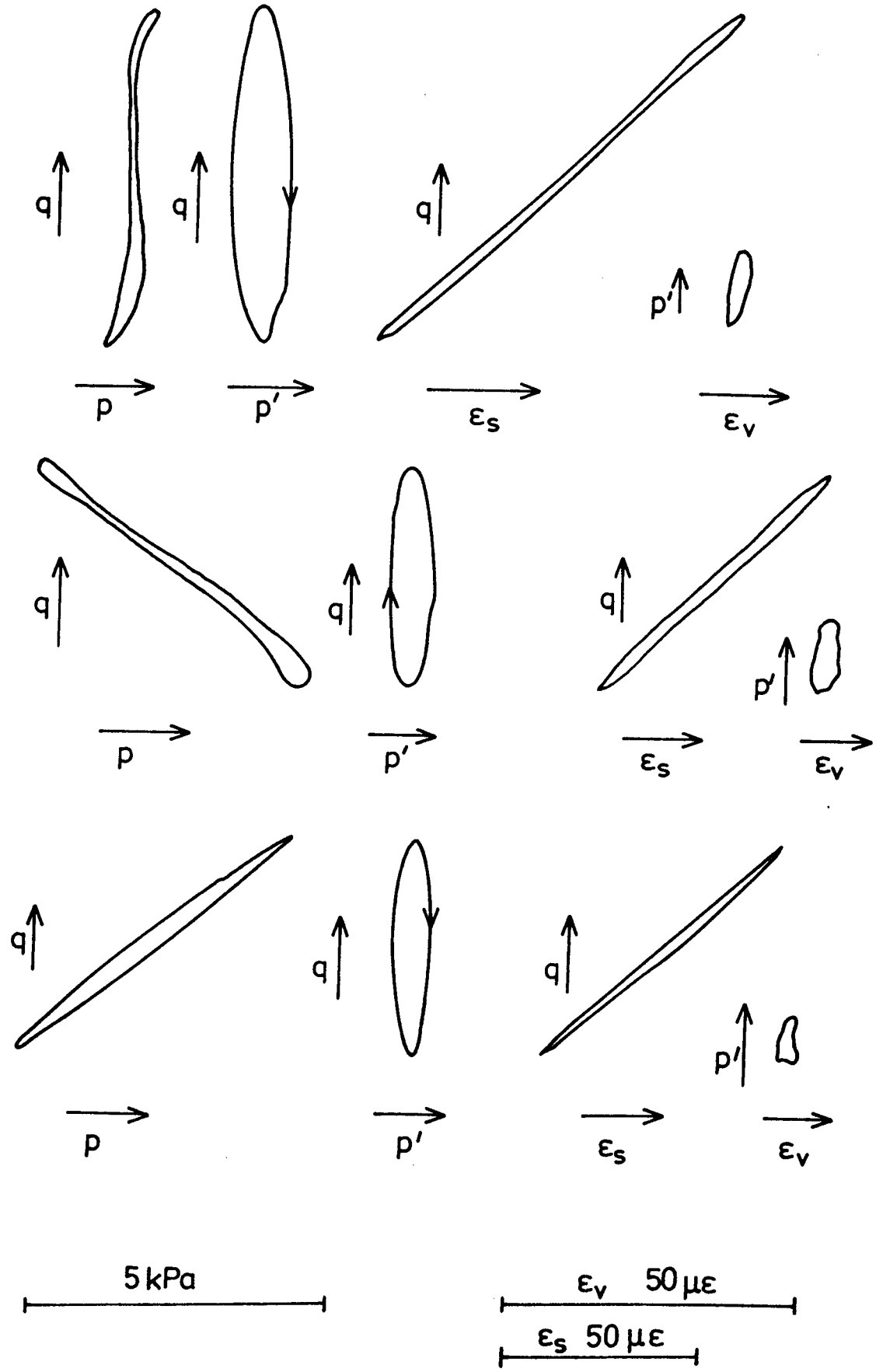

FIGURE 6.4b SOME STRESS PATH TEST RESULTS FROM SAMPLE 100/18

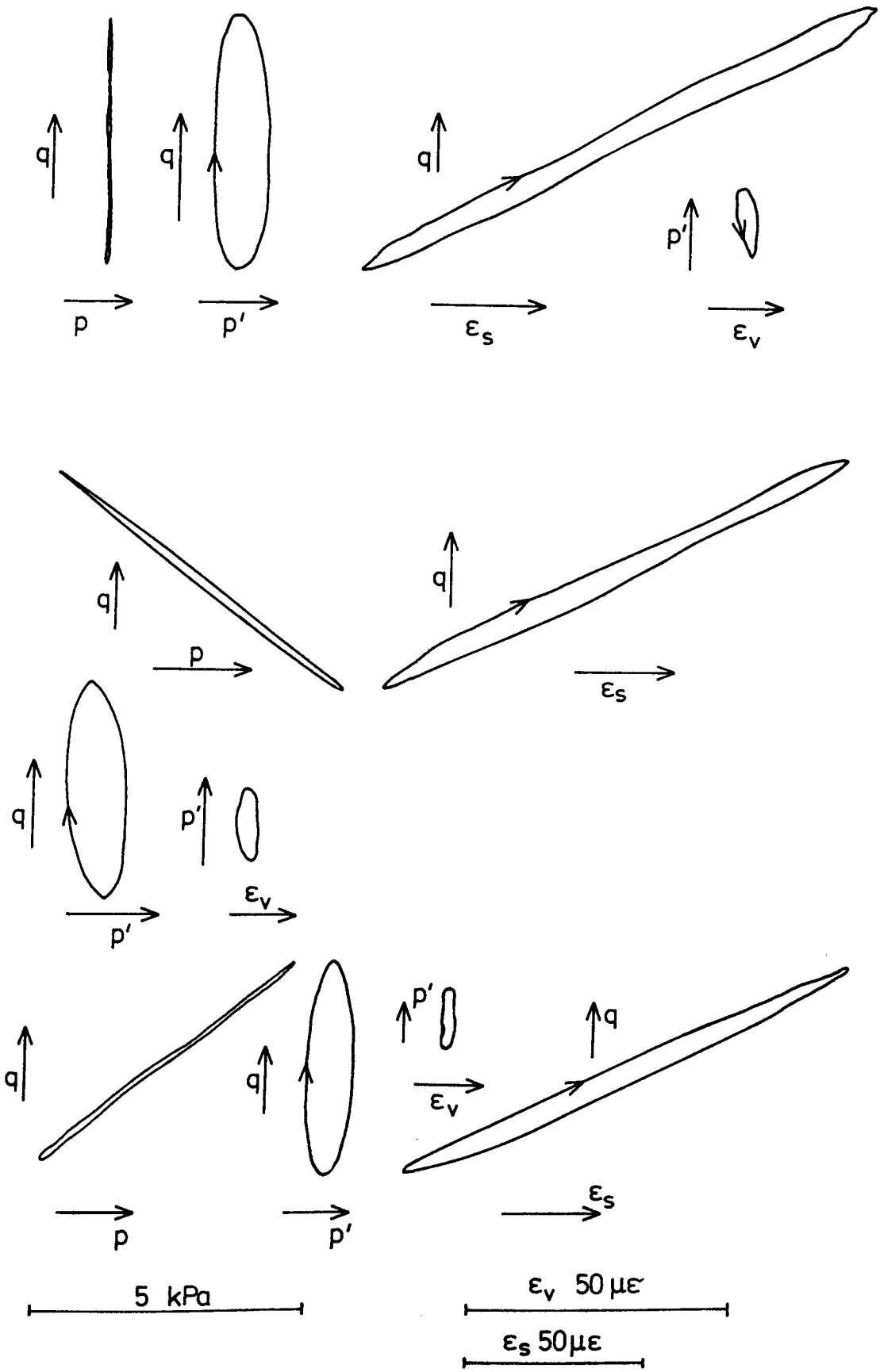

FIGURE 6.4c SOME STRESS PATH TEST RESULTS FROM SAMPLE 33/6

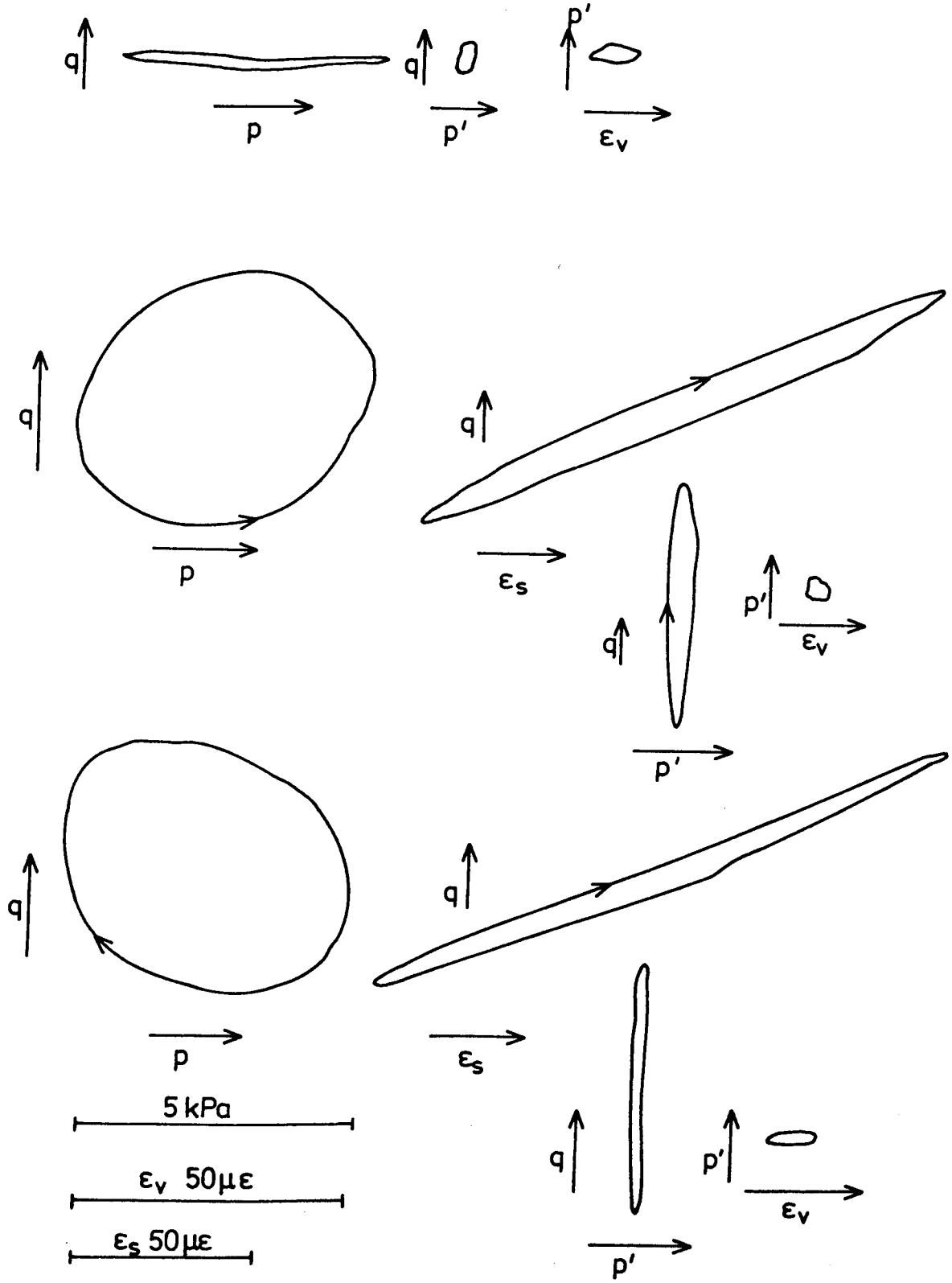

FIGURE 6.4d SOME STRESS PATH TEST RESULTS FROM SAMPLE 33/6

indicates that the sample is behaving in an isotropic elastic manner.

Graham and Houlsby (1983) working on a naturally anisotropically consolidated clay demonstrated that changes in shear stress affected the volumetric strain and that changes in the mean normal effective stress affected the shear strain. This led to effective stress paths where p' did not remain constant although the effective stress path in q-p' space remained linear. The sign of the gradient of the stress path in q-p' space indicated whether the sample was stiffer axially or radially. This behaviour is not apparent from the results of this research or that of Overy (1982) although the samples were carefully anisotropically consolidated. Further work should include examining samples of clay consolidated in this equipment under an electron microscope as it is possible that the samples are not consolidated from a wet enough slurry to induce anisotropy.

6.3.2 One Second Stress Pulse Tests

These tests were performed just prior to and immediately after the permanent strain tests, see Figure 3.2. The tests consisted of a range of undrained deviator stress pulses of 1 second duration. The peaks only were recorded, so the complete stress paths cannot be plotted. Figure 6.5 shows the peak resilient axial strain plotted against the peak resilient radial strain for a number of tests and shows that Poisson's Ratio is approximately 0.5 within the experimental scatter. Figure 6.6 shows that on average the change in pore pressure is approximately one third of the change in the deviator stress, although the value appears to increase as the deviator stress pulse increases. This may be due to the transducer affecting the stress distribution at the higher strain levels. The ratio of a third between the deviator stress pulse and the change in pore pressure indicated that p' remains constant during this type of loading as:-

$$q = \sigma_v - \sigma_r \qquad 6.2$$

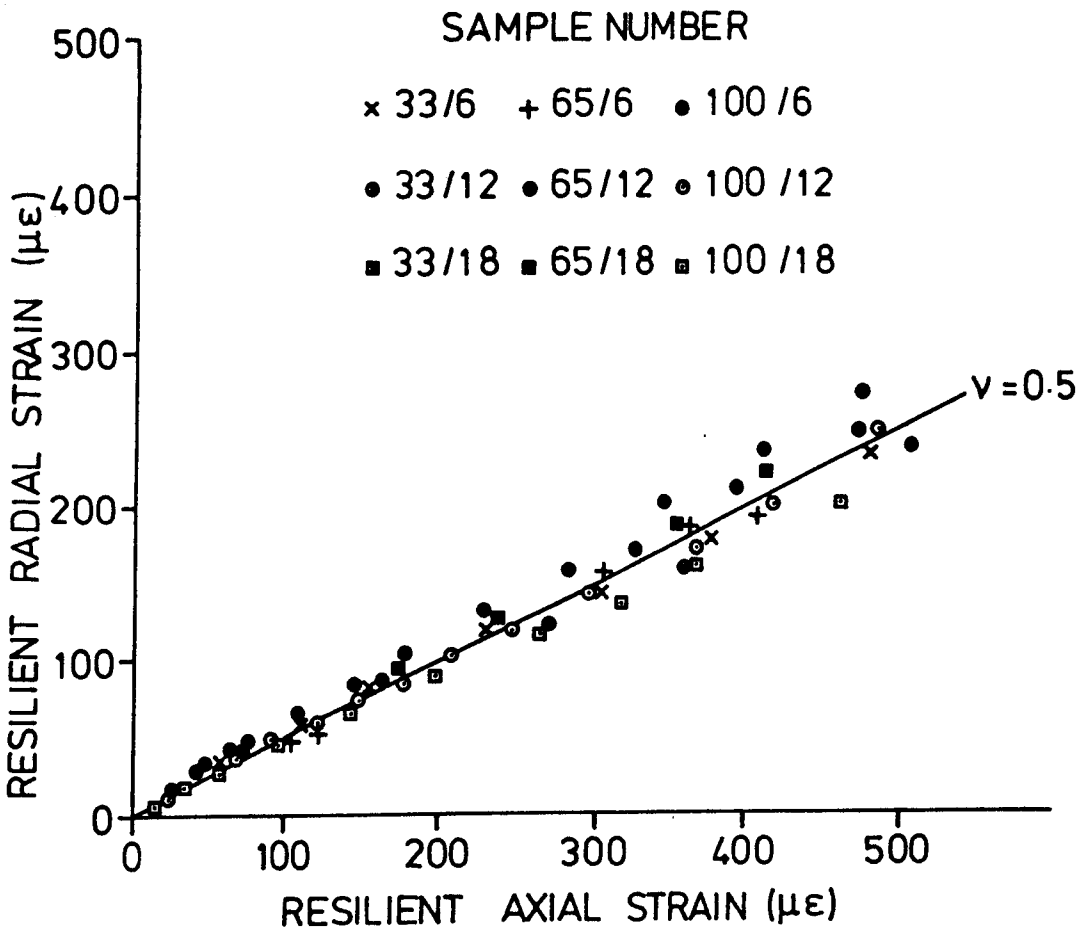

FIGURE 6.5 RESILIENT AXIAL STRAIN vs RESILIENT RADIAL STRAIN FOR CONSOLIDATED SAMPLES OF KEUPER MARL. 1 SECOND PULSE DURATION

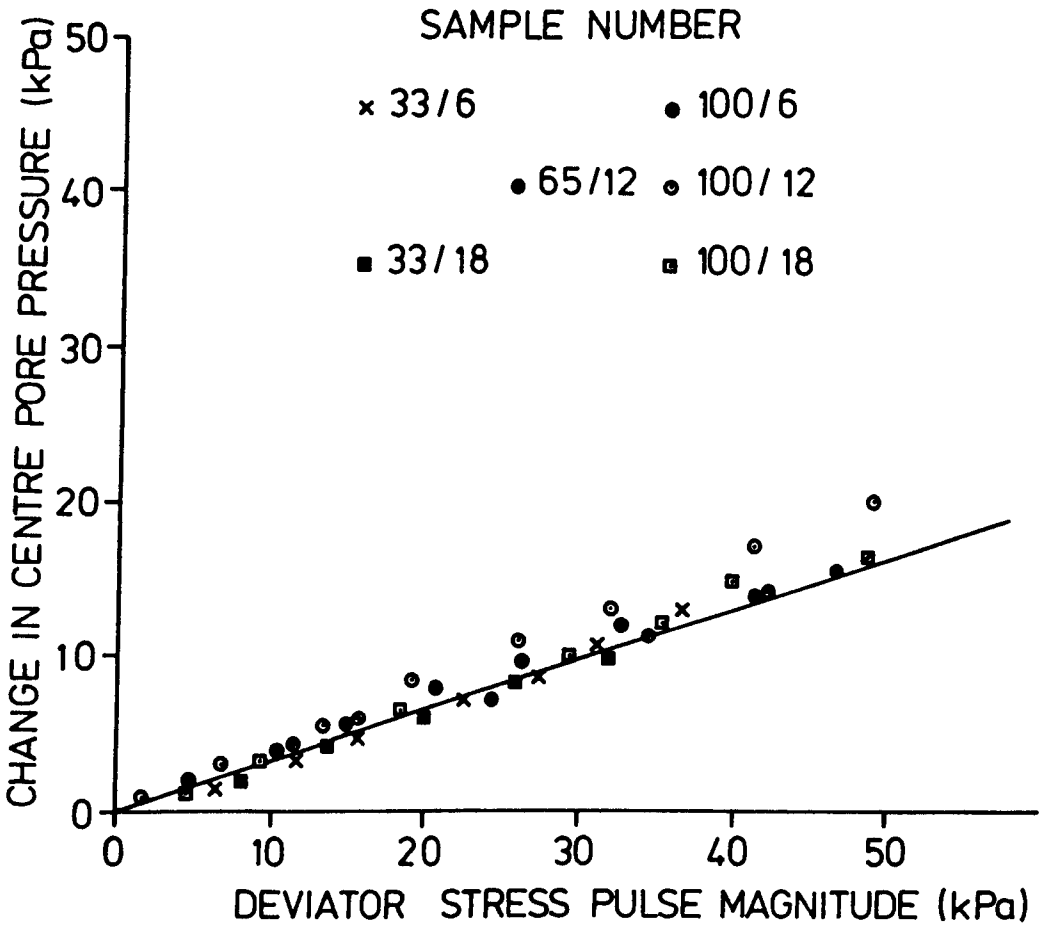

FIGURE 6.6 PORE PRESSURE RESPONSE TO DEVIATOR STRESS PULSE OF 1 SECOND DURATION (CENTRE PROBE)

Therefore as the cell pressure remains constant

$$\Delta q = \Delta\sigma_v \qquad 6.3$$

The total mean normal stress $p = \frac{1}{3}(\sigma_v + 2\sigma_r)$ 6.4

therefore $\Delta p = \frac{\Delta\sigma_v}{3}$ 6.5

substituting $\Delta p = \frac{\Delta q}{3}$ 6.6

However as $\Delta u = \frac{\Delta q}{3}$ from Figure 6.6 it follows

that $\Delta p = \Delta u$ 6.7

as $p' = p - u$ 6.8

therefore as $\Delta p' = \Delta p - \Delta u$ 6.9

it follows that $\Delta p' = 0$

6.3.3 One Tenth Second Stress Pulse Tests

These tests were carried out at a variety of undrained pulsed deviator stress magnitudes of 0.1 second duration with a rest period of approximately 0.25 seconds. The early tests were recorded on an ultra violet chart recorder and consequently only

the peak valves were available. Following the introduction of the analogue to digital converter and the computer data acquisition system it was possible to record the full pulse and consequently the effective stress path resulting from the applied loading.

Figure 6.7 shows some of the effective stress paths recorded and demonstrated that p' remained essentially constant during these tests. The centre pore pressure transducer was shown to be capable of following stress pulses of this duration by supplementary tests detailed in Appendix C.

Overy (1982) reported a loss in response from the base pore pressure transducer at a maximum frequency of 0.005 Hz, and at approximately 0.1Hz for the centre pore pressure transducer in most cases. Samples exhibiting this sort of response would be unlikely to show a B value of 1 in the initial saturation tests described in Chapter 5 and would have been rejected under the conditions applied during this research.

The pulsed deviator stress resilient axial strain paths for a number of deviator stress pulse magnitudes for samples 33/6 and 100/12 are shown in Figures 6.8, and 6.9. Figure 6.10a shows the stress softening behaviour of the material evident at the start of the tests, and Figure 6.10b shows the effect of 10,000 pulses on the shape of the stress strain paths. The resilient modulus seems to reduce with increasing number of stress applications. Figures 6.8 and 6.9 shows the effect of numbers of cycles on the stress strain paths in more detail for samples 33/6 and 100/12 respectively.

It was found that between 5 and 15 deviator stress pulses were applied to the samples before the correct magnitude was achieved. This depended to a large extent on the magnitude of the deviator stress pulse. Therefore the first full pulse recorded by the computer was not the first pulse applied to the sample and some change in the shape of the hysteresis loop may have already occurred.

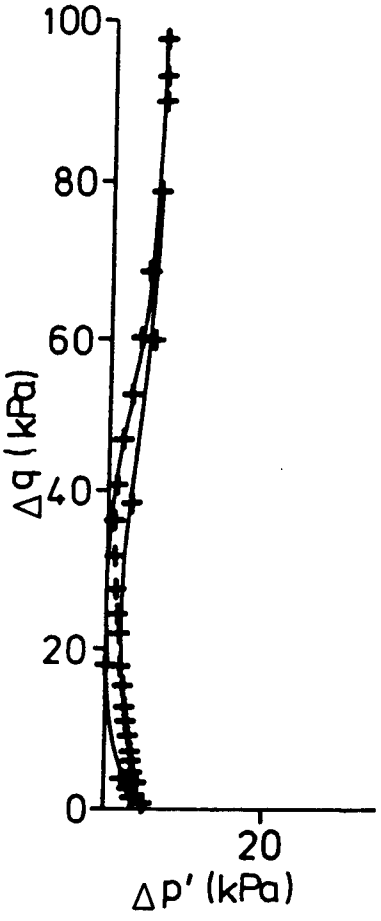

Sample 100/12
q_r = 100 kPa
N = ~10

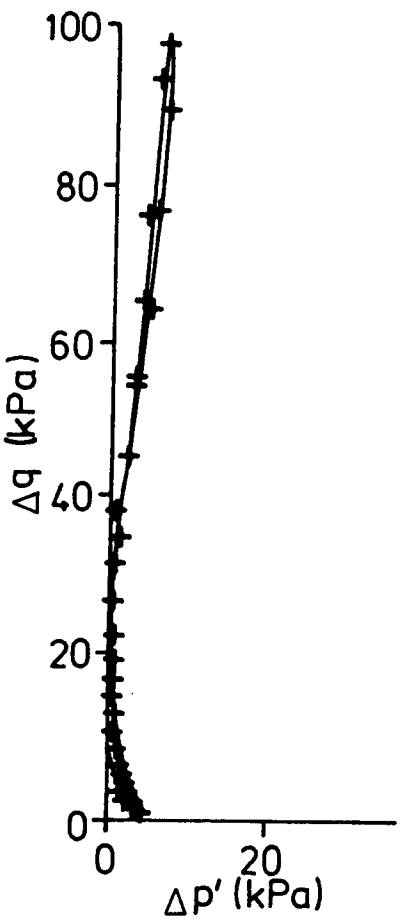

Sample 100/12
q_r = 100 kPa
N = 100 000

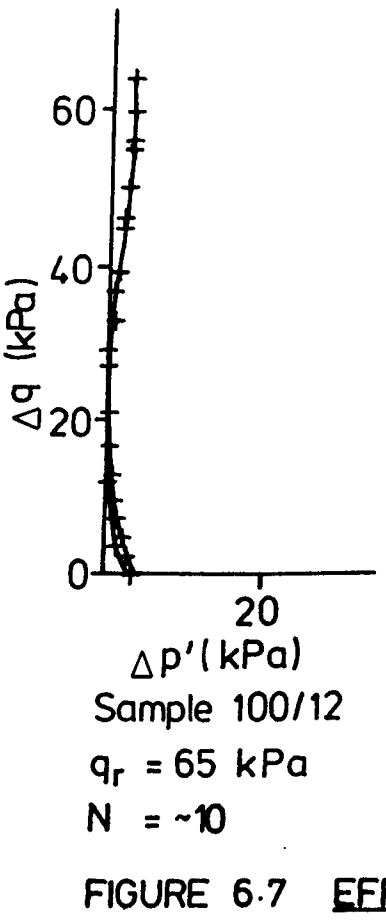

Sample 100/12
q_r = 65 kPa
N = ~10

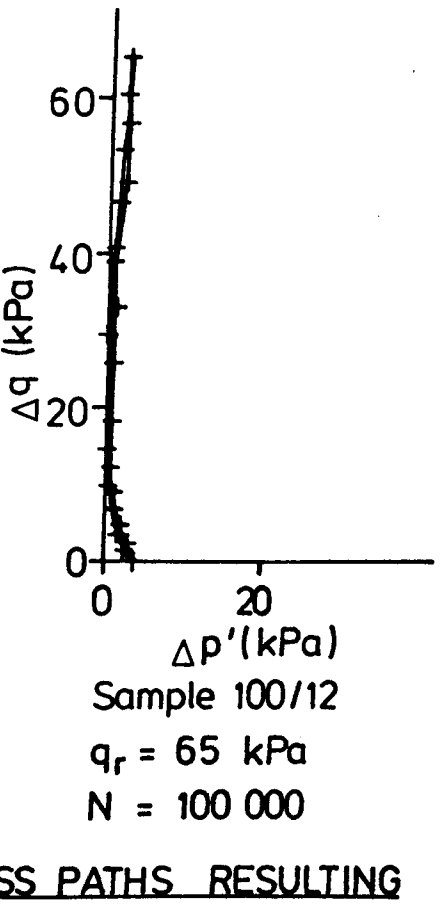

Sample 100/12
q_r = 65 kPa
N = 100 000

FIGURE 6.7 EFFECTIVE STRESS PATHS RESULTING FROM PULSED DEVIATOR STRESSES AT 0.1 SECOND DURATION

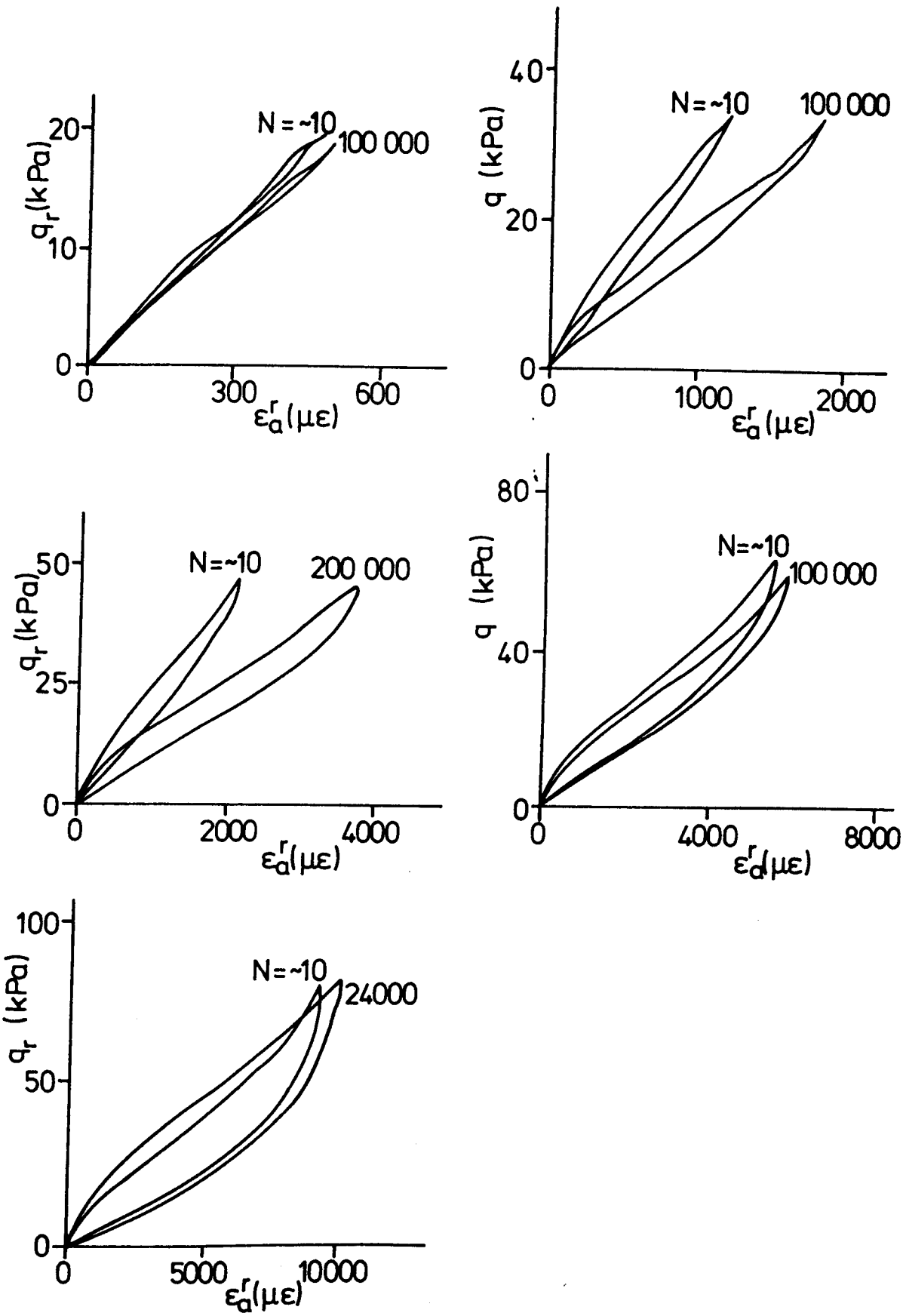

FIGURE 6-8 DEVIATOR STRESS PULSE RESILIENT AXIAL STRAIN PATHS FOR SAMPLE 33/6

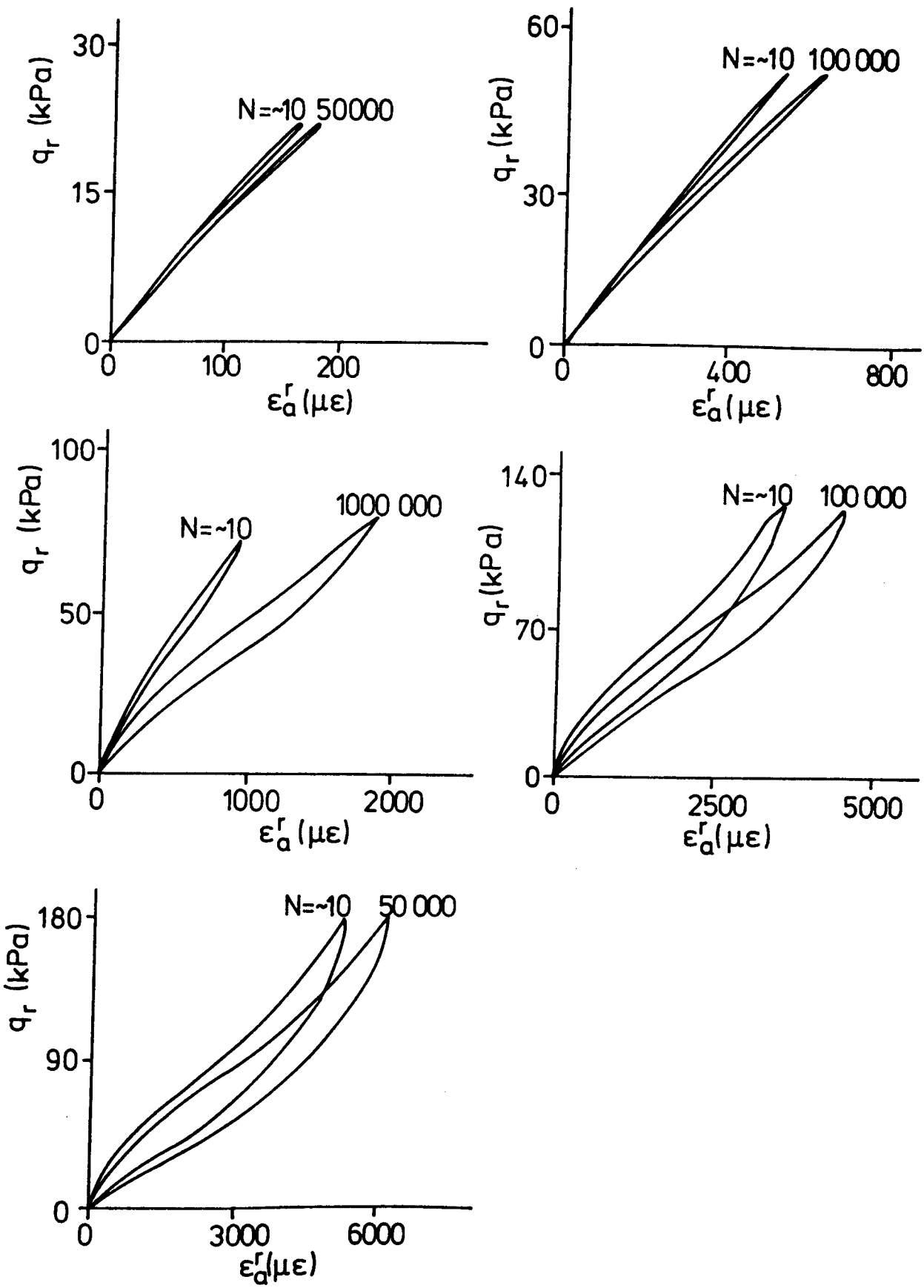

FIGURE 6.9 DEVIATOR STRESS PULSE RESILIENT AXIAL STRAIN PATHS FOR SAMPLE 100/12

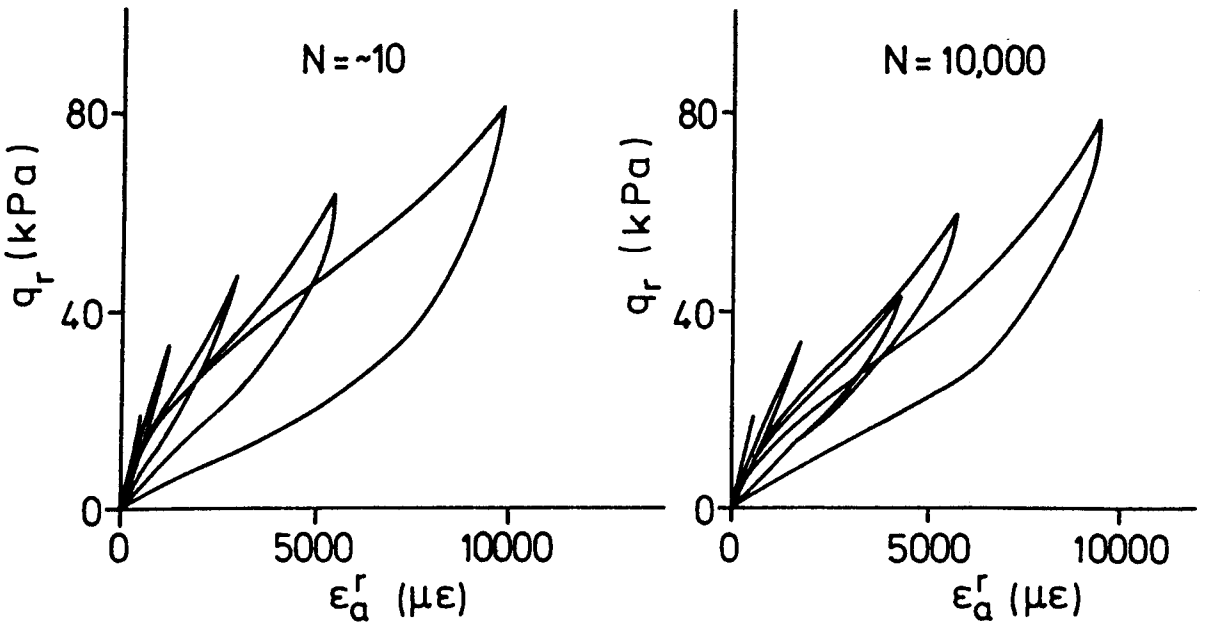

FIGURE 6.10a EFFECT OF DEVIATOR STRESS PULSE MAGNITUDE AND NUMBER OF CYCLES ON THE STRESS STRAIN RESPONSE OF SAMPLE 33/6

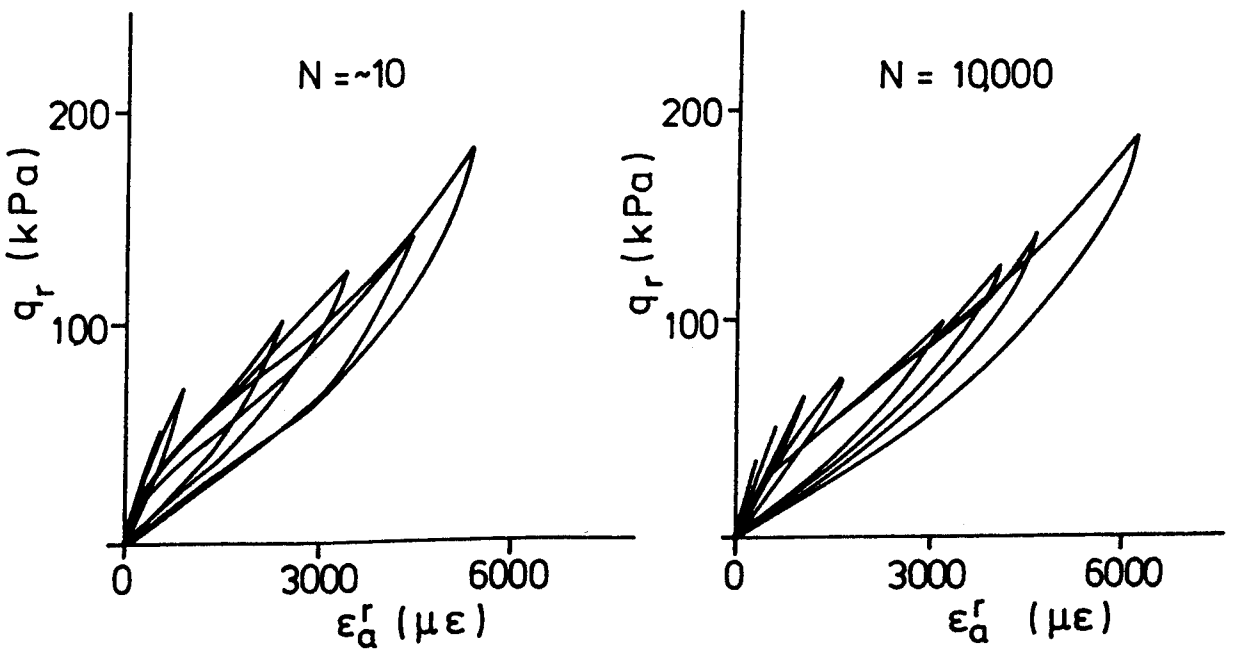

FIGURE 6.10b EFFECT OF DEVIATOR STRESS PULSE MAGNITUDE AND NUMBER OF CYCLES ON THE STRESS STRAIN RESPONSE OF SAMPLE 100/12

There is an indication however from Figures 6.8 and 6.9 that the loops do degenerate with increasing number of cycles, with the top of the loop becoming similar in shape to the end of the S shape hysteresis loops generally found by other researchers, and discussed more fully in Chapter 2. The S shaped loops referred to are the result of two way loading whereas the above tests were all one way.

At low repeated deviator stress levels the hysteresis loops in Figures 6.8 and 6.9 are closed and do not appear to change with frequency, indicating that the loading is having little effect on the sample, which is therefore behaving elastically. As the repeated deviator stress increases then the loops tend to get wider. The area enclosed by the hysteresis loop is a measure of the energy absorbed by the sample during each stress pulse, and it follows that as the magnitude of the stress pulse increases, and therefore the magnitude of resilient strain, then the work done on the sample must also increase.

6.4 RESILIENT RESPONSE

The main bulk of the data comes from the tests carried out with a pulsed loading time of 1 second as the stress levels were sufficiently high to produce reasonable resilient strains without causing any permanent deformation. The data from these tests is presented first and the data from the remaining tests with shorter and longer stress pulse durations is then presented and compared with the main results.

6.4.1 One Second Stress Pulse Tests

All the results from the tests showed a stress softening effect with increasing deviator stress pulse magnitude. Figure 6.11 shows a typical result for a single test. Each point represents the resilient axial strain measured at that value of pulsed deviator stress and was determined over 3 or 4 cycles. Figure 6.11 demonstrates that if the sample was unloaded then the material was softer than it was on the initial loading sequence,

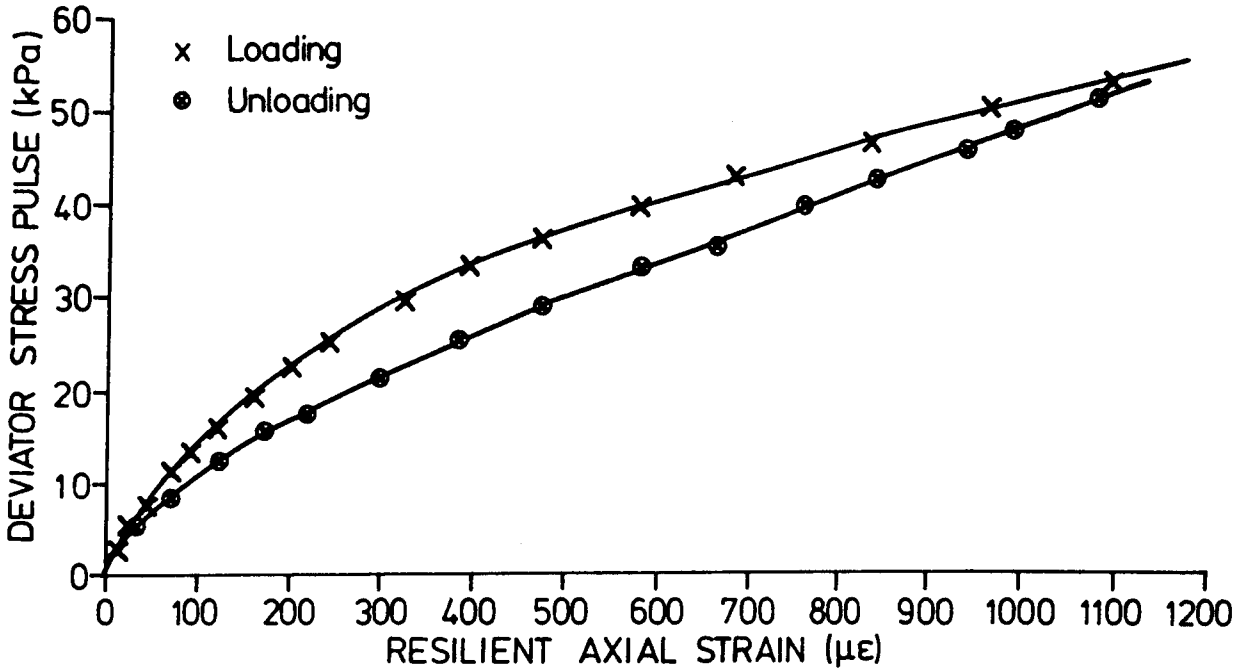

FIGURE 6.11 TYPICAL DEVIATOR STRESS PULSE vs RESILIENT SHEAR STRAIN PLOT FOR SATURATED KEUPER MARL.1 SECOND LOADING

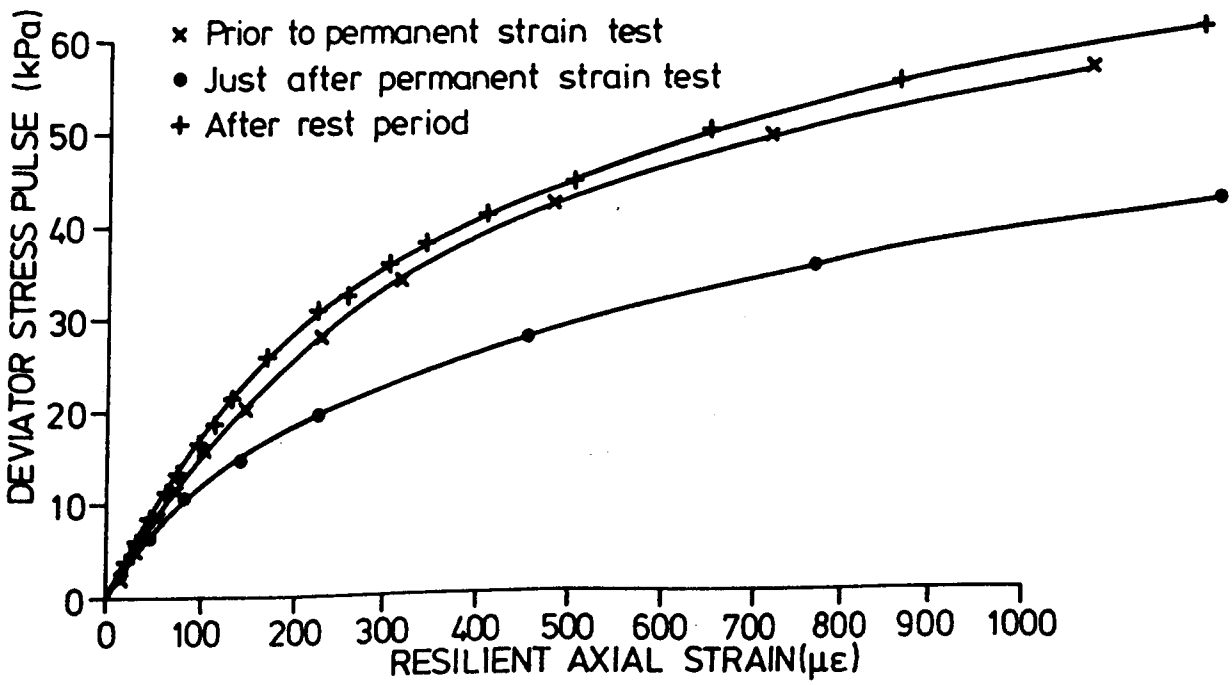

FIGURE 6.12 THE EFFECT OF LOADING AND REST PERIODS ON THE STRESS STRAIN RESPONSE OF KEUPER MARL. 1 SECOND LOADING. SAMPLE 100/18.

although there was no measurable change in pore pressure or any development of permanent strain.

Figure 6.12 shows a typical comparison between the results of these tests immediately prior to and immediately following a permanent strain test. The samples were found to be a lot softer after the permanent strain test even if there was negligible pore pressure development, as was the case for most of the permanent strain tests. The permanent strain tests are discussed more fully in Section 6.5. A comparison between typical stress-strain curves measured just prior to each permanent strain test on a particular sample is shown in Figure 6.13 for sample 100/18 and demonstrates that the sample recovers its original stiffness during the rest period between the permanent strain tests. This was found to be the case for all the samples. As there was very little excess pore pressure developed during the permanent strain tests there was consequently very little volume change during the drained rest periods and therefore no significant change in the sample's stress state. It is thought that this softening and stiffening is due to a thixotropic type effect and the sample recovered its original stiffness because it was allowed to rest without being loaded rather than because it was allowed to drain.

The stress strain curves from the initial 1 second deviator stress pulse tests on all the samples were used to infer the required deviator stress pulse magnitudes to give resilient axial strains of 100, 200, 300, 400, and 500 microstrain in each case. Figure 6.14 shows these values of pulsed deviator stress plotted against the mean normal effective stress at the end of consolidation. The curves for the strain contours are the best fit lines drawn through the points and the origin. Table 6.2 gives the intercept for the curves if the origin is not specified and demonstrates that drawing the strain contours through the origin is a reasonable assumption. The contours get closer together as the magnitude of the resilient shear strain increases which is the result of the non-linearity in the stress strain response evident in Figure 6.13.

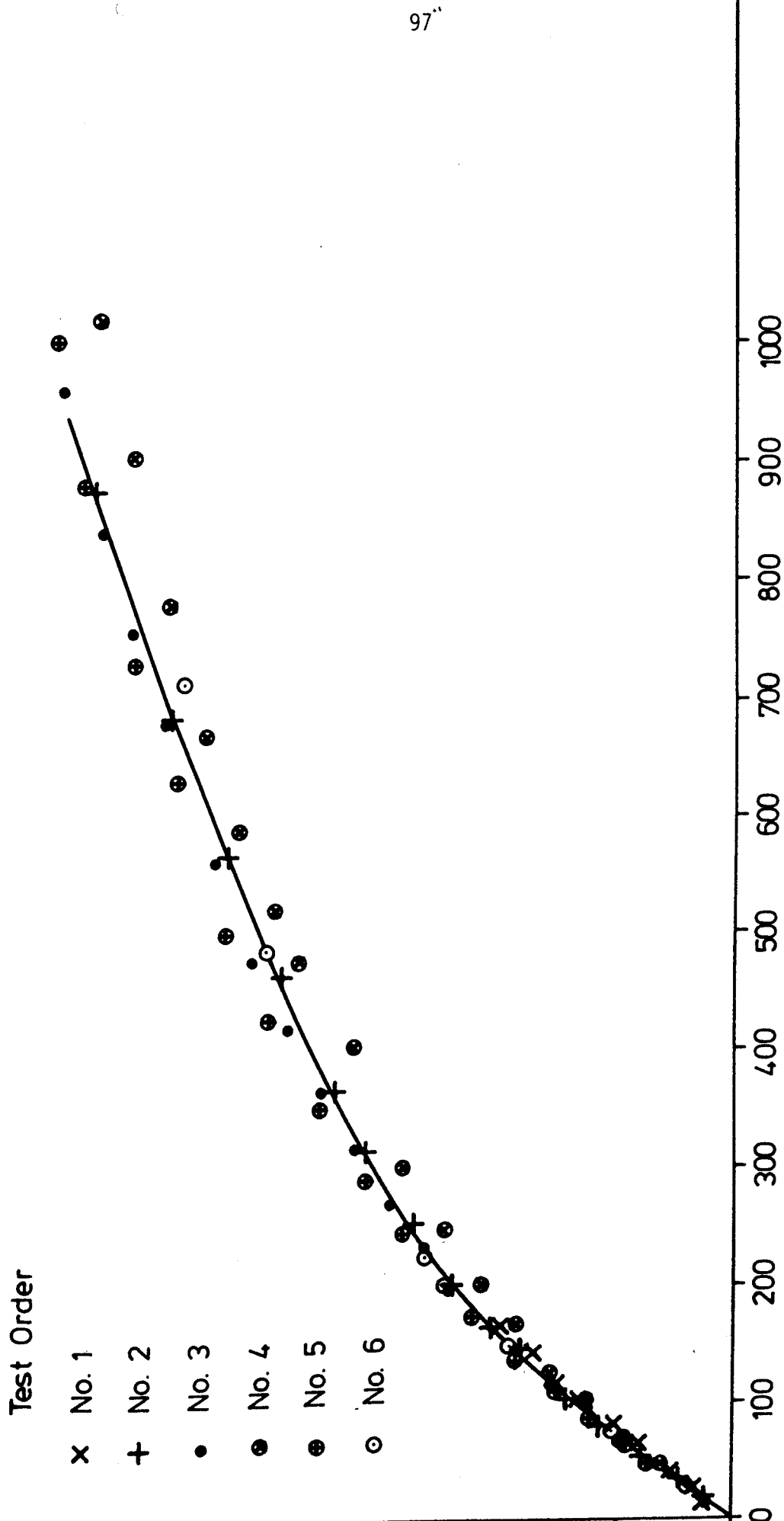

FIGURE 6.13 STRESS STRAIN RESPONSE OF SATURATED KEUPER MARL JUST PRIOR TO EACH PERMANENT STRAIN TEST. SAMPLE 100/18

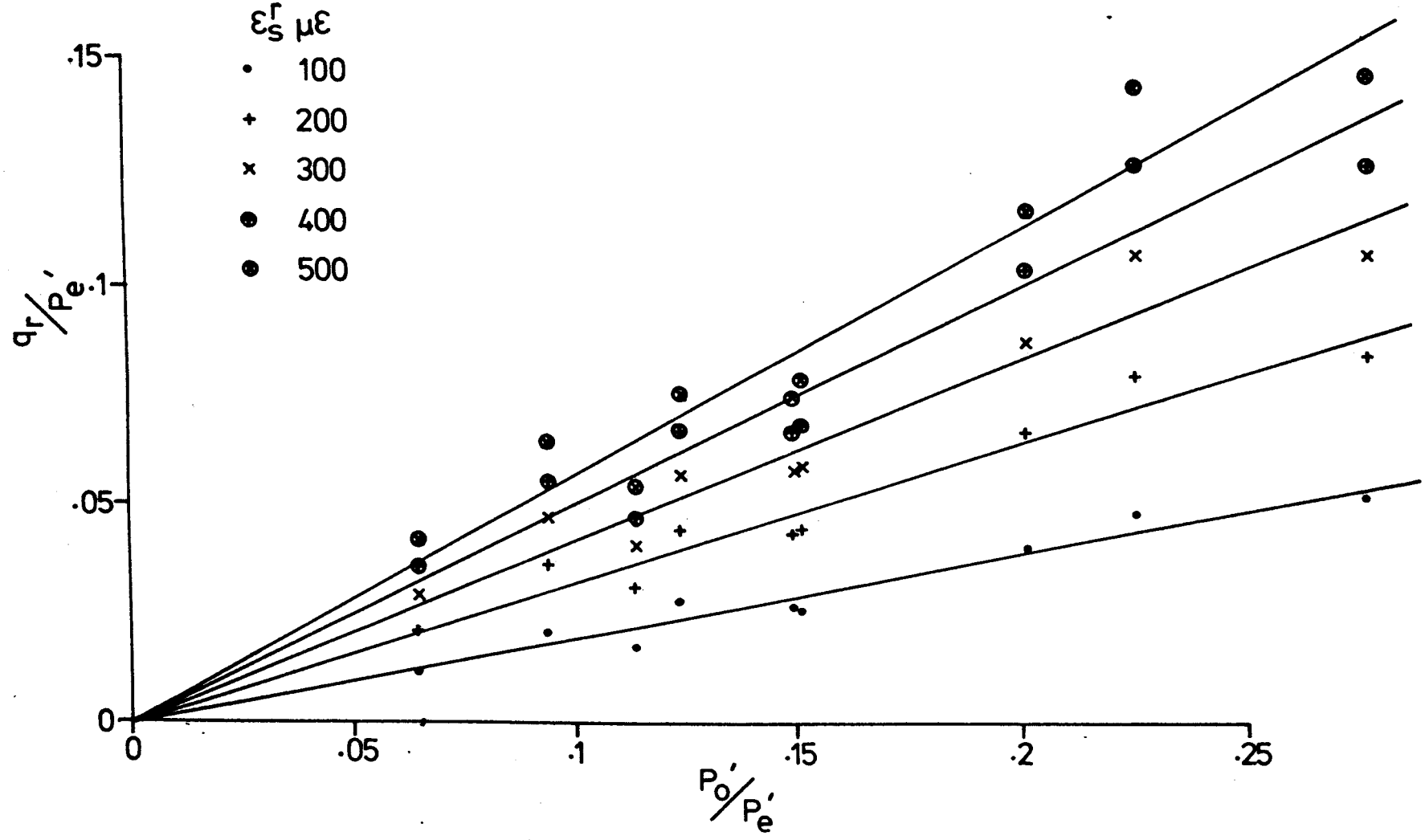

FIGURE 6.14 RESILIENT SHEAR STRAIN CONTOURS FOR CONSOLIDATED KEUPER MARL

Table 6.2 Intercept of strain contours for consolidated Keuper Marl under 1 second pulsed loading

Resilient shear strain (microstrain)	Intercept on P_o'/P_e' at $q_r/P_e' = 0$
100	0
200	-.004
300	-.007
400	-.007
500	-.004

Figure 6.15 shows the gradient of the strain contours plotted against the magnitude of the resilient shear strain. The curve is reasonably linear and leads to the relationship

$$\varepsilon_s^r = A\left[\frac{q_r}{p'_o}\right]^B \qquad 6.10$$

where A and B are material constants and are equal to 1110 and 1.552 respectively with the stresses in kPa and the strains in microstrain.

Equation 6.10 does not include the ambient deviator stress. The ambient deviator stress varied considerably for these samples and was positive in some cases. This was caused by the method of consolidation as discussed in section 6.2. However the stress paths followed by these tests are within the yield locus for these samples, and have been shown to be elastic. The ambient deviator stress is also a small proportion of the yield stress for the range of stress conditions chosen for the test programme, and therefore the ambient deviator stress is unlikely to have much effect.

An indication of the accuracy of the model, or the scatter of the results, is shown in Figure 6.16 where calculated values of the resilient strain are shown against the measured values. Approximately 90% of the results are accurate to $\pm$ 20%, which considering the type of test and the magnitude of the strains, is considered to be quite reasonable.

6.4.2 One Tenth Second Stress Pulse Tests

These tests were carried out with a constant deviator stress pulse magnitude of 0.1 second duration and were intended to investigate the development of permanent deformation and effective stress change with number of cycles. The resilient response was also monitored during these tests which covered a range of different stress levels and the stress softening behaviour was again

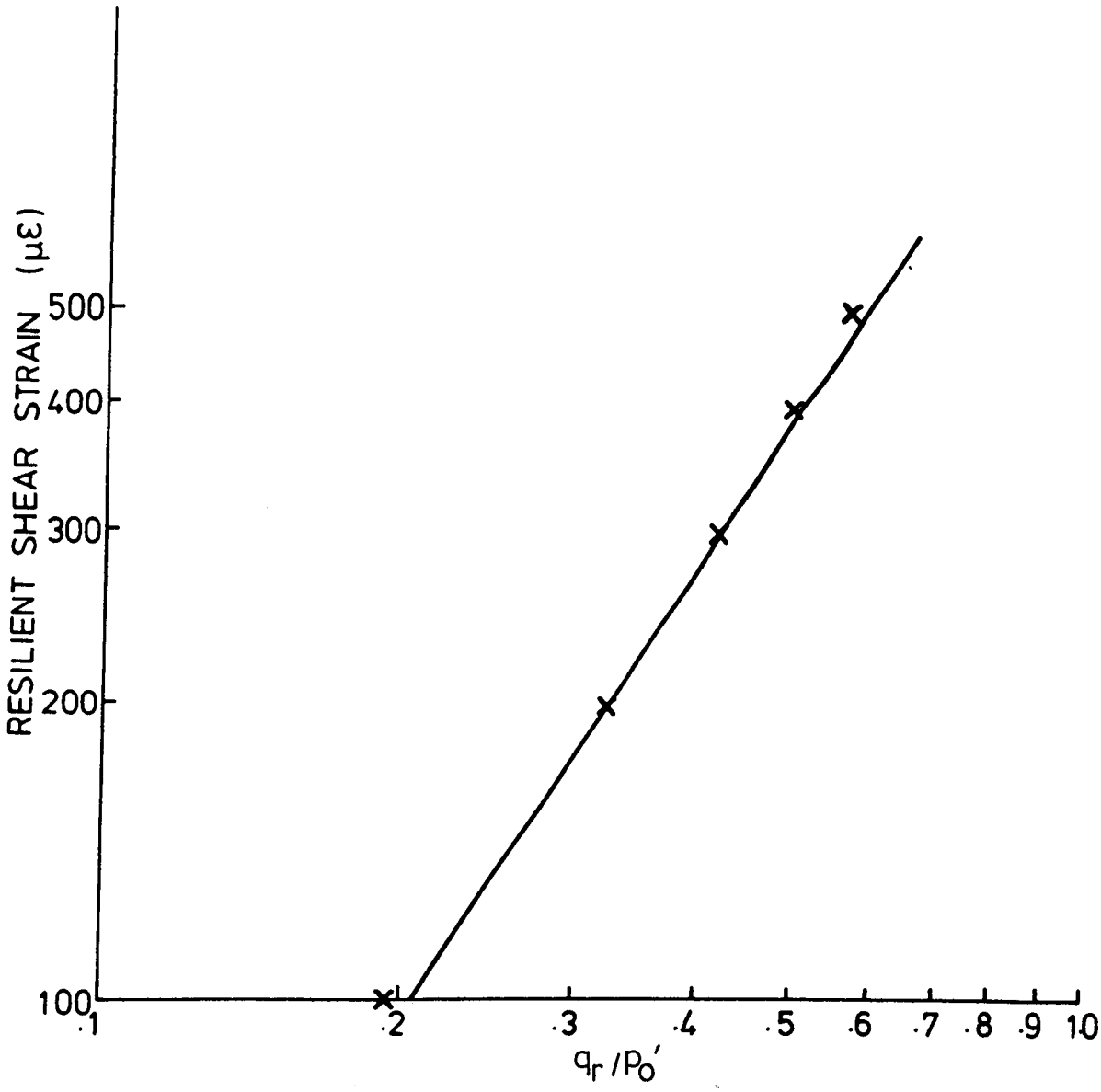

FIGURE 6.15 MODEL DEVELOPMENT FOR SATURATED KEUPER MARL SAMPLES UNDER 1 SECOND LOADING

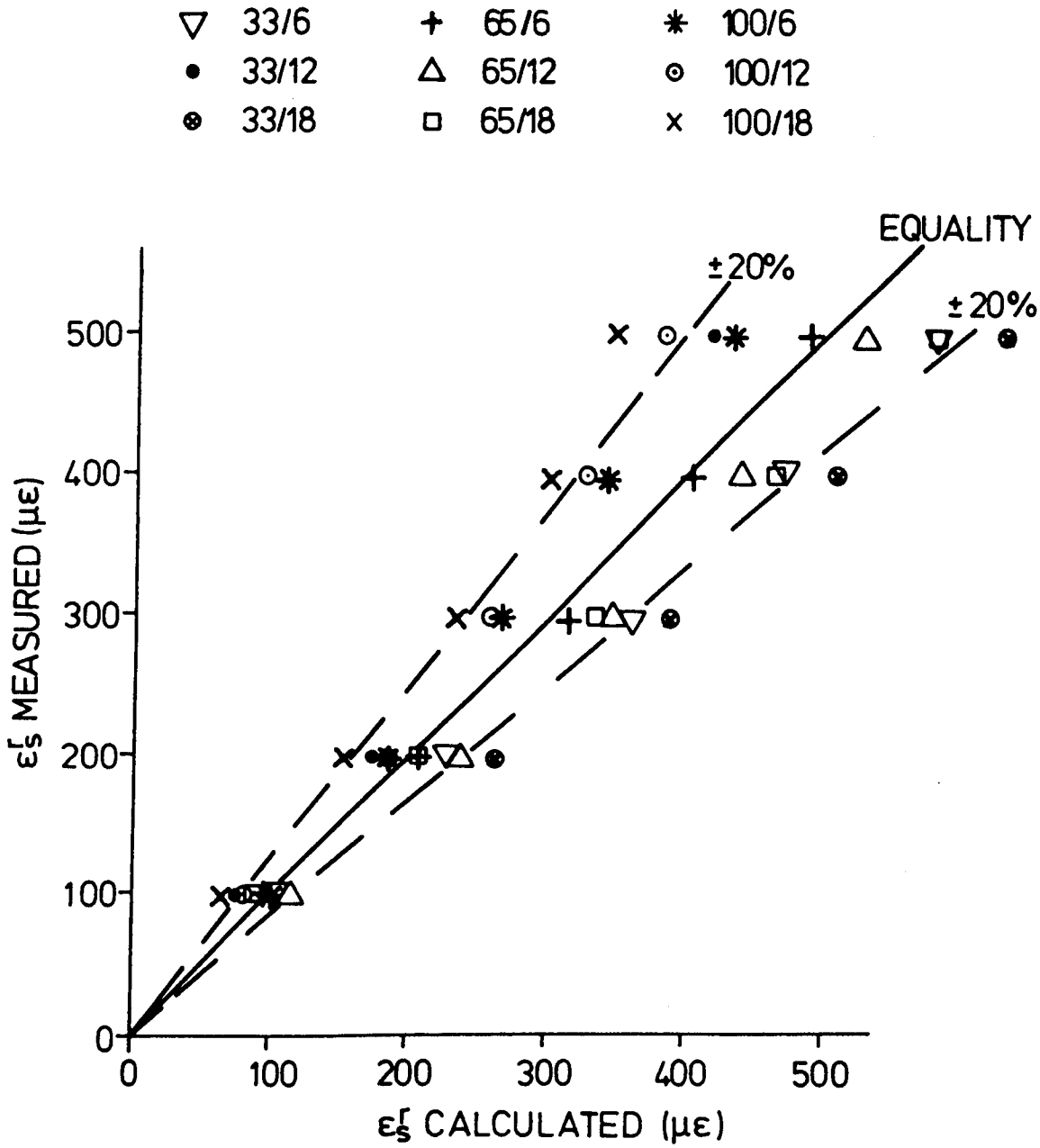

FIGURE 6.16 RESILIENT SHEAR STRAIN CALCULATED vs RESILIENT SHEAR STRAIN MEASURED

apparent. Figure 6.17 shows the pulsed deviator stress resilient axial strain response for sample 100/12, which had the largest number of different stress levels applied to it. There was insufficient data from the different samples to draw any strain contours but the results are shown in Figure 6.18 for all the tests as resilient axial strain against the deviator stress pulse magnitude divided by the mean normal effective stress. The shear strain has not been plotted as there was some doubt as to the accuracy of the radial strain measurements for this type of test. Figure 6.18 indicates that there is a linear relationship, although there is quite a scatter of results, of the form

$$\varepsilon_a{}^r = C \left[\frac{q_r}{P'_o} \right]^D \qquad 6.11$$

where C and D are material constants and are equal to 2000 and 1.62 respectively. The strain is given in microstrain.

The model is of the same form as that derived from the tests with a 1 second pulse length, but the material constants are different. One of the main factors which could influence the material constants is likely to be the stress pulse duration which controls the rate of loading.

6.4.3 Total stress path tests

These tests were carried out over a small range of low stress pulse magnitudes and low frequencies. The samples did not show any sign of stress softening, which consequently gave a constant resilient modulus for each sample tested as shown in Figure 6.19. It is unclear whether this linearity is due to the low stress pulse magnitude, or the low test frequency, or a combination of both. It is felt that the effect is due to a combination of low frequency and low stress level, and that if the stress levels had been increased whilst maintaining that frequency or the frequency increased whilst maintaining those stress levels then the stress softening effect would have been

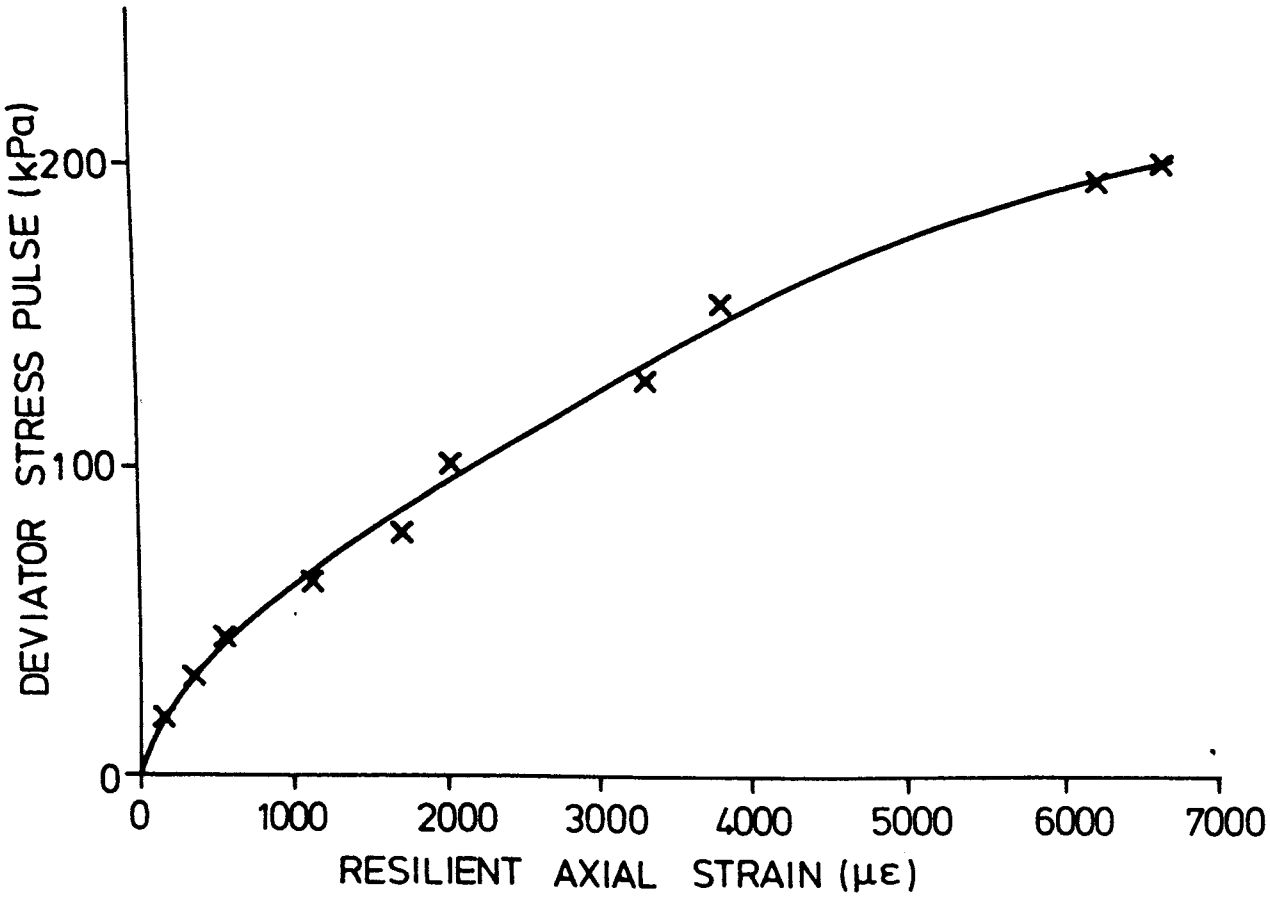

FIGURE 6.17 DEVIATOR STRESS PULSE vs RESILIENT AXIAL STRAIN FOR SAMPLE 100/12 (0.1 SECOND PULSES)

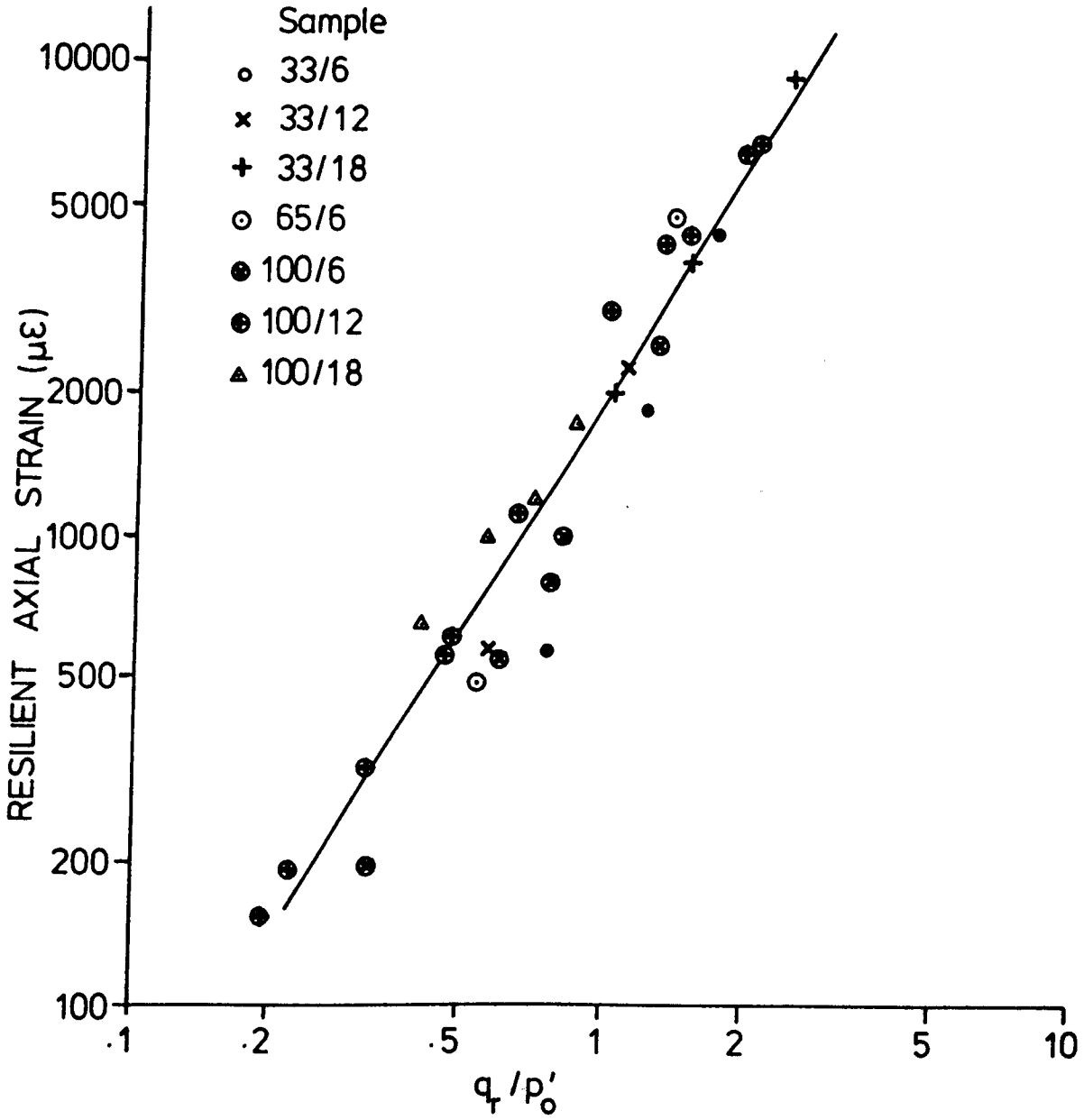

FIGURE 6·18 RESILIENT SHEAR STRAIN RESULTS FROM 0·1 SECOND STRESS PULSE TESTS

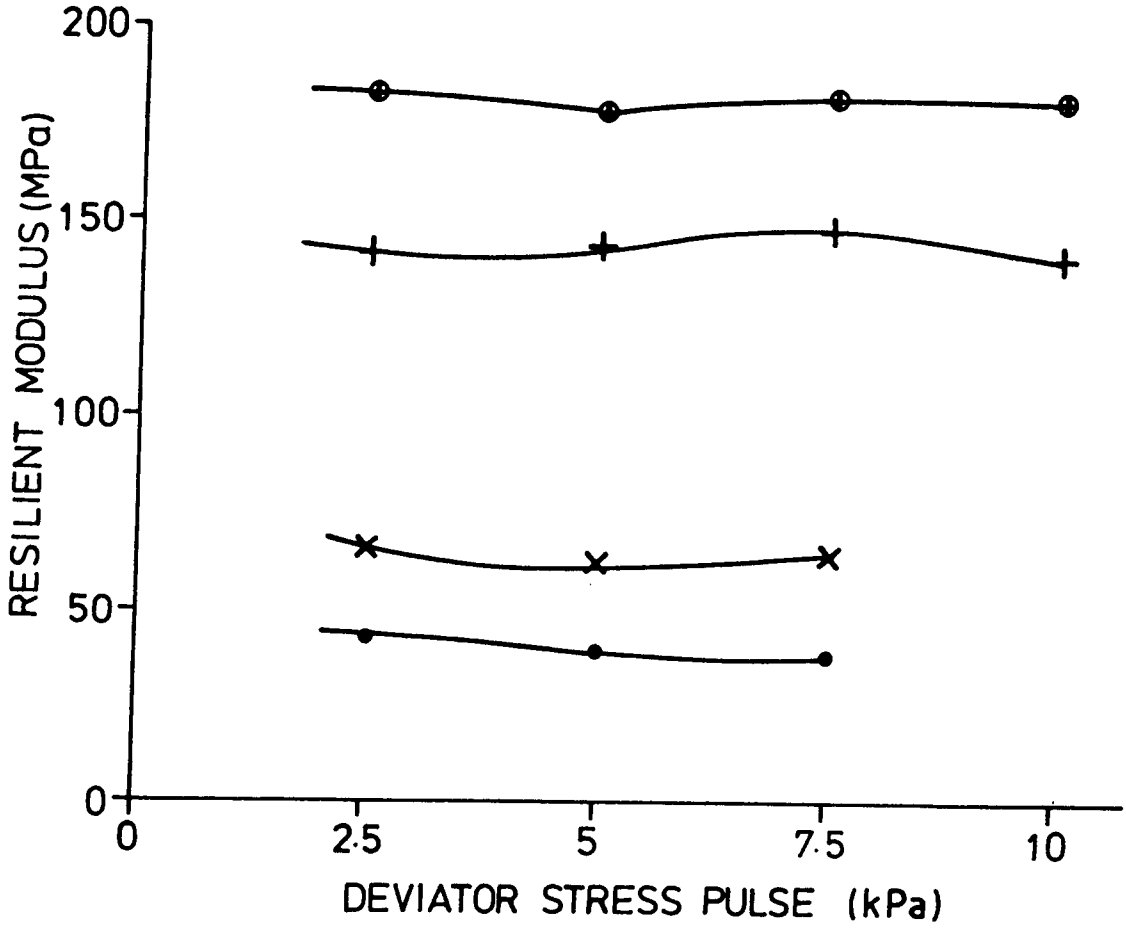

FIGURE 6·19 VARIATION OF RESILIENT MODULUS WITH STRESS PULSE MAGNITUDE -LOW FREQUENCY PULSES

apparent.

Figure 6.20 shows the results from the low frequency tests plotted as the resilient shear strain against the deviator stress pulse magnitude divided by the mean normal effective pressure. The results show good correlation and lead to an equation of the form

$$\varepsilon_s{}^r = E \left[\frac{q_r}{P'_o}\right]^F \qquad 6.12$$

where E and F are material constants and equal 690 and 1.06 respectively. The strain is given in microstrain.

6.4.4 Comparison with previous research at Nottingham

The earlier soil model was of the form

$$\varepsilon_a{}^r = \frac{q_r}{A} \left[\frac{q_r}{\sigma_r}\right]^B \qquad 6.13$$

It was developed from the results of the repeated load triaxial tests of Hyde (1974) and is described by Brown et al (1975). Hyde (1974) also presents some results attributed to Lashine (1971) and Figure 6.21 shows those results and those of Hyde replotted in the form used in this thesis. Hyde's results are measured after 10^5 cycles. It is apparent from Figure 6.21 that there is a reasonable line through all the points for each cell pressure, but that dividing by the mean normal effective stress does not result in a unique relationship. Lashine and Hyde both used an external pore pressure transducer and an external LVDT, and Lashine also used an external load cell. The external LVDT may have caused some errors in the measurement of the resilient strain, especially after 10^5 cycles when the sample may be behaving in a non uniform manner, due to the development of

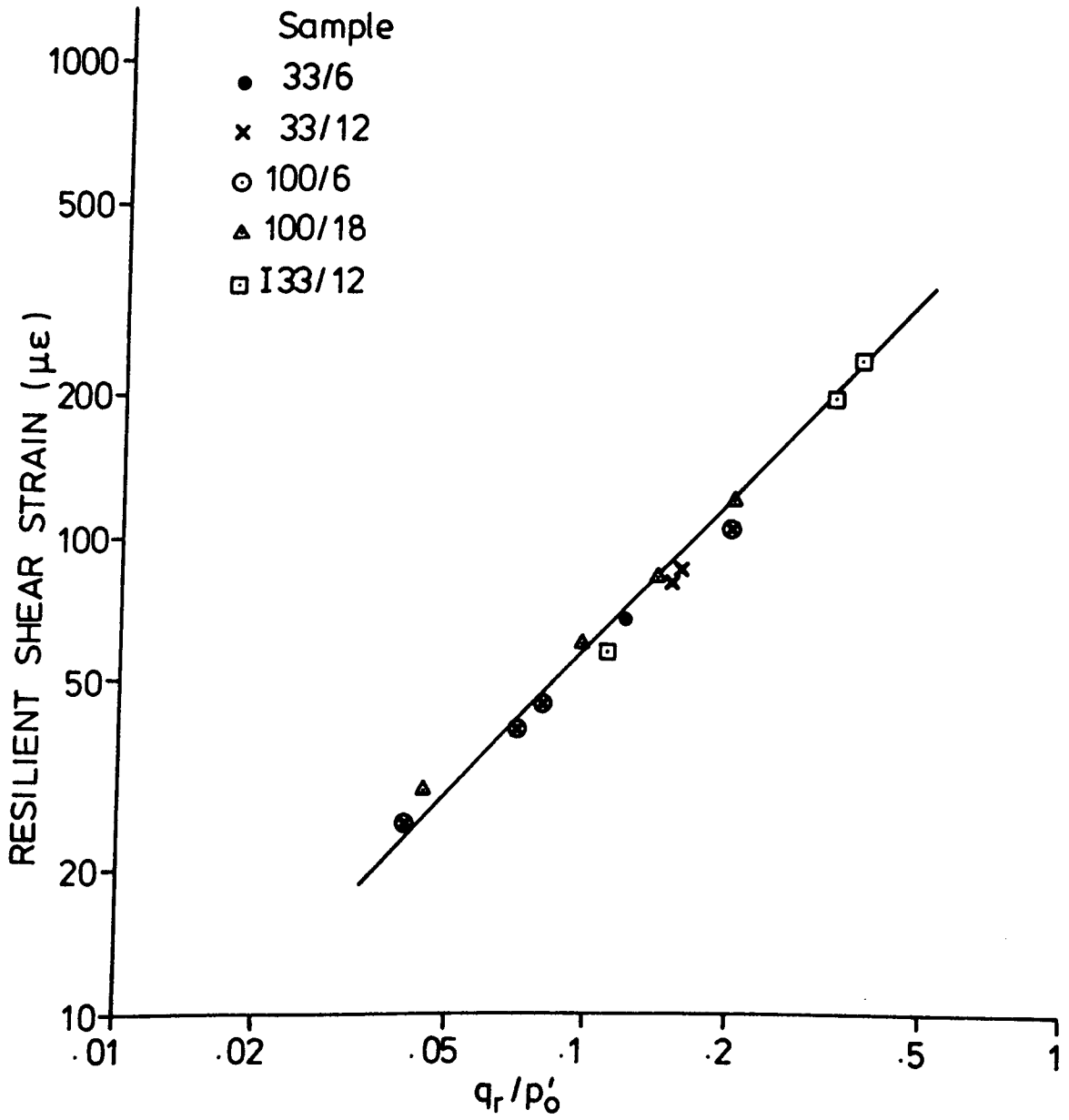

FIGURE 6.20 RESILIENT SHEAR STRAIN RESULTS FROM 20 SECOND STRESS PULSE TESTS

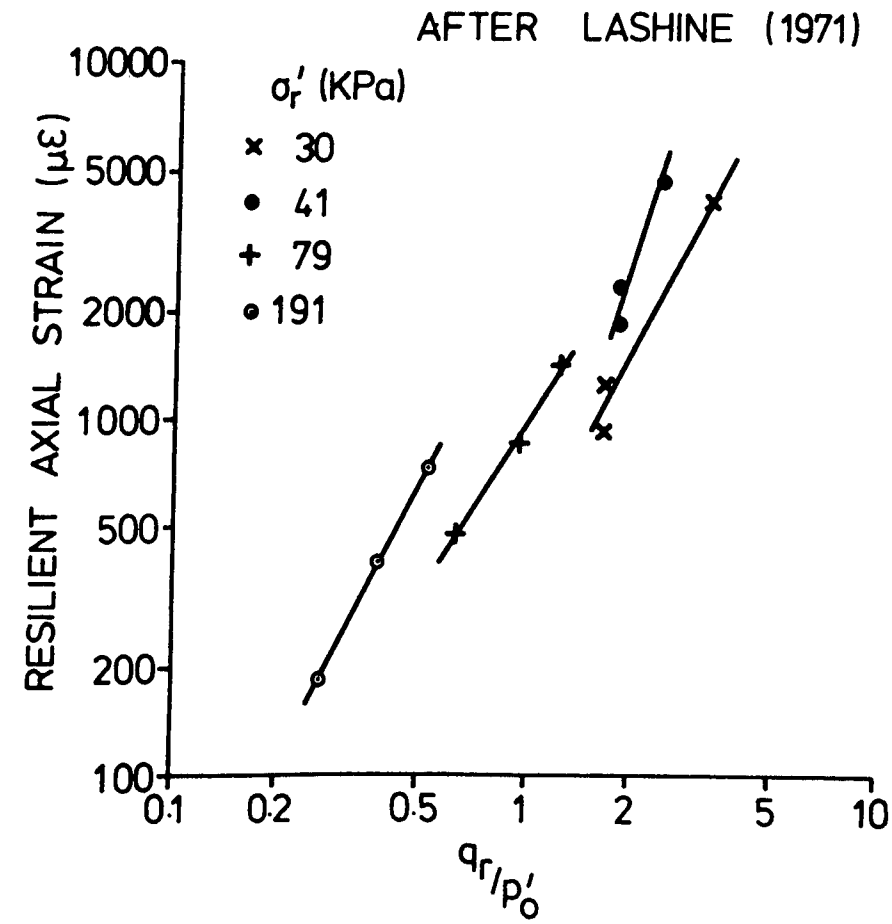

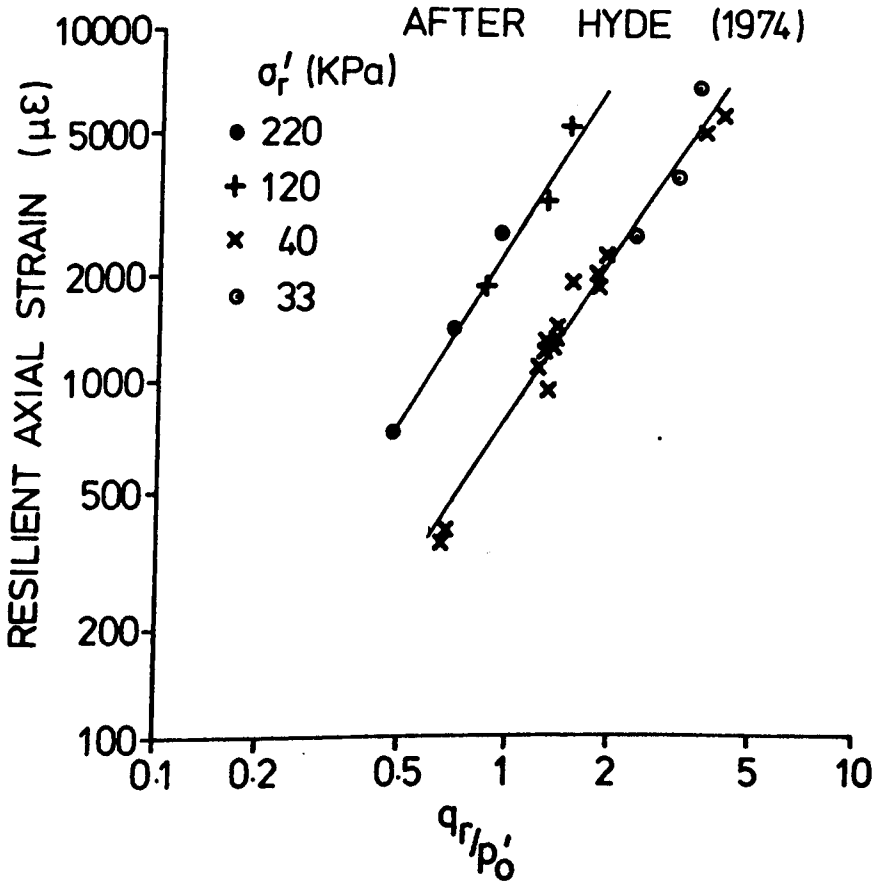

FIGURE 6·21 RESILIENT BEHAVIOUR OF KEUPER MARL AFTER LASHINE (1971) AND HYDE (1974).

permanent strain and the end effects caused by friction on the platens. There will be some errors introduced into Lashine's results from friction on the bearing through the cell top.

It is considered by the author that the difference in behaviour is unlikely to be due to the fact that Hyde's and Lashine's samples were isotropically consolidated, as the results indicate that the anisotropically consolidated samples were behaving istropically and that the resilient behaviour is independent of moisture content. Overy (1982) also found that the stress paths to failure for isotropically overconsolidated and anisotropically overconsolidated samples were similar. The differences therefore are more likely to be due to the different, and more accurate, measuring systems used in this research.

6.4.5 Discussion of resilient model

A simple model of the form

$$\varepsilon_s{}^r = A \left[\frac{q_r}{P'_o} \right]^B \qquad 6.14$$

has been shown to fit the experimental results from the different tests on the overconsolidated saturated Keuper Marl samples. Stress pulses of three different durations were used with a range of different stress pulse magnitudes for each pulse length. The values of A and B were found to differ for each of the three stress pulse lengths. Table 6.3 gives the values of A and B together with the length of the stress pulse and the variation in deviator stress pulse magnitude divided by the mean normal effective stress. There is some overlap in the stress pulse magnitudes for each test as expressed in the form q_r/P'_o and the values of A and B were found to increase as the duration of the stress pulse decreases. The results show that as the duration of a particular stress pulse decreases i.e. the rate of loading increases, then the stiffness of the sample increases. This was as expected and is in agreement with the findings of other

Table 6.3 Model details from tests on overconsolidated Keuper Marl

Model form $\varepsilon_s^r = A\left[\frac{q_r}{p'_o}\right]^B$ (microstrain)

Duration of stress pulse secs	q_r/p'_o		A	B
	min value	max value		
20	0.04	0.36	690	1.061
1	0.2	0.57	1110	1.522
0.1	0.2	2.5	2000	1.62

researchers. The soil has been shown to be behaving elastically, certainly in the range of stress pulse magnitudes that are covered for all three frequencies, and therefore the variation in A and B is likely to be due to the change in frequency rather than the change in stress pulse magnitude. However a plot of A or B against frequency shows no apparent simple relationship.

6.5 SAMPLE BEHAVIOUR UNDER REPEATED LOADING

6.5.1 Introduction

The development of permanent strain and change in pore pressure under large numbers of constant amplitude pulsed loads of 0.1 second duration was investigated in this section of the test programme. Generally each test was allowed to run until it was judged that equilibrium had been attained or the sample had failed. An average of approximately 400,000 stress pulses were applied to each sample at each pulsed stress level.

The response of the sample to the loading sequence was difficult to define accurately as the equipment was not capable of maintaining the constant ambient deviator stress required during the test period, although the cyclic component was in fact reasonably constant except at high amplitudes. It is thought that the variation in deviator stress was caused by two separate effects. The first was a drift in the control system over a period of time which caused slow changes in the deviator stress level. The second was sudden pulsed loads caused by electrical interference which affected the control system. The interference could have been airborne or in the mains supply and would have been caused by other items of electrical equipment in the laboratory switching on and off. This had the effect of applying an unknown and uncontrolled stress pulse to the sample, after which the system would stabilise close to the original stress conditions, although it may have caused significant strains and pore pressures to develop.

6.5.2 Development of Permanent Strain

As described previously the change in ambient deviator stress affected the strains recorded during each test and typical results of axial strain against the logarithm of the number of cycles is shown on Figure 6.22. Also shown is the change in ambient deviator stress and it is apparent that there is good correlation between the peaks and troughs in the stress and strain curves.

Figures 6.23 and 6.24 show the results of all the permanent strain tests on samples 100/6 and 100/18 respectively, and indicate that the lower repeated stress levels have little effect on the sample, but that above a certain level the sample begins to deform. It is interesting to note that sample 100/6 showed a continuous build up of permanent strain which then accelerated to failure, while sample 100/18 showed very little development of permanent strain initially, and then failed suddenly. The results generally tend to support the proposition of a threshold stress level, loading above which causes the sample to fail by a build up of permanent deformation.

Figure 6.25 shows the permanent strain against the logarithm of the number of cycles for the highest stress level applied to each of the samples tested under these conditions. Apart from sample 100/18 there is a gradual build up of strain with numbers of cycles, although there is evidence of drift and interference in the load control system.

Figure 6.26 shows the effective stress paths for the tests shown on Figure 6.25. The paths are based on the peak pore pressure recorded by the centre probe from each of the stress levels applied to that sample at that frequency. The base pore pressure probe was unable to follow the stress pulse at these frequencies, see Appendix C. Samples 33/18, 100/6 and 33/6 failed under the repeated loading with a reasonably steady build up of strain, the rate of which then increased to failure. Sample 100/12 did not fail and sample 100/18 failed quite suddenly after a relatively

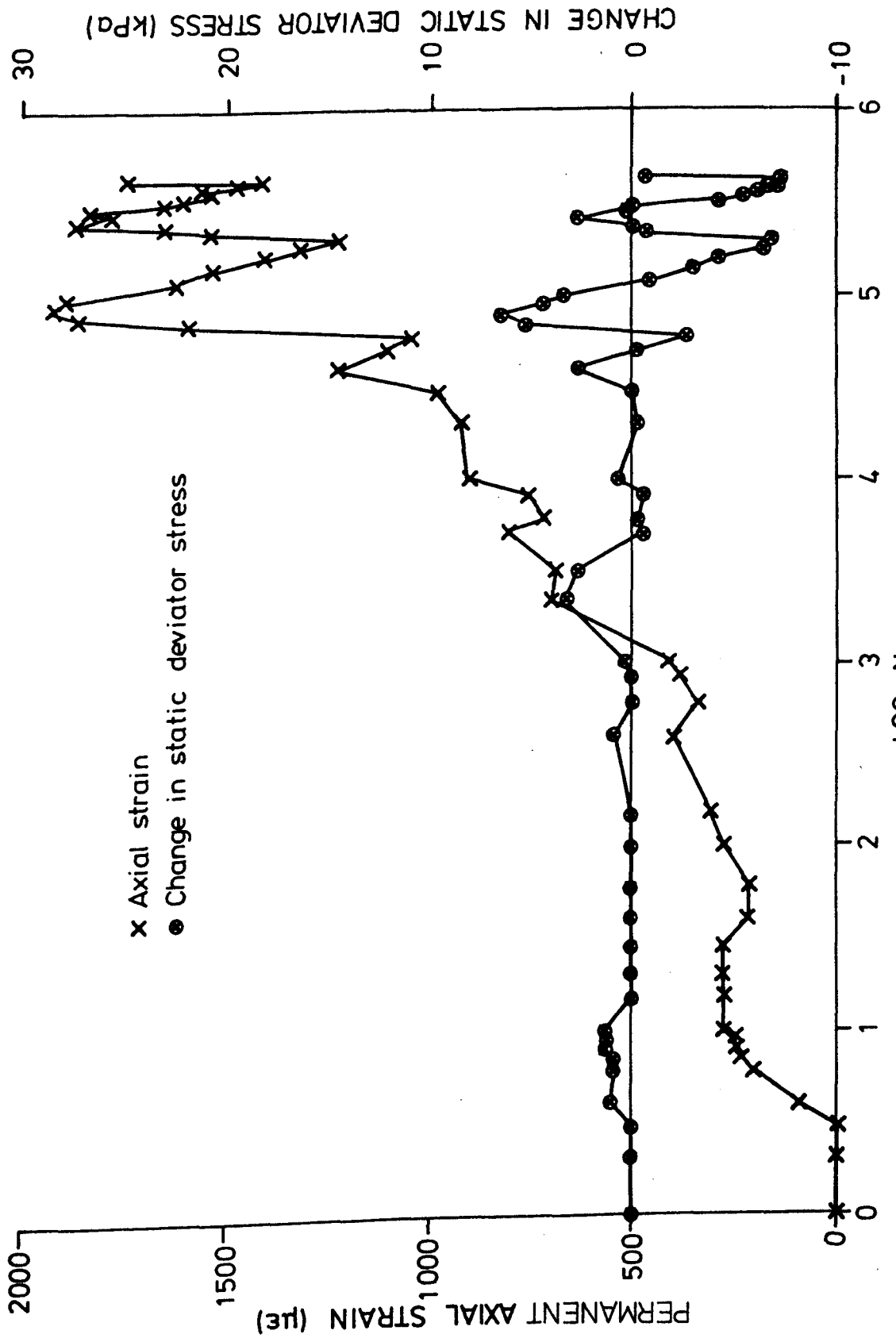

FIGURE 6.22 TYPICAL PERMANENT STRAIN vs LOG CYCLE NUMBER SHOWING THE EFFECT OF THE VARIATION IN THE STATIC DEVIATOR STRESS

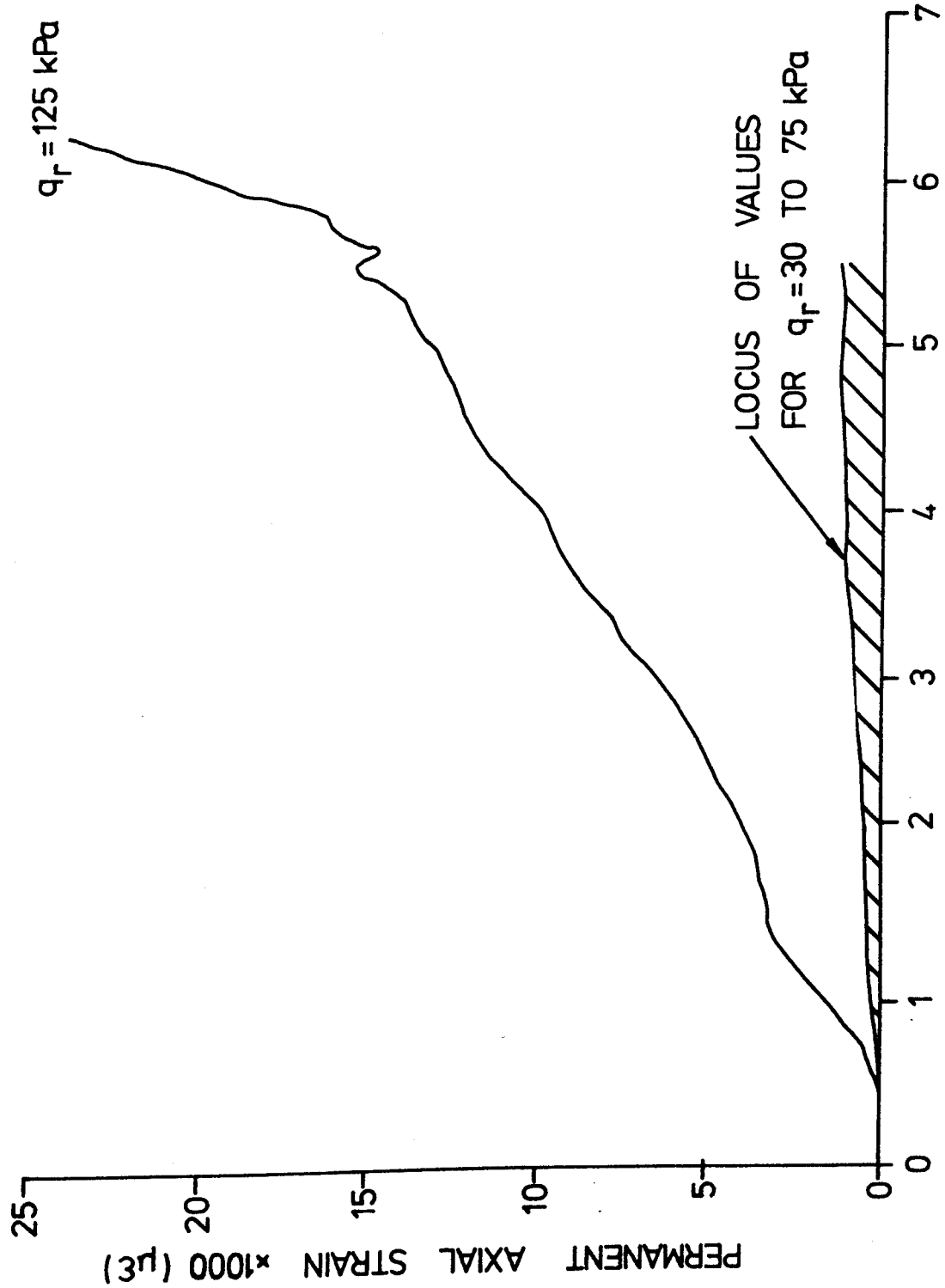

FIGURE 6.23 PERMANENT STRAIN DEVELOPMENT WITH NUMBER OF LOAD PULSES FOR SAMPLE 100/6

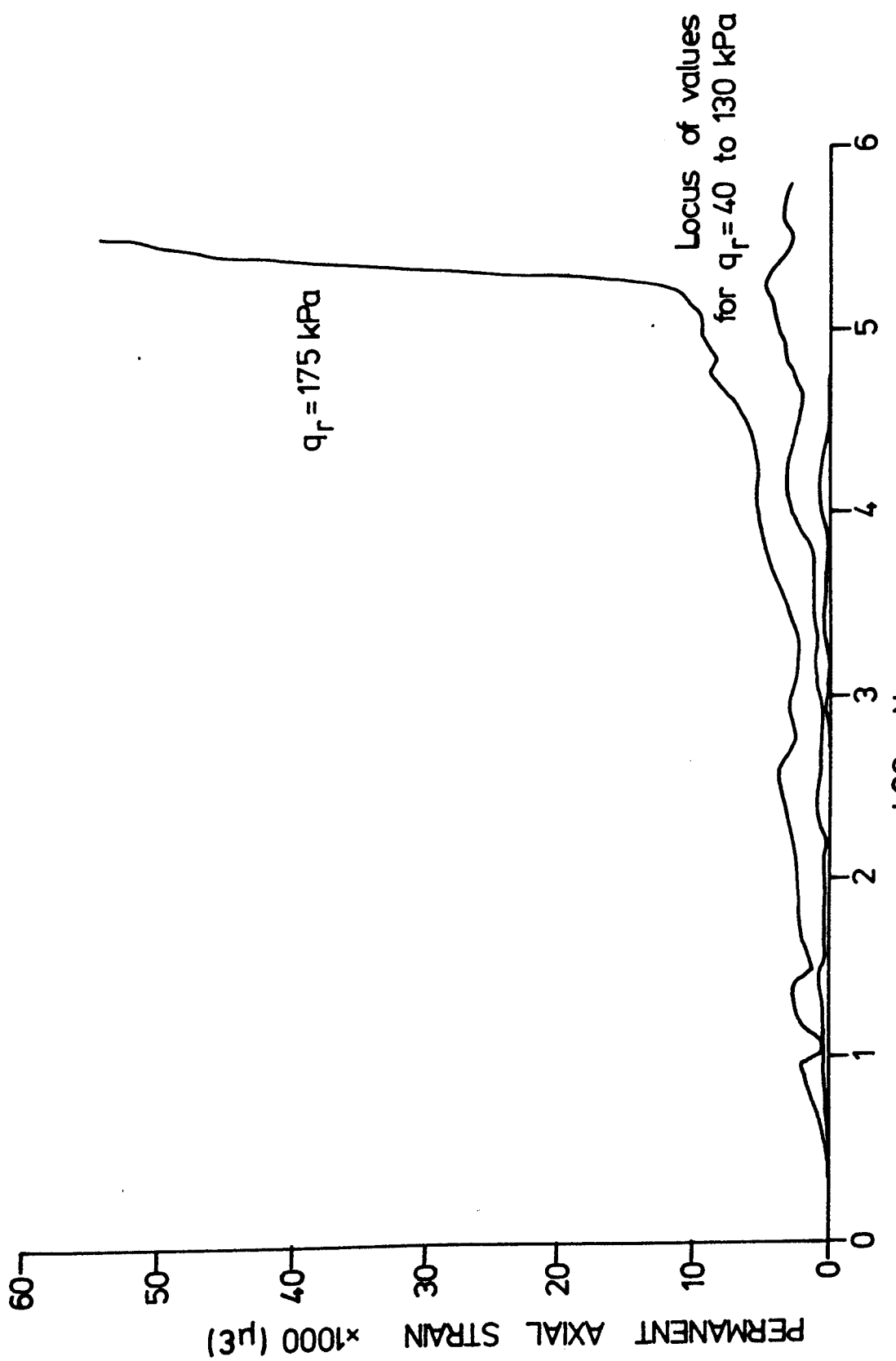

FIGURE 624 PERMANENT STRAIN DEVELOPMENT WITH NUMBER OF LOAD PULSES FOR SAMPLE 100/18

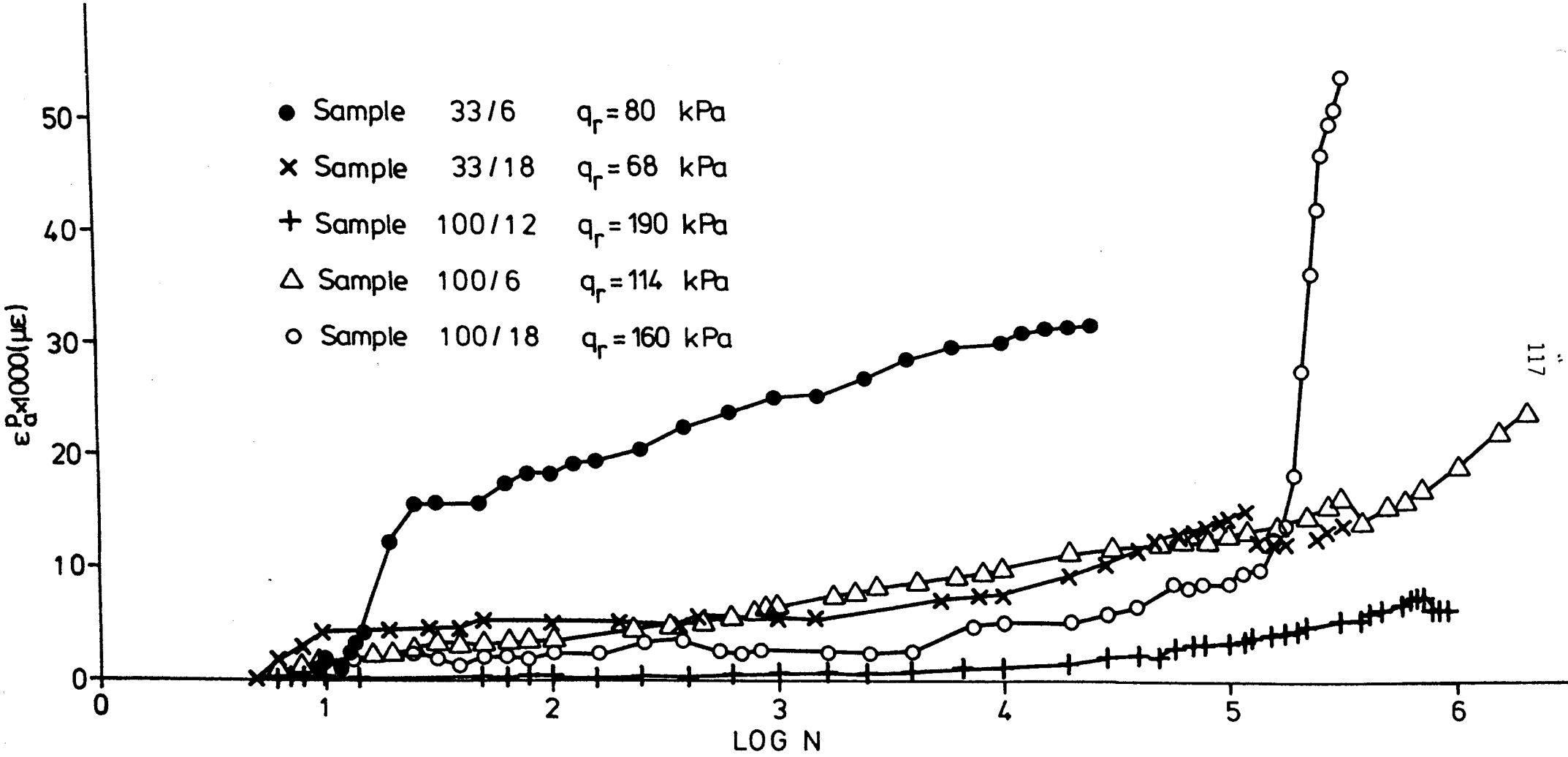

FIGURE 6.25 DEVELOPMENT OF AXIAL STRAIN vs LOG CYCLE NUMBER FOR SATURATED SAMPLES OF KEUPER MARL

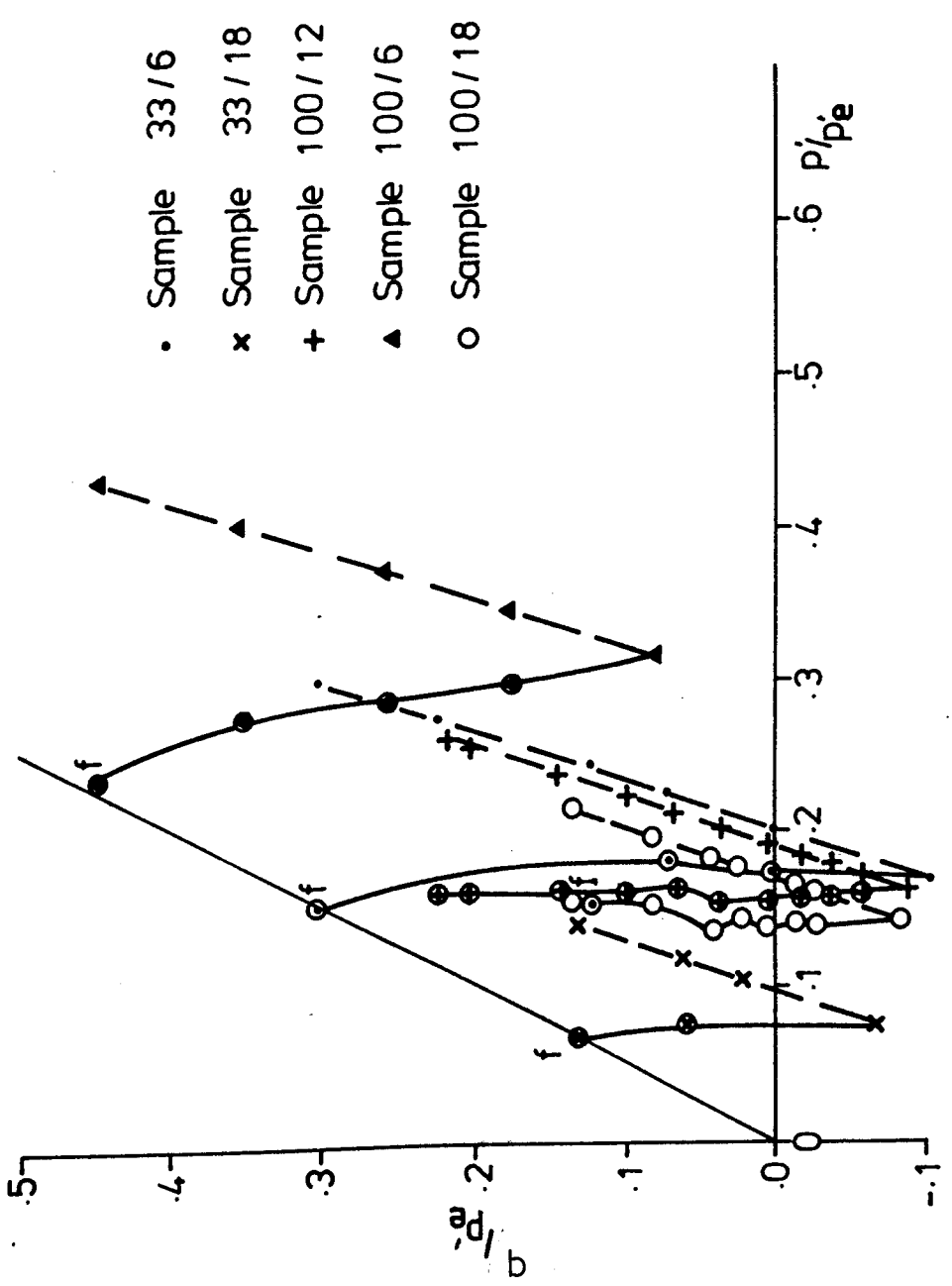

FIGURE 6.26 NORMALISED EFFECTIVE STRESS PATHS FOR SATURATED SAMPLES OF KEUPER MARL

small build up of strain. This may have been caused by interference. Figure 6.26 suggests that there is a threshold stress which can be expressed as a single line on the normalised plot, and that effective stress paths crossing this line are likely to cause excessive deformation and eventually failure, as was the case for samples 33/18, 100/6 and 33/6. Effective stress paths approaching this line are likely to cause significant deformation, as sample 100/12.

The mean normal effective stress paths tend to become curved as they approach the failure level, although it is not clear if this is a true measurement, or if it is due to inaccuracies of measurement when the sample deformations become large and the pulsing of the load ram affects the cell pressure. At large deformations it is also unlikely that the sample is behaving uniformly.

6.5.3 Development of pore pressure

The pore pressure was monitored during the tests using the base and centre pore pressure probes. The lack of any significant pore pressure development during any of the tests except those at the highest stress level corresponds to the lack of any permanent strain development and supports the supposition that the samples are generally behaving elastically. There was no significant volume change recorded in the drained rest periods between tests at the lower stress levels, which is as expected as there was negligible pore pressure development. The volume change measuring system could resolve to 0.01 cm^3. There was no evidence that the sample states progressed to equilibrium positions determined from the previous stress history as reported by Sangrey et al (1969) and discussed in Chapter 2.

Figure 6.27 shows the change in ambient pore pressure as measured by the centre probe for the samples tested with the highest repeated deviator stress. The tests are the same as those shown in Figure 6.25. The general trend is for a negative excess pore pressure to develop, although the magnitudes recorded

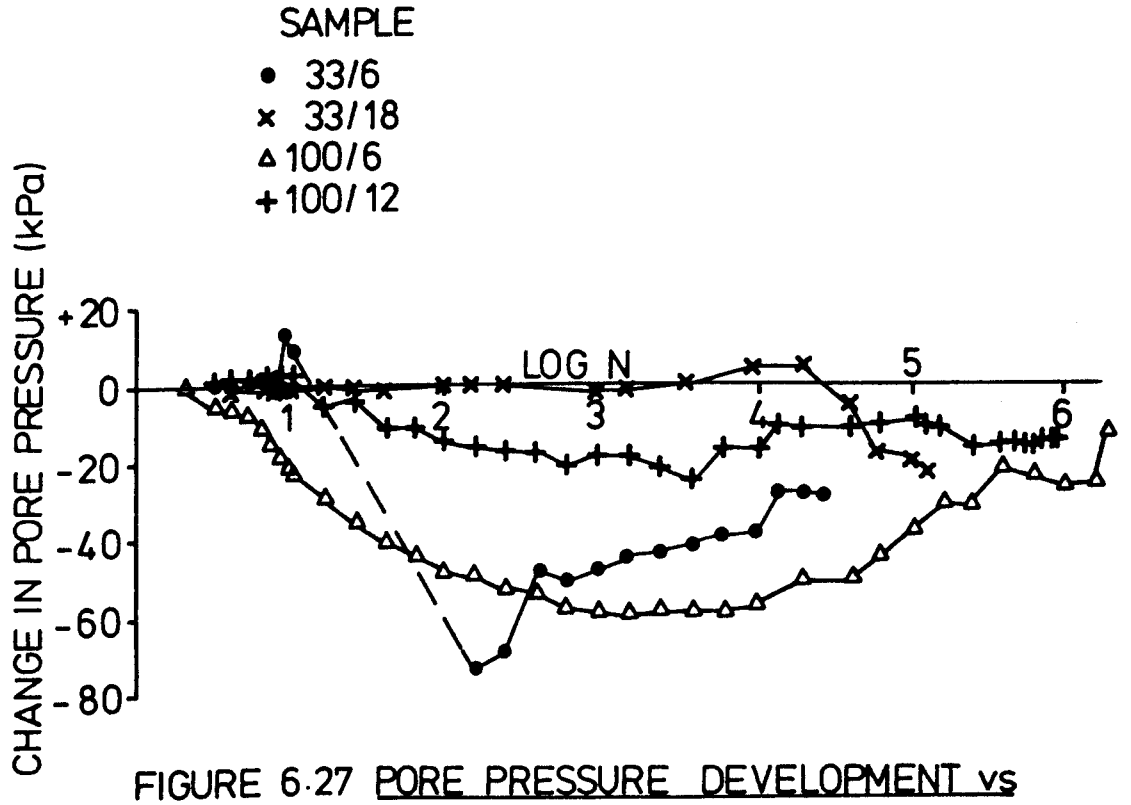

FIGURE 6·27 PORE PRESSURE DEVELOPMENT vs NUMBER OF LOAD APPLICATIONS FOR CONSOLIDATED KEUPER MARL SAMPLES. CENTRE PROBE

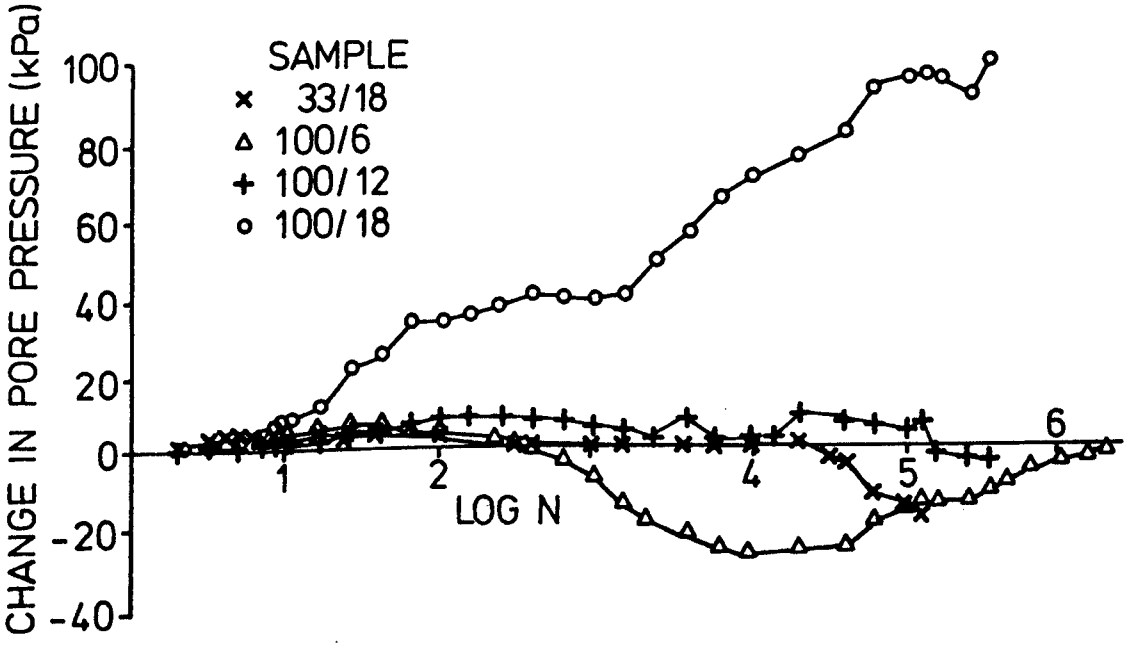

FIGURE 6·28 PORE PRESSURE DEVELOPMENT vs NUMBER OF LOAD APPLICATIONS FOR CONSOLIDATED KEUPER MARL SAMPLES. BASE PROBE

and the rate of development are all very variable. The pore pressure also changed as the ambient deviator stress changed which masked the behaviour under cyclic loading. The change in both axial strain and pore pressure for sample 33/6 shown in Figures 6.25 and 6.27 respectively are examples of this. Unfortunately the centre pore pressure probe had failed in sample 100/18 and the change in the centre pore pressure just prior to the sudden failure, see Figure 6.25, was not recorded.

Figure 6.28 shows the change in ambient pore pressure as measured by the base probe for the same tests as shown in Figure 6.27. All samples showed an initial positive excess pressure, which is opposite to that recorded by the centre probe, which either continued to build up or decreased and became negative, depending on the sample. All the samples were overconsolidated sufficiently to be on the dry side of critical where a negative excess pore pressure would be expected on shearing. Figure 6.28 shows that one of the samples with the highest overconsolidation ratio, sample 100/18, in fact recorded the highest positive excess pore pressure. Unfortunately the centre pore pressure transducer in this sample was not working. It is the opinion of the author that the base probe is affected considerably by sample non uniformity caused by the end restraint when the sample begins to deform, and that the centre probe gives a more accurate measure of the pore pressure. However overconsolidated samples develop negative excess pore pressure when sheared which tends to cause non uniformity in the sample generally and leads to discrete failure planes, in which case a centre pore pressure probe is unlikely to provide a true measure of the pore pressure as the sample fails.

6.5.4 Variation in Resilient Modulus with numbers of Cycles

Generally the resilient modulus was found to remain fairly constant with number of stress applications for low level deviator stress pulses, and to decrease with increasing number of cycles as the deviator stress pulse magnitude increased as shown on Figure 6.29. It is interesting to note that the greatest

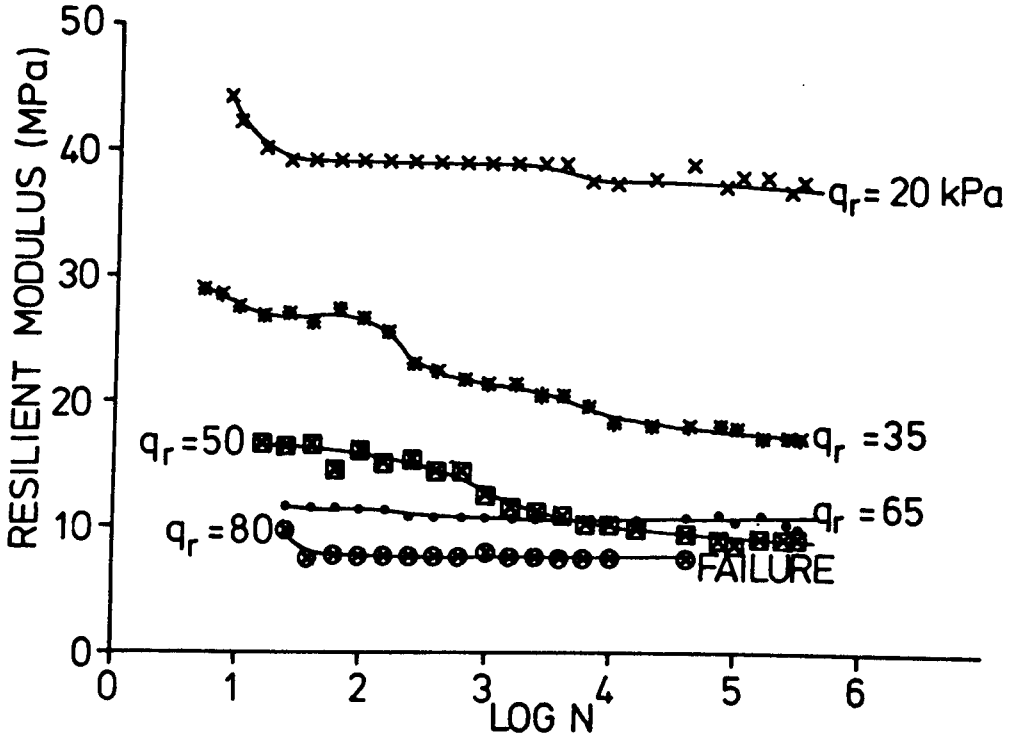

FIGURE 6.29a VARIATION OF RESILIENT MODULUS WITH NUMBER OF CYCLES FOR SAMPLE 33/6

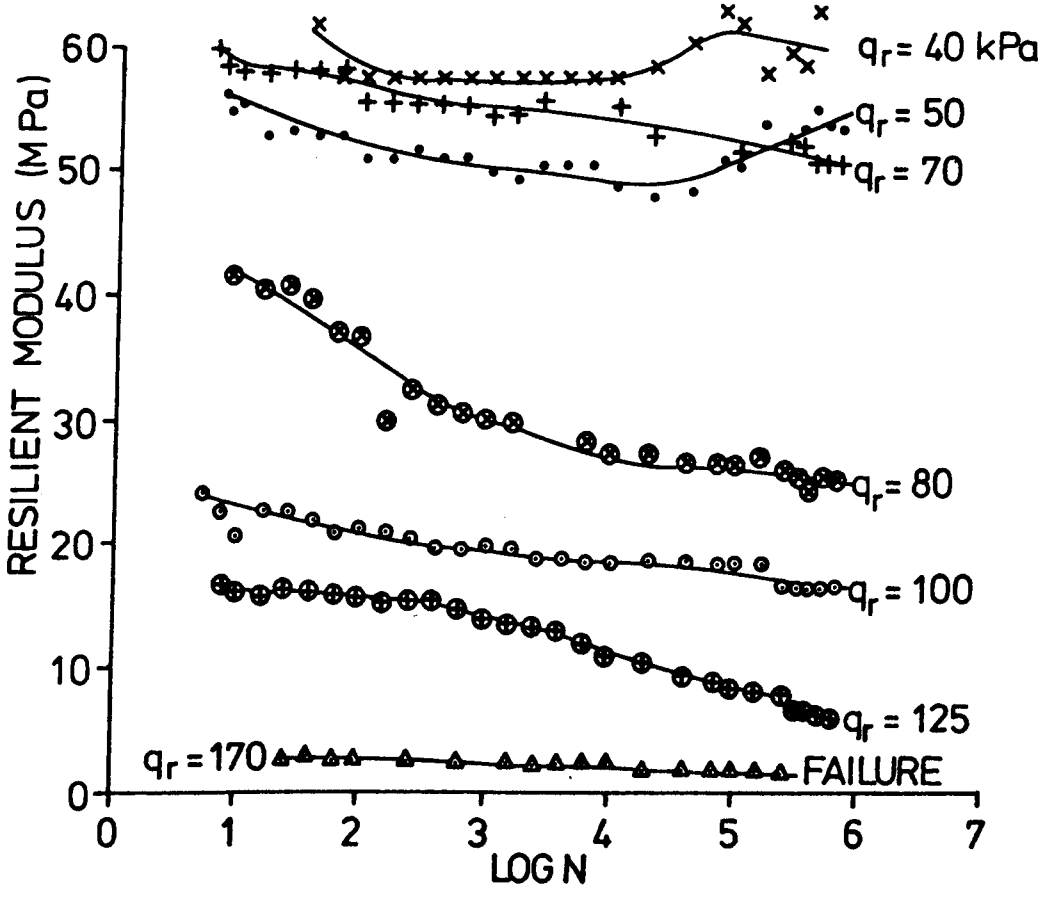

FIGURE 6.29b VARIATION OF RESILIENT MODULUS WITH NUMBER OF CYCLES FOR SAMPLE 100/18

reduction in resilient modulus occurred for the midrange deviator stress pulse magnitudes, and that the resilient modulus remained fairly constant during the tests at the deviator stress pulse magnitude which caused failure for samples 33/6 and 100/18.

The rate of change of deviator stress with number of cycles appears to be reasonably constant for a particular value of deviator stress pulse magnitude, and these results do not suggest any relationship between this rate and the magnitude of the deviator stress pulse. Hyde (1974) reported some results from similar tests on isotropically overconsolidated samples of Keuper Marl. Hyde used a smaller range of repeated deviator stresses, which were generally higher than those used in this research. Hyde demonstrated that the modulus decreased with increasing stress pulse magnitude, and that those samples with the smaller repeated deviator stress showed the greatest reduction in resilient modulus with increasing number of cycles.

The effects described above may be due to the thixotropy of the material, as it is the energy input from the external applied loading which breaks down the thixotropic bonds. Under low external loads the thixotropic bonds remain essentially intact and the modulus therefore remains constant. As the external loading increases in magnitude the thixotropic bonds begin to be disrupted and the sample becomes softer. As the magnitude of the loading increases the number of stress applications required to break the majority of the bonds reduces until at high external loads, i.e. those approaching the failure level, the bonds are all broken in the first few cycles.

The first few cycles for each repeated stress level are not shown in Figure 6.29 as the applied stress level was being adjusted and any change in thixotropic behaviour was masked by the nonlinearity of the stress strain response.

6.6 UNDRAINED STRENGTH

Three samples were loaded to failure at a constant rate of deformation. The tests were undrained and a rate of deformation of 0.1mm/min was used. Figure 6.30 shows the deviator stress-axial strain plot and the excess pore pressure axial strain plot. The deviator stress plots do not show the peak and residual strength normally associated with overconsolidated material. The curves show a general shape of an initial stiff section followed by an approximately linear, much less stiff section, followed by a flat section at failure where the deviator stress no longer increases with increasing strain. It is thought that the initial stiff section is where the stress path is within the yield surface defined by the Hvorslev surface, and that the first change in behaviour is when the effective stress path reaches the Hvorslev surface and curves to follow that surface. The second change in behaviour, then, would be when the sample reaches the critical state at the intersection of the Hvorslev and Roscoe surfaces.

Figure 6.31 shows the stress paths plotted in normalised stress space with the stresses indicated at which the changes in behaviour occurred. The curves show a similar shape but there is some variation in the failure points and the curves do not follow a single line up to failure. It is thought that this is due to the non uniformity present in overconsolidated samples once yield has occurred. The initial yield points marked on the curve seem a little low to coincide with the Hvorslev surface. Although Hyde (1974), Overy (1982) and Hyde and Ward (1985) were all working with Keuper Marl the various material parameters quoted differ and so does the location of the critical state point in nomalised q-p' stress pace. The material used by Hyde and Ward is closest in terms of the Atterberg limits and the clay content, and Figure 6.31 shows the Hvorslev surface drawn from their failure tests. It is apparent that the results agree quite reasonably though all the results tend to show a scatter and sample failure before the critical state is attained. Hyde and Ward plot the critical state at a value of the normalised mean

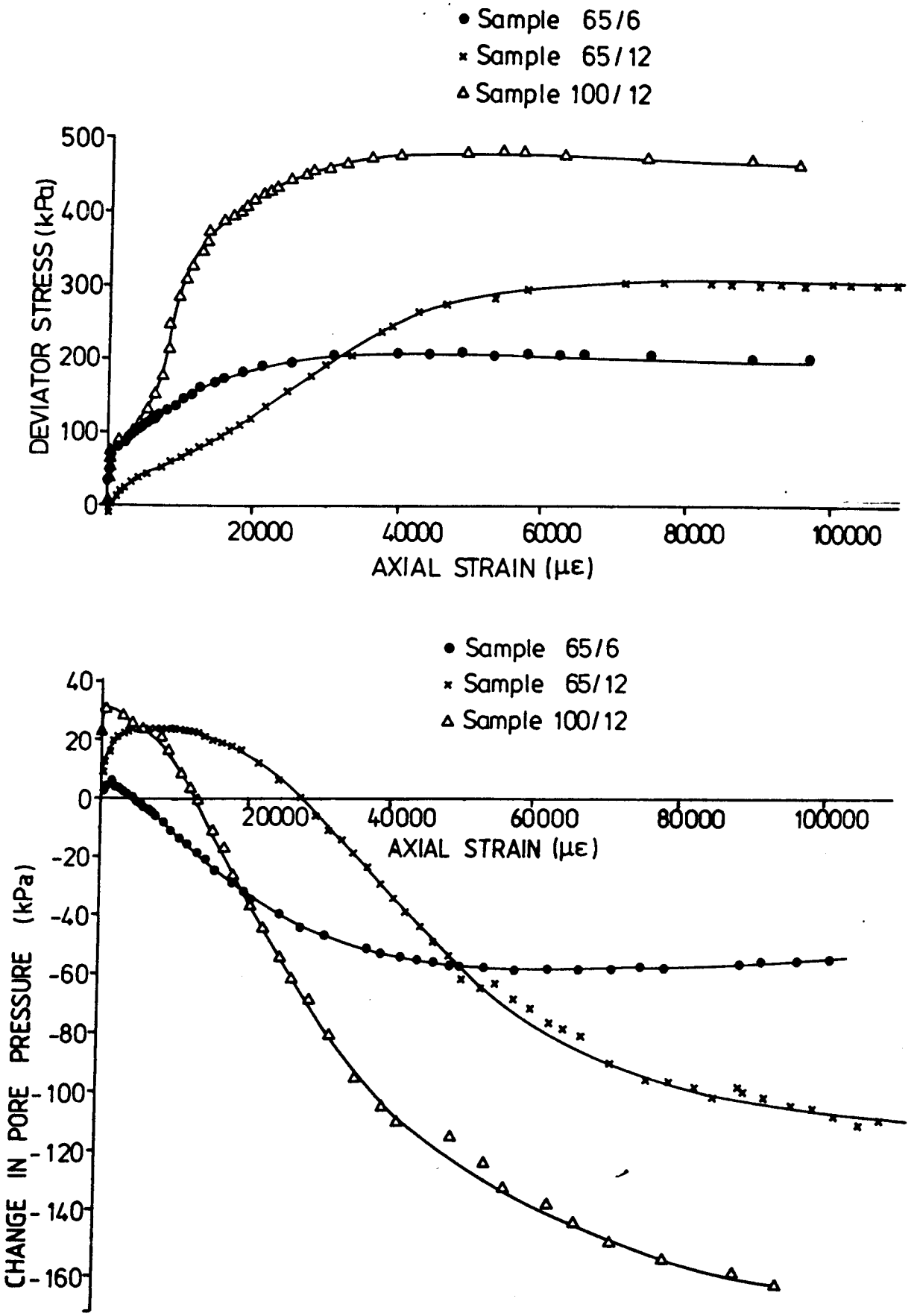

FIGURE 6.30 DEVIATOR STRESS AND EXCESS PORE PRESSURE vs AXIAL STRAIN FOR UNDRAINED STRENGTH TESTS

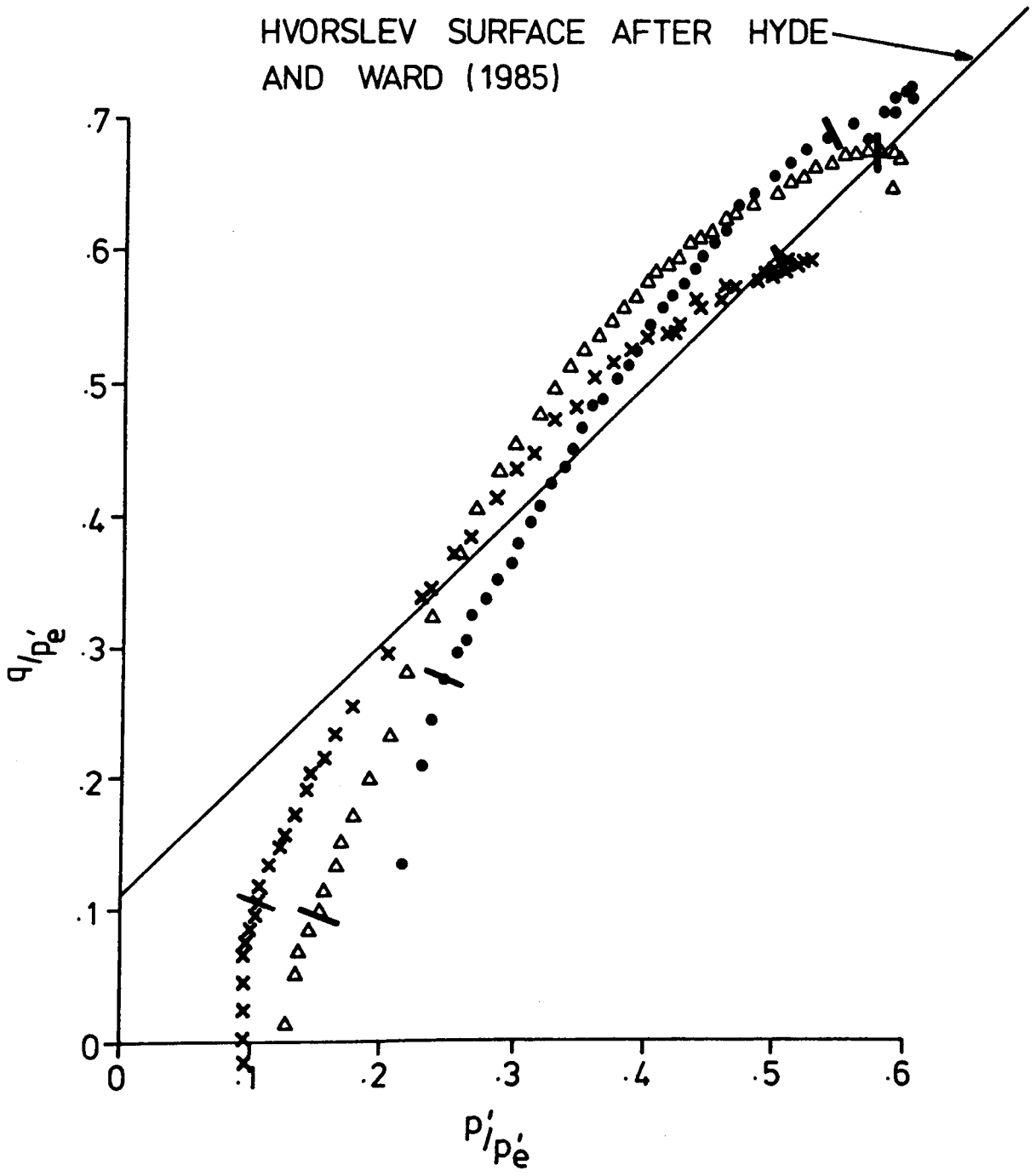

FIGURE 6.31 NORMALISED STRESS PATHS FOR UNDRAINED STRENGTH PLOTS

normal stress of 0.77, and a value of 0.83 for the normalised deviator stress. None of their failure tests on overconsolidated samples attained the critical state. This is due to the formation of discrete failure planes as the sample dilates on shearing and therefore the transducers are unlikely to measure the true failure conditions on the shear plane. Figure 6.32 shows the Mohr circles for the samples which show good agreement with an effective angle of friction of 28.5°, and no effective cohesion.

6.7 EQUIPMENT PERFORMANCE

6.7.1 The Consolidation Control System

A number of samples were failed during the consolidation phase by breakdowns in the consolidation control unit. As discussed in Chapter 4 the control unit and servo system were modified and improved as far as possible without completely redesigning the control system, and the bellofram piston system supplying the axial consolidation load. This was originally designed by Overy (1982), and was modified to supply the higher axial loads required to produce heavily overconsolidated samples.

One major problem with the system was that there was still interference between the circuits for each cell. The six proximity transducers were wired with one acting as a master oscillator driving five slave oscillators. It was found that if one transducer was moved over its full range then it affected the outputs from the other five. This was only of the order of a few millivolts in a full range output of 1v, but it was sufficient to significantly disrupt the servo systems which were operating. Unplugging a sensor from a proximity transducer to install it on a triaxial cell for example also affected the outputs of the others.

The bellofram units incorporated into the cell top by Overy (1982) to apply axial load to the sample during the consolidation phase also proved troublesome. The modified clamping system between the piston and the load ram was not easy to operate and still proved troublesome at high consolidation loads. There was

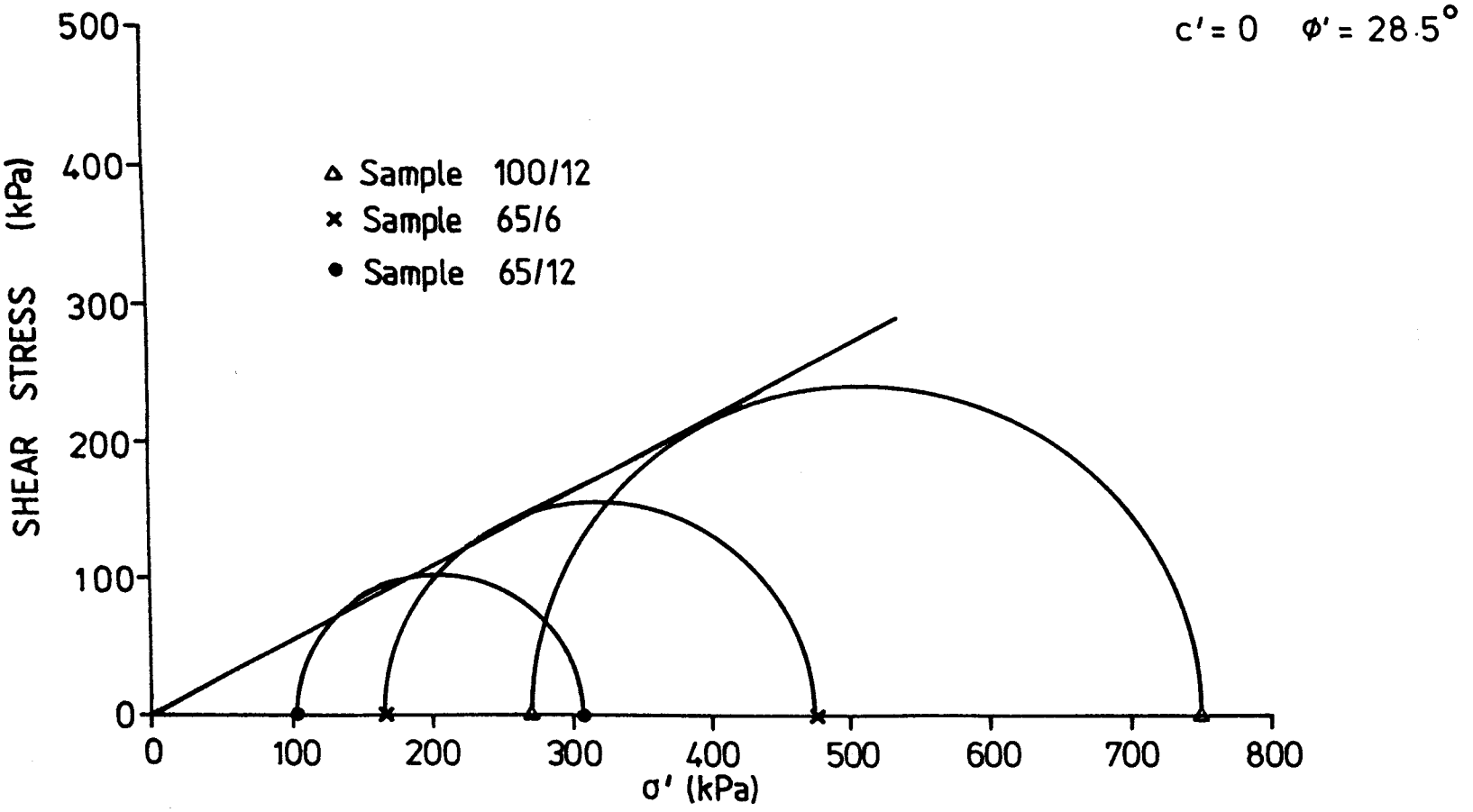

FIGURE 6.32 MOHR'S CIRCLES FOR CONSOLIDATED KEUPER MARL SAMPLES

insufficient travel in the bellofram unit to accommodate the sample movement during consolidation, which necessitated unclamping and repositioning the piston during consolidation. The unit also contained a small bellofram seal against the cell pressure, and consequently any significant movement of the load ram caused a change in cell pressure.

The concept of the anisotropic consolidation control system has been shown to work well for the consolidation phase but requires some modification to provide accurately controlled anisotropic overconsolidation. Significant shortcomings in the consolidation control equipment have been found.

6.7.2 Data Monitoring System

The digital recording system fitted to the equipment part of the way through the research project proved to be accurate and repeatable. There were almost no spurious signals recorded and no trouble was experienced from electrical interference. The system extended the range of the test facility considerably as stress paths could be plotted over a much higher frequency range than with conventional X-Y plotters. The signal conditioning unit and ultra violet chart recorder also worked satisfactorily following the modifications to reduce the electrical noise on the signals. The system is limited though as only peak values can be determined from the traces.

Both systems could resolve axial and radial strains to five microstrain.

6.7.3 Instrumentation

Generally the electrical transducers worked satisfactorily. The latest disc load cells, the pressure transducers and the LVDTs were all found to be sufficiently stable for this type of test. The crosstalk between the proximity transducers has been discussed above, and in addition they were found to need recalibrating over their linear range at the end of each test.

The volume change system using burettes with dyed water paraffin interfaces were found to be temperamental and required frequent cleaning. It was difficult to achieve a water tight seal each time the system was dismantled for cleaning. The meniscus was not always even and this led to inaccuracies in the volume change measurements.

6.7.4 The Control System

Once the hydraulic system and servo valves were overhauled the system proved adequate for short term tests where the load was continually monitored and could be frequently adjusted. As discussed earlier in Chapter 6 both the static and cyclic components of the axial load drifted in the long term, which made analysis of the long term tests rather difficult.

The control system was capable of following a haversine load signal of 0.1 second duration where the sample was stiff and consequently the deflection was small. With higher load signals and deflections the unload part of the pulse degenerated as shown in Figure 6.33 for samples 33/6 and 100/12. The pulse shape only degenerates so far and further increases in load do not then cause any more degeneration of the load pulse shape, as shown by comparing the pulse shapes for repeated loads of 100kPa and above for sample 100/12, and 50kPa and above for sample 33/6. This degeneration was not noticeable when the stress pulse duration was 1 second or longer, partly because the rate of loading was slower and also because the magnitudes of the load pulses were smaller.

The lack of response at the higher amplitudes and frequencies is maybe a consequence of using a low flow rate servo valve. Low flow rate servo valves were originally fitted to try and improve the stability of the system, and therefore a balance must be struck between stability and response at the higher frequencies and amplitudes which may be required during a test programme.

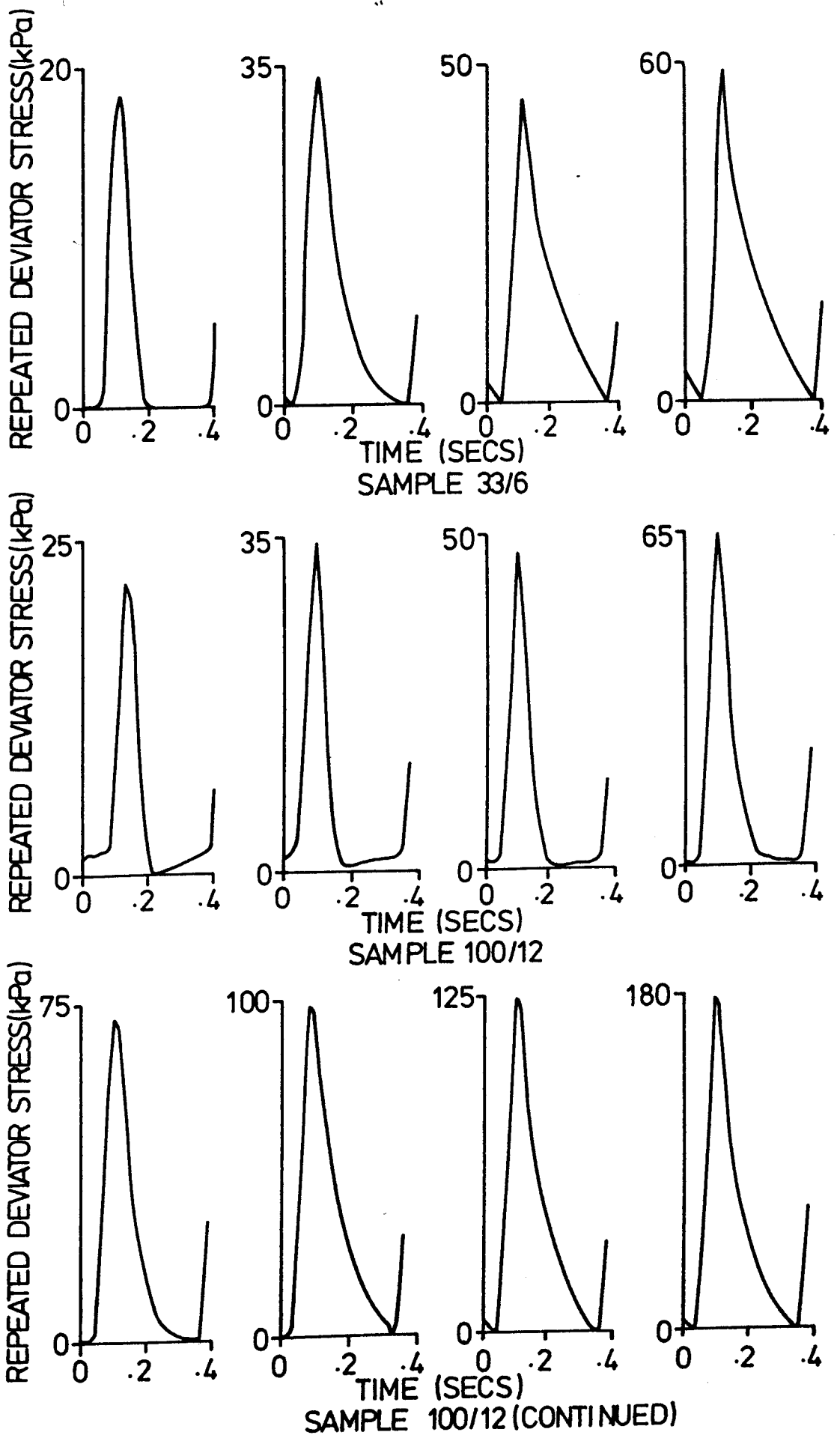

FIGURE 6.33 TYPICAL DEGENERATION OF STRESS PULSE SHAPE WITH INCREASING STRESS PULSE MAGNITUDE

CHAPTER SEVEN

BEHAVIOUR OF COMPACTED TRIAXIAL SAMPLES

7.1 INTRODUCTION

This chapter presents the results of the suction measurements and repeated load triaxial tests on compacted samples of the three clays used in the research project (Keuper Marl, Gault clay and London clay). The suction moisture content curves are presented first, and then the results from the pneumatic repeated load triaxial rig. The test programme is detailed in Chapter 3, and the equipment is detailed in Chapter 4.

7.2 SUCTION MEASUREMENTS

The suction/moisture content curves measured for the Keuper Marl, Gault clay and London clay are shown in Figures 7.1, 7.2 and 7.3 respectively. Measurements from both types of apparatus described in Chapter 4 are shown for comparison. Two sets of measurements using the equilibrium method were made for the Gault and London clays. For the first set the clay was mixed to approximately the equilibrium moisture content for the suction applied to the sample, and for the second set the three samples were all mixed to the same moisture content as that estimated as the equilibrium value for the middle value of suction used in the experiment.

The two types of test on the Keuper Marl, Figure 7.1, show general agreement. A small air bleed was discovered at higher suctions in the 'araldite' sealing the porous stone to the glass tube. It would seem likely that this gave rise to the points scattered to the left of the line shown in Figure 7.1. The leak was sealed and the remaining tests gave satisfactory results.

The agreement between the two types of test on the Gault and London clays, Figures 7.2 and 7.3, is not very good. It was found that the porous stones used in the equilibrium apparatus tended to dry out and admit air after three or four days under

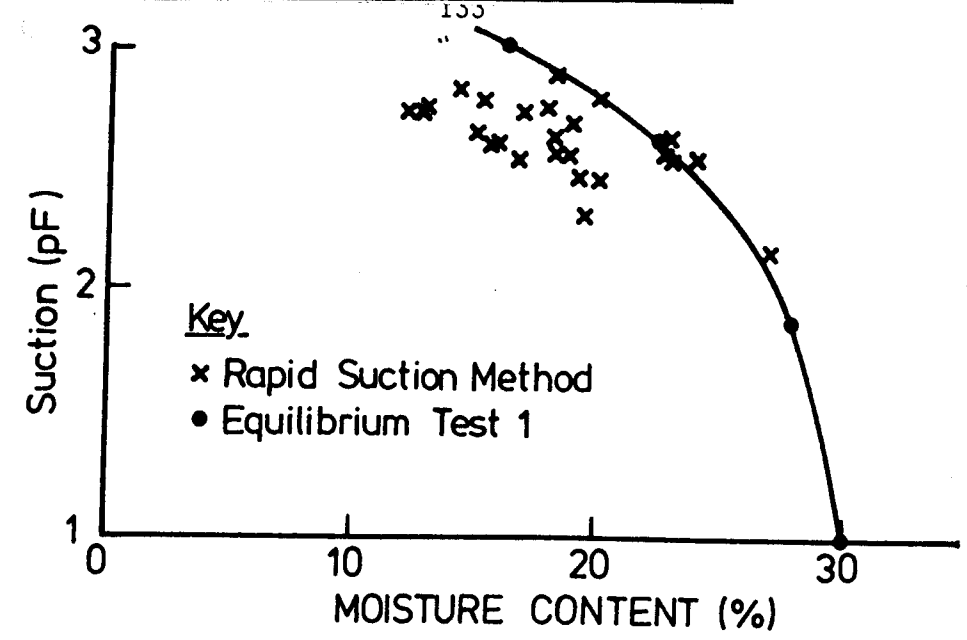

7.1 Keuper Marl

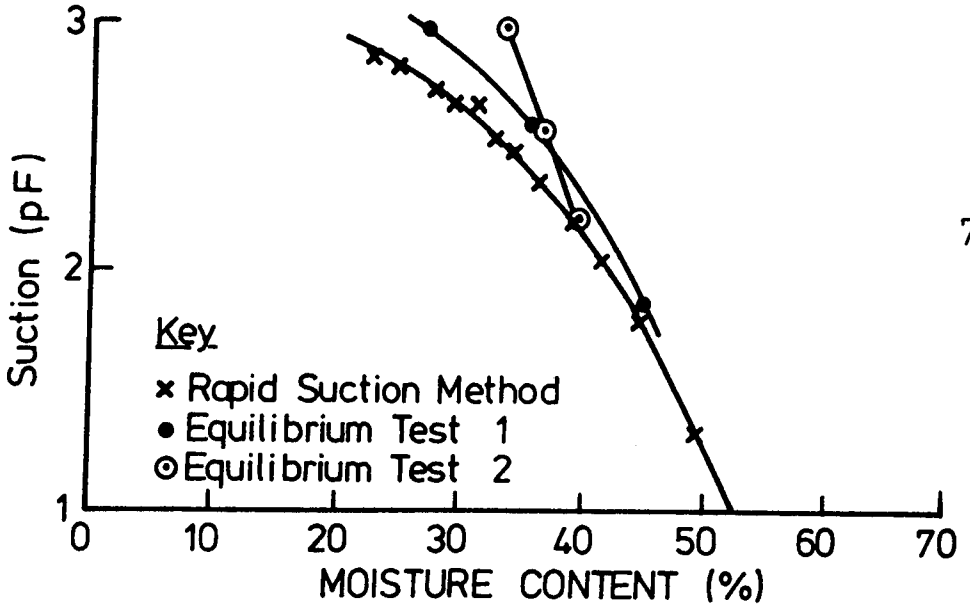

7.2 Gault Clay

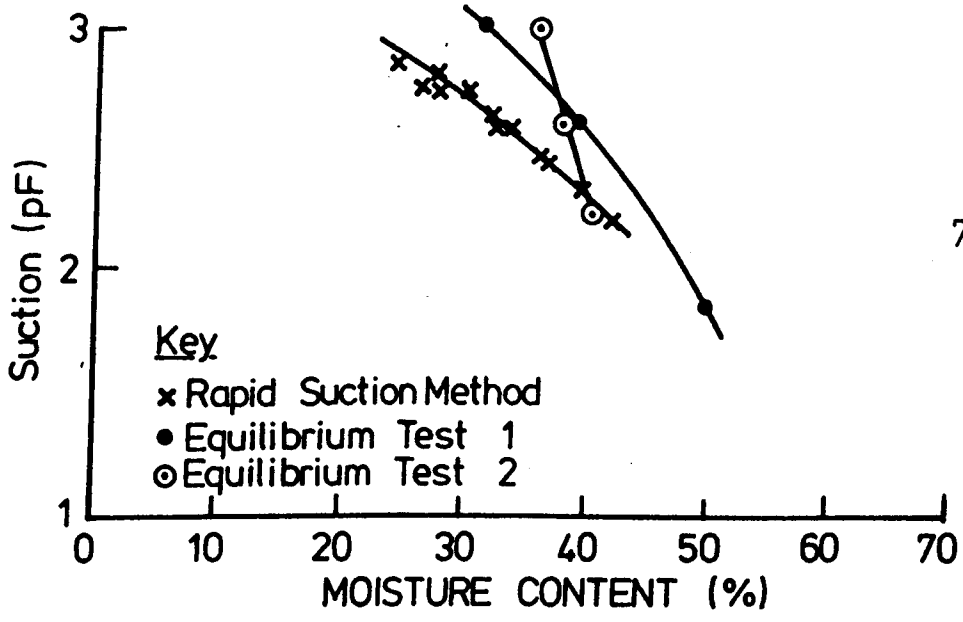

7.3 London Clay

FIGURES 7.1, 7.2 & 7.3 RESULTS FROM SUCTION - MOISTURE CONTENT TESTS

vacuum. This would seem to be insufficient time for the low permeable clays, like the Gault and London, to reach equilibrium before the tests had to be terminated. This is indicated by the difference between the gradients of the test results from the first and second tests using the equilibrium method. The second test, when all three samples started at the middle moisture content, produced a steeper line than the first test when the samples started nearer the equilibrium moisture content for each suction. The fact that the tests were terminated after the porous stones started leaking throws some doubt on the accuracy of the moisture contents and the curves derived from the rapid suction measurements are used to give the values of suction quoted in this thesis.

The three clays seem to have similar suctions at their plastic limits and therefore an attempt was made to 'normalise' the moisture content using the plasticity index. Figure 7.4 shows the suction plotted against the liquidity index for all three clays and demonstrates that the suction moisture content curve is approximately linear for each clay over this range of suctions. The plastic limit is difficult to determine accurately using the standard test (BS 1377) and this will cause some variation in the results. The minearology of the three clays is also different and this may also influence the suction moisture content relationship. The factors affecting suction are discussed more fully in Chapter 2, section 12. However, the relationship between liquidity index and moisture content shown in Figure 7.4 would seem reasonable enough to enable suctions to be estimated from a knowledge of the Atterberg limits and moisture content for the three clays tested. Also shown on Figure 7.4 are some results, presented by Croney (1977) for a variety of heavy clays which do not fit the pattern of results found in this research. Croney measured the suction on the drying part of the curve, if the suction was measured on the wetting part then the suctions would be lower in each case, though the agreement between the results would not improve.

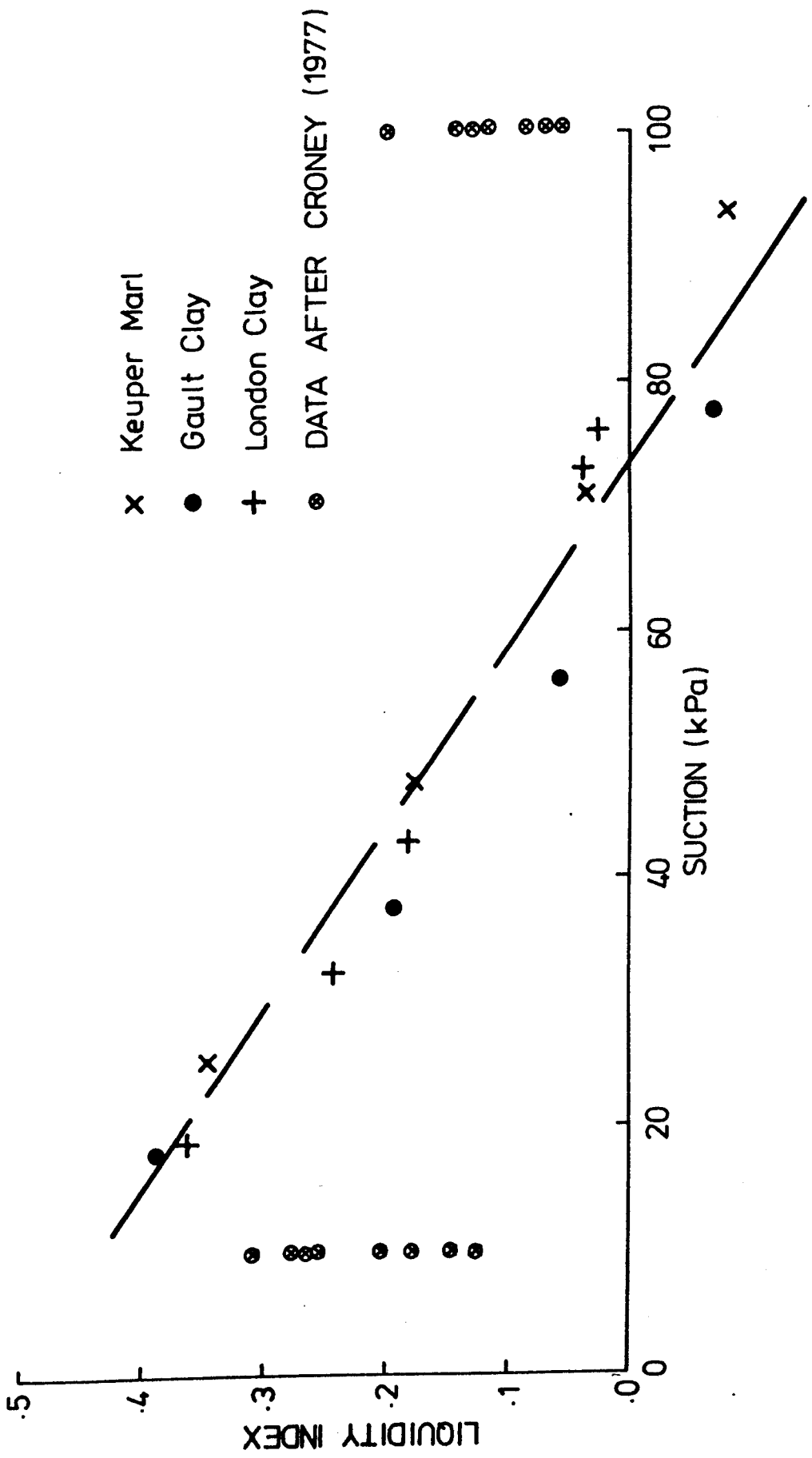

FIGURE 7.4 LIQUIDITY INDEX vs SUCTION FOR COMPACTED CLAY SAMPLES

7.3 COMPACTED TRIAXIAL SAMPLES

7.3.1 Introduction

The sample details for the Keuper Marl, Gault clay and London clay are given in Tables 7.1, 7.2 and 7.3 respectively.

The test programme on the compacted samples was designed to investigate the initial resilient response of the material when subjected to various deviator stress pulse magnitudes. However, some samples were tested for up to 4000 stress pulses at each stress level and some samples were subjected to load-reload tests. The onset of permanent strain was determined but there were insufficient tests to correlate the development of permanent strain with number of cycles.

7.3.2 General behaviour

All samples from all three clays were subjected to at least one test which consisted of pulsing the deviator stress at a certain value and monitoring the resilient strains at 1 and 100 cycles. The deviator stress pulse magnitude was then increased and the measurements repeated. The load sequence was reversed when the resilient strains were approximately 3500 microstrain.

Figure 7.5 shows a typical deviator stress pulse magnitude versus resilient axial strain plot. The samples all exhibit typical stress softening behaviour, and also above a certain pulsed deviator stress level the resilient strain starts to increase from 0 to 100 cycles. The unload line appears nearly linear at the higher repeated deviator stress, but joins the loading curve at the lower deviator stress pulse magnitudes. There is also no difference between the axial resilient strain measured after 1 and 100 cycles when the sample was being unloaded.

Six of the tests on the Keuper Marl were repeated, four of them three times. In all cases the samples were stiffer with each reloading. Figure 7.6 shows a typical plot. These tests were

Table 7.1 Results from triaxial tests on Keuper Marl

Sample Number	Cell Pressure kPa	Moisture Content %	Suction kPa	Dry Density kg/m³	Degree of saturation %	Poisson's Ratio
1	30	20.48	64	1705	94.5	Unreliable
2	30	19.17	76	1710	90.7	Unreliable
3	30	22.29	49	1610	89.1	0.082
4	30	14.94	122	1880	93.5	0.050
5	30	17.20	95.5	1810	94.6	0.093
6	15	23.03	40	1590	89.2	0.073
7	15	20.34	61.5	1690	91.5	0.071
8	15	17.62	87	1765	90.5	0.034
9	15	15.85	106	1855	94.9	0.059
10	0	24.47	25.5	1530	88.0	0.070
11	0	21.39	48	1640	90.7	0.064
12	0	18.69	72	1745	92.6	0.051
13	0	16.56	93.5	]820	93.7	0.070

Table 7.2 Results from unconfined triaxial tests on Gault Clay

Sample Number	Moisture Content %	Suction kPa	Dry Density kg/m³	Degree of saturation %	Poisson's Ratio
1	38.96	18	1230	88.7	0.116
2	31.93	37.5	1390	92.1	0.087
3	27.11	56	1525	95.4	0.071
4	22.54	77.5	1670	98.6	0.121

Table 7.3 Results from unconfined triaxial tests on London clay

Sample Number	Moisture Content %	Suction kPa	Dry Density kg/m³	Degree of saturation %	Poisson's Ratio
1	40.33	19	1245	92.3	0.093
2	31.81	43	1410	92.7	0.072
3	24.31	76	1570	89.5	0.028
4	34.73	32.5	1330	90.3	0.084
5	24.92	73	1520	-	Unreliable

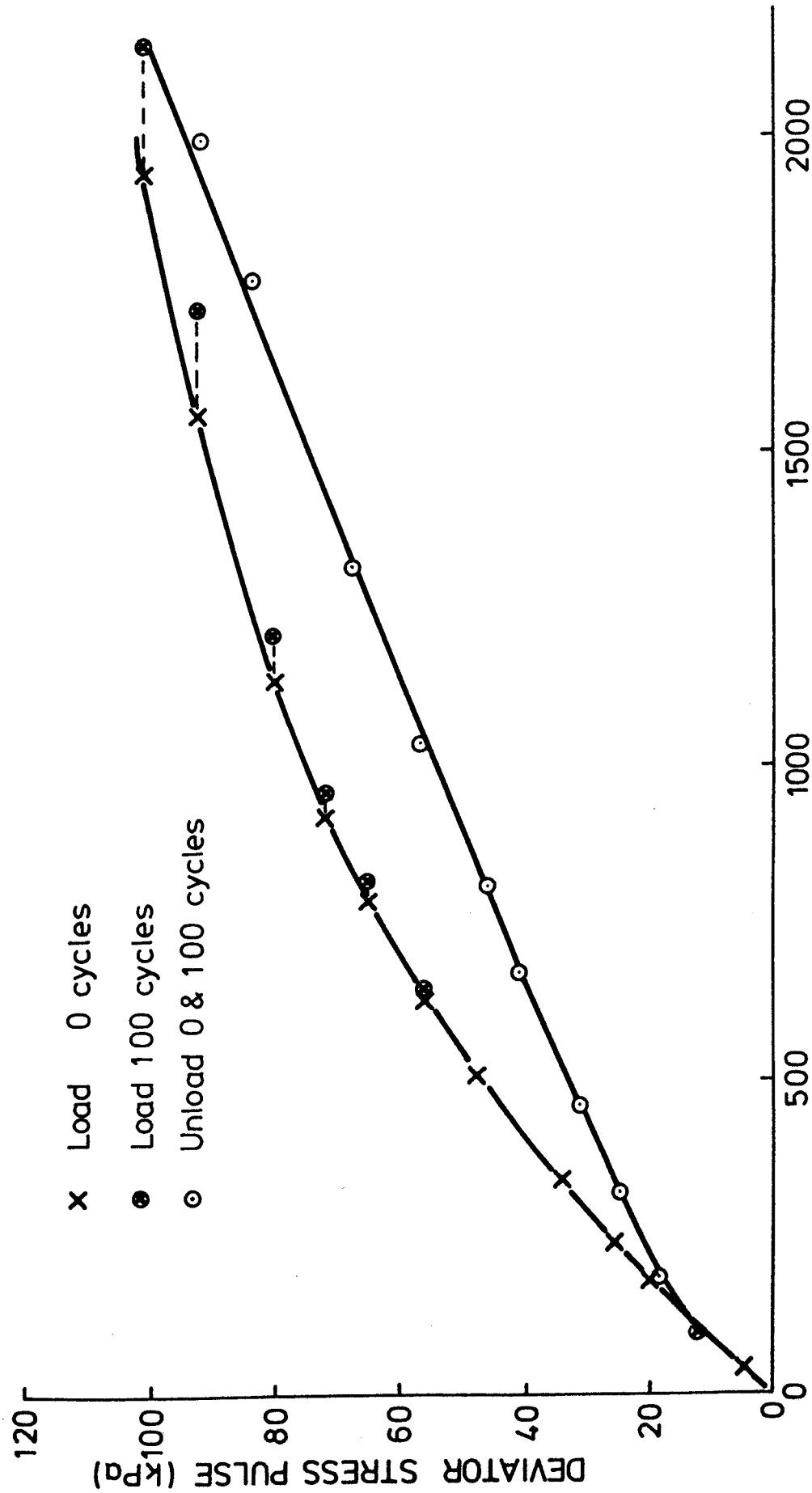

FIGURE 7.5 TYPICAL DEVIATOR STRESS PULSE vs RESILIENT AXIAL STRAIN PLOT LONDON CLAY SAMPLE 2

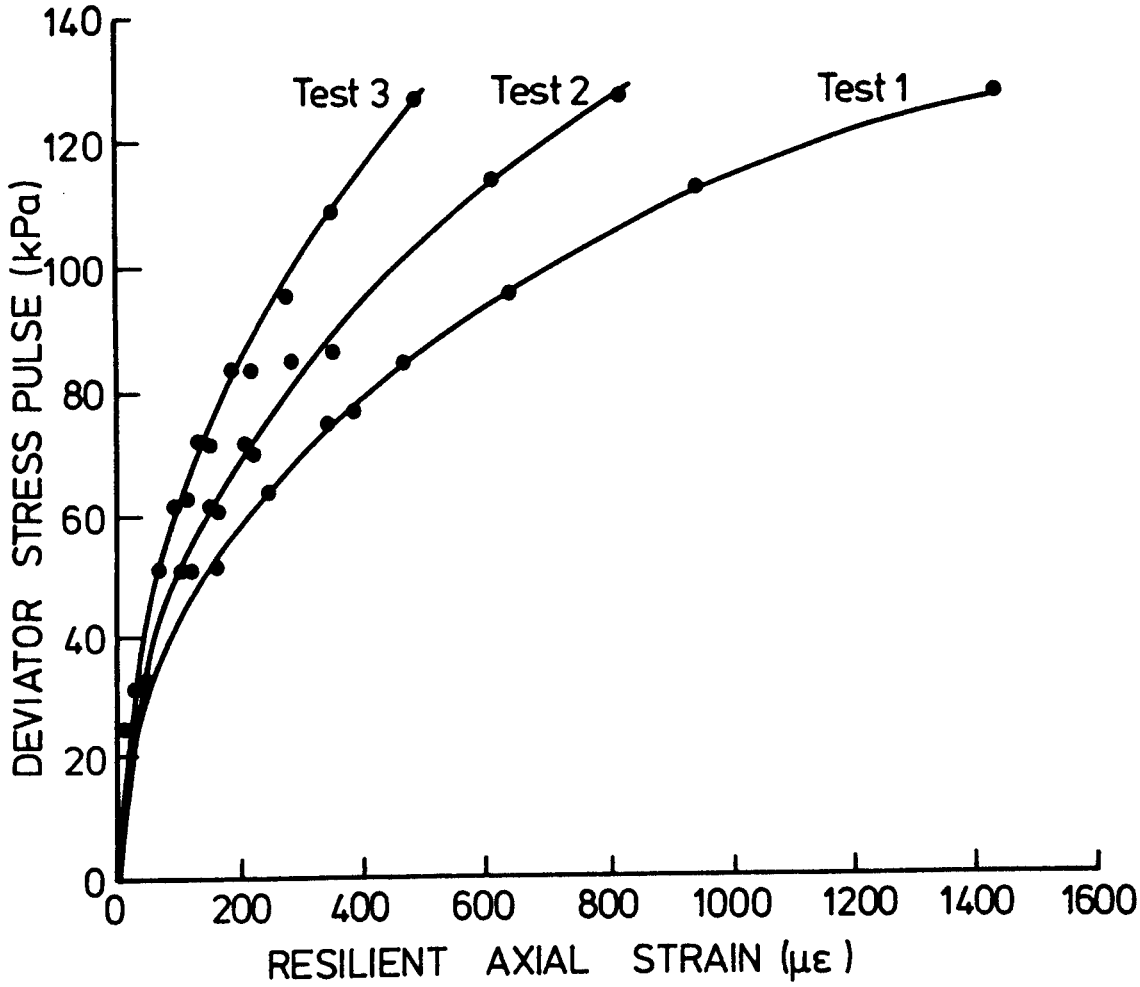

FIGURE 7.6 DATA FROM REPEAT TESTING AFTER AT LEAST 24 HOUR DELAY

carried out after at least 24 hours had elapsed since the last test. The samples were left undrained during that time.

A single load, partial unload, reload and final unload test was performed on Keuper Marl sample 7, see Figure 7.7, which indicated that the previous highest repeated stress level affected the modulus at lower repeated stress levels even on the reload section of the curve. This behaviour must be time dependent as the same trend is not shown when the tests are repeated with a rest period, see Figure 7.6.

Some attempt was made to monitor the effect of a larger number of cycles at each pulsed deviator stress level. The results are shown in Figure 7.8 and show that the modulus decreases with increasing numbers of cycles at each stress level. It is not clear whether the samples would reach equilibrium or fail and at what stress level this would occur. This type of test was considered too time consuming and outside the original brief for this section of the research and no further tests of this type were performed.

7.3.3 Resilient behaviour

7.3.3.1 Axial Strain

All modulus and strain contour values plotted for each sample were taken from the initial loading curve from the tests described above. The modulus used is a secant resilient modulus defined as q_r/ε_a^r where q_r is the repeated deviator stress and ε_a^r the resilient axial strain.

The values of repeated deviator stress for set resilient axial strains were read off the basic stress strain loading curves and these were plotted against the suction. The suction of the sample was obtained from the suction moisture content curves derived using the rapid suction method. The strain contour plots for the unconfined samples of Keuper Marl, Gault clay and London

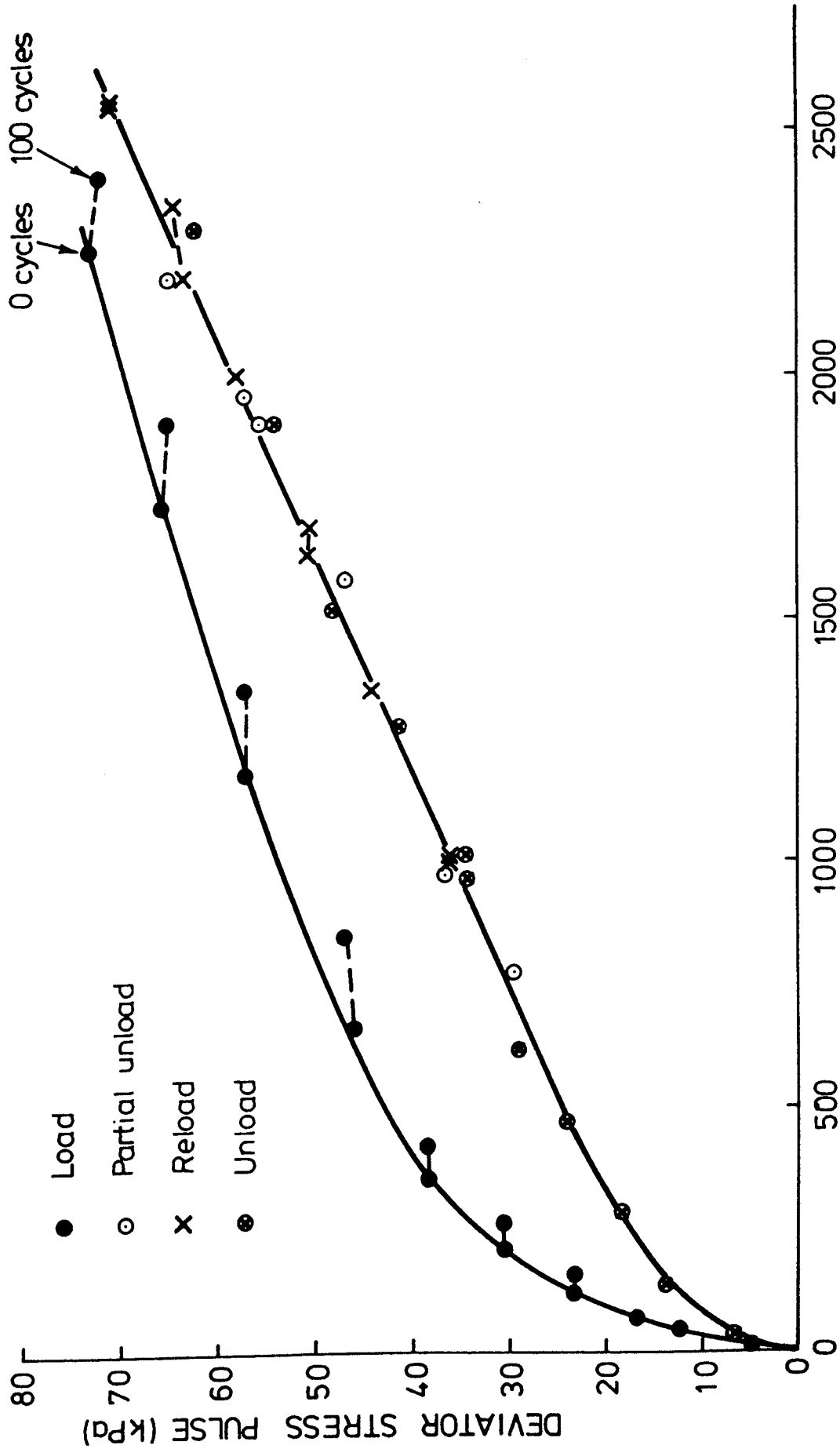

FIGURE 7.7 EFFECT OF LOADING SEQUENCE ON KEUPER MARL SAMPLE 7

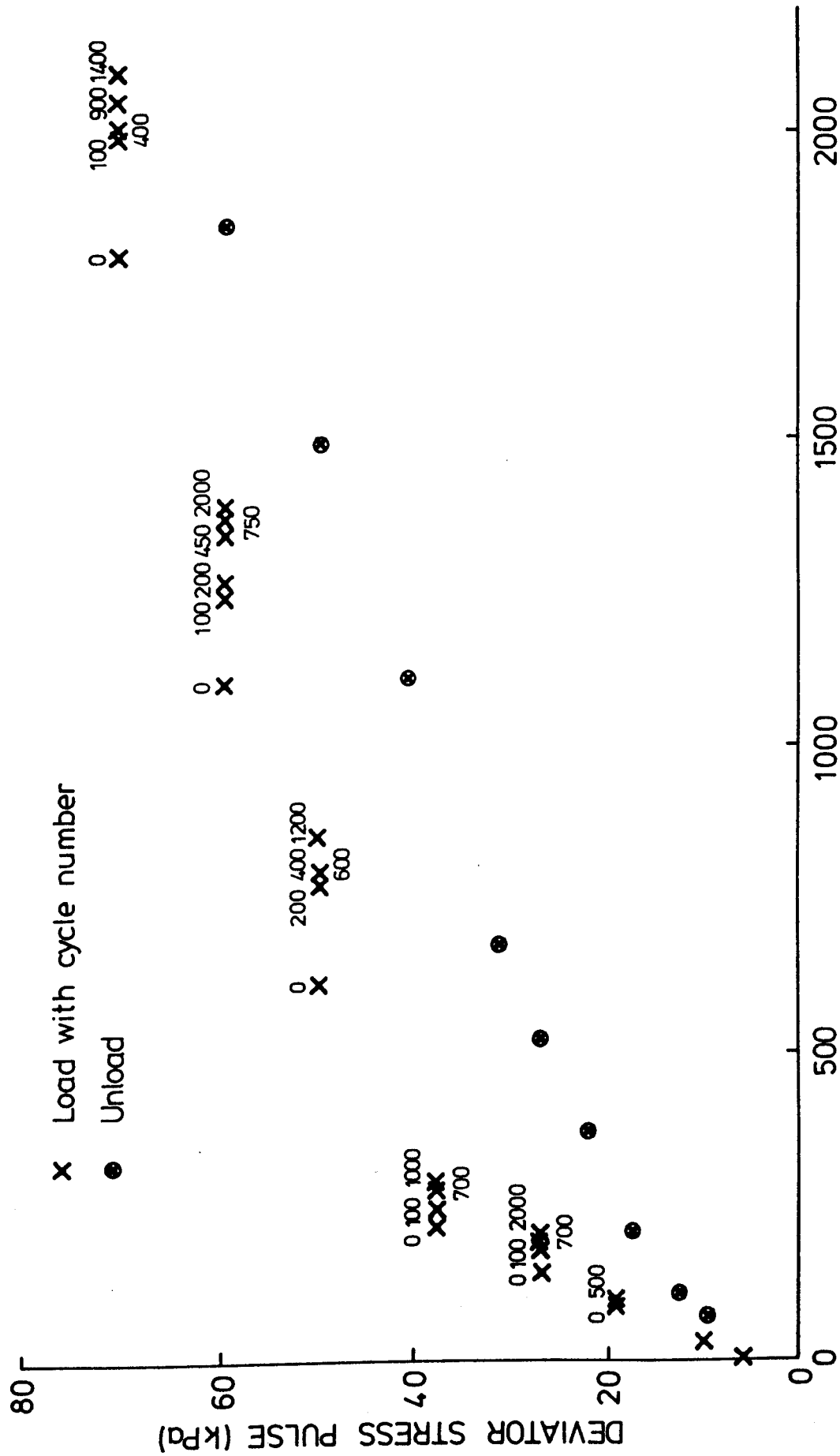

FIGURE 7.8 EFFECT OF NUMBER OF CYCLES ON DEVIATOR STRESS PULSE vs RESILIENT AXIAL STRAIN, KEUPER MARL SAMPLE 7

clay are shown in Figures 7.9, 7.10 and 7.11 respectively. The results have been plotted in terms of resilient axial strain rather than resilient shear strain as the low values of Poisson's Ratio measured indicate that the resilient radial strains measured may not be correct.

The results for the London clay, Figure 7.11, show good correlation, with strain contours radiating from the origin and getting closer together as the strains increase, demonstrating the stress softening behaviour. The Gault clay and Keuper Marl plots follow the same sort of pattern though not as convincingly. There appears to be a change in slope of the contours at higher suctions for both the Keuper Marl and the Gault clay. These changes occur at suctions approximately equivalent to the plastic limit and perhaps do not appear on the London clay results as all those tests were conducted at moisture contents above the plastic limit.

A comparison between results in Figures 7.9, 7.10, and 7.11 and those in Figure 6.14 indicate that the suction of a compacted sample could be analogous to the mean normal effective stress of a consolidated saturated sample. The resilient axial strains from the confined Keuper Marl samples are shown in Figure 7.12 and indicate that increasing the confining pressure increases the stiffness of the sample. An attempt was made to allow for the effect of cell pressure on the suction by using the relationship

$$S = u + \alpha p \qquad 7.1$$

with u as the suction corresponding solely to the moisture content of the sample, p as the cell pressure, and α was taken as 0.3 as used by Croney (1977) for this material. Figure 7.13 shows the effect of adding αp to the suctions in Figure 7.12. Generally the trend is correct although the magnitudes are not. This may be due to inaccuracies in monitoring the cell pressure as the cell medium was air and the pressure was measured using a

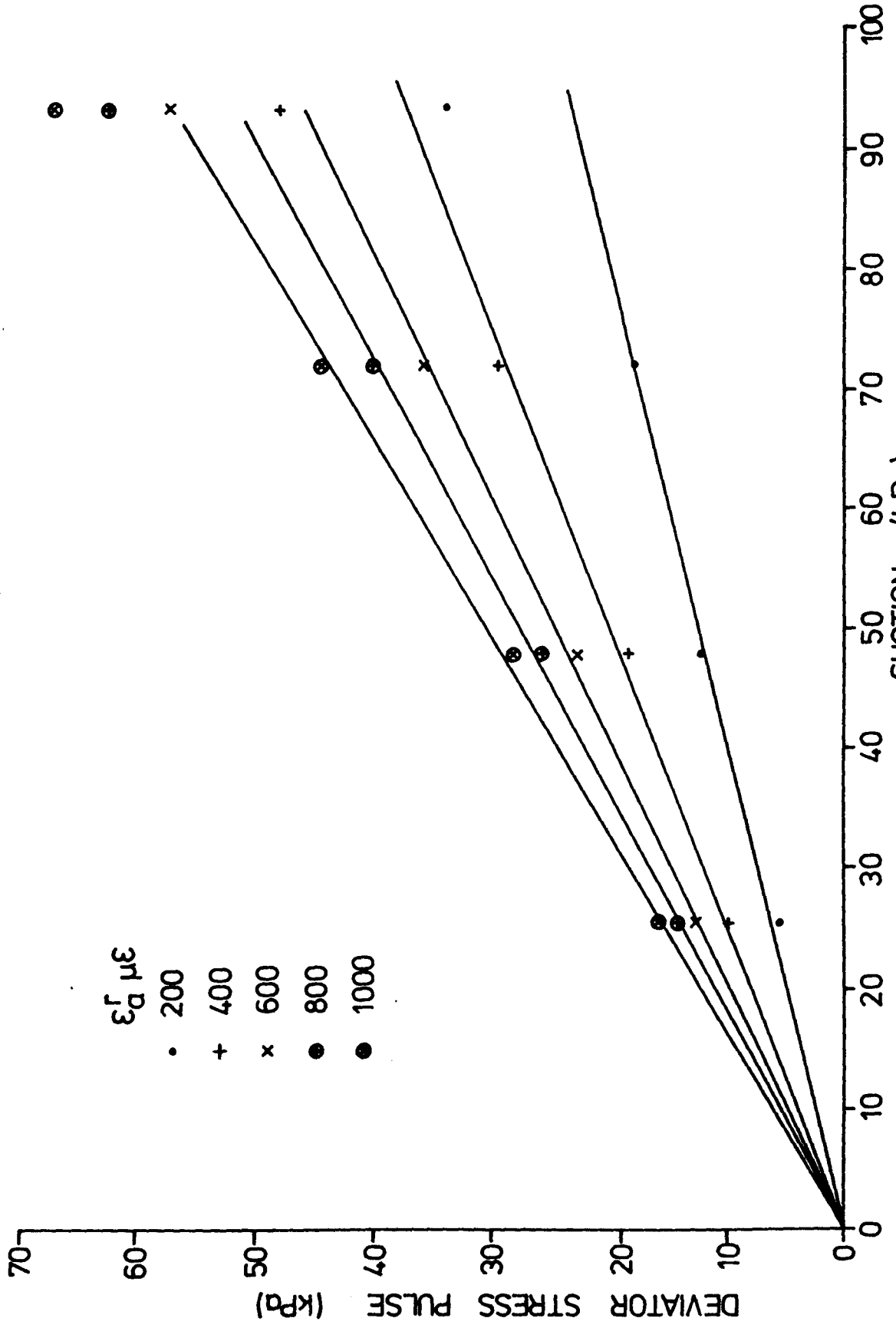

FIGURE 7.9 RESILIENT AXIAL STRAIN CONTOURS FOR COMPACTED KEUPER MARL

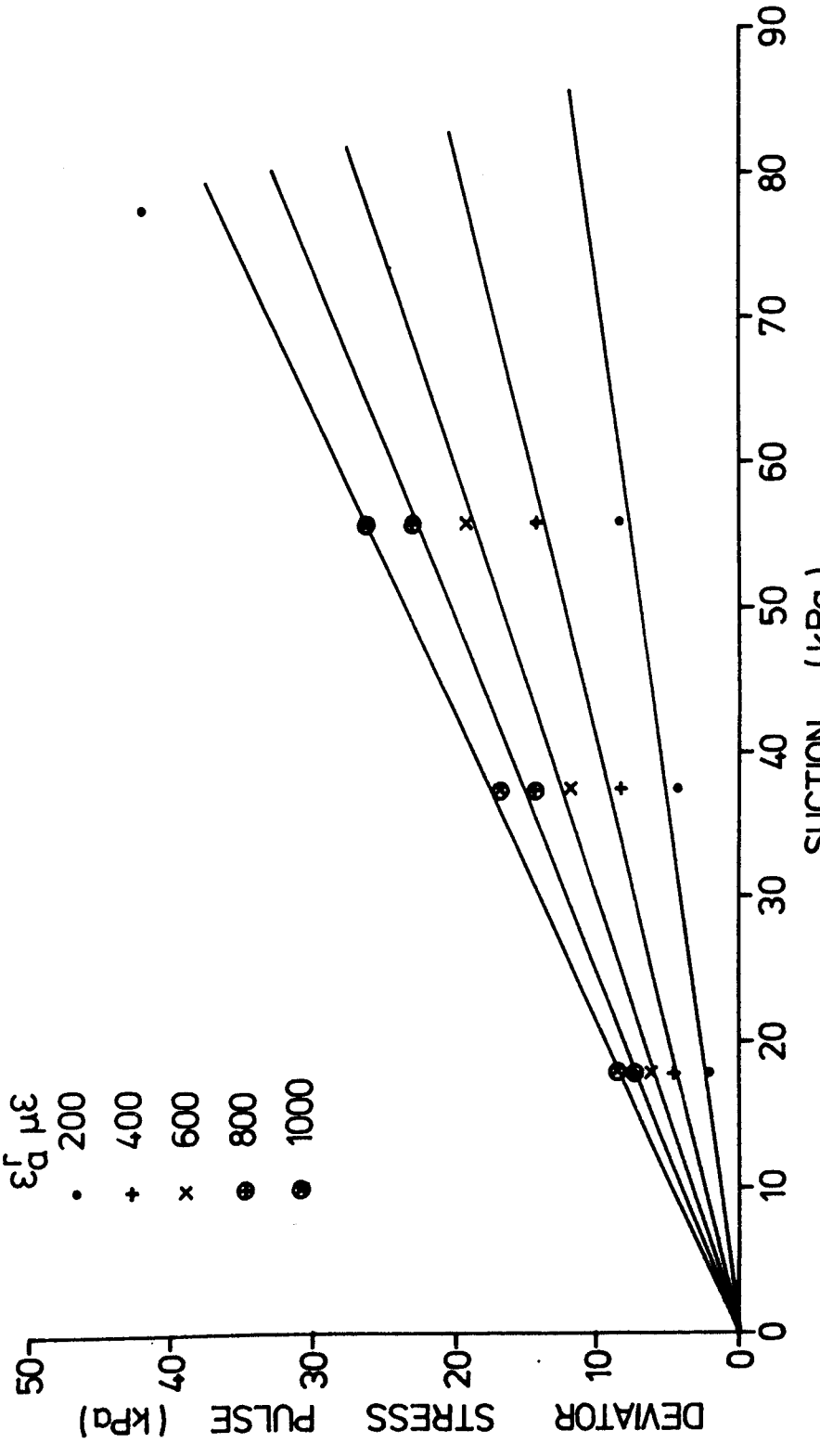

FIGURE 7.10 RESILIENT AXIAL STRAIN CONTOURS FOR COMPACTED GAULT CLAY

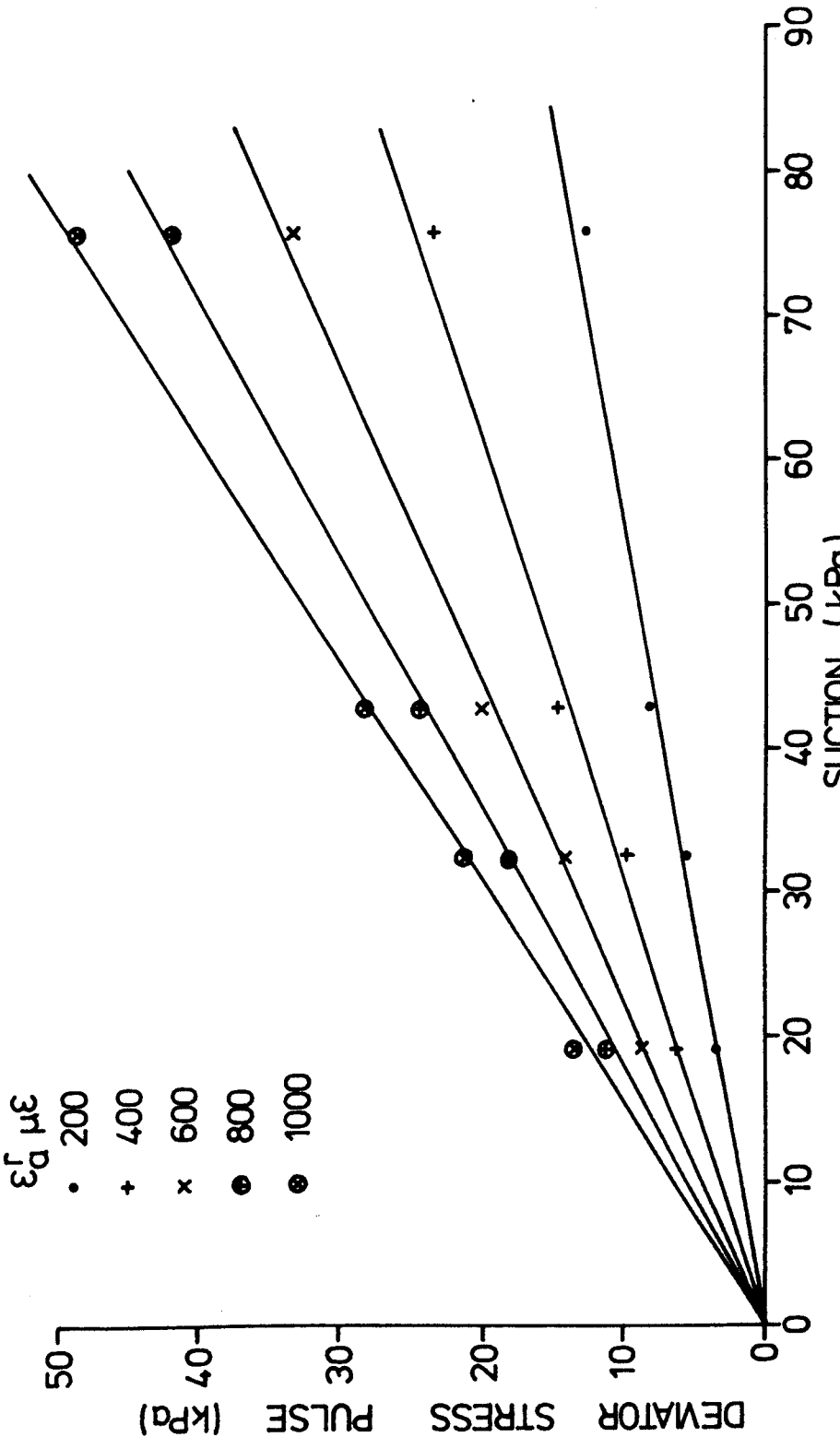

FIGURE 7.11 RESILIENT AXIAL STRAIN CONTOURS FOR COMPACTED LONDON CLAY

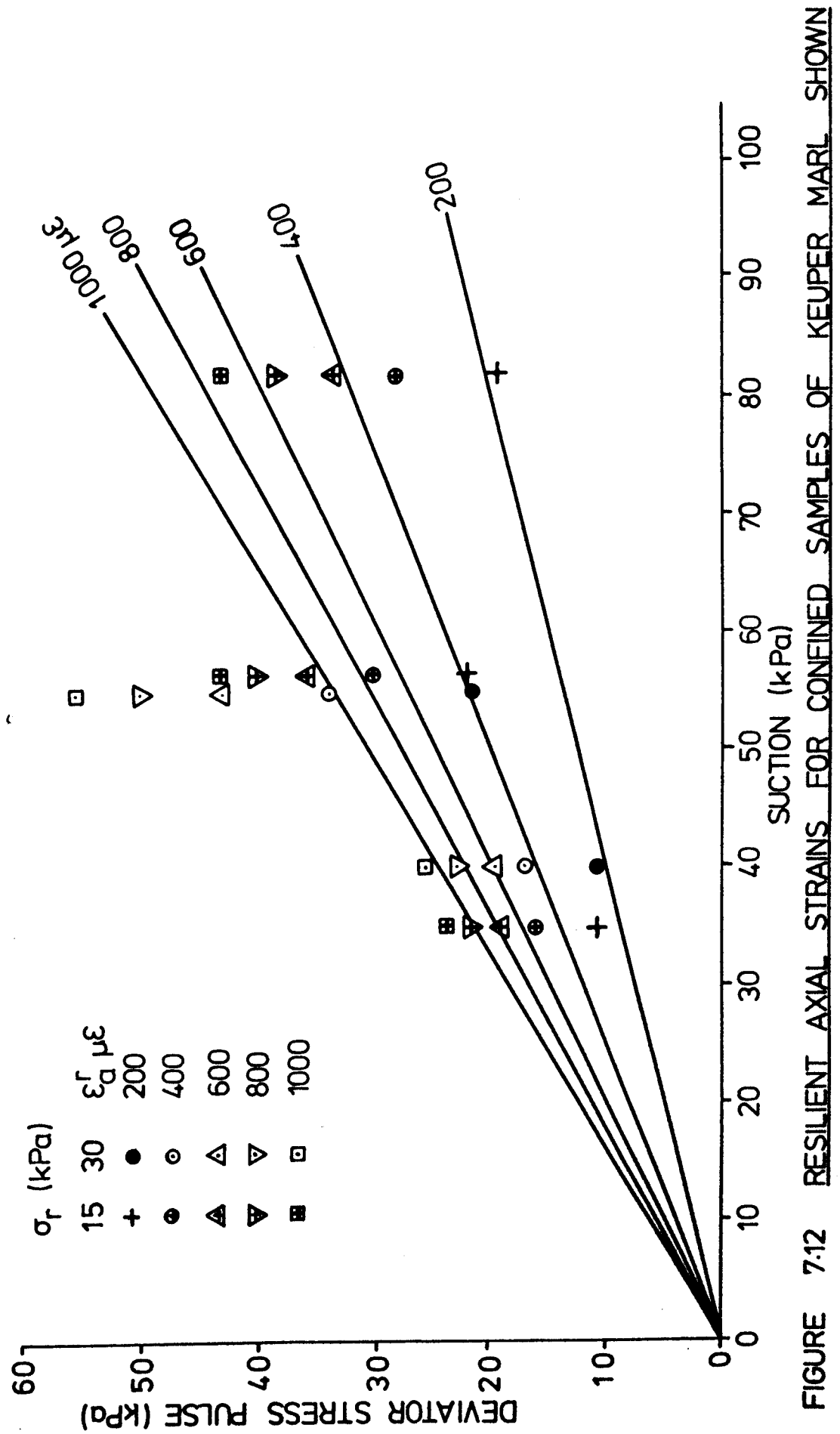

FIGURE 7.12 RESILIENT AXIAL STRAINS FOR CONFINED SAMPLES OF KEUPER MARL SHOWN STRAIN CONTOURS FROM UNCONFINED SAMPLES OF KEUPER MARL.

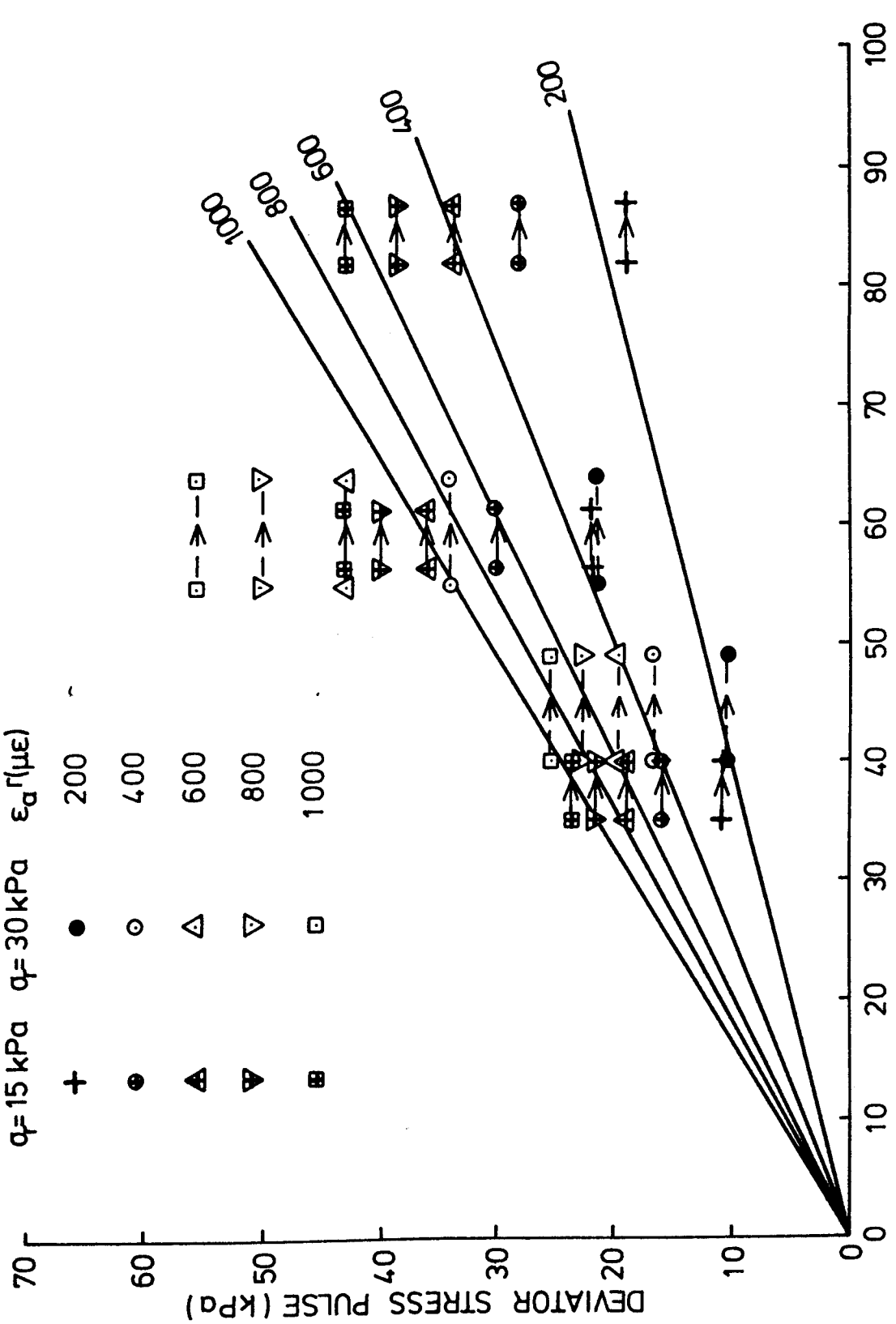

FIGURE 7.13 RESILIENT AXIAL STRAINS FOR CONFINED SAMPLES PLOTTED ON STRAIN CONTOURS FOR UNCONFINED SAMPLES OF KEUPER MARL

relatively insensitive pressure gauge. The system was not improved as further work concentrated on unconfined specimens.

Figures 7.14, 7.15 and 7.16 show the strain contour gradient plotted against resilient axial strain for the Keuper Marl, Gault clay and London clay respectively. These figures give reasonable approximations to straight lines and lead to relationships of the form

$$\varepsilon_a^r = A \left[\frac{q_r}{S} \right]^B \qquad 7.2$$

where A and B are constants. This can be rearranged to give an equation for the resilient modulus.

$$M_r = \frac{q_r}{A} \left[\frac{S}{q_r} \right]^B \qquad 7.3$$

Table 7.4 gives the values of A and B obtained from Figures 7.14, 7.15 and 7.16. Plots of calculated resilient axial strain against measured resilient axial strain for the Keuper Marl, Gault clay and London clay are shown in Figures 7.17, 7.18 and 7.19 respectively. Apart from the test results from samples at moisture contents below the plastic limit the calculated resilient axial strains are all within 20% of the measured values.

7.3.3.2 **Poisson's Ratio**

The resilient radial strain was recorded for each test. Figure 7.20 shows a typical plot similar for all three clays and demonstrates that the Poisson's Ratio was not stress dependent. The values obtained for each test for the Keuper Marl, Gault clay and London clay are given in Tables 7.1, 7.2 and 7.3.

The value of Poisson's Ratio measured for saturated samples in similar undrained tests was 0.5 for the range of moisture contents tested. The dry density of the saturated samples varied

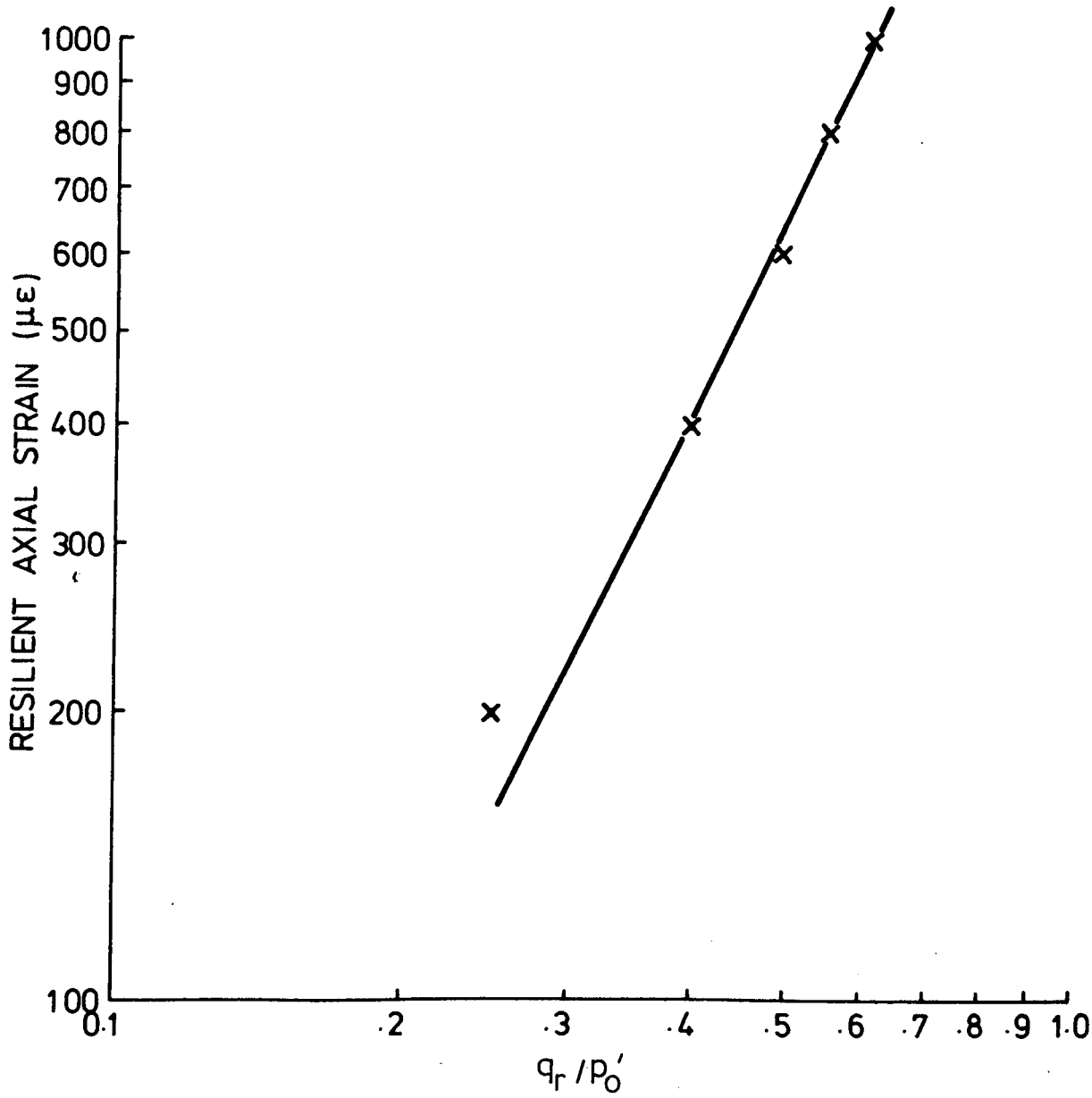

FIGURE 7.14 LOG RESILIENT AXIAL STRAIN vs LOG GRADIENT OF STRAIN CONTOUR FOR KEUPER MARL

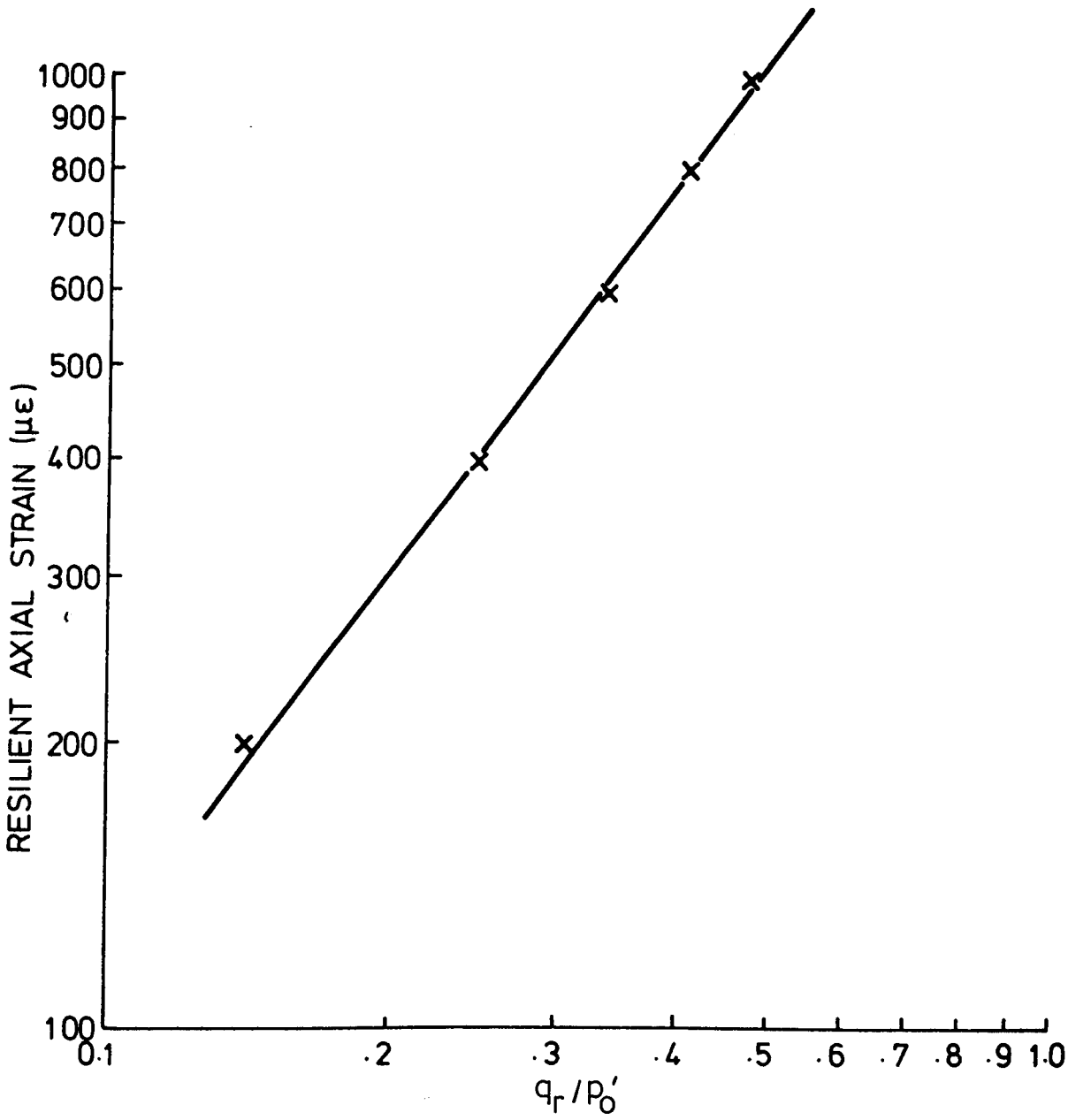

FIGURE 7·15 LOG RESILIENT AXIAL STRAIN vs LOG STRAIN CONTOUR GRADIENT FOR GAULT CLAY

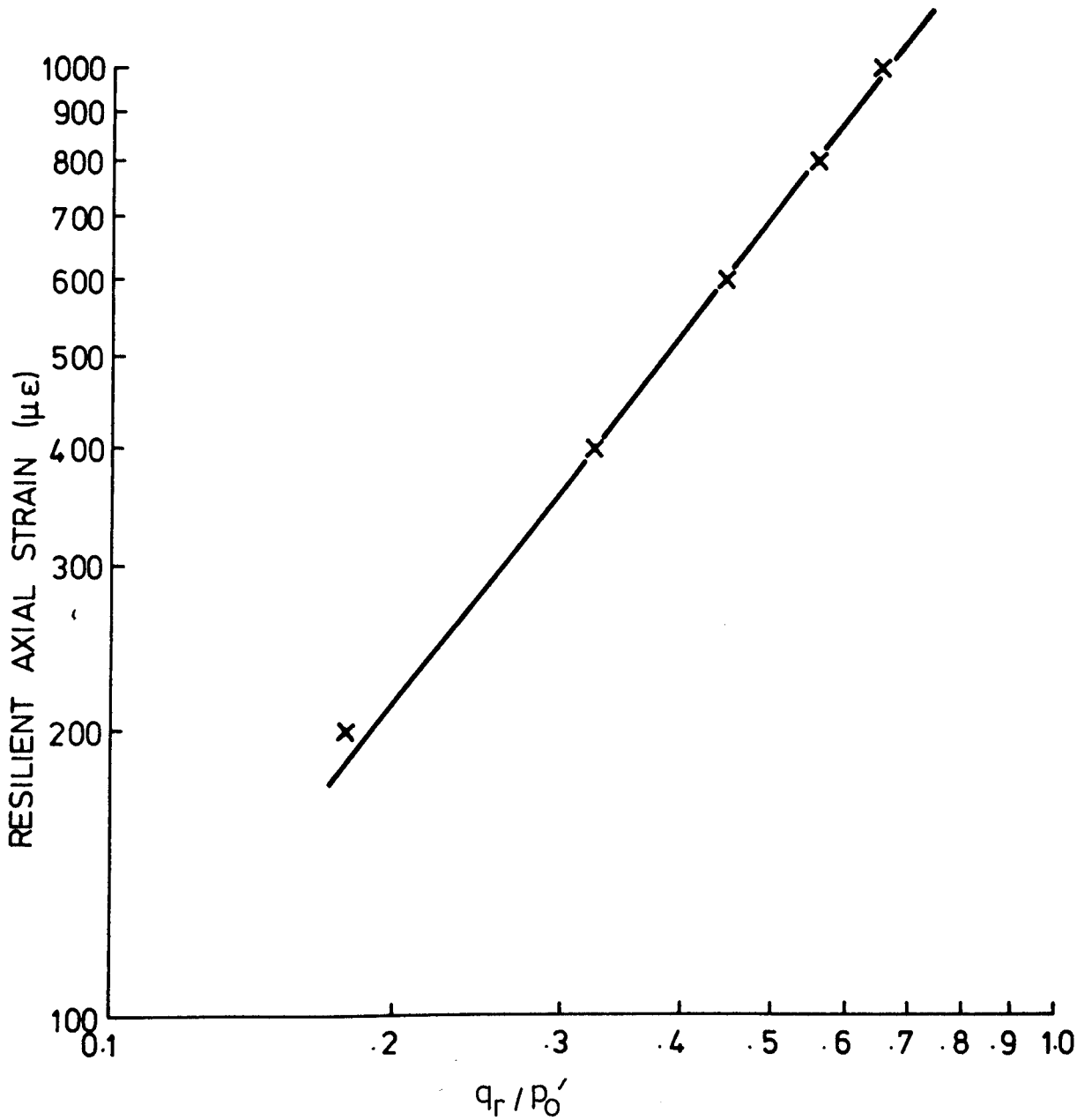

FIGURE 7·16 LOG RESILIENT AXIAL STRAIN vs LOG STRAIN CONTOUR GRADIENT FOR LONDON CLAY

Table 7.4 Coefficients for equation 7.2

Materials	A microstrain	B
Keuper Marl	2740	2.1
Gault clay	2640	1.35
London clay	1690	1.27

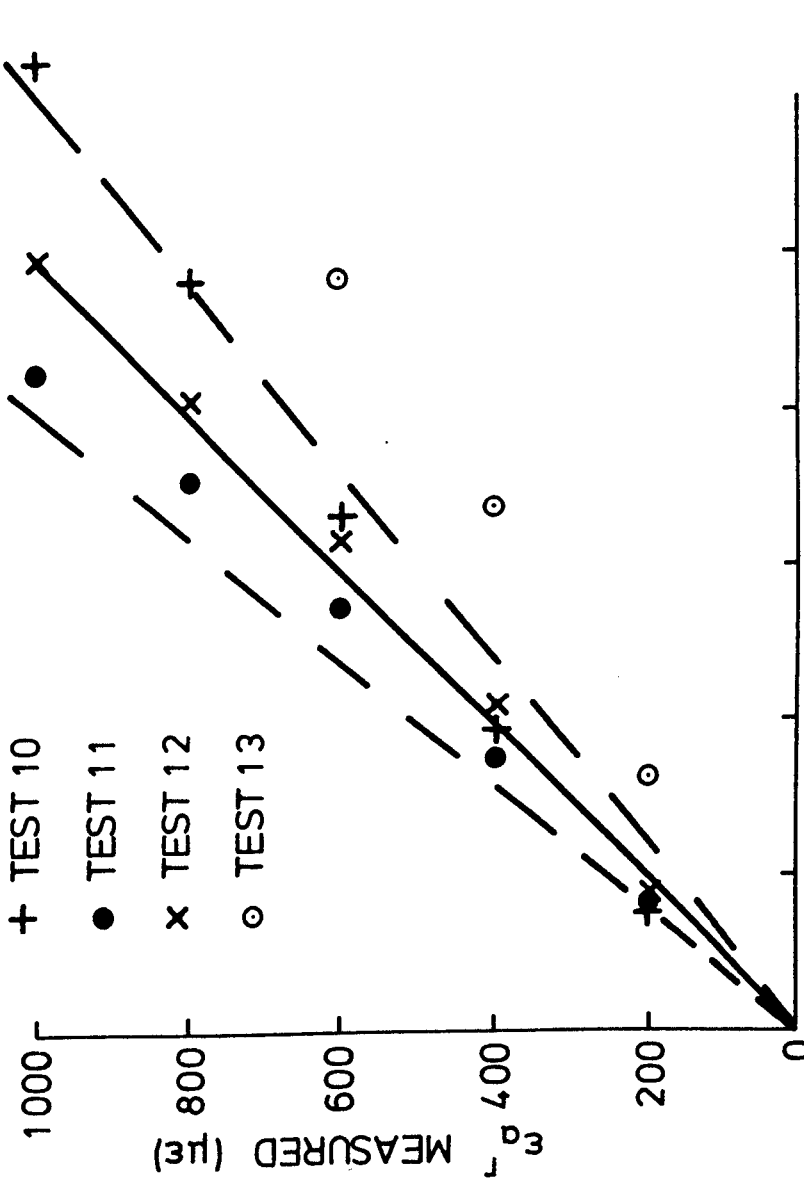

FIGURE 7.17 COMPARISON BETWEEN PREDICTED AND MEASURED RESILIENT AXIAL STRAINS FOR KEUPER MARL

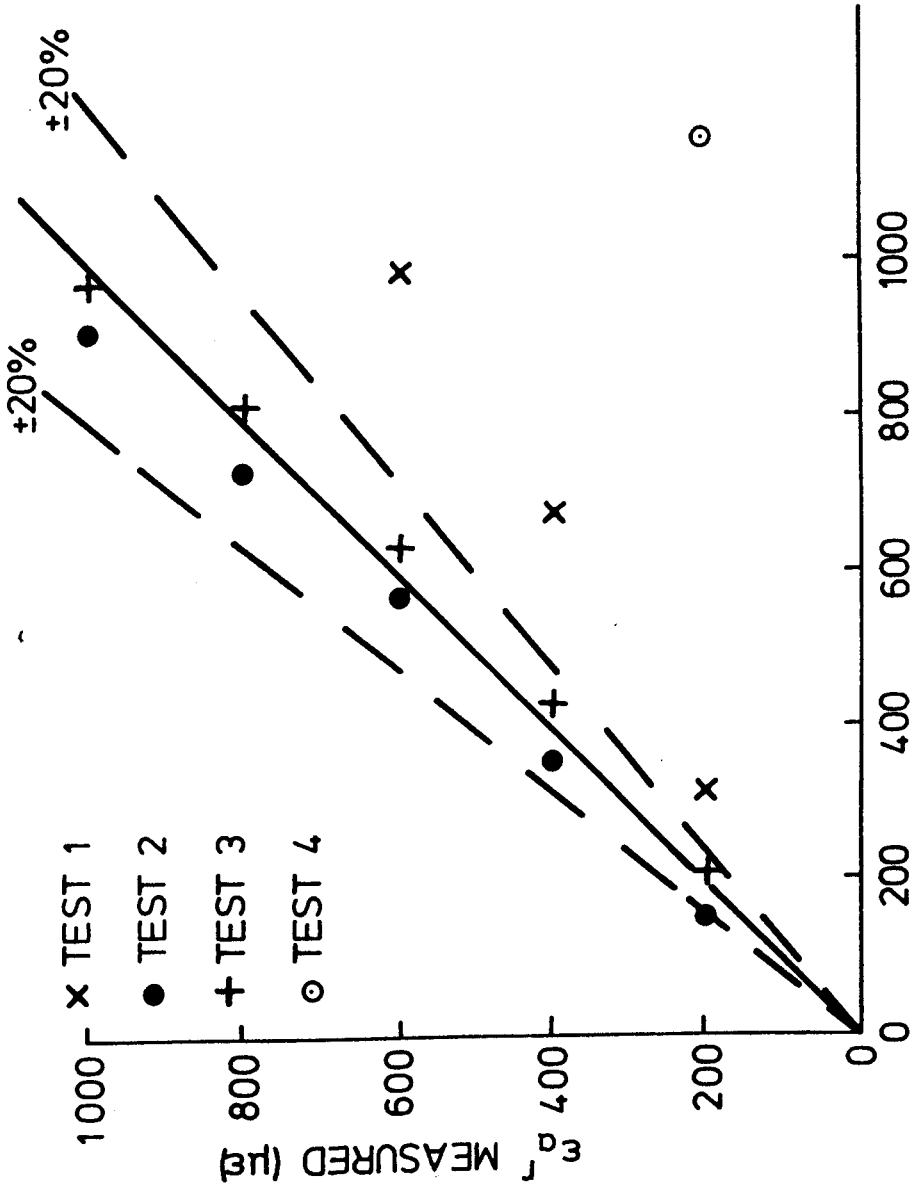

FIGURE 7.18 COMPARISON BETWEEN PREDICTED AND MEASURED RESILIENT AXIAL STRAINS FOR GAULT CLAY

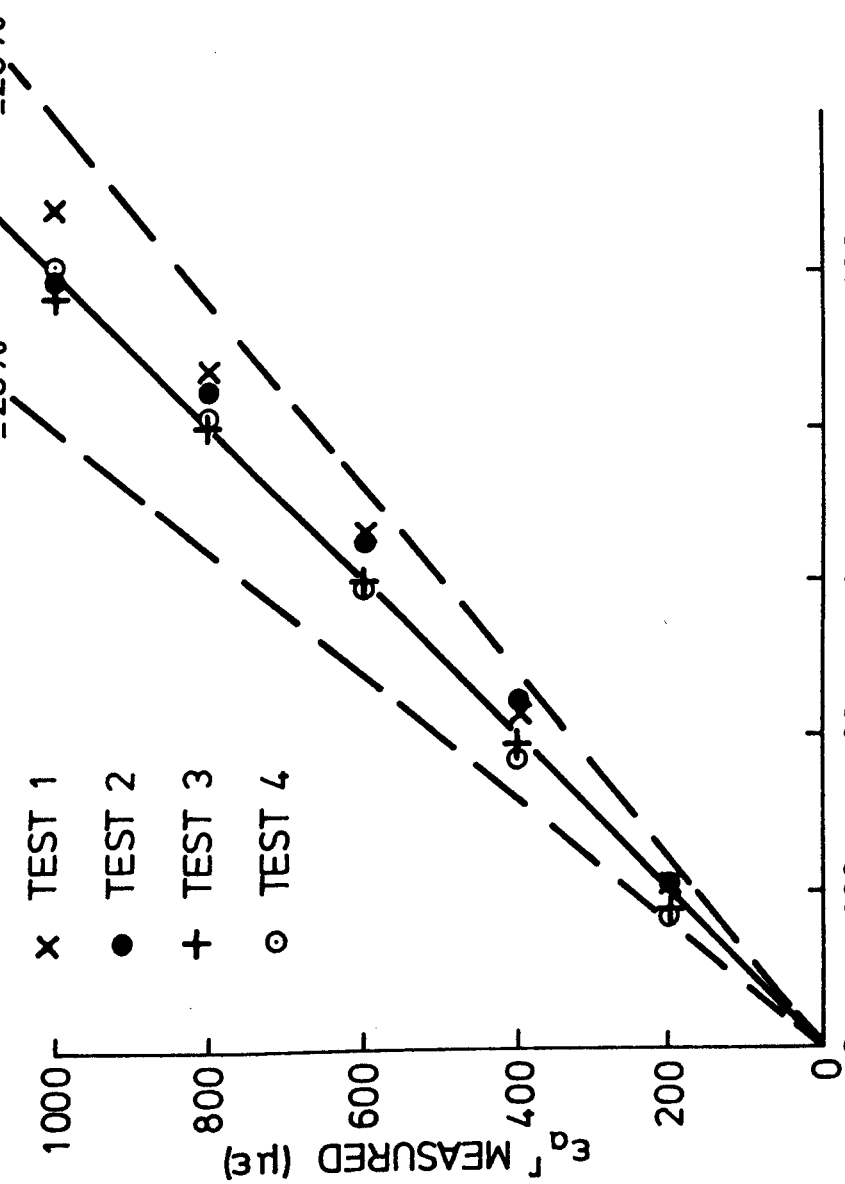

FIGURE 7.19 COMPARISON BETWEEN PREDICTED AND MEASURED RESILIENT AXIAL STRAINS FOR LONDON CLAY

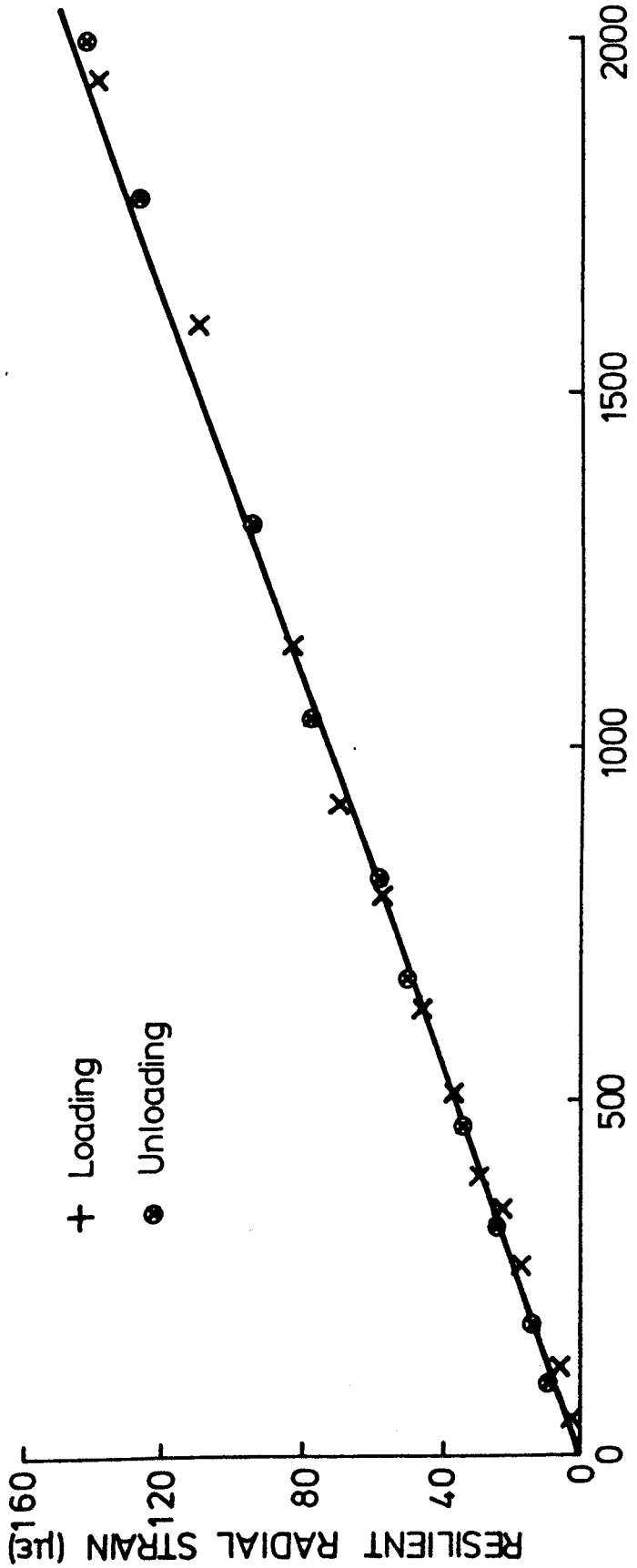

FIGURE 7.20 TYPICAL PLOT OF RESILIENT RADIAL STRAIN vs RESILIENT AXIAL STRAIN, LONDON CLAY 2

with moisture content though the degree of saturation was 100%. The behaviour of the compacted samples is rather different and gives much lower values for Poisson's Ratio. The London clay, for example, gives a decreasing Poisson's Ratio with decreasing moisture content at a roughly constant degree of saturation. The Gault clay and Keuper Marl also seem to show a similar trend except when the degree of saturation is close to 100% when the value of Poisson's Ratio is rather higher than the other results would indicate, for example Gault clay sample 4 and to a lesser extent Keuper Marl, sample 13. The value of Poisson's Ratio would seem to depend on the degree of saturation and also to some extent on the moisture content. Rather more tests would be required to confirm this conclusion.

7.3.3.3 **Permanent Strain**

The cyclic deviator stress at which a measurable amount of permanent strain had accumulated was determined for each test and was plotted against the suction of the sample, see Figure 7.21. The figure shows that there is an approximate linear relationship which holds for all three clays. Expressions relating permanent strain in the subgrade to the repeated vertical stress would be very useful for the analytical design of road pavements, as one of the modes of failure of a road is by rutting caused by subgrade deformation. The spread in the results may be due to the inaccuracies in determining the onset of plastic strain in the tests, or because the results are from three different clays with three different minearologies and stress strain relationships.

7.4 UNDRAINED SHEAR STRENGTH

The four Gault clay samples and two of the London clay samples were subjected to undrained constant strain rate failure tests. A Wykeham Farrance constant strain rate machine was used at a strain rate of 0.3040mm/minute.

The deviator stress axial strain plots are shown in Figures 7.22 and 7.23 for the Gault and London clays respectively. As would

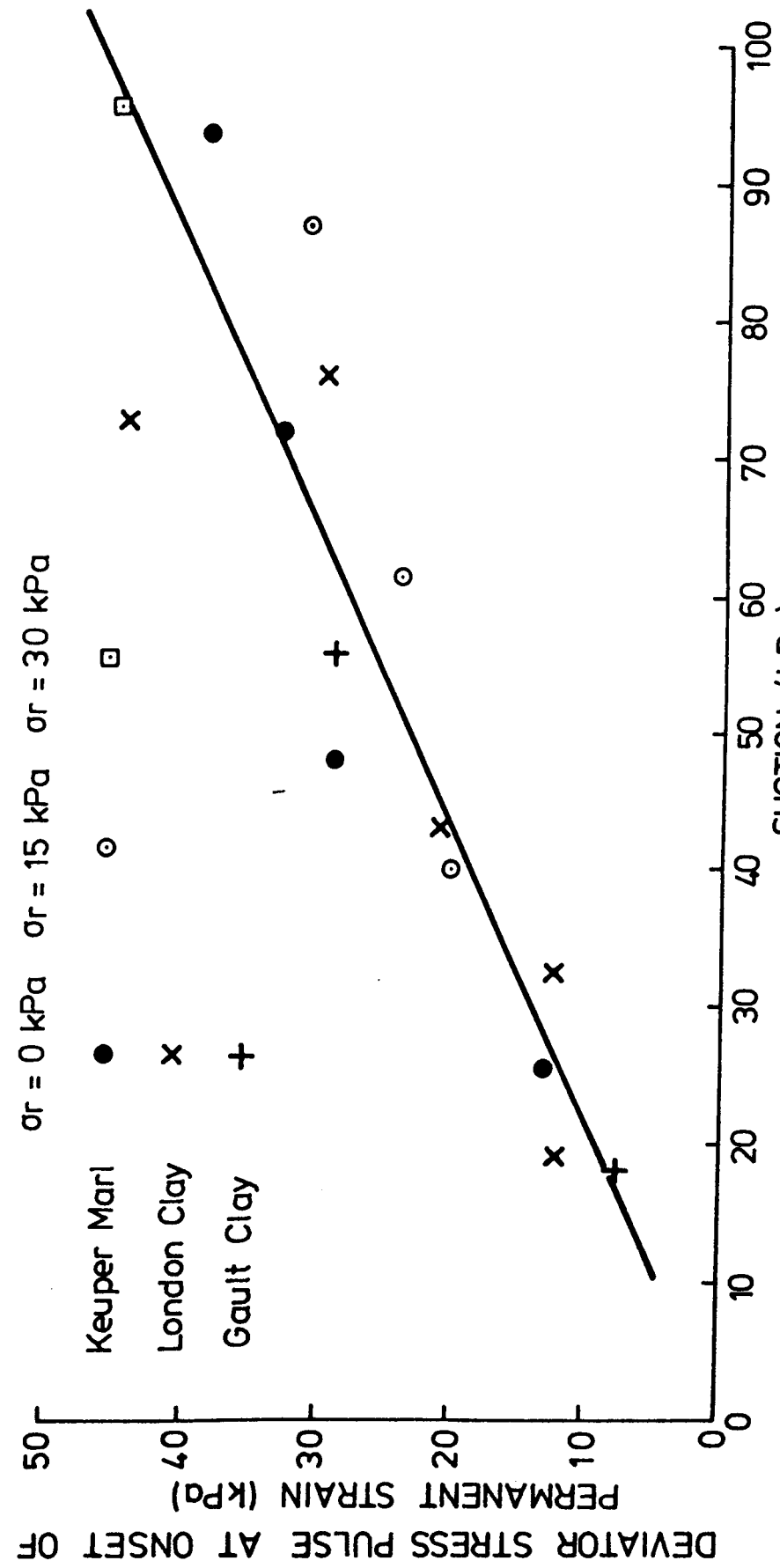

FIGURE 7.21 DEVIATOR STRESS PULSE MAGNITUDE AT THE ONSET OF PERMANENT STRAIN vs SUCTION

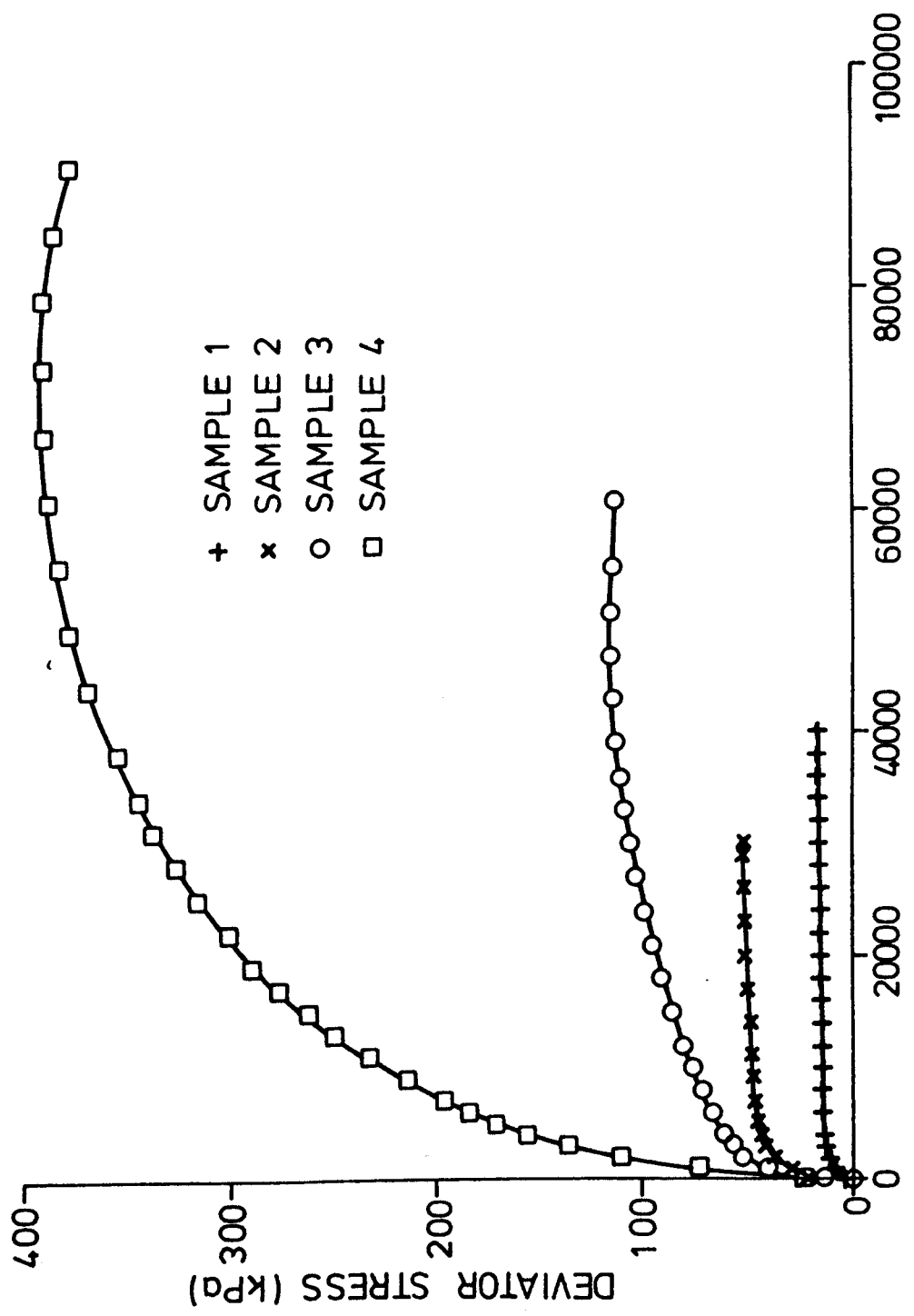

FIGURE 7.22 DEVIATOR STRESS vs AXIAL STRAIN FOR CONSTANT STRAIN RATE FAILURE TESTS, GAULT CLAY

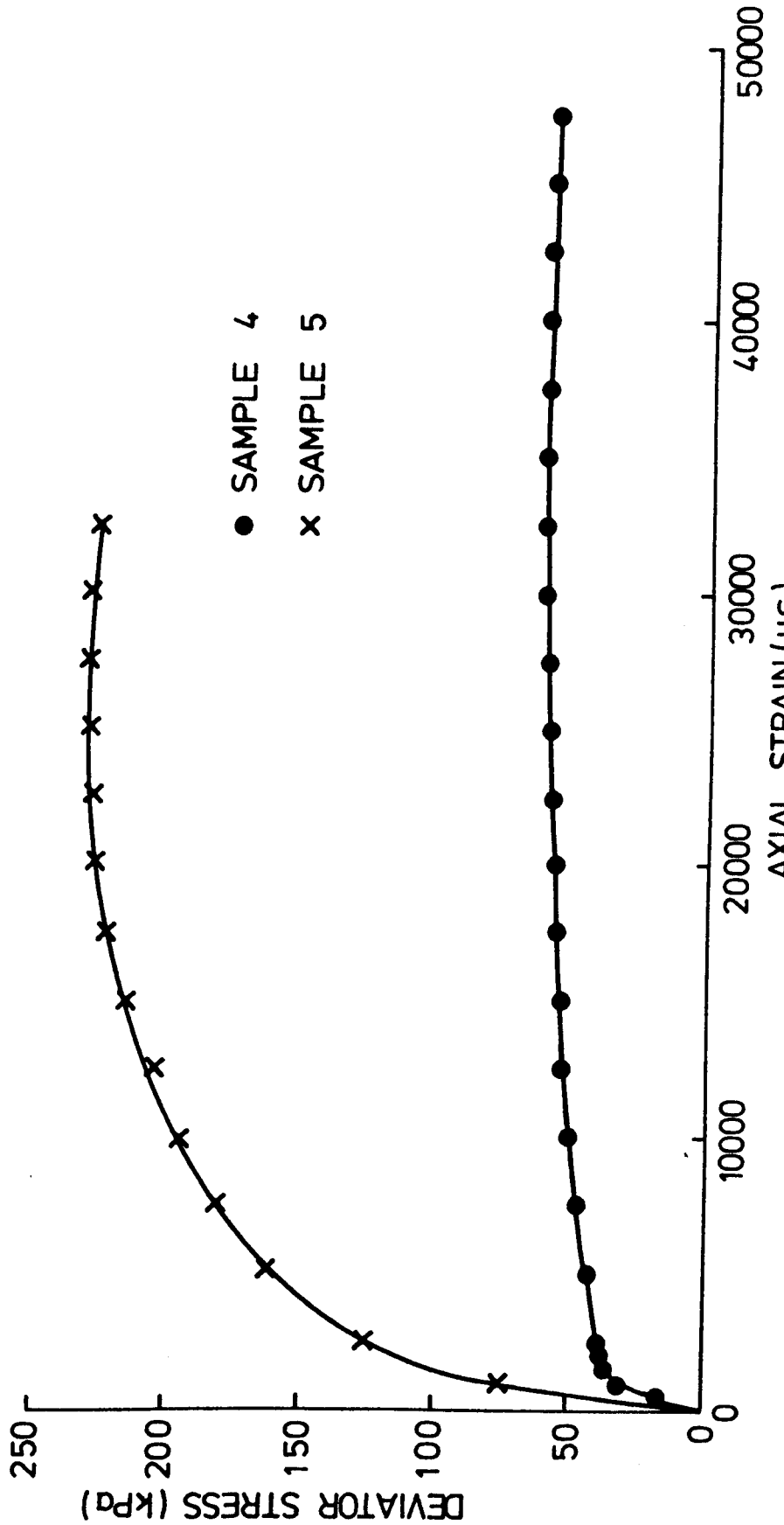

FIGURE 7.23 DEVIATOR STRESS vs AXIAL STRAIN FOR CONSTANT STRAIN RATE FAILURE TESTS, LONDON CLAY

be expected the drier samples sustained the higher values of deviator stress. As shown previously the drier samples also have the higher suctions.

The type of failure varied with the moisture content. The wettest Gault clay sample, sample 1, showed no signs of failure planes and deformed into a uniform barrel shape. Gault clay sample 2 developed an appreciable barrelled shape but there was evidence at the surface of small failure planes. Gault clay samples 3 and 4 failed with excessive deformation on a discrete failure plane, with the rest of the sample showing little distress. The two samples of London clay also failed along discrete failure planes.

These two types of failure, the uniform barrelling and the discrete failure planes, would indicate a change in overconsolidation ratios for saturated samples. Those with low overconsolidation ratios would be wet of critical state and consequently deform uniformly, while those with overconsolidation ratios greater than about 4 would be dry of critical and become non uniform with the resultant shear planes. Schofield and Wroth (1968) report that when soil is completely sheared by remoulding the overconsolidation ratio is often between 4 and 5. This was limited to saturated soils but it would seem reasonable that compacted unsaturated soils would also show some signs of overconsolidation. It is likely that compacted soils would also have a locked in radial stress caused by the compaction process. The results suggest that there is a change from plastic to brittle behaviour as the moisture content decreases, but that this does not coincide with the conventional plastic limit.

Figure 7.24 shows the peak values of deviator stress plotted against suctions at the start of the test on a log-linear scale. The results for the Gault clay give a good linear relationship, showing a direct relationship between the suction and log peak deviator stress. There are only two results from the London clay and these are shown to fit the curve from the Gault clay quite reasonably.

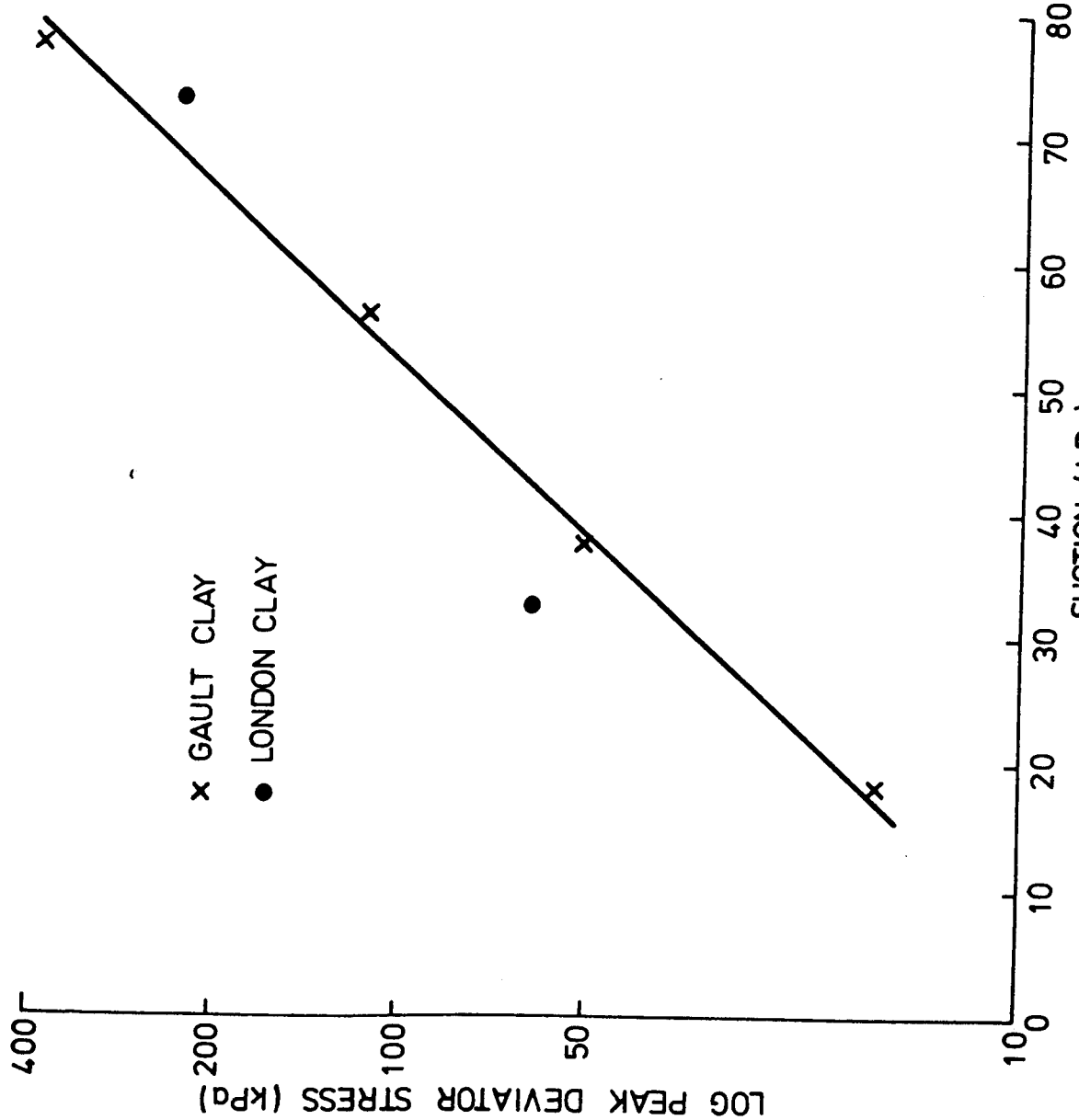

FIGURE 7.24 LOG PEAK DEVIATOR STRESS vs SUCTION FOR CONSTANT STRAIN RATE UNDRAINED FAILURE TESTS

Saturated samples tested to failure under undrained conditions fail on the critical state line at the same voids ratio as they had initially. The failure point is independent of p' and therefore independent of the overconsolidation ratio. The undrained shear strength can be expressed as a function of the specific volume as

$$C_u = \frac{1}{2} M \exp\left[(\Gamma - v_o)/\lambda \right] \qquad 7.4$$

It follows therefore that for saturated samples a plot of log C_u against specific volume or moisture content will give a linear relationship.

Figure 7.24 shows that for unsaturated Gault clay there is a linear relationship between log C_u and suction. It has been shown previously that there is a linear relationship between suction and moisture content, and therefore between log C_u and moisture content for the unsaturated samples.

An equation similar to 7.4 can be seen to describe the behaviour of the unsaturated samples as well as saturated samples, although the various constants would be different.

The two results from the London clay tests do not give sufficient information to describe the behaviour of London clay and rather more tests on Gault clay would be required before a firm conclusion could be drawn.

CHAPTER EIGHT

CBR TEST RESULTS

8.1 INTRODUCTION

This chapter presents the results from the tests on the consolidated CBR samples of Keuper Marl, and on the compacted CBR samples of Keuper Marl, Gault clay and London clay. The sample preparation is detailed in Chapter 5, and the test programme is discussed in Chapter 3.

8.2 CONSOLIDATED CBR SAMPLES

The sample details from the tests on the consolidated Keuper Marl samples are given in Table 8.1. The CBR was determined at the top of each sample. The preconsolidation pressure was determined from oedometer tests carried out on two samples cut from the bottom of each CBR sample. The shear strength was determined by a 19mm shear' vane and is the average of at least three readings, which generally showed a scatter of ± 2 kPa.

The results from the CBR tests are shown in Table 8.1. The trends are generally as expected, with a decreasing moisture content leading to an increase in CBR and also in shear strength as measured by the shear vane. The overconsolidation ratio also behaves as expected with an increase in the moisture content leading to a decrease in OCR. This is because the samples were all swelled back to approximately the same vertical effective stress therefore the overconsolidation ratio depends mainly on the preconsolidation pressure.

Figure 8.1 shows a typical plot of one of the CBR tests showing the effects of the load unload cycle. The shape of the curve compares well with that produced when a sample of annealed copper is loaded and unloaded axially in tension to successively higher stress levels. The curve shows a predominantly plastic behaviour for the virgin loading section with the recoverable part of the

Table 8.1 Consolidated Keuper Marl CBR samples - sample details and results

Sample Number	Moisture Content Top %	Moisture Content Bottom %	OCR $Pm'/_{Po'}$	CBR % 2.5 mm	CBR % 5.0 mm	Cu Shear Vane kPa	Cu Pocket Pen kPa	Dry Density kg/m^3
2	20.75	20.40	11.1	5.0	3.9	40.8	-	1780
6	21.36	21.17	9.8	5.9	3.9	44.4	40	1750
4	21.71	21.68	8.8	4.3	2.9	33.4	-	1740
3	22.42	21.26	9.6	4.2	2.8	31.8	-	1750
1	22.47	22.42	8.5	3.8	2.9	28.8	-	1730
5	23.60	23.47	6.5	2.8	2.0	20.0	19	1670
7	24.34	23.83	5.85	2.4	1.7	19.0	-	1700

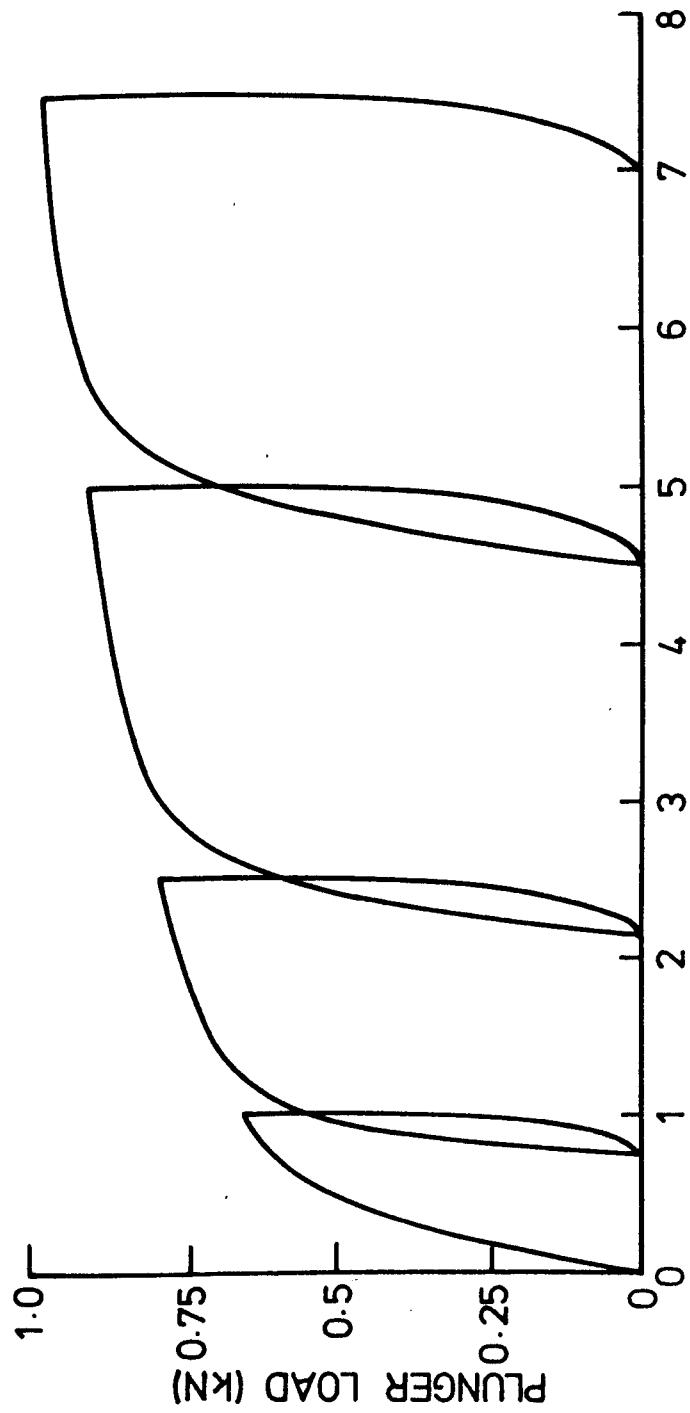

FIGURE 8.1 TYPICAL RESULT FROM A CBR TEST ON AN OVERCONSOLIDATED SAMPLE OF KEUPER MARL

deformation becoming apparent on the unloading sections. The reload part of the curve is of a similar gradient to the unload section of the curve (allowing for the hysteresis), until the load approaches the previous maximum load when the gradient decreases sharply as the sample starts to yield again.

Figure 8.2 shows the complete load deflection curves plotted for all the consolidated samples with the unload reload sections omitted for clarity. Figure 8.3 shows the loads recorded for the first millimetre penetration together with the unloading and reloading section of three of the curves. The curves on Figure 8.2 are all fairly similar and the relative strengths apparent in the initial stages of the test continue on to the maximum deflections. It is interesting to note from Table 8.1 that the ratio of the CBR values at 2.5mm penetration to 5mm penetration is approximately 1.4 to 1 for all the tests. This may indicate that the material under the plunger is already in a general state of failure at 2.5mm penetration and that the stress distributions are similar at 2.5mm penetration and 5mm penetration although the amount of sample affected will obviously be greater with the larger penetration. Therefore to determine the stiffness of samples before yield it might be prudent to use the results from the early part of the CBR test. Hight and Stevens (1982) reported a similar conclusion from their work which consisted of a finite element analysis of the CBR test on soils with various load deformation characteristics.

The initial part of the curves shown in Figure 8.3 suggest that the stronger the sample the greater the initial gradient. However, the initial part of the curve is very dependent on how well the plunger is seated on the sample and is therefore difficult to measure accurately. To some extent this applied to the unload reload parts of the curves as well as the penetration at zero load after unloading is difficult to measure accurately and was found to be time dependent as the samples continued to recover slowly. The reload parts of the curves shown in Figure 8.3 also show that the stronger the sample the greater the gradient of the reload curve.

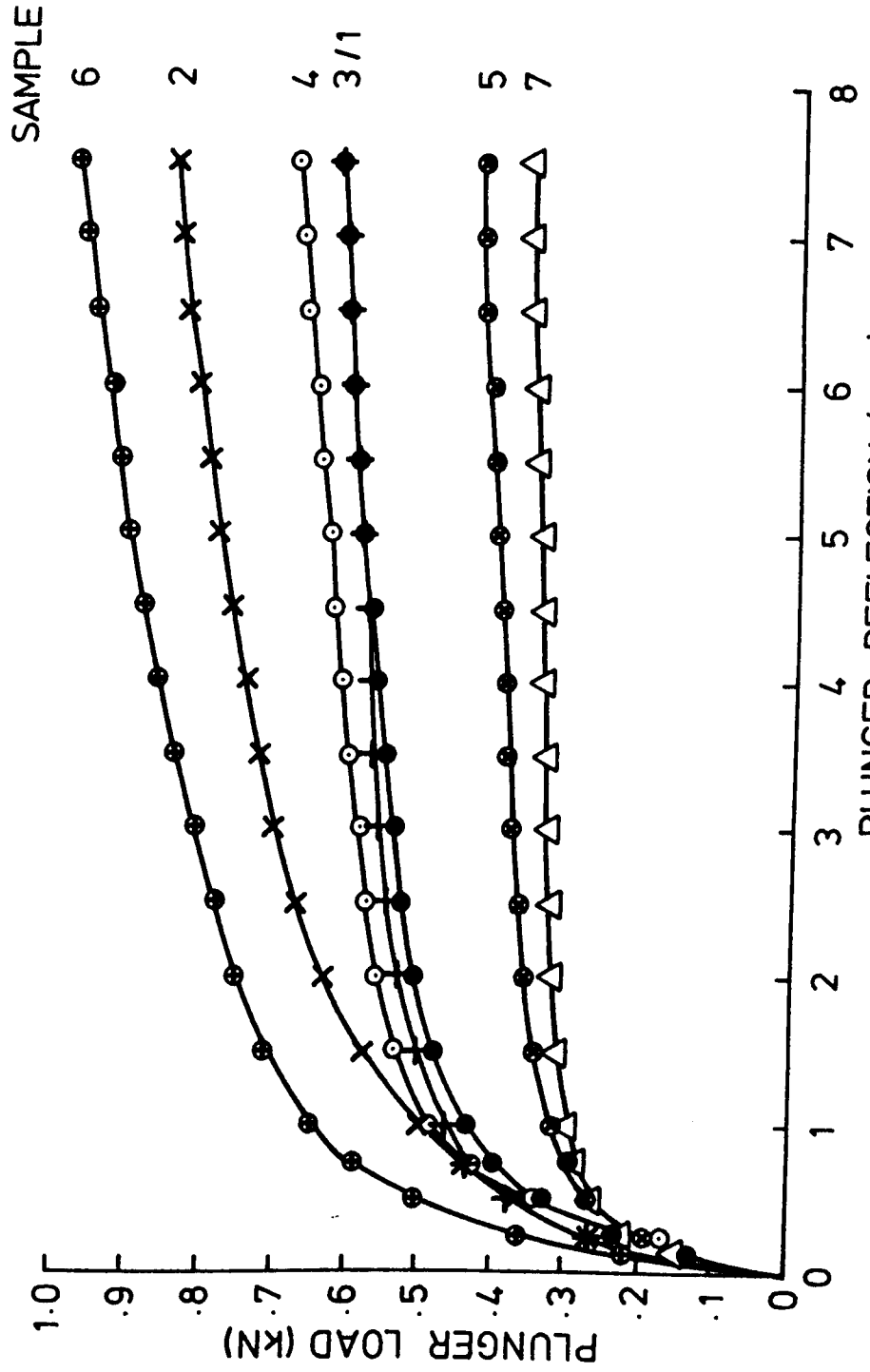

FIGURE 8.2 CONSOLIDATED KEUPER MARL CBR LOAD DEFLECTION CURVES

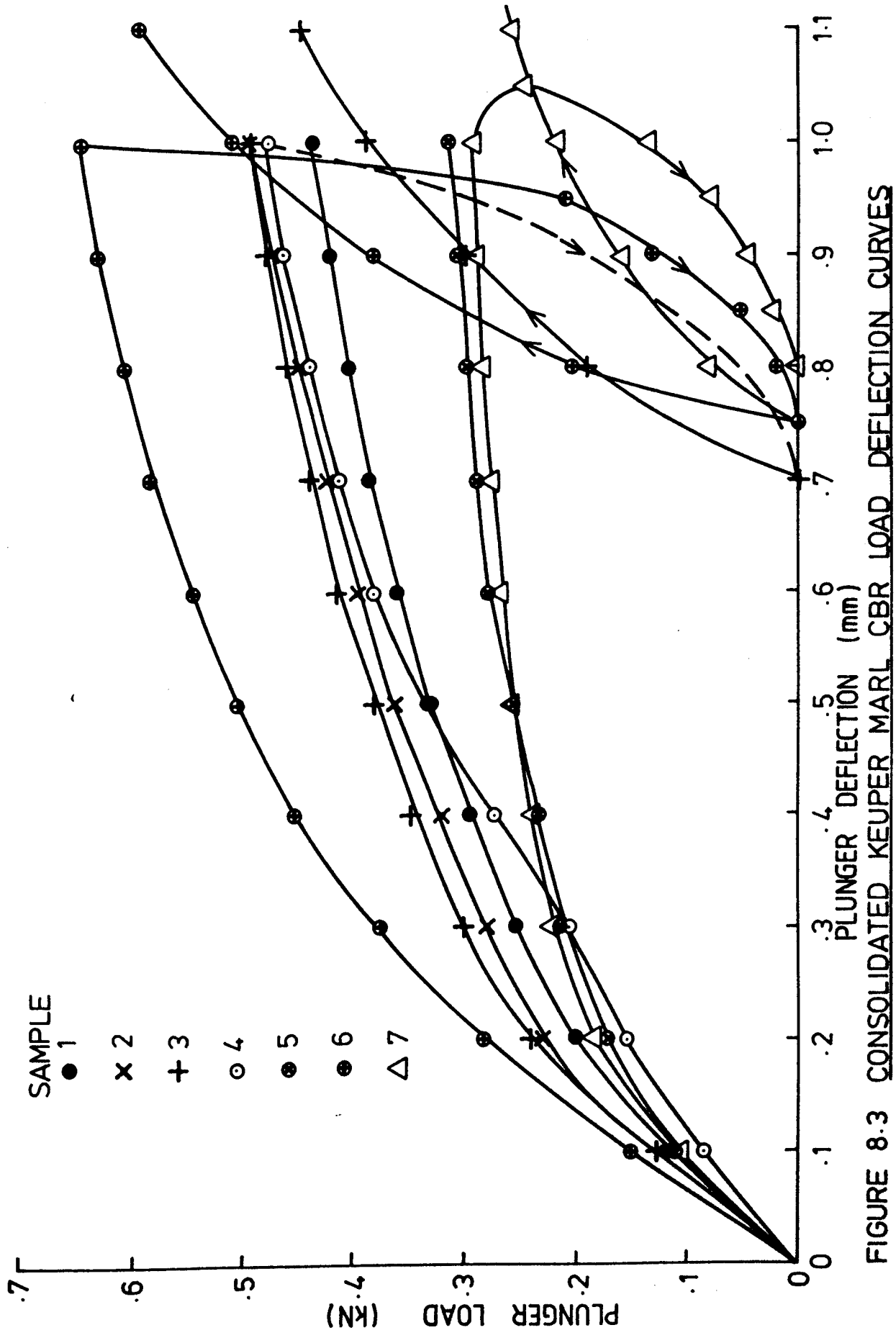

FIGURE 8.3 CONSOLIDATED KEUPER MARL CBR LOAD DEFLECTION CURVES

There was too much scatter in the gradients of the reload curves to suggest any form of relationship with the CBR value other than that the gradient increased as the CBR increased. This scatter is probably due to the experimental errors discussed above and also as there was only one sample tested at each moisture content. It would seem reasonable to assume that there would be some form of relationship if the samples were uniform, prepared in the same manner, and of the same material.

Figure 8.4 shows the CBR value plotted against the undrained shear strength as determined by the shear vane for each sample, and a pocket penetrometer for samples 5 and 6. The penetrometer results show reasonable agreement with the shear vane results for the two samples. The CBR and undrained shear strength (in kPa) are related by the expression $C_u = 7.8 \times CBR$ for this material over the range of moisture contents tested. Black (1979) quotes the relationship between CBR and undrained shear strength as $C_u = 11.5 \times CBR$ for undisturbed overconsolidated soil. Black used a cone penetrometer to measure C_u. The results quoted by Black show a range of factors from 8.6 to 11.0, so the results from Figure 8.4 are at the low end of this range.

Figure 8.5 shows that there is a linear relationship between the moisture content and the logarithm of the undrained shear strength. This result is as expected from critical state theory for undrained strength tests on saturated samples as the sample fails on the critical state line at a constant specific volume. This is discussed more fully in Chapter 7, section 7.4.

8.3 COMPACTED CBR SAMPLES

Tables 8.2, 8.3 and 8.4 give the sample details and test results from the tests on the compacted samples of Keuper Marl, Gault clay and London clay respectively. The CBR, moisture content and undrained shear strength were determined at each end of the sample. The undrained shear strength was determined using a 19mm shear vane and a pocket penetrometer.

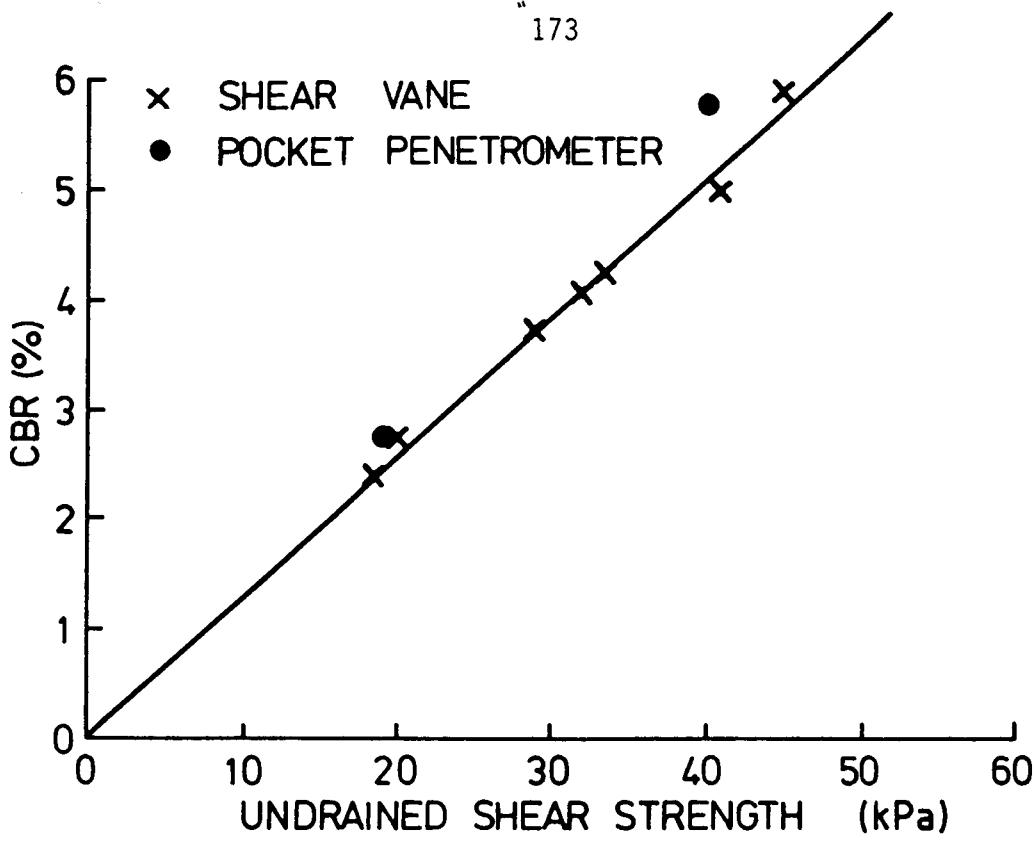

FIGURE 8.4 CBR AGAINST UNDRAINED SHEAR STRENGTH FOR OVERCONSOLIDATED SAMPLES OF KEUPER MARL

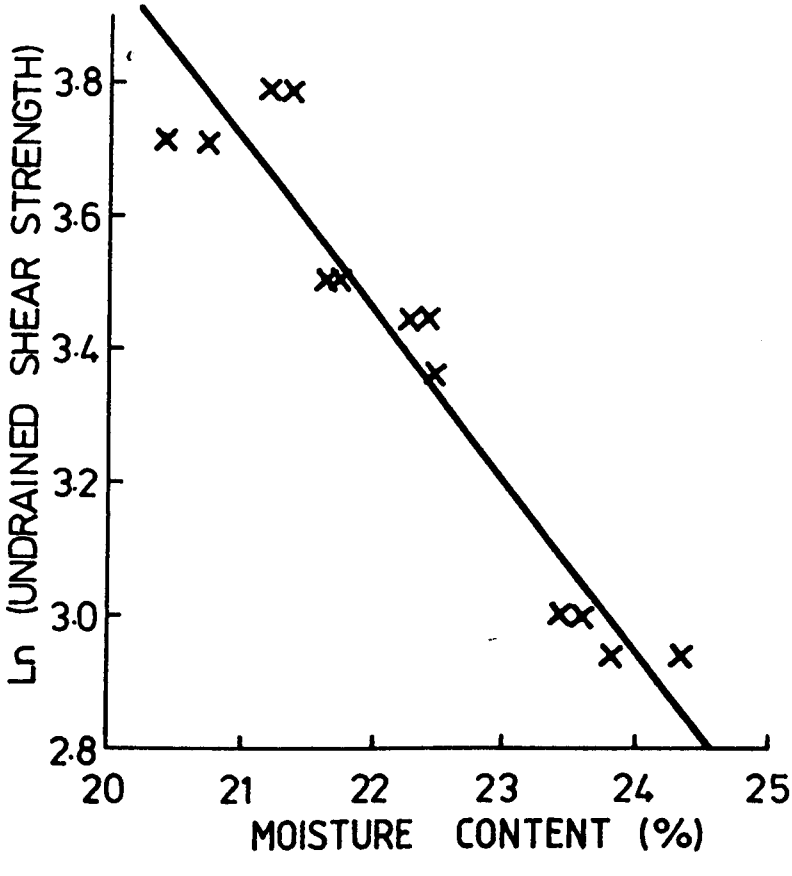

FIGURE 8.5 LOGARITHM (UNDRAINED SHEAR STRENGTH) AGAINST MOISTURE CONTENT FOR CONSOLIDATED CBR SAMPLES OF KEUPER MARL

Table 8.2 Compacted Keuper Marl CBR samples - sample details and results

Sample Number	Moisture Content %		CBR %				Cu Shear Vane kPa		Cu Pocket Pen kPa		Dry Density kg/m³		Degree of Saturation %		Suction kPa	
			T		B											
	T	B	2.5	5.0	2.5	5.0	T	B	T	B	T	B	T	B	T	B
2	24.37	24.06	0.6	0.6	0.6	0.6	13	13	14	14	1600	1600	0.96	0.95	27	28
5	22.25	22.25	1.0	0.9	1.0	0.9	-	-	32	30	1640	1640	0.93	0.93	42	42
1	20.26	21.44	1.4	1.5	1.0	1.0	33	27	55	55	1730	1715	0.98	1.0	58	47
3	18.08	18.89	3.3	3.1	3.0	2.6	59	46	98	89	1805	1790	0.99	1.0	78	69
4	16.03	16.53	5.9	5.0	4.9	4.6	110	99	190	153	1785	1775	0.84	0.86	100	94

Table 8.3 Compacted Gault clay CBR samples - sample details and results

Sample Number	Moisture Content %		CBR %				Cu Shear Vane kPa		Cu Pocket Pen kPa		Dry Density kg/m³		Degree of Saturation %		Suction kPa	
			T		B											
	T	B	2.5	5.0	2.5	5.0	T	B	T	B	T	B	T	B	T	B
1	39.35	39.40	0.8	0.6	0.8	0.6	9.5	8.8	18	18	1250	1250	0.92	0.92	17	17
2	32.19	32.28	1.8	1.6	2.1	1.7	26.2	26.3	45	43	1360	1360	0.89	0.89	36	36
3	26.59	27.11	4.4	4.0	4.4	4.0	56	55	102	115	1525	1520	0.94	0.95	58	56
4	21.96	23.13	12.6	8.0	9.7	8.0	>130	108	490	330	1615	1600	0.89	0.91	80	74

Table 8.4 Compacted London clay CBR samples - sample details and results

Sample Number	Moisture Content %		CBR %				Cu Shear Vane kPa		Cu Pocket Pen kPa		Dry Density kg/m³		Degree of Saturation %		Suction kPa	
			T		B											
	T	B	2.5	5.0	2.5	5.0	T	B	T	B	T	B	T	B	T	B
3	35.35	35.31	2.3	1.9	2.3	1.9	-	-	99	100	1318	1318	0.90	0.90	31	31
1	32.15	32.39	3.1	2.3	3.7	2.8	-	-	86	85	1370	1370	0.89	0.89	41	41
4	26.40	27.33	9.0	7.0	8.0	6.4	103	87	310	280	1520	1510	0.91	0.93	65	61
2	25.15	26.49	13.2	11.0	11.4	9.4	-	-	440	330	1570	1550	0.93	0.95	72	65

Figures 8.6 and 8.7 show the results for the Keuper Marl, Figures 8.8 and 8.9 show the results for the Gault clay, and Figures 8.10 and 8.11 show the results for the London clay. The unload and reload sections of the curves have been omitted from Figures 8.6, 8.8 and 8.10 for clarity. As for the consolidated samples discussed in section 8.2 the curves are a fairly similar shape, and the relative strengths are apparent in the initial stages of the tests. Again as for the consolidated samples the samples with the higher CBR values showed the larger initial gradients and reload gradients. There was too much variability in the measured gradients to indicate any relationship with the CBR.

A comparison between Figures 8.2, 8.6, 8.8 and 8.10 show that the curves for the Gault and London clays are approximately the same shape, while those of the consolidated Keuper Marl samples are stiffer initially, and those of the compacted Keuper Marl are somewhat flatter. This is reflected in the ratios between the CBR at 2.5mm and 5.0mm penetration which are very approximately 1.25 for the Gault clay and London clay, 1.4 for the consolidated Keuper Marl and approximately 1.1 for the compacted Keuper Marl.

Figure 8.12 shows that there is a good relationship between the CBR value and the undrained shear strength as measured by a pocket penetrometer. The relationship can be approximated to a straight line of the form $C_u = 3.7 \times CBR\ (kPa)$ The pocket penetrometer is in reality a small scale version of the CBR test and a linear relationship is not surprising. Figure 8.13 shows the relationship between the undrained shear strength as measured by the shear vane and the CBR value. The relationship for the Keuper Marl and Gault clays can be approximated to straight lines, although of different gradients. There are only two results for the London clay and these suggest that the behaviour might be similar to the Gault clay. The relationships are approximately $C_u = 20 \times CBR$ for the Keuper Marl, and $C_u = 12.5 \times CBR$ for the Gault clay, with C in kPa.

Black (1979) suggests that $C = 23 \times CBR\ (kPa)$ for remoulded soils. The results from the Keuper Marl are in reasonable agreement with

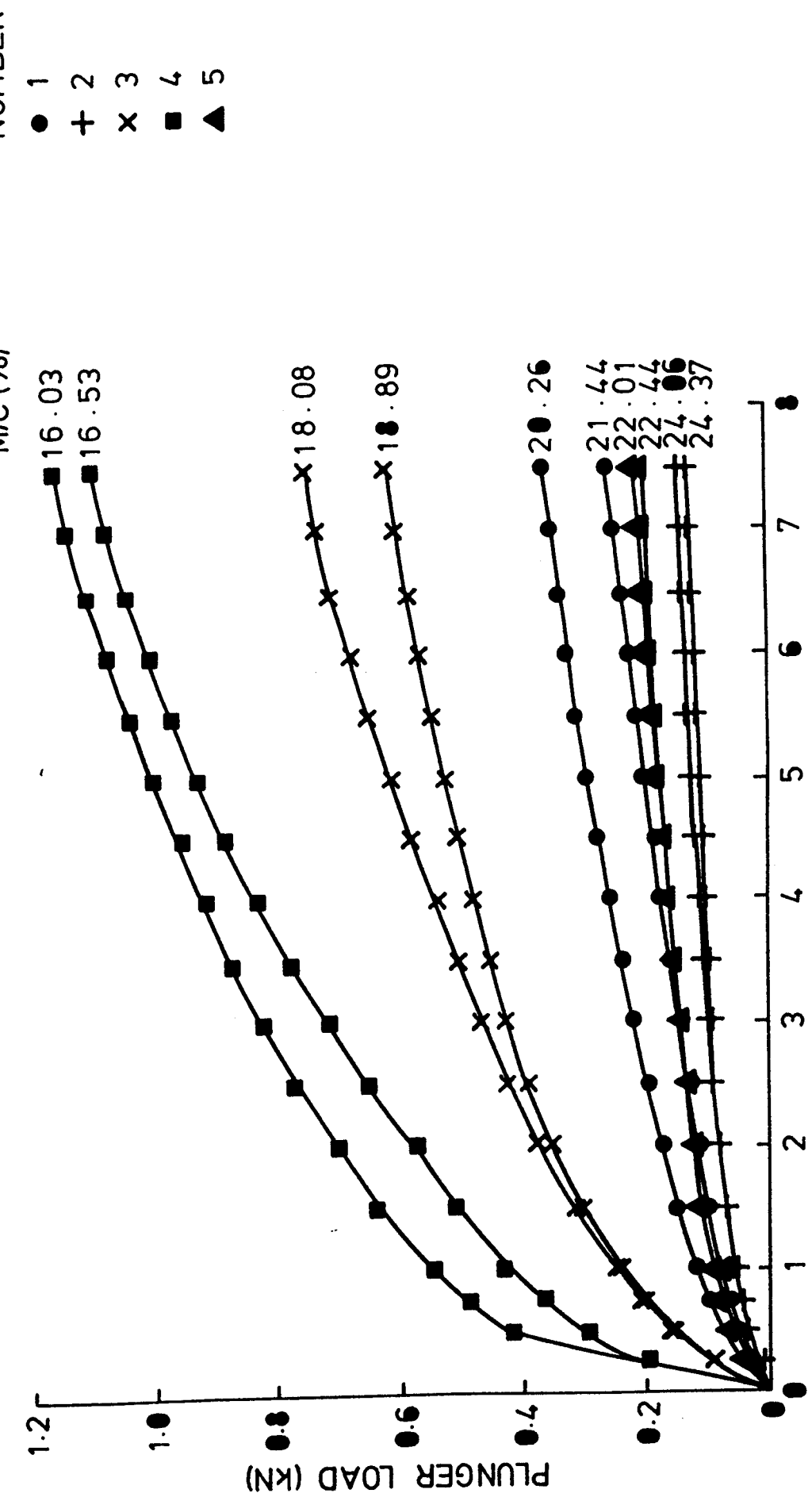

FIGURE 8.6 COMPACTED KEUPER MARL CBR TEST RESULTS

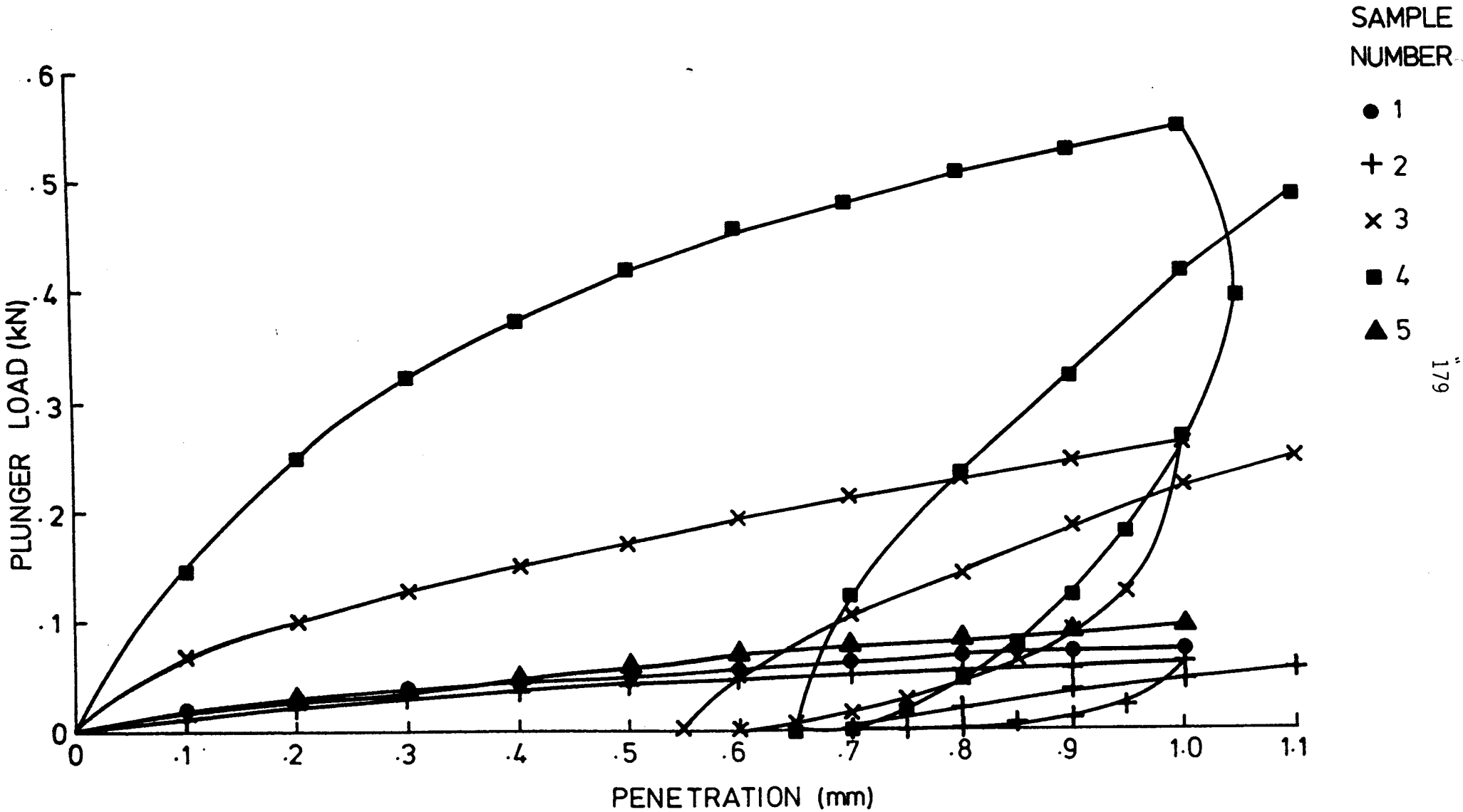

FIGURE 8.7 COMPACTED KEUPER MARL CBR PART TEST RESULTS

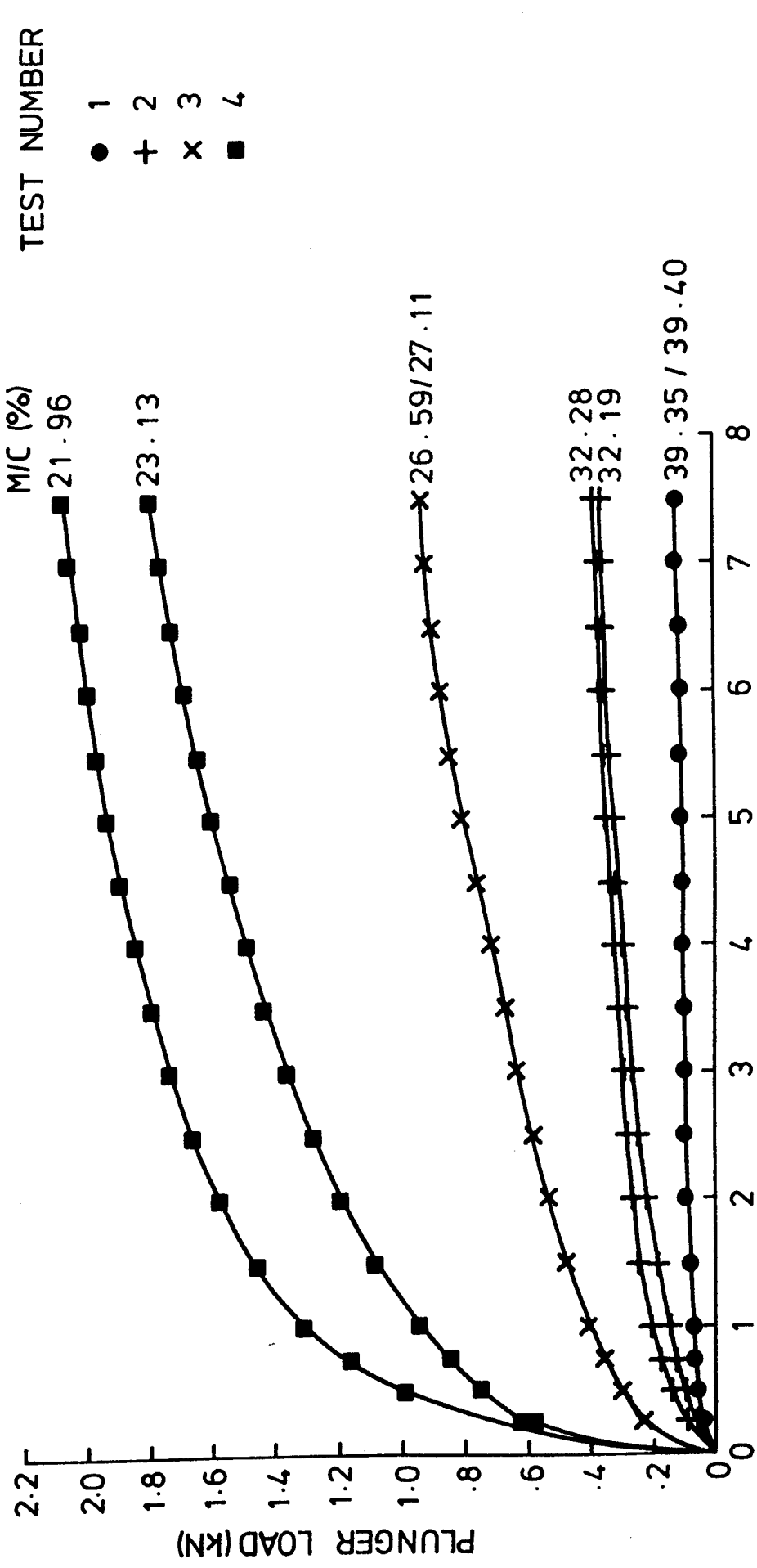

FIGURE 8.8 COMPACTED GAULT CLAY CBR TEST RESULTS

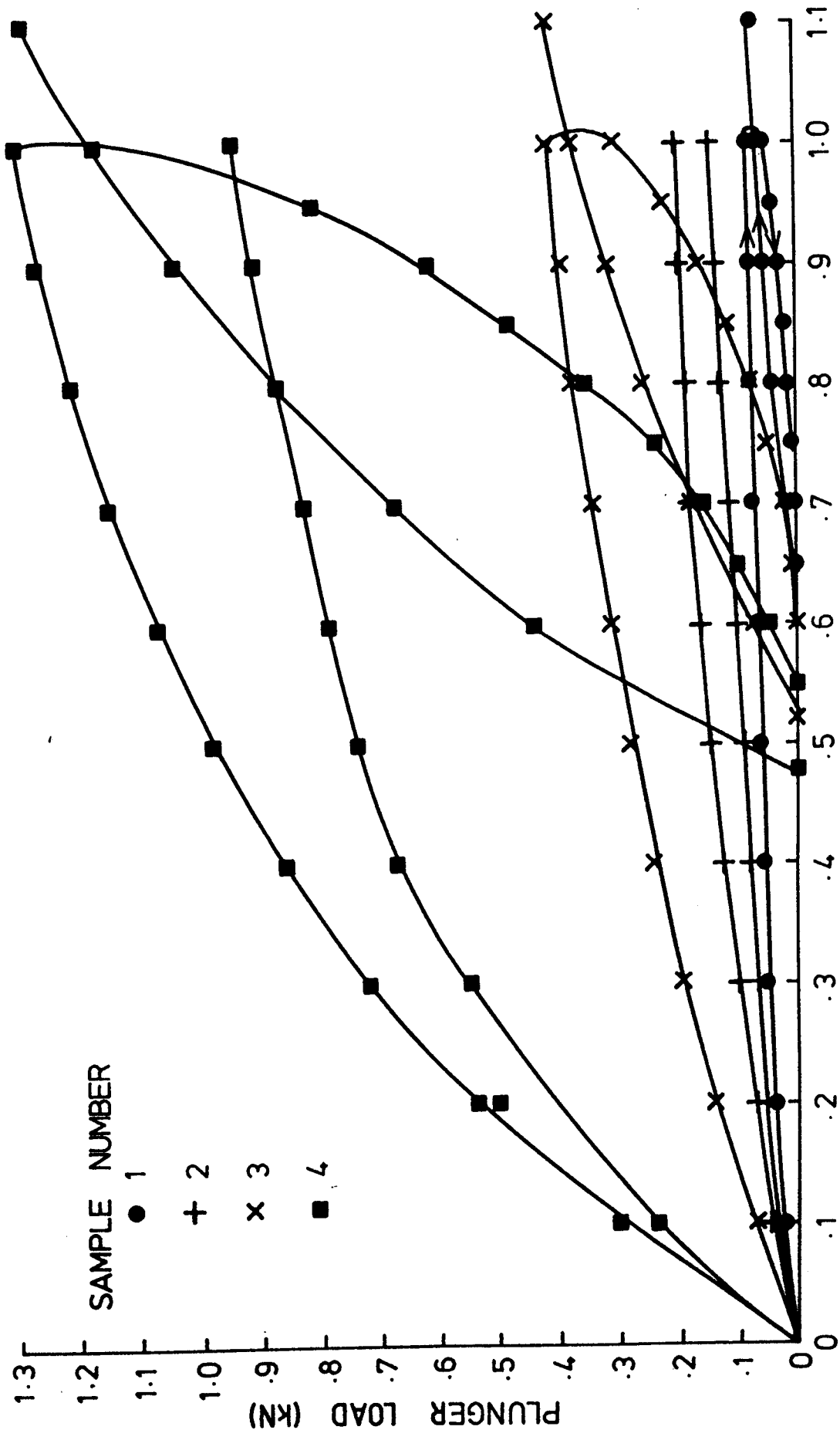

FIGURE 8.9 COMPACTED GAULT CLAY PART CBR TEST RESULTS

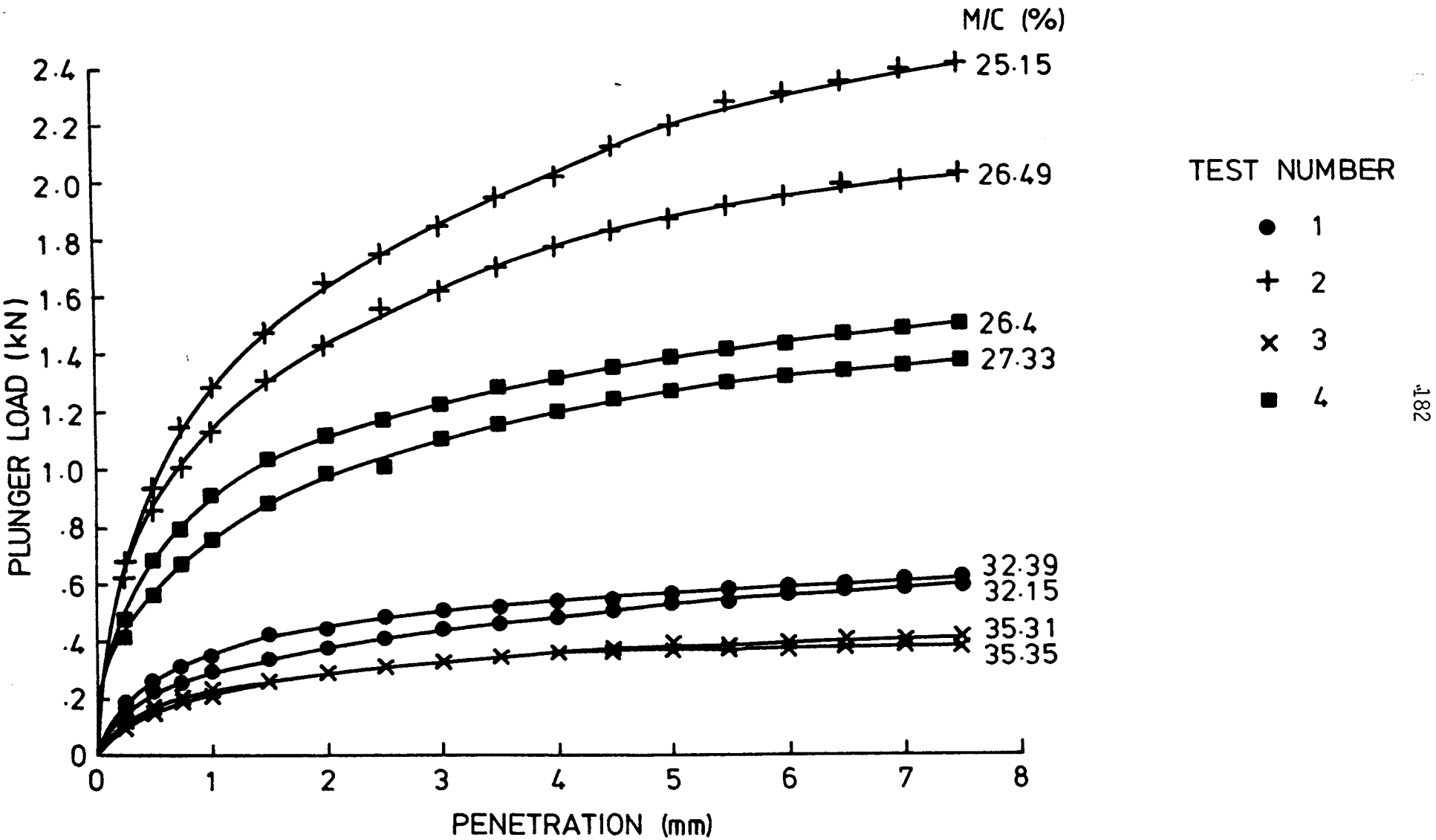

FIGURE 8.10 COMPACTED LONDON CLAY CBR TEST RESULTS

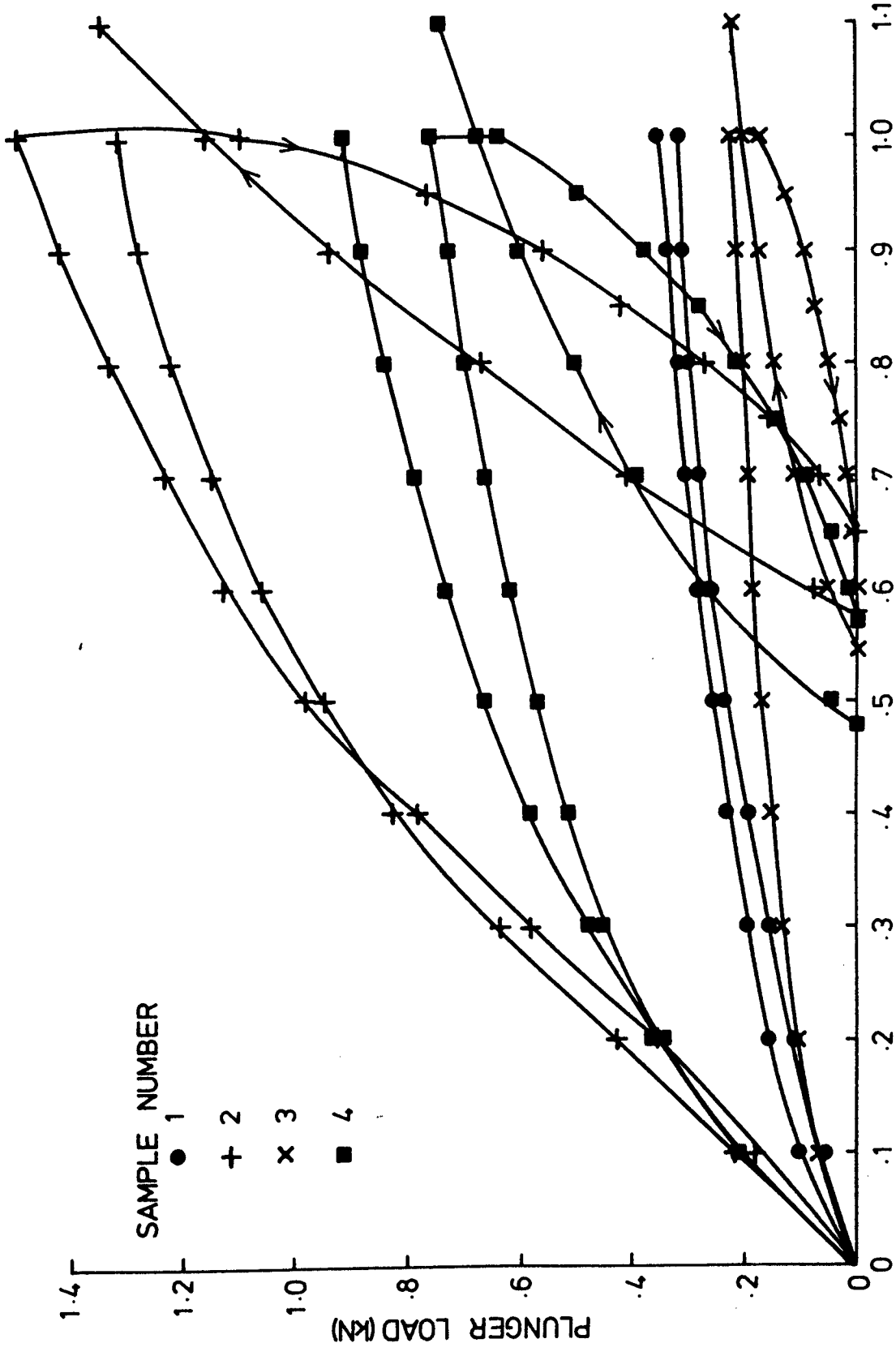

FIGURE 8.11 COMPACTED LONDON CLAY C B R PART RESULTS

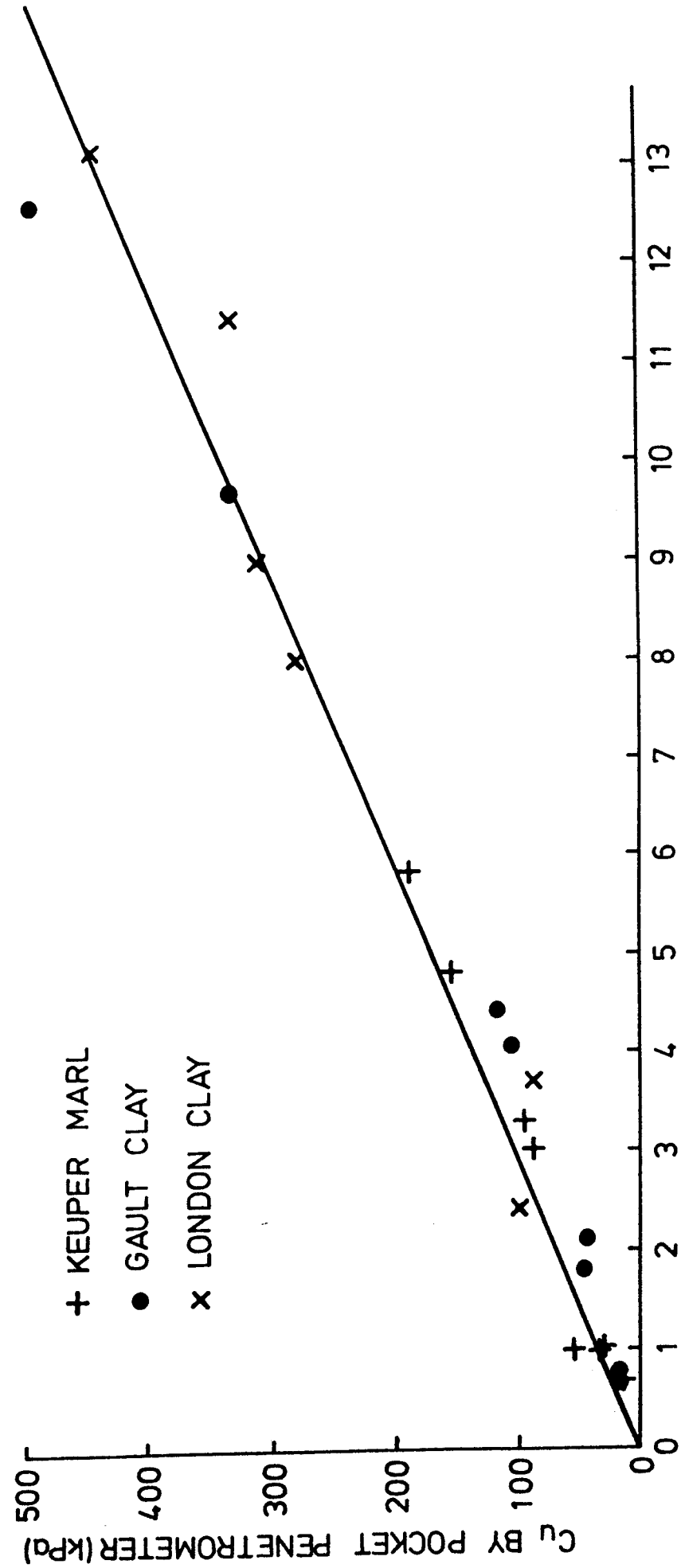

FIGURE 8.12 C B R AGAINST UNDRAINED SHEAR STRENGTH MEASURED BY A POCKET PENETROMETER FOR THE COMPACTED SAMPLES

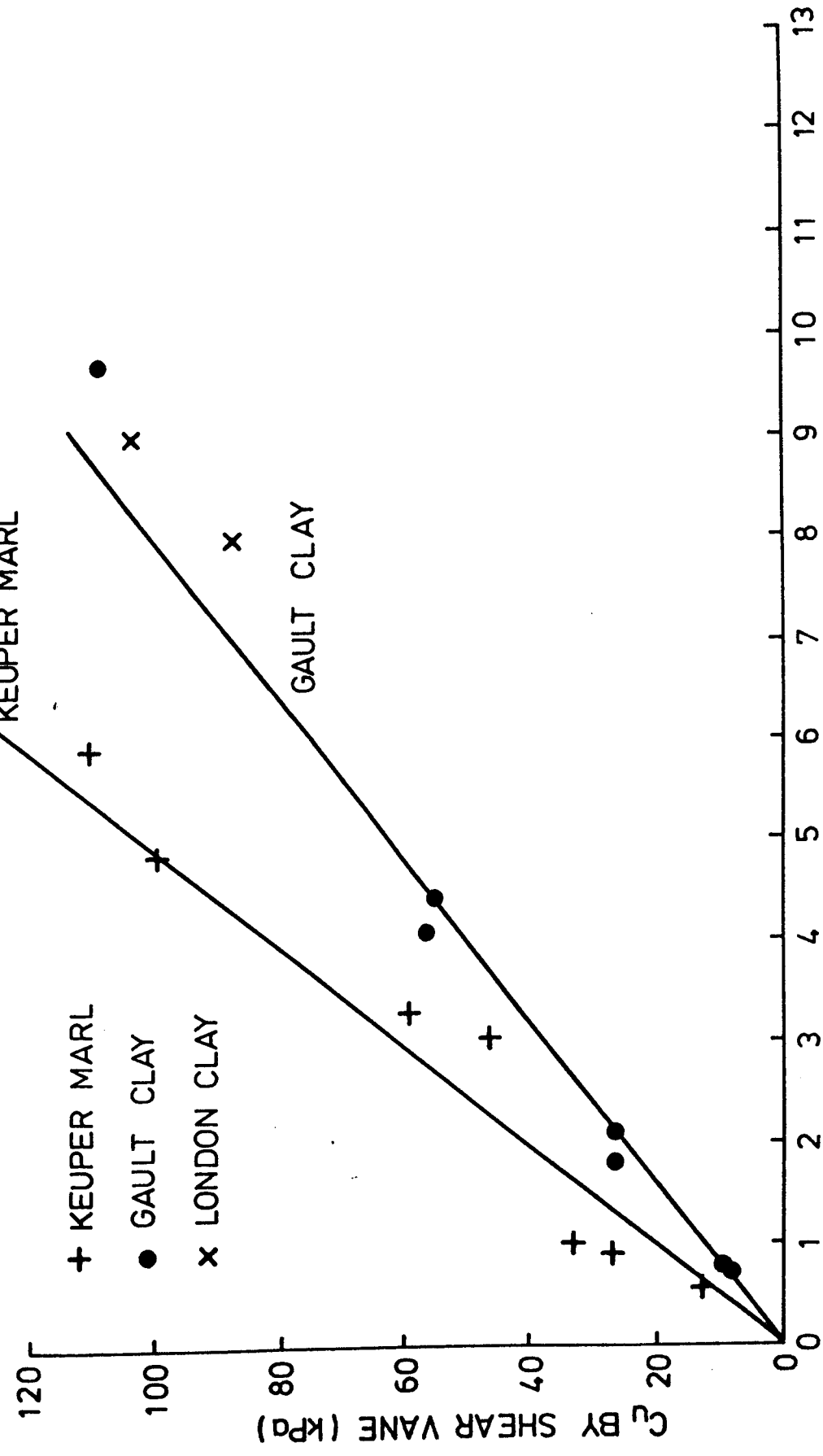

FIGURE 8.13 CBR AGAINST UNDRAINED SHEAR STRENGTH MEASURED BY A SHEAR VANE FOR THE COMPACTED SAMPLES

this, but those from the Gault clay are rather lower, and more in agreement with the relationship he proposed for undisturbed overconsolidated material (C_u = 11.5 x CBR). Black states that many compacted fills at low equilibrium suctions can behave as though they were 'undisturbed overconsolidated soils' as the act of shearing them causes a negative change in pore pressure which results in small strain at failure. As shown in Chapter 7 the behaviour of compacted samples changes in nature from plastic to brittle as the moisture content decreases. The liquidity index at which this occurs does not correlate with the plastic limit and may vary with different clays. The difference in behaviour then may just be the result of the two clays having different mineralogies and Atterberg limits.

Figures 8.14, 8.15 and 8.16 show that there is an approximately linear relationship between the suction of the compacted samples of Keuper Marl, Gault clay and London clay respectively, and the logarithm of the CBR value. The CBR value for these samples was found to correlate directly with the undrained shear strength as measured by the shear vane or pocket penetrometer, and consequently Figures 8.14, 8.15 and 8.16 show the same type of behaviour as the compacted triaxial samples, where there was a linear relationship between the logarithm of the undrained shear strength as measured in an undrained constant strain rate triaxial test, and the suction, as shown in Figure 7.25.

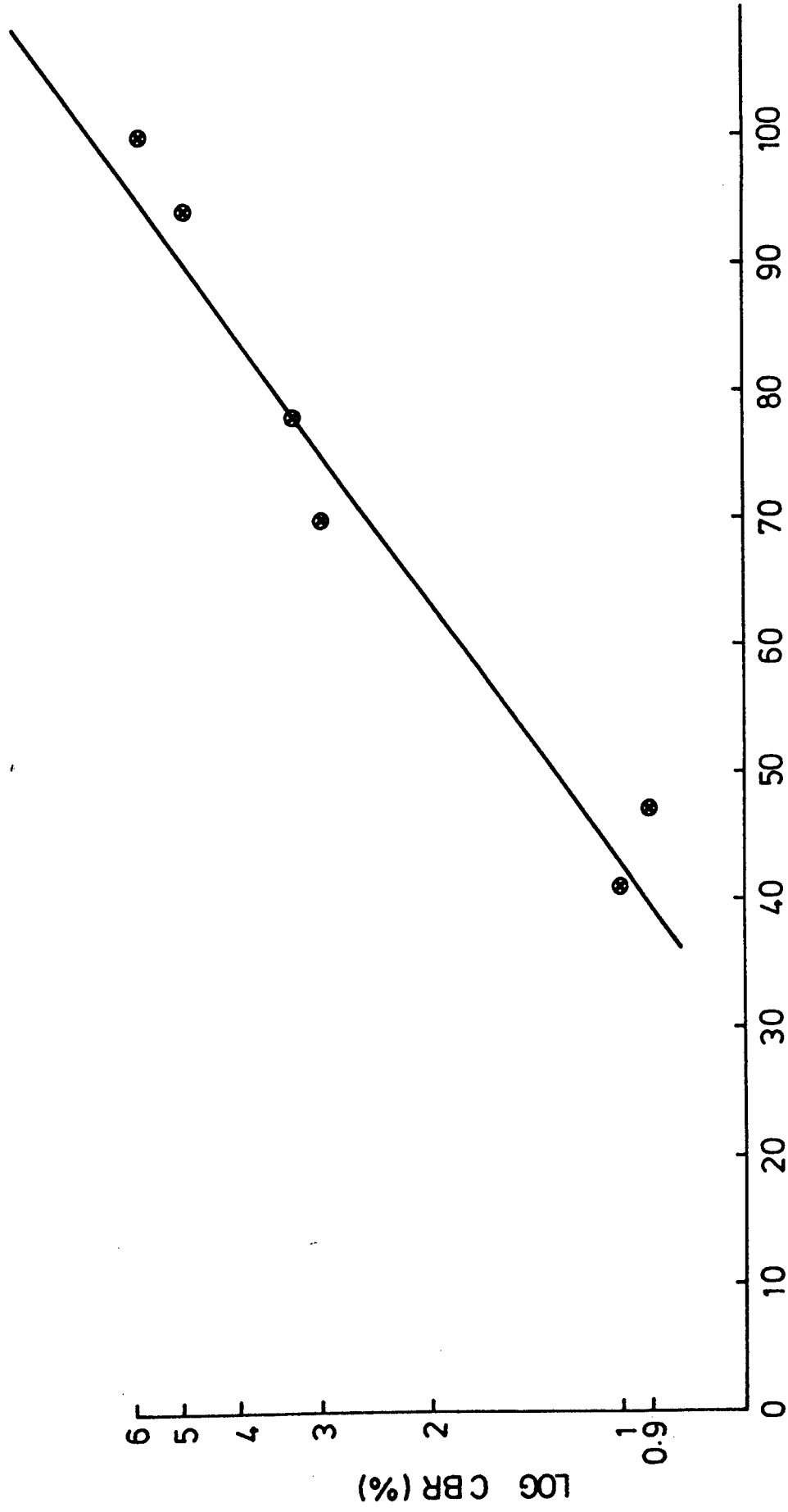

FIGURE 8.14 LOG CBR AGAINST SUCTION FOR COMPACTED KEUPER MARL SAMPLES

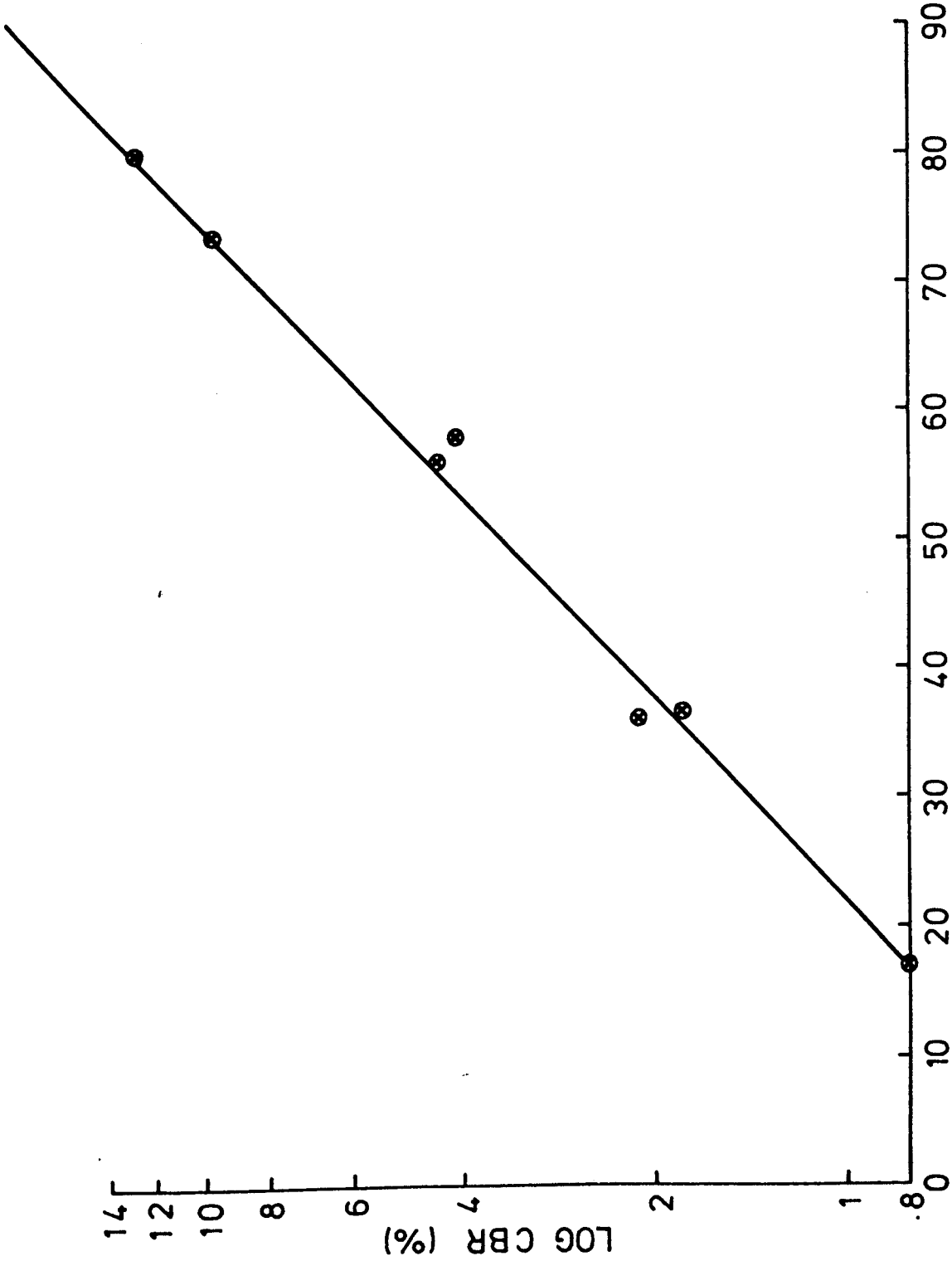

FIGURE 8.15 LOG CBR AGAINST SUCTION FOR COMPACTED GAULT CLAY SAMPLES

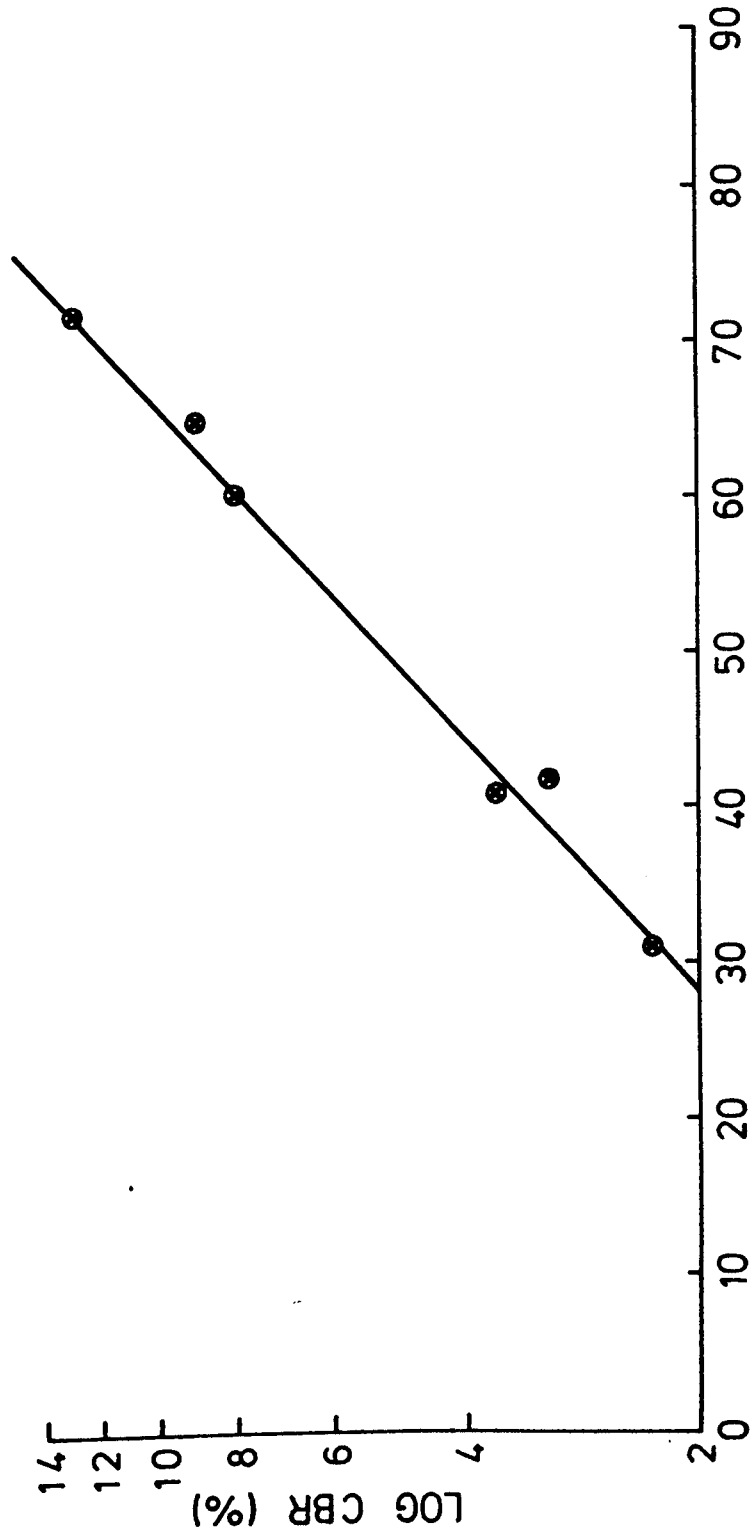

FIGURE 8.16 LOG CBR AGAINST SUCTION FOR COMPACTED LONDON CLAY SAMPLES

CHAPTER NINE

UNDISTURBED SAMPLES

9.1 THE SAMPLES

To try and obtain a measure of the natural overconsolidation ratio of road subgrades some undisturbed samples from under two roads in the south of England were obtained and tested. The samples were taken in U4 sample tubes and were kindly supplied by Somerset County Council and Northampton County Council.

The samples from Somerset were taken from under the hard shoulder of the M5 in a cutting approximately 10m deep and consisted of a Keuper Marl. Those from Northamptonshire were taken from a section of the M1 which was being rebuilt and consisted of clay with some sand. The area was generally flat. There were no records available indicating the ground water level at either site.

Some of the samples were tested in standard Rowe cells to determine the natural overconsolidation ratio, and the remaining samples were placed in the pneumatic repeated load triaxial rig and tested in the same manner as the compacted samples.

9.2 DETERMINATION OF NATURAL OVERCONSOLIDATION RATIO

The equipment is described in Chapter 4. Some difficulty was experienced in extruding and cutting good samples, especially from the Keuper Marl, as the natural material contained stones and harder natural lumps of Marl.

The results from the tests on the Somerset samples are shown in Figure 9.1, and those on the Northamptonshire soil in Figure 9.2. The water table was assumed to be at the top of the subgrade in each case to allow an estimate of the overconsolidation ratio to be made. The overconsolidation ratio was estimated from the vertical effective stresses. The Somerset

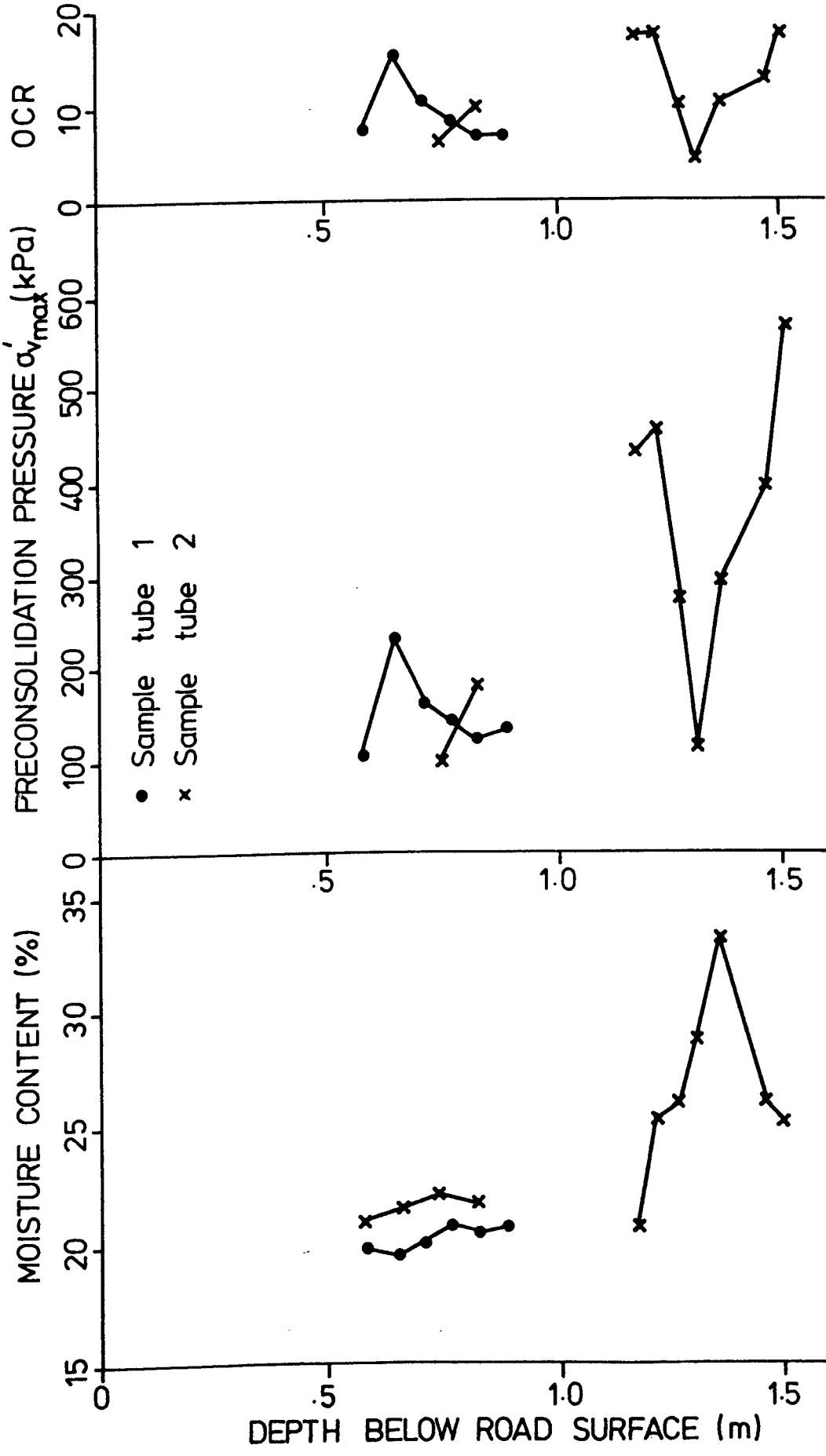

FIGURE 9.1 ROWE CELL RESULTS - SOMERSET SAMPLES

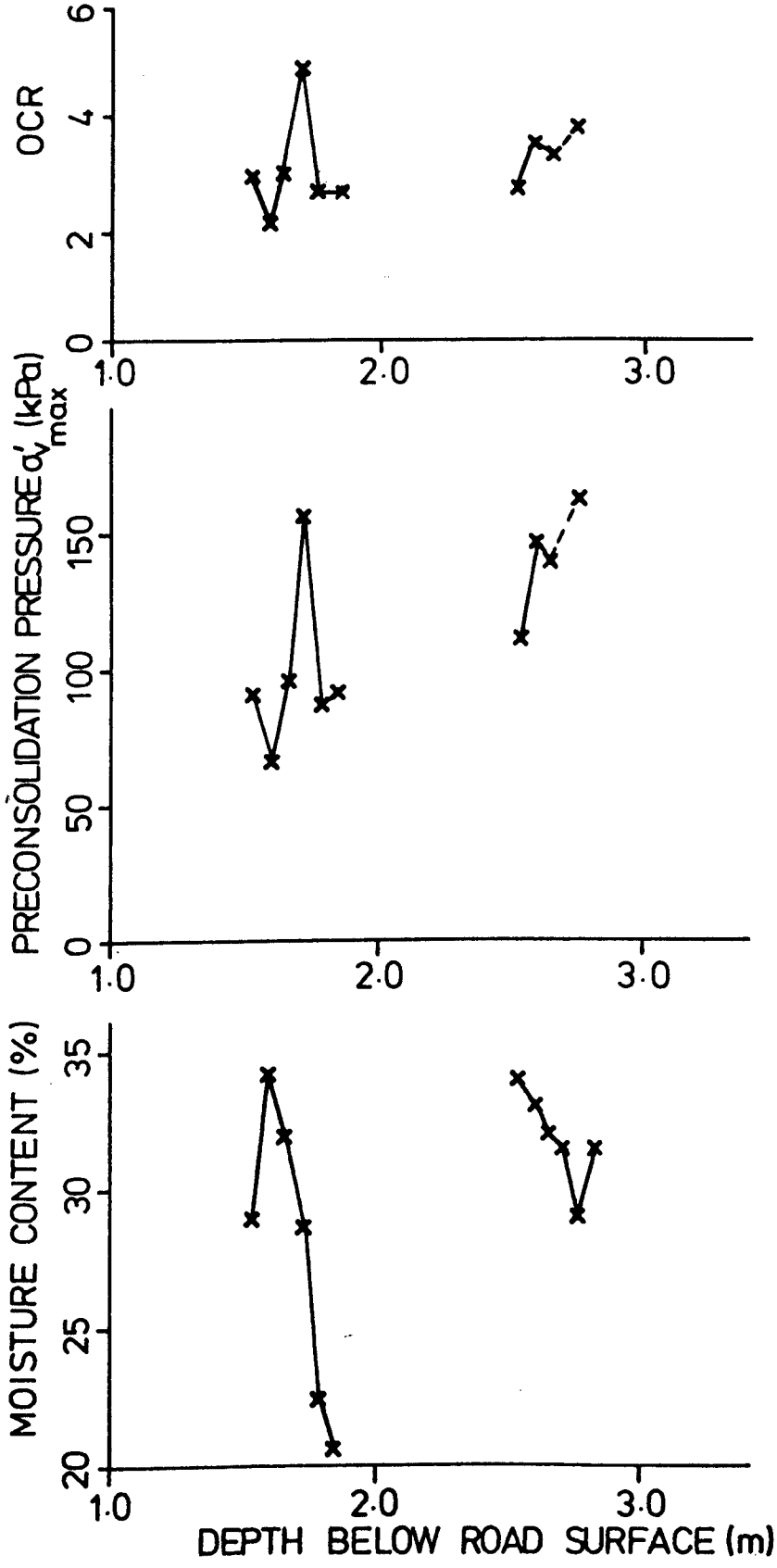

FIGURE 9.2 ROWE CELL RESULTS ON NORTHAMPTON SAMPLES

samples show a range of overconsolidation ratios similar to that chosen for the test programme, while those from Northamptonshire indicate a rather less overconsolidated material.

Natural Keuper Marl is mudstone which ages and weathers into a stiff and overconsolidated clay. The results shown in Figure 9.1 indicate that the material is overconsolidated, though not as much as might have been expected. There is likely to have been some sample disturbance at the top of the subgrade during road construction although the samples are natural, not fill, as they were obtained from the bottom of a cutting. As stated previously there was some difficulty in cutting samples to fit accurately in the Rowe cell, which would result in the measured values of preconsolidation pressure erring on the low side. The Northampton material was fill as various bits of glass and wood were discovered, and it is interesting to note that it does seem to be slightly overconsolidated which is in agreement with Schofield and Wroth (1968), who stated that soil completely sheared on remoulding exhibits some degree of overconsolidation.

The moisture content appeared very variable with depth. The moisture content was determined from trimmings around the edges and ends of each Rowe cell sample, and generally did not include the least disturbed material from the centre of U4 tubes.

Both samples indicate that as the moisture content increased, and therefore the specific volume, the preconsolidation pressure decreased. There does not appear to be any link between overconsolidation ratio and the depth of the sample. The depth range is very small though and would need to be increased to investigate this aspect more fully.

The variable results are thought to be due to the fact that the natural material was not uniform and therefore difficult to extrude and cut neatly. The point of steepest curvature on the load deformation curve was difficult to determine accurately which caused variations in the results.

9.3 DETERMINATION OF RESILIENT MODULUS

It was impossible to cut 78mm diameter triaxial samples from the Keuper Marl extruded from the U4 tubes without excessive sample disturbance. Five triaxial samples were successfully cut from the Northamptonshire material and installed and tested in the pneumatic triaxial repeated load rig in the same manner as the compacted triaxial sample. Table 9.1 gives the sample details.

There was no provision for drainage and the samples were tested unconfined. Figure 9.3 shows the results plotted as repeated deviator stress against resilient axial strain. There is reasonably good agreement between four of the tests which would indicate that the material is fairly uniform over the depth range tested. The unload part of the test follows the load section more closely than for the compacted samples and would suggest that the material is less thixotropic than the Keuper Marl, Gault clay and London clays tested in the research project. The plasticity index of the Northamptonshire material lay somewhere between that of the laboratory Keuper Marl and Gault clay, and the difference in thixotropic behaviour may be due to the larger percentage of sand sized material.

The resilient radial strains were also measured and are shown plotted against the resilient axial strain in Figure 9.4. The value of Poisson's Ratio varies quite considerably for the five samples tested as shown in Figure 9.4 and does not appear to relate to either the moisture content or dry density. The variation may be due to inaccuracies of measurement, or due to the natural variability of undisturbed soil samples. The values of Poisson's Ratio recorded are much lower than those which are generally associated with this type of material.

The estimated suction for each sample given in Table 9.1 was calculated using the Atterberg limits for this material and the approximate relationship between suction and liquidity index discussed in Chapter 7. Figure 9.5 shows the resilient axial strain plotted against the repeated deviator stress divided by

Table 9.1 Simple details on undisturbed triaxial samples from Northamptonshire

Sample Number	Depth below ground surface m	Dry Density kg/m³	Moisture Content of samples (Av of 3)%	Moisture Content of trimmings (Av of 7)%	Range	Liquidity Index	Suction kPa
1	1.8	-	25.05		-	.059	65
2	1.6	1530	25.72	27.26	25.35 - 28.82	.078	61
3	1.85	1510	25.14	28.31	24.30 - 32.61	.061	64.5
4	2.2	1440	30.47	29.82	26.37 - 32.60	.213	42
5	2.35	1400	32.22	32.72	31.82 - 33.97	.263	35

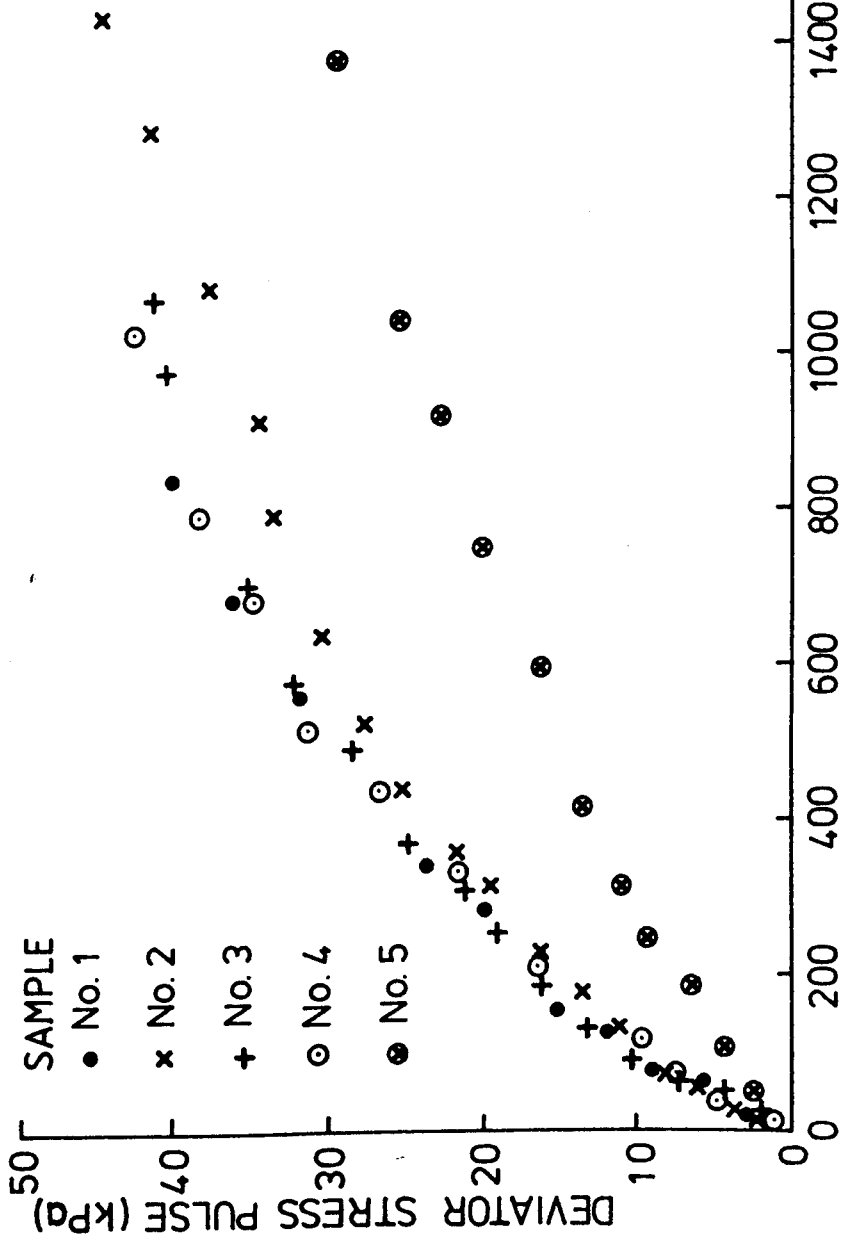

FIGURE 9.3 STRESS STRAIN RESPONSE FOR UNDISTURBED NORTHAMPTON SAMPLES UNDER 1 SECOND PULSED LOADING

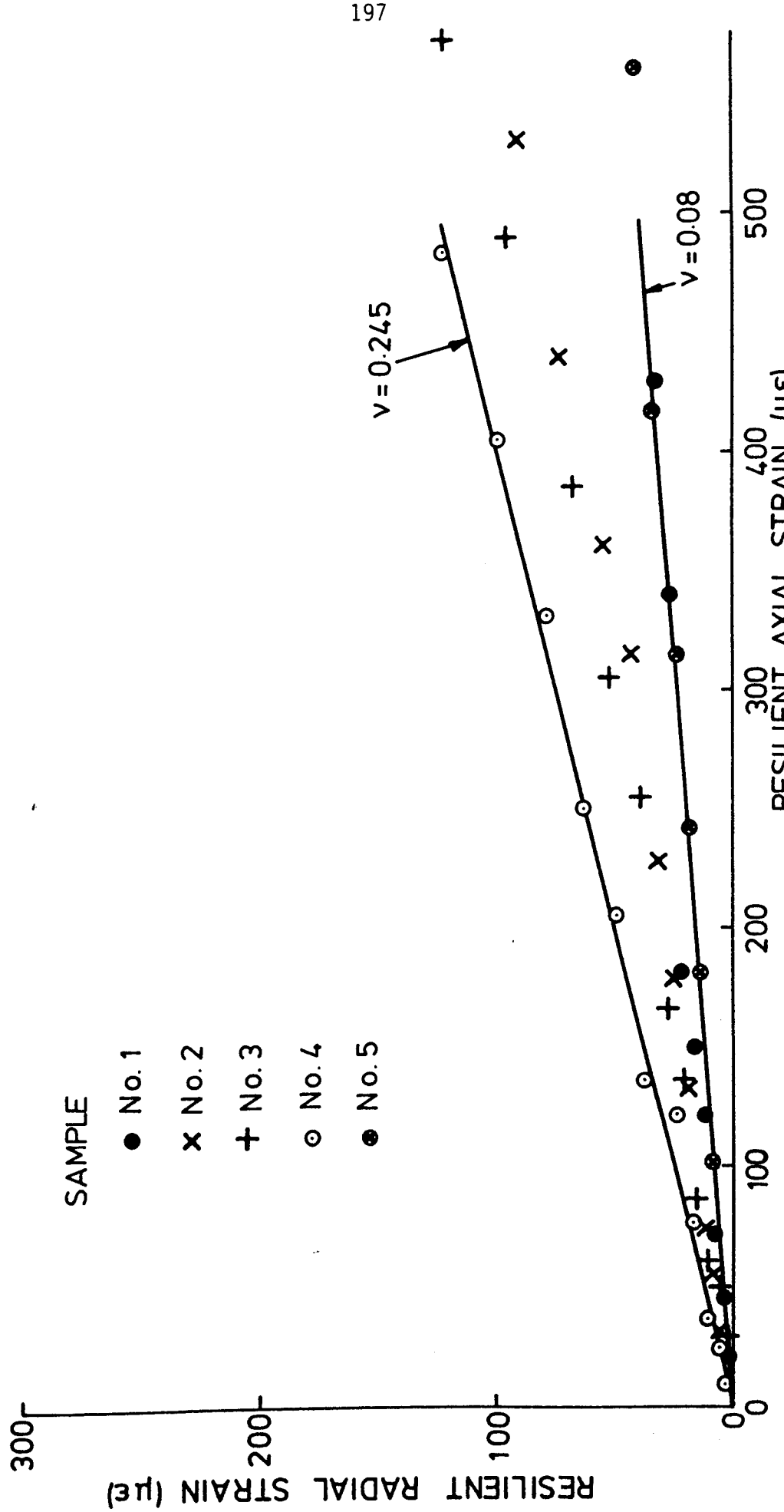

FIGURE 9.4 RESILIENT AXIAL STRAIN AGAINST RESILIENT RADIAL STRAIN FOR THE UNDISTURBED SOIL SAMPLES FROM NORTHAMPTON

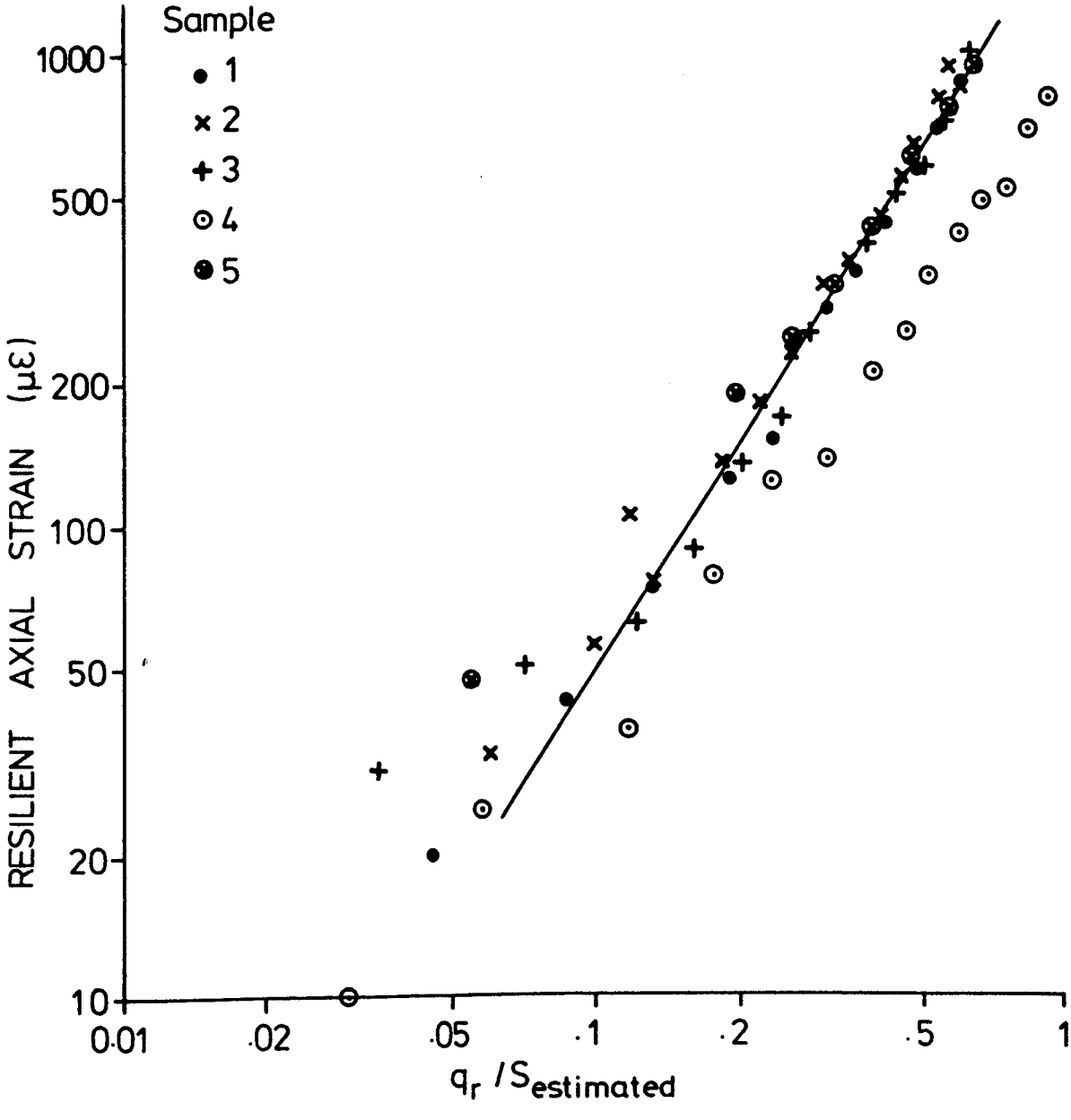

FIGURE 9·5 RESILIENT AXIAL STRAIN vs REPEATED DEVIATOR STRESS DIVIDED BY SUCTION FOR THE UNDISTURBED NORTHAMPTON SAMPLES

the suction. Samples 1, 2, 3 and 5 show reasonable agreement above a resilient axial strain of approximately 200 microstrain. The results from sample 4 show a similar gradient to the others, but a different intercept. The spread in the results below 100 microstrain is thought to be due to inaccuracies in measuring strains of this magnitude.

The resilient response of the samples above a resilient axial strain of 100 microstrain can be described by the soil model developed in Chapters 6 and 7, which is of the form

$$\varepsilon_a^r = A \left[\frac{q_r}{s}\right]^B \qquad 9.1$$

where A and B are material constants and equal 1870 and 1.61 respectively.

Although the stiffness of the samples did not increase with depth when they were tested unconfined, they would be stiffer with increasing depth due to the effect of the surrounding material. A subgrade consisting of this material would appear stiffer with depth in a non linear manner to a pulsed load as the material is stress softening, see Figure 9.3, and the stress pulse magnitude decreases with depth as the load is spread over a greater area.

CHAPTER TEN

PAVEMENT ANALYSIS

10.1 INTRODUCTION

Two different pavements were analysed using a finite element computer program which can cater for non linear elastic materials. The original non linear soil models developed at Nottingham by Brown and Pappin (1982) from data by Brown et al (1975) were used initially to give an indication of stress pulse magnitude, and pulse shape under a standard wheel load for use in the experimental programme.

The subgrade model developed in Chapter 6 has been incorporated into the program and these results are compared with those produced using the original subgrade model, by re-analysing the same road structures under the same conditions.

10.2 PAVEMENTS ANALYSED

The two pavements which were analysed are shown in Figure 10.1 together with the loading details. The difference between the two pavements was in the thickness of the granular layer only, and they are referred to as 'thin' and 'thick' pavements (200mm and 700mm granular layer respectively). The pavements do not correspond to any specific design but are two of a number of structures previously analysed using the finite element program, and described more fully by Brown and Pappin (1985).

Three different pore pressures were chosen and used in the computer program to cover the range of effective stresses used in the main test programme. These were 0kPa, -50kPa and -100kPa.

10.3 THE COMPUTER PROGRAM

The finite element program, called SENOL (SEcant NOn Linear), had been developed at Nottingham by Pappin (1979) from an original

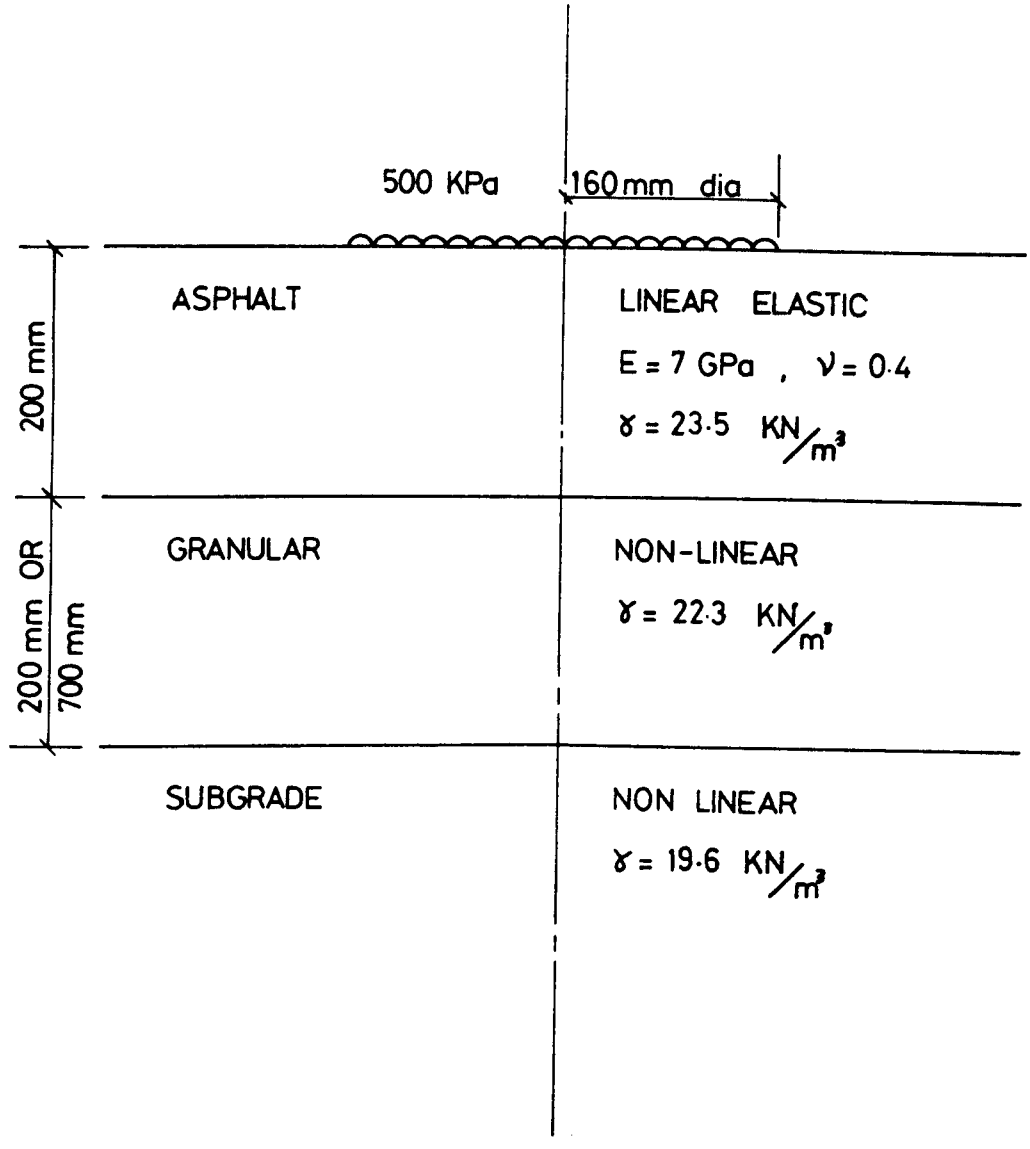

FIGURE 10.1 PAVEMENT DETAILS FOR ANALYSIS

program by Barksdale. It can cater for any practical number of layers and any layer can be specified to behave elastically using either a linear or a non linear model. The program is arranged to allow different soil models to be incorporated easily for each layer. Each model must produce stress dependent shear and bulk moduli G and K for use in the main program.

The program output consists of the stresses and strains for each element together with the total deformation. Careful account is taken of the overburden pressure. An equivalent modulus and Poisson's ratio is also estimated for each element assuming isotropic behaviour.

10.4 THE SOIL MODELS

10.4.1 The Granular Model

The granular model was developed at Nottingham from a series of stress path tests on crushed limestone in a repeated load triaxial apparatus. The test programmes produced sufficient information about the resilient shear and volumetric strains to allow these to be modelled mathematically. Consequently the model incorporated into SENOL is quite sophisticated in that G and K are calculated separately and Poisson's ratio is therefore not constant. Full details of the test results on the crushed limestone and the development of the model are given by Shaw (1982) and Pappin (1979).

10.4.2 The Subgrade Model

The earlier subgrade model referred to above was developed by Brown and Pappin (1982) from repeated load triaxial tests on saturated overconsolidated samples of Keuper Marl in an earlier version of the triaxial rig used for the research. The differences between the rigs used and experimental programmes are detailed in the discussion section of this Chapter. The model details are described below.

The earlier model relates the resilient axial strain to the deviator stress and mean normal effective stress as

$$\varepsilon_a{}^r = \frac{q_{max}}{F}\left[\frac{q_{max}}{P_o'}\right]^S \qquad 10.1$$

where $\varepsilon_a{}^r$ is the resilient axial strain in microstrain
q_{max} is the maximum value of the deviator stress in kPa
P_o' is the initial mean normal effective stress in kPa
and for this material
F = 50 MPa
S = 0.7

The new model is of the form

$$\varepsilon_a{}^r = A\left[\frac{q_r}{P_o'}\right]^B \qquad 10.2$$

where $\varepsilon_a{}^r$ and P_o' are as before
q_r is the magnitude of the deviator stress pulse in kPa
and for this material
A = 1110
B = 1.52

There was no resilient volumetric strain measured during the tests which gave rise to this model as the soil was behaving elastically with a Poisson's ratio of 0.5. The test results are discussed in Chapter 6.

10.5 USE OF THE MODELS IN THE PROGRAM

The load was applied in ten increments and the total resilient shear strain after each increment was obtained by adding the resilient shear strain calculated for that increment using the expressions above to the total resilient shear strains calculated before the last increment. In the case of the first increment

the initial shear strain was calculated from the overburden pressures.

The shear modulus G for each increment was obtained from the expression

$$G = \frac{q_r}{3\epsilon_a^r} \qquad 10.3$$

using values of q_r and ϵ_a^r calculated after the last increment of deviator stress. The bulk modulus K was calculated from the expression

$$K = \frac{2\ (1 + \nu)G}{3\ (1 - \nu)} \qquad 10.4$$

However a Poisson's ratio of 0.5 results in an infinite bulk modulus using this relationship. The earlier work assumed that

$$K = 3.233 \times G \qquad 10.5$$

which gives a Poisson's ratio of 0.36. This value has been used here to allow for a direct comparison between the results from the new model and those obtained from the earlier model.

10.6 THE FINITE ELEMENT MESH

The finite element mesh consists of a grid of 336 rectangular elements, made up of 26 rows of 14 elements. Figure 10.2 gives the mesh dimensions. The mesh can be considered as a section along a radius of a vertical cylinder, with the centreline of the load down one edge of the mesh.

The boundary conditions allow for vertical movement only of the mesh at the sides and the base is taken as rigid to simulate a section of soil restrained by the surrounding material and founded on stiffer material.

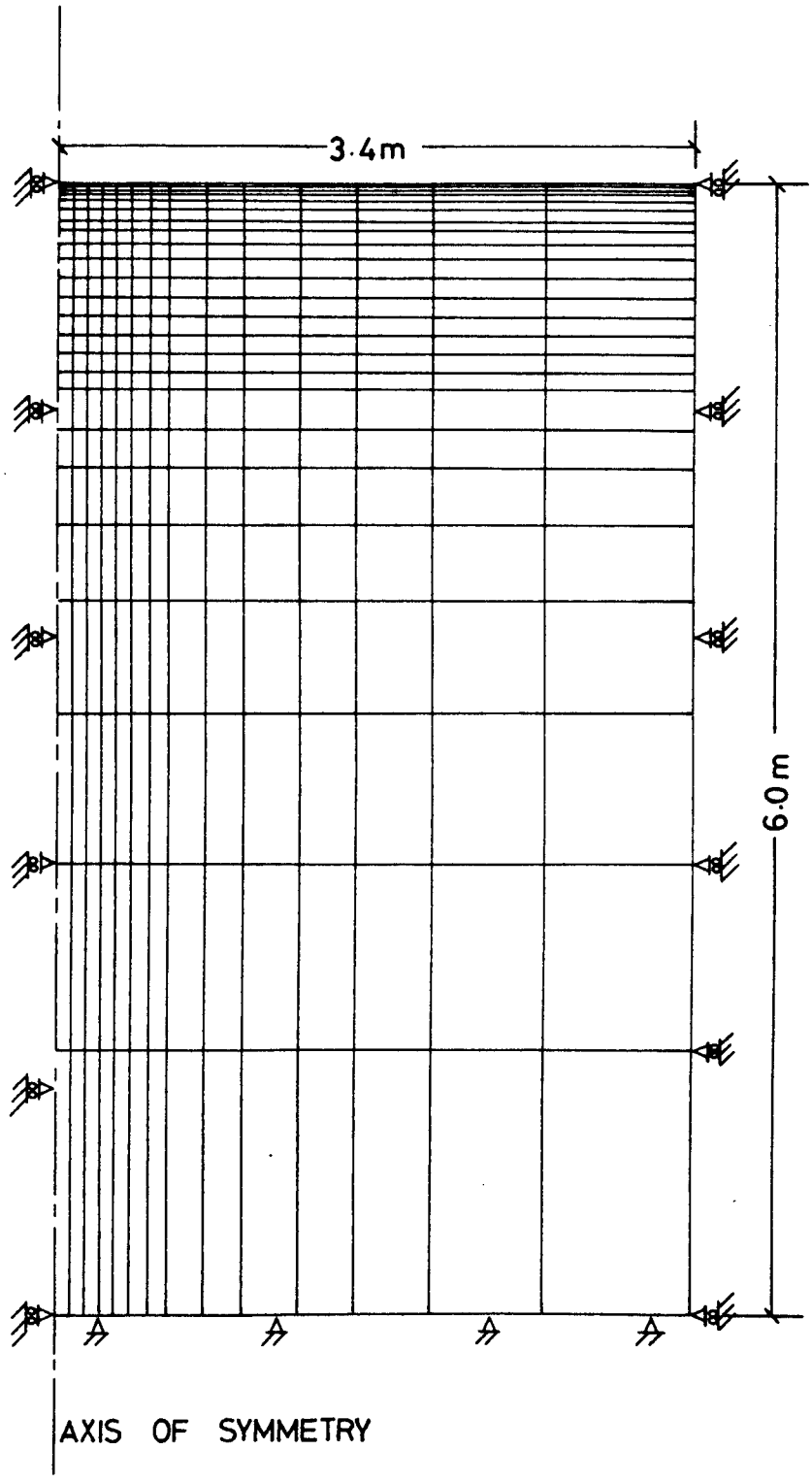

FIGURE 10.2 FINITE ELEMENT GRID USED FOR ANALYSIS

10.7 RESULTS AND DISCUSSION

Figures 10.3, 10.4, 10.5 and 10.6 show the equivalent modulus plotted against depth on the load centreline for the thin and thick pavements with pore pressures in the subgrade of 0kPa and -50kPa respectively. The program did not give a satisfactory convergence for the pavements with a pore pressure of -100kPa, and therefore the results have not been included. The results from the new model indicate a very rapid increase in subgrade stiffness with depth, while those from the earlier model predict a subgrade stiffness which is approximately linear with depth. Figures 10.3 and 10.5 also show the modulus variation with depth assuming a linear elastic subgrade. The stiffness predicted by both models increases as the pore pressure becomes more negative, which results in a higher mean normal effective stress. The increase in stiffness would be expected as the more confined a particulate sample the smaller the effect of a stress pulse of a certain magnitude. Equations 10.1 and 10.2 demonstrate that the higher P'_o the smaller the resilient axial strain which results therefore in a larger value of modulus.

The main difference between the earlier and new models is the behaviour of stiffness with depth. The earlier model predicts a small increase in modulus as the depth increases followed by a decrease in modulus, which is more pronounced when the mean normal effective stress is higher. The new model predicts quite a rapid increase in the subgrade modulus with depth for all the pore pressures examined. This would seem reasonable as the stress pulse magnitude decreases with depth as the load spreads, and therefore the material would be expected to increase in stiffness non linearly from the general non linear stress softening behaviour of the soil.

Figure 10.7 shows the stress pulse shape at the top of the subgrade for the thin and thick pavements with the water table at the top of the subgrade (u = 0kPa). The new model gives a lower peak value of deviator stress in both cases, although the stress pulse is wider to compensate. Also shown on Figure 10.7 are

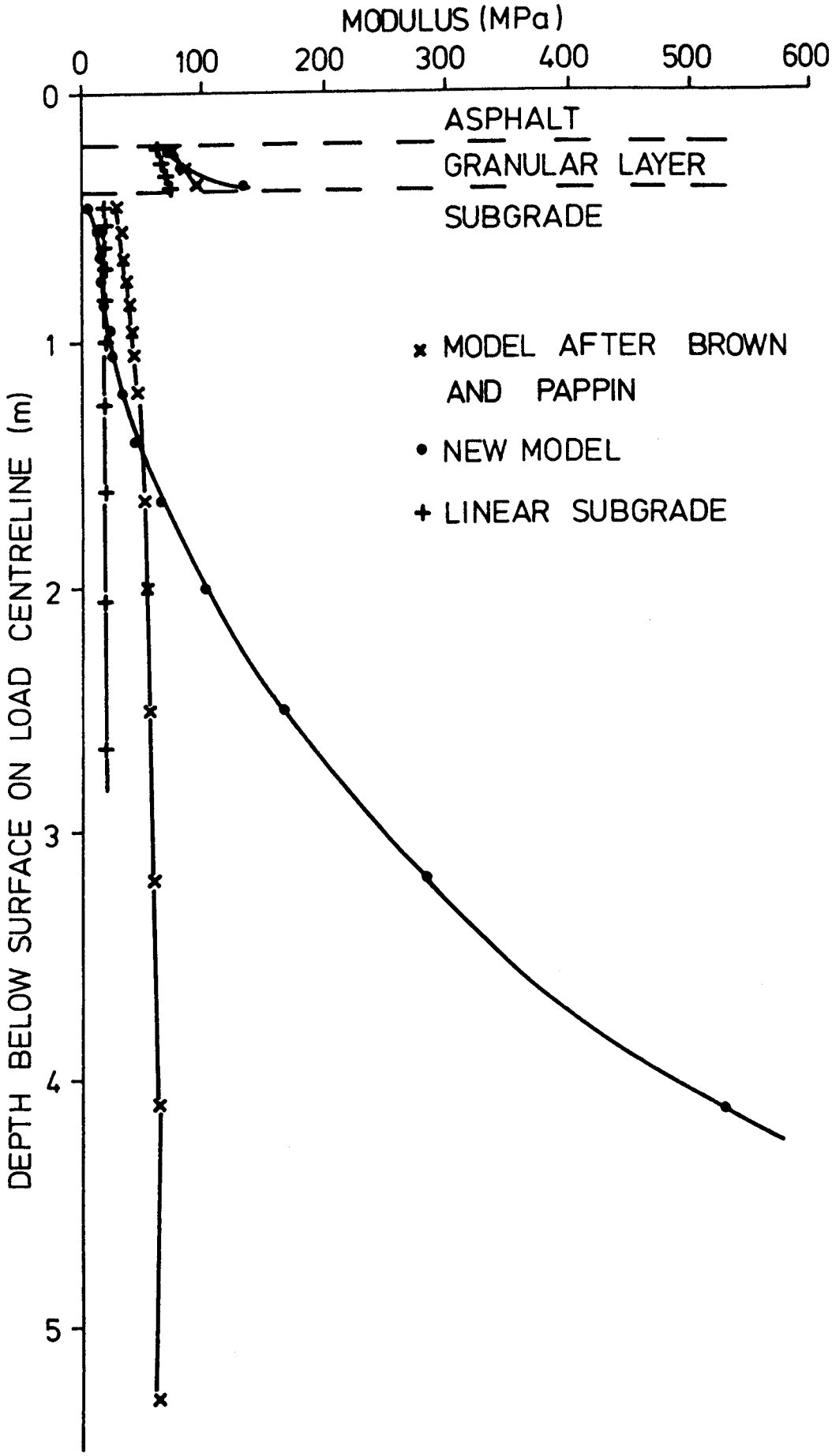

FIGURE 10.3 EQUIVALENT MODULUS VARIATION WITH DEPTH FOR THIN PAVEMENT SUBGRADE PORE PRESSURE = 0 kPa

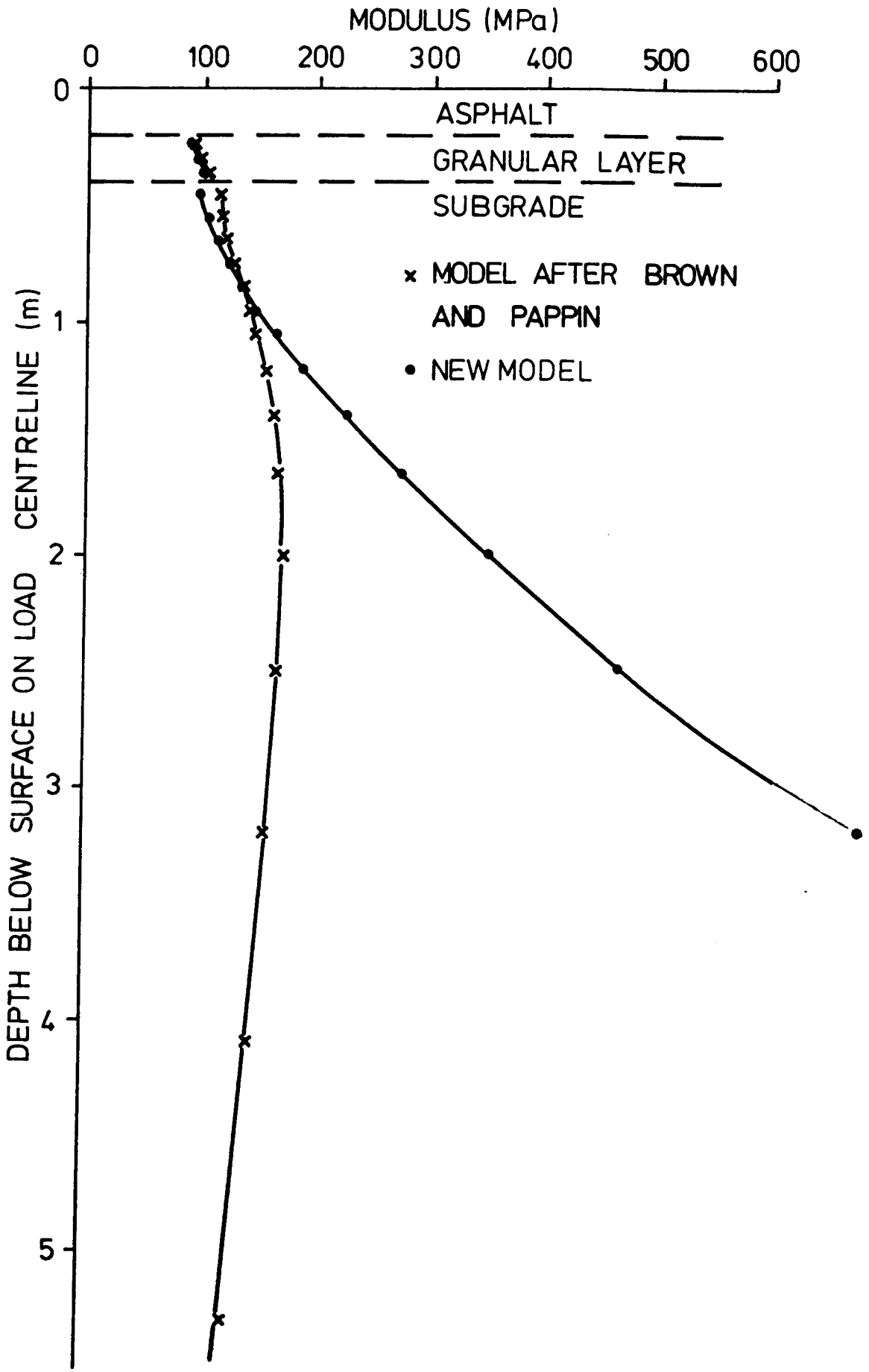

FIGURE 10.4 EQUIVALENT MODULUS VARIATION WITH DEPTH FOR THIN PAVEMENT. SUBGRADE PORE PRESSURE = -50 kPa

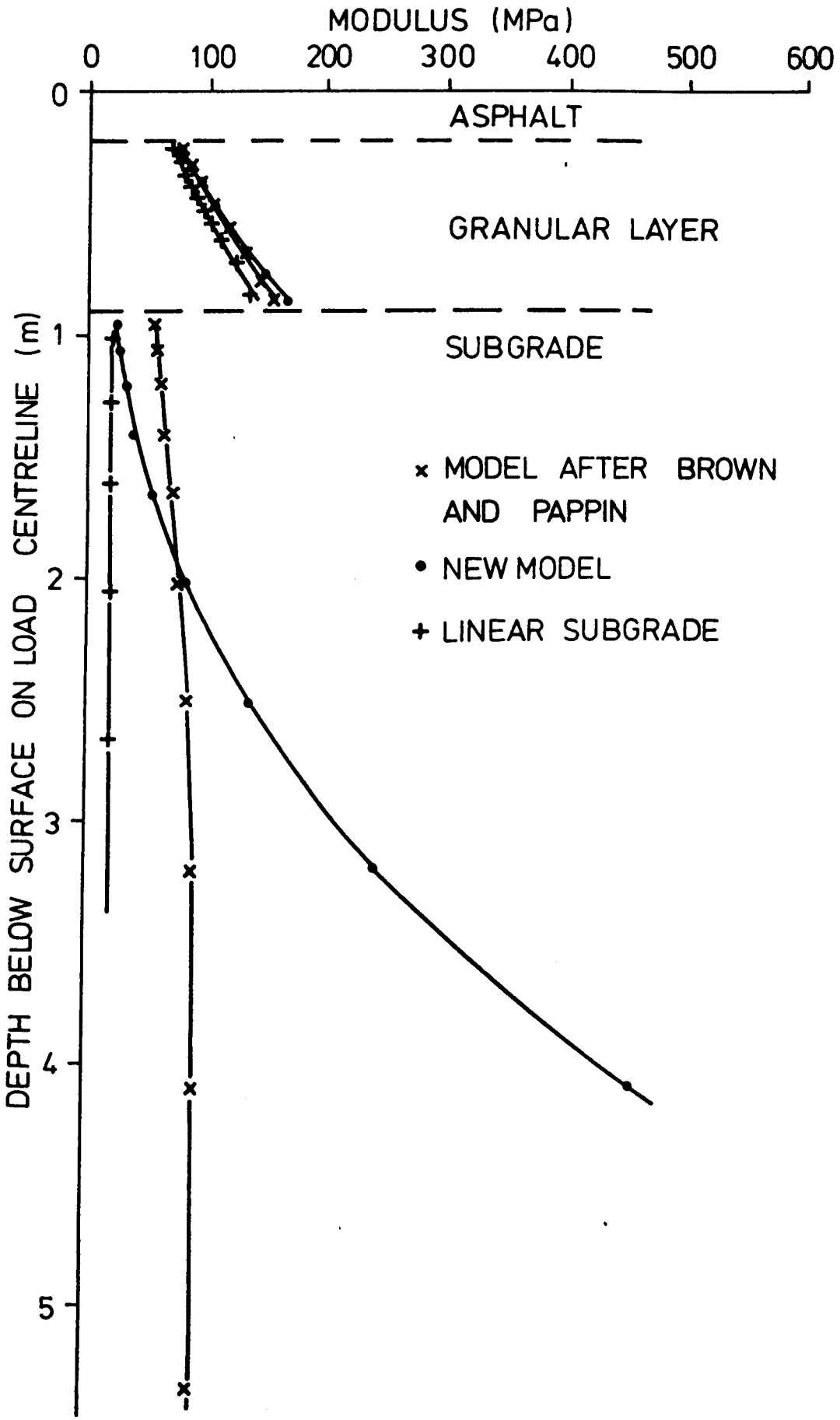

FIGURE 10.5 EQUIVALENT MODULUS VARIATION WITH DEPTH FOR THICK PAVEMENT. SUBGRADE PORE PRESSURE = 0 kPa

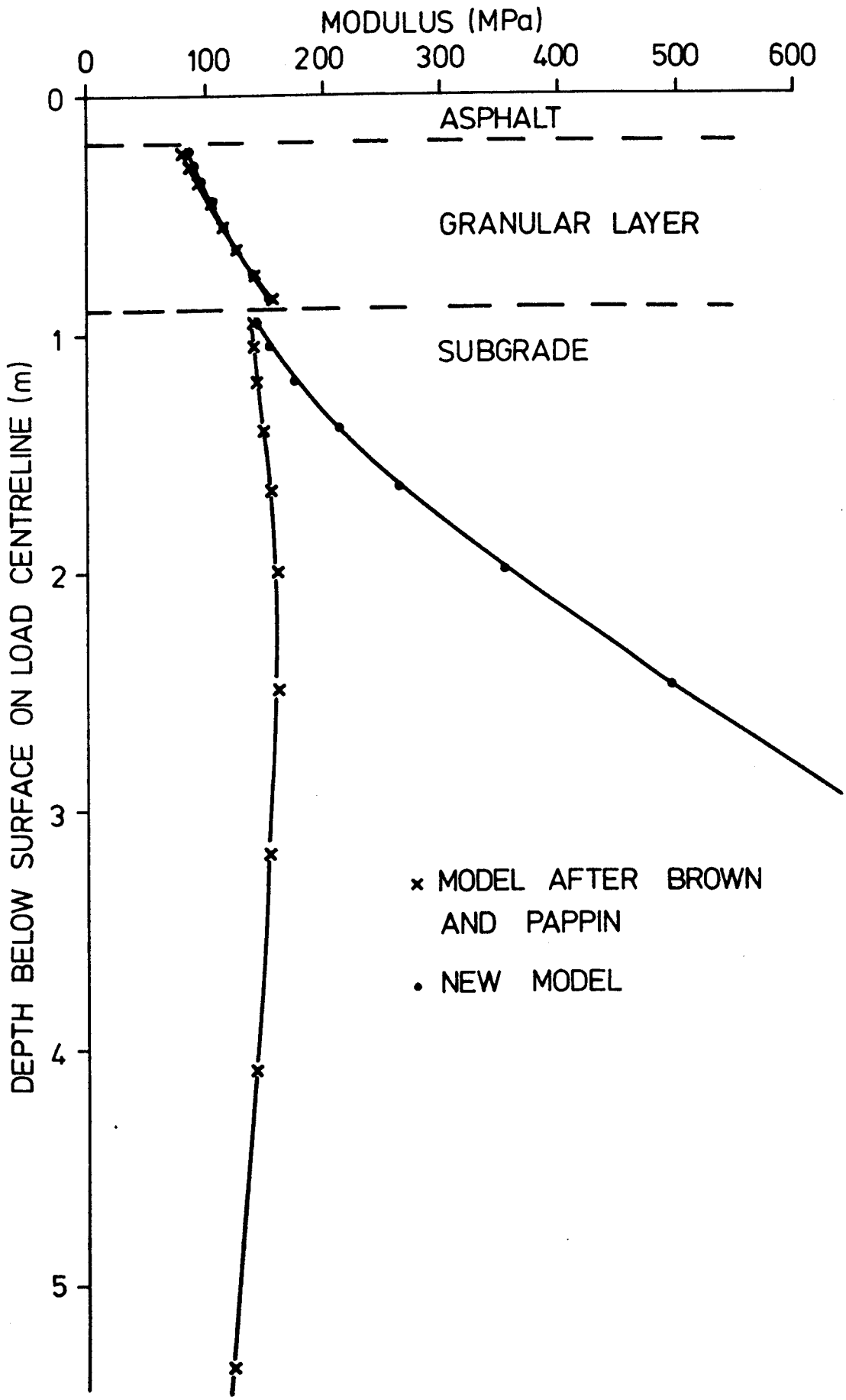

FIGURE 10·6 EQUIVALENT MODULUS VARIATION WITH DEPTH FOR THICK PAVEMENT. SUBGRADE PORE PRESSURE = - 50 kPa

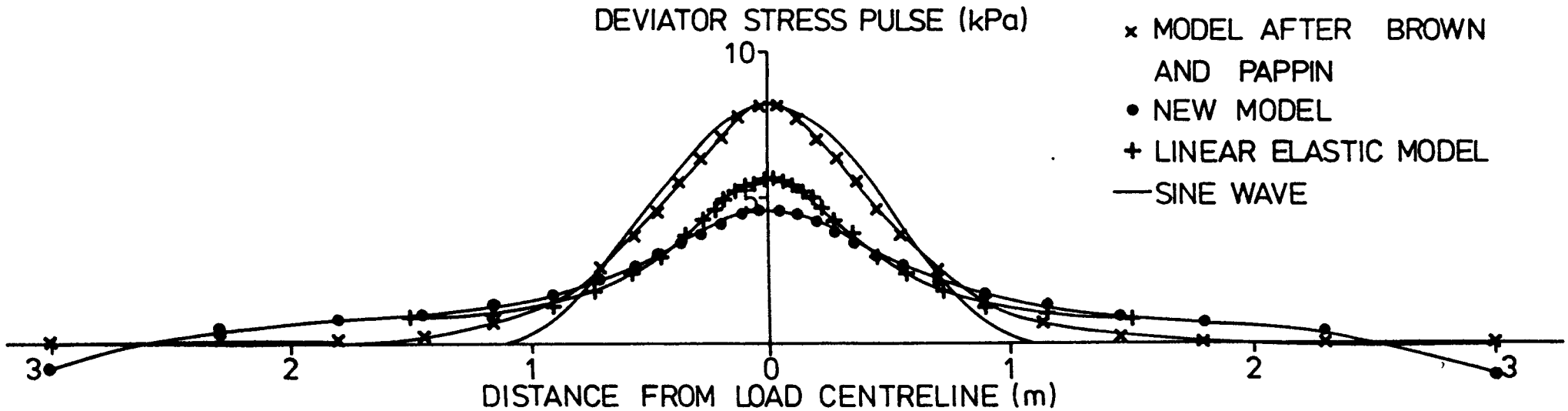

FIGURE 10·7a STRESS PULSE PREDICTION AT THE TOP OF THE SUBGRADE. THIN PAVEMENT. u = 0 kPa

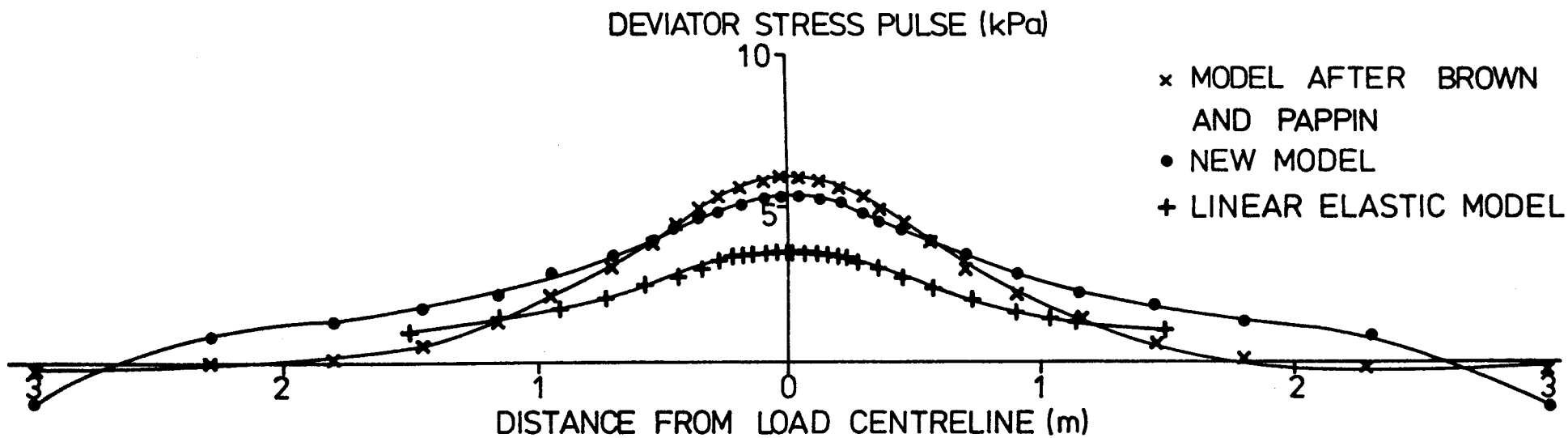

FIGURE 10·7b STRESS PULSE PREDICTION AT THE TOP OF THE SUBGRADE. THICK PAVEMENT. u = 0 kPa

the results from earlier computations using the same pavements, but with a linear elastic soil model. The mesh in this case was only 1.5m wide although there were the same number of elements. The stress increment at the edge is not zero. For this reason the mesh was doubled in size for the later computations. However this does not seem sufficient for the new model as the behaviour at the edge of the mesh appears to be inaccurate, and a mesh with a larger number of elements is required to correct this.

A sine wave is shown plotted on Figure 10.7. The period has been adjusted to give the best fit to the central portion of the pulse shape, but this leads to a rather shorter stress pulse than that produced from the calculations. It can be seen though that of the standard waveforms available from signal generators the sine wave gives the best fit to the pulse shape, and it is easier for a servo system to follow as there are no step changes in the rate of loading.

CHAPTER ELEVEN

COMPARISON BETWEEN THE BEHAVIOUR OF CONSOLIDATED AND COMPACTED SAMPLES

11.1 INTRODUCTION

This chapter contains a comparison and discussion of the results from the different test series on the consolidated and compacted samples. It can be divided into two sections: the first contains a comparison between the results obtained from the compacted and consolidated samples in the same type of test, and the second part compares the results of the CBR test series and triaxial test series from the consolidated and then the compacted samples.

11.2 COMPARISON BETWEEN THE BEHAVIOUR OF COMPACTED AND CONSOLIDATED TRIAXIAL SAMPLES OF KEUPER MARL

11.2.1 Resilient Modulus

The resilient modulus determined from the consolidated samples has been shown to depend on the mean normal effective stress and not on the moisture content. Overconsolidated samples with different stress histories giving different moisture contents at the same effective stress will therefore have the same modulus.

The model proposed for calculating the resilient modulus of the compacted samples is identical to that proposed for the consolidated samples except that the suction is substituted for the mean normal effective stress term. The suction referred to is the matrix suction and evidence from other researchers (Chapter 2, section 2.12) indicates that it depends on moisture content and is relatively insensitive to changes in dry density. Therefore samples with different dry densities at the same moisture content may be expected to have similiar suctions and therefore a similar resilient modulus.

The Keuper Marl was the only material to be tested in the

consolidated and compacted states and the results from both series of tests demonstrate that increasing the confining pressure increases the resilient modulus. For the saturated samples the term P'_0 in equation 6.10 is the actual effective stress within the sample and naturally includes the confining pressure. The soil model for the compacted samples was developed from the results on unconfined samples and therefore the suction term in the equation is the matrix suction of the sample under no external load. There were insufficient confined triaxial tests on the compacted samples to quantify the effect of a cell pressure.

A comparison between the results for the compacted and consolidated samples cannot be made by using the same moisture content in each case as the resilient modulus of the consolidated samples does not depend on moisture content. If the suction is taken as the negative pore pressure of the compacted samples then in the absence of an external load it is equivalent to the mean normal effective stress for the consolidated samples. Equating the suction and mean normal effective stress terms in the models demonstrates that the stiffnesses obtained from each model are of the same order, see Figure 11.1, with the best agreement occurring at the lower deviator stress pulse magnitudes. The suctions used in the model to plot Figure 11.1 are the suctions of the samples with no external load. Applying a confining pressure to the compacted samples will increase the effective stress even in undrained condition, as the air in the sample compresses, and will therefore lead to higher resilient moduli. An increase in the confining stress of 20 kPa, representing approximately 1m of overburden, for the compacted samples will increase the calculated stiffness by increasing the suction term. According to Croney (1977) the actual value of the increase will depend on the value of α in the equation

$$u = s + \alpha p \qquad 11.1$$

where u is the pore pressure
s is the suction
p is the overburden pressure
α is the compressibility factor

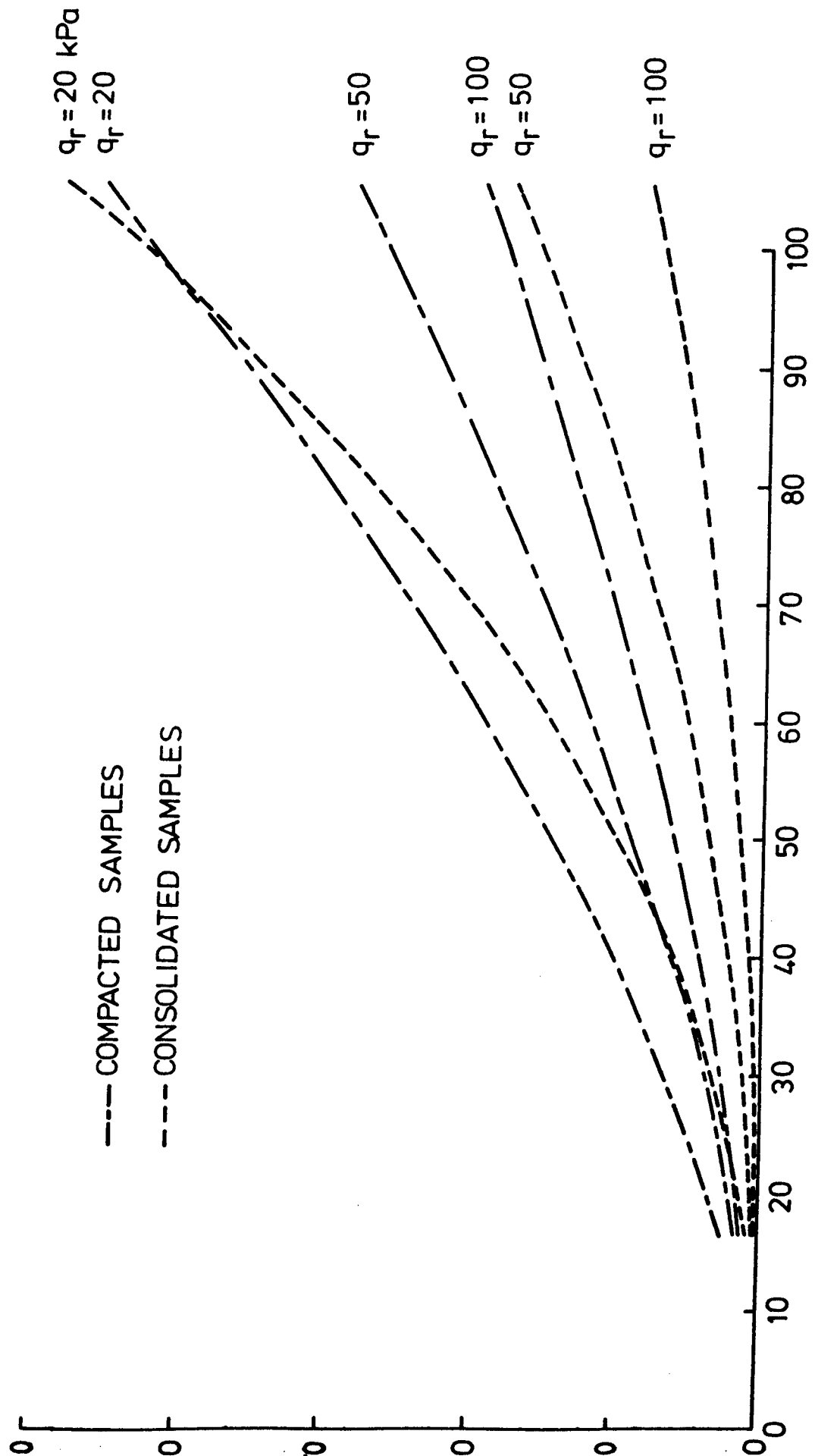

FIGURE 11.1 COMPARISON BETWEEN SOIL MODELS FOR COMPACTED AND CONSOLIDATED SAMPLES

There were insufficient tests on confined samples to determine a value of α for the Keuper Marl.

11.2.2 Thixotropy

Both the compacted and consolidated samples exhibited thixotropy, with the measured stiffness at a certain stress pulse smaller if any of the preceeding stress pulses were larger, within a certain time period. However the consolidated samples tended to regain their original stiffness when they were left to recover, but the results from the compacted samples suggest that they tended to become stiffer after recovering from periods of loading than they were when loaded for the first time. Drainage was allowed in between tests for the consolidated samples, although there was a negligible change in volume in most cases. The compacted samples were not provided with any provision for drainage. The gain in stiffness of the samples following cyclic loading would then be due to a slow reorganisation of the internal structure without any change in state. The interparticulate forces would be sufficiently small that they could be disrupted by quite low external stresses and hence the sample would soften on reloading even if the pore pressure remained constant. This is discussed more fully in Chapter 2, section 2.10.

11.2.3 Development of permanent strain

The test programme on the compacted samples was not designed to investigate the development of permanent strain. However, the approximate repeated deviator stress level which caused the onset of permanent strain was recorded and was found to be linearly related to the suction of the sample.

The test programme on the consolidated samples demonstrated that there was a threshold repeated stress level, above which failure was likely to occur, but below which equlibrium was attained. As discussed previously the deviator control system was not sufficiently stable to allow the onset of permanent strain to be detected with any confidence for the consolidated samples.

11.3 COMPARISON BETWEEN THE BEHAVIOUR OF COMPACTED AND CONSOLIDATED CBR SAMPLES OF KEUPER MARL

The CBR values determined for the compacted and consolidated samples of Keuper Marl are shown plotted against moisture content in Figure 11.2, and it is apparent that the consolidated samples show a considerably higher CBR than the compacted samples. Neither sample was tested with any surcharge weights, although the consolidated samples were allowed to swell back under a vertical effective stress of 20 kPa. This was removed just prior to testing the sample and the consequent change in pore pressure would maintain the vertical effective stress at 20 kPa. Hight and Stevens (1982) report that initial stresses affect the slope of the CBR curves at low penetrations but do not affect the CBR value for stiff samples (CBR approximately equal to 10%). For samples with CBR's of 4 or 5 they found that there was some effect on the CBR value as well as on the initial stiffness. The compacted samples would have some residual radial stresses caused by the compaction process.

The consolidated samples were consolidated anisotropically and the sample structure would be expected to be anisotropic with the clay plate like particles arranged horizontally. The structure would then be stiffer along the axes perpendicular to the platelets than parallel to them. However, the anisotropically consolidated triaxial samples did not exhibit any evidence of anisotropy. This is discussed more fully in Chapter 6. The compacted samples were compacted to relatively high degrees of saturation by a small tamper. Seed et al (1962) report that this type of compaction in samples with high degrees of saturation is likely to result in some reorientation of the clay particles into a parallel structure. Seed et al found that soil with this type of structure is very much softer than the same soil compacted by static compaction which results in a randomly orientated structure.

The other difference between the two types of sample is the degree of saturation. The consolidated samples were all

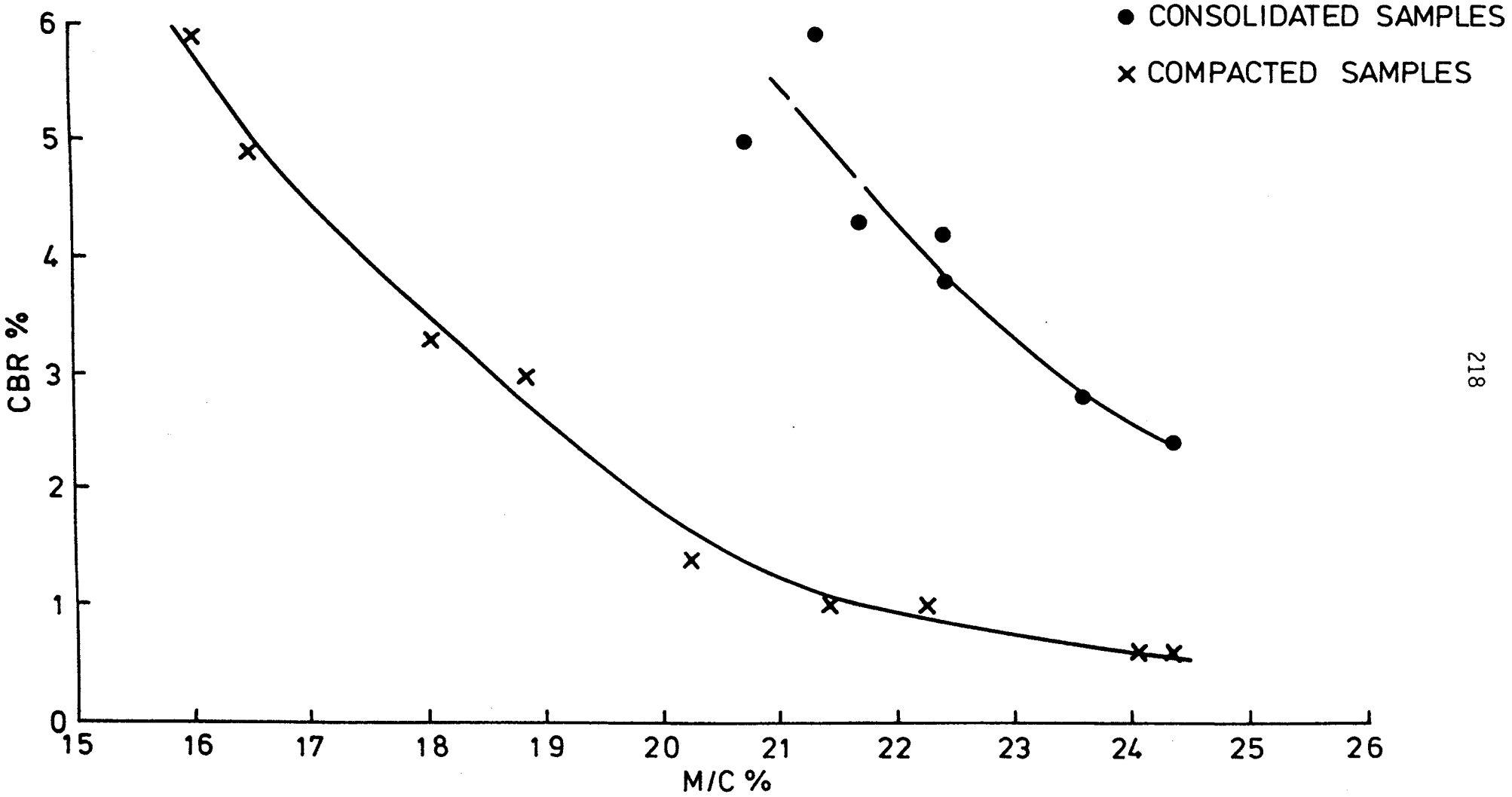

FIGURE 11.2 COMPARISON BETWEEN THE CBR VALUES FOR THE COMPACTED AND CONSOLIDATED SAMPLES OF KEUPER MARL

saturated, while all the compacted samples, apart from the driest, varied from 93% to 100% saturation. It seems likely that samples compacted to this high a degree of saturation would behave similarly to saturated samples, as the air pockets would be small and not continuous.

The difference in response between the two types of sample would seem to be due to a combination of the differences in structure and the initial stresses.

11.4 CONSOLIDATED SAMPLES OF KEUPER MARL - RESILIENT MODULUS AND CBR

The model developed in Chapter 6 from test results on a variety of samples with different moisture contents and mean normal effective stresses demonstrates that the resilient behaviour of the overconsolidated samples of Keuper Marl depends on P'_0 and is independent of the moisture content and hence the consolidation history. The model was developed from low stress pulse tests on fairly heavily overconsolidated samples and the stress paths were well within the yield locus.

The CBR test results covered a similar range of moisture contents but the samples were all allowed to swell back to approximately the same effective stress. A standard CBR test at 1mm/min is completed in 7.5 minutes, and this can be compared with approximately 150 minutes for 90% consolidation assuming that the coefficient of consolidation equals 2.28 m^2/year (Overy 1982) and assuming a zone of failure 30mm thick under the CBR plunger at 2.5mm penetration. This value was taken from the results of the finite element analysis of the CBR test by Hight and Stevens (1982). The tests can therefore be considered undrained.

The undrained shear strength for saturated soils depends on the moisture content, not the overconsolidation ratio and consequently not the mean normal effective stress at the start of the test. The measured CBR value was found to be linearly related to the undrained shear strength as measured by a shear

vane. This may not be the case at other mean normal effective pressures outside the range of the test programme as Hight and Stevens found that the CBR reflected the strength of stiff samples, and a combination of strength and stiffness for samples with lower CBRs. The initial gradients of the load penetration curves, and the gradients from the reload sections of the curves showed no apparent correlation with any other measured parameter. Hight and Stevens suggest that the initial slope of the load penetration curve depends to some extent on the initial stress and does not relate directly to the stiffness. It is the author's opinion that the CBR tests in this instance reflect the undrained shear strength rather than the stiffness, although it is possible that the initial gradients do correlate with stiffness and the variability found in the results is due to experimental error.

Figure 11.3 shows a plot of resilient modulus against CBR, where the CBR is the measured value, and the resilient modulus is calculated from the soil model using the mean normal effective stress estimated for the CBR sample. However a 50% increase in the mean normal effective stress almost doubles the resilient modulus and probably has much less of an effect on the CBR value. The calculated values for resilient modulus for a deviator stress pulse of 40kPa then lie on either side of the relationship M_r = 10 x CBR.

11.5 COMPACTED SAMPLES - RESILIENT MODULUS AND CBR

The model developed in Chapter 7 from repeated load triaxial tests on unconfined samples of three different clays demonstrated that the resilient axial strains were controlled by the suction of the sample as well as the level of the repeated deviator stress. The material constants in the model differed for the three clays. The suction was found to be related to the moisture content of the sample, and, as discussed in Chapter 2, would appear to be relatively insensitive to changes in dry density.

The CBR test results demonstrated that the CBR was related to the suction for each clay, although the constants in the equations

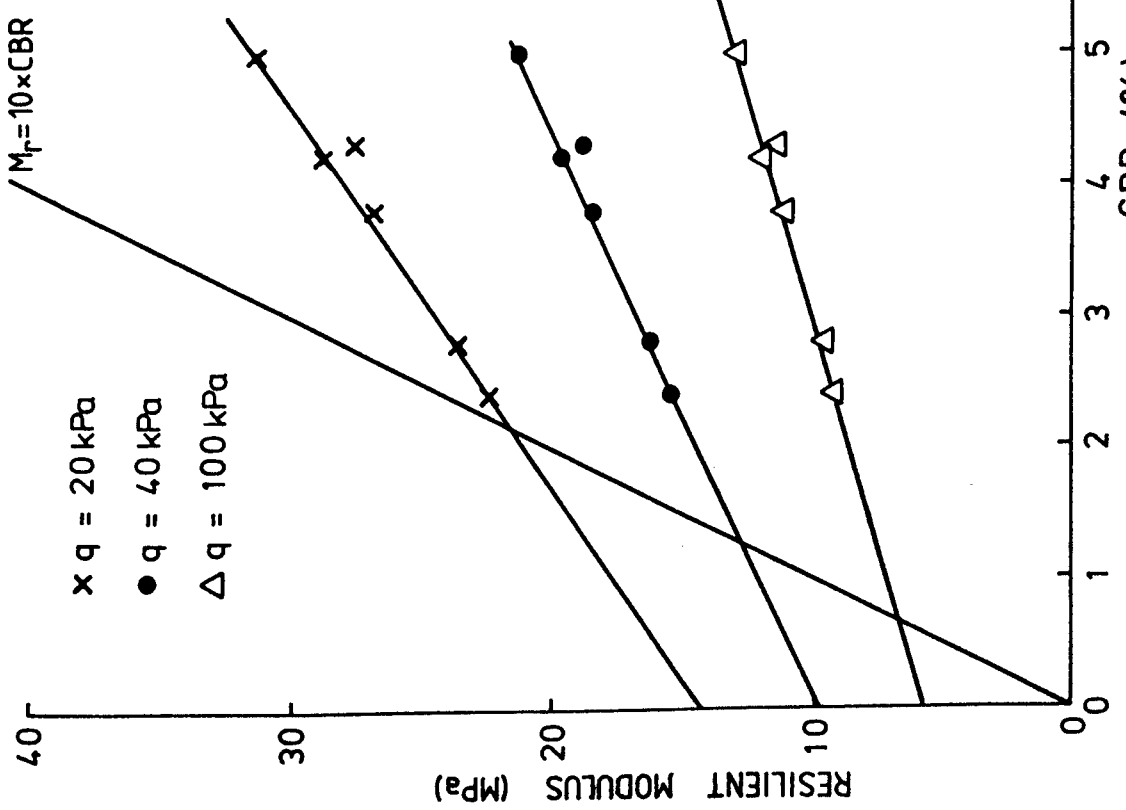

FIGURE 11.3 RELATIONSHIP BETWEEN THE CBR AND RESILIENT MODULUS FOR CONSOLIDATED SAMPLES OF KEUPER MARL

again differed with the different materials.

Figures 11.4, 11.5 and 11.6 show the relationship between CBR and resilient modulus for different values of pulsed deviator stress for the Keuper Marl, Gault clay and London clay respectively. The figures were plotted using the soil model derived in Chapter 7, rearranged to give the resilient modulus

$$M_r = \frac{q_r}{A} \left[\frac{S}{q_r} \right]^B \qquad 11.2$$

and the relationship found between the CBR and suction and described in Chapter 8.

$$\log CBR = CS + D \qquad 11.3$$

where C and D are constants and equal 0.019 and -0.417 respectively

combining these equations gives

$$M_r = \frac{q_r}{A} \left[\frac{(\log(CBR)-D)}{C \times q_r} \right]^B \qquad 11.4$$

The empirical relationships $M_r = 10 \times CBR$, originally derived by Heukelom and Klomp (1962), and $M_r = 17.6\ (CBR)^{0.64}$ from Powell et al (1984) are also shown on the figures.

The results indicate that the magnitude of the repeated deviator stress pulse has a significant effect for all three clays, although the effect is greatest for the Keuper Marl, which is the least plastic. The marl however exhibits less non linearity in its stiffness - CBR relationship than either of the other two soils.

The empirical relationships give a reasonable approximation to the stiffness of the marl, but overestimate the stiffness of the London clay and Gault clay at the higher CBR values. Kirwan et al (1982) reported similar inaccuracies at CBR values of 5% and above, although they were working with glacial tills with

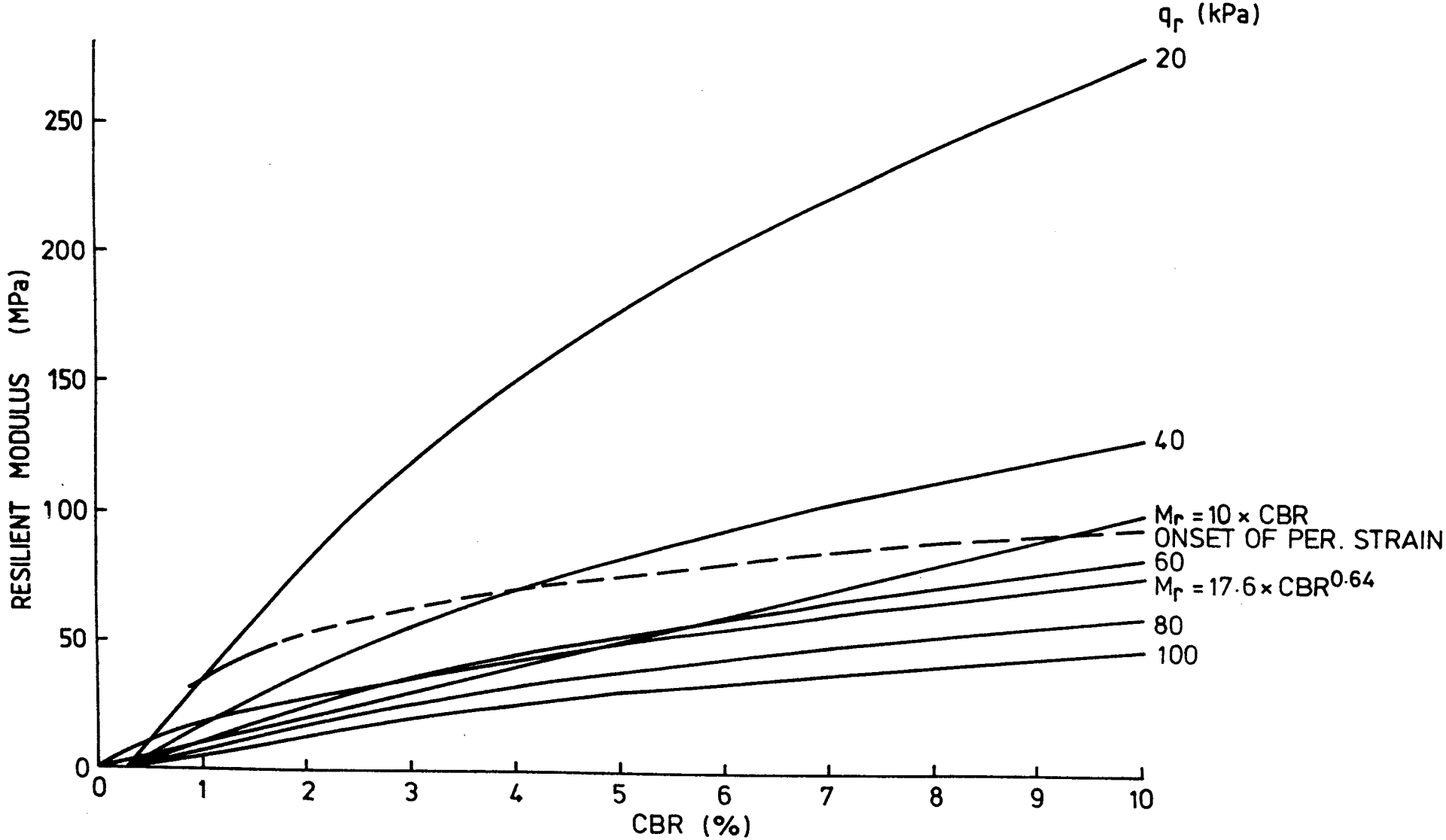

FIGURE 11.4 THE RELATIONSHIP BETWEEN STIFFNESS AND CBR FOR COMPACTED SAMPLES OF KEUPER MARL FOR A RANGE OF STRESS PULSE AMPLITUDES

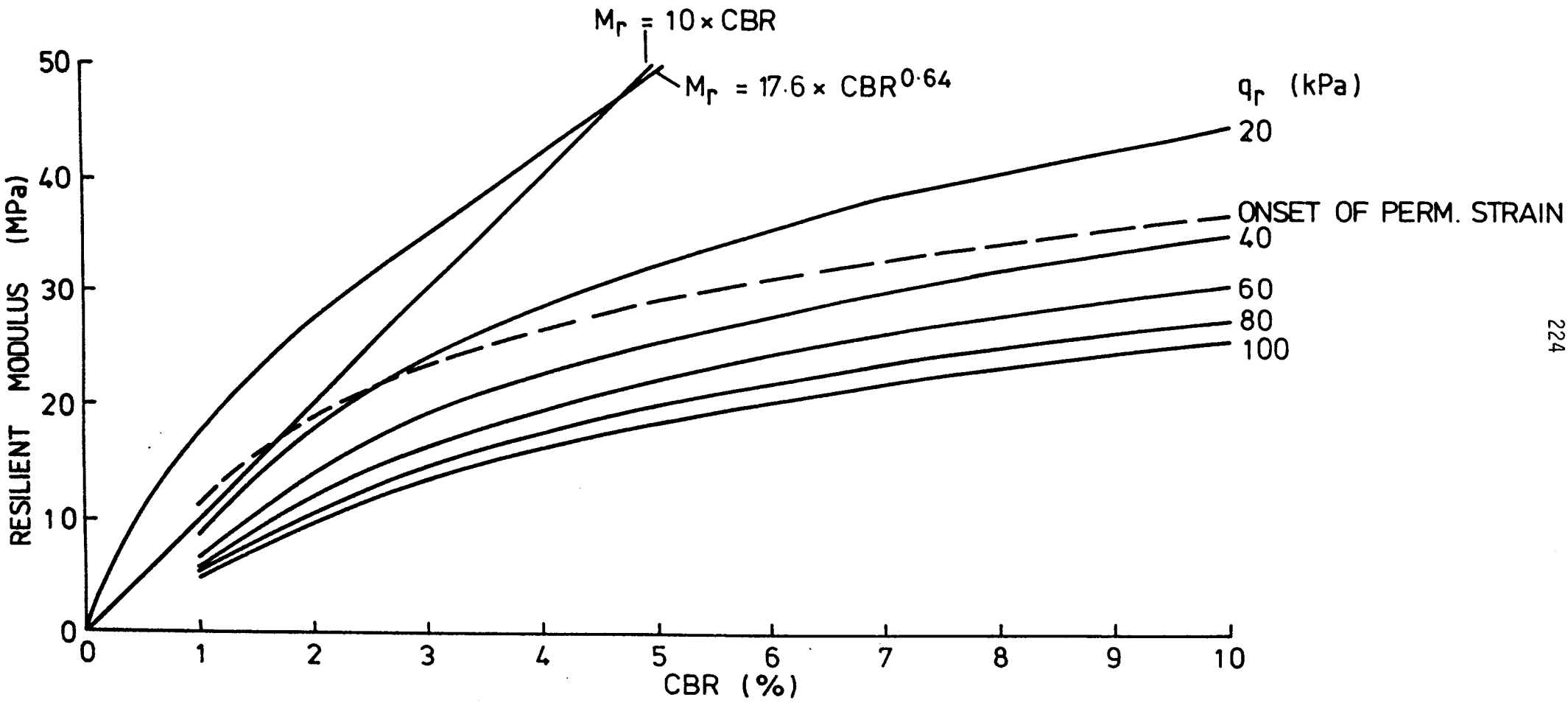

FIGURE 11.5 THE RELATIONSHIP BETWEEN STIFFNESS AND CBR FOR COMPACTED SAMPLES OF GAULT CLAY FOR A RANGE OF STRESS PULSE AMPLITUDES

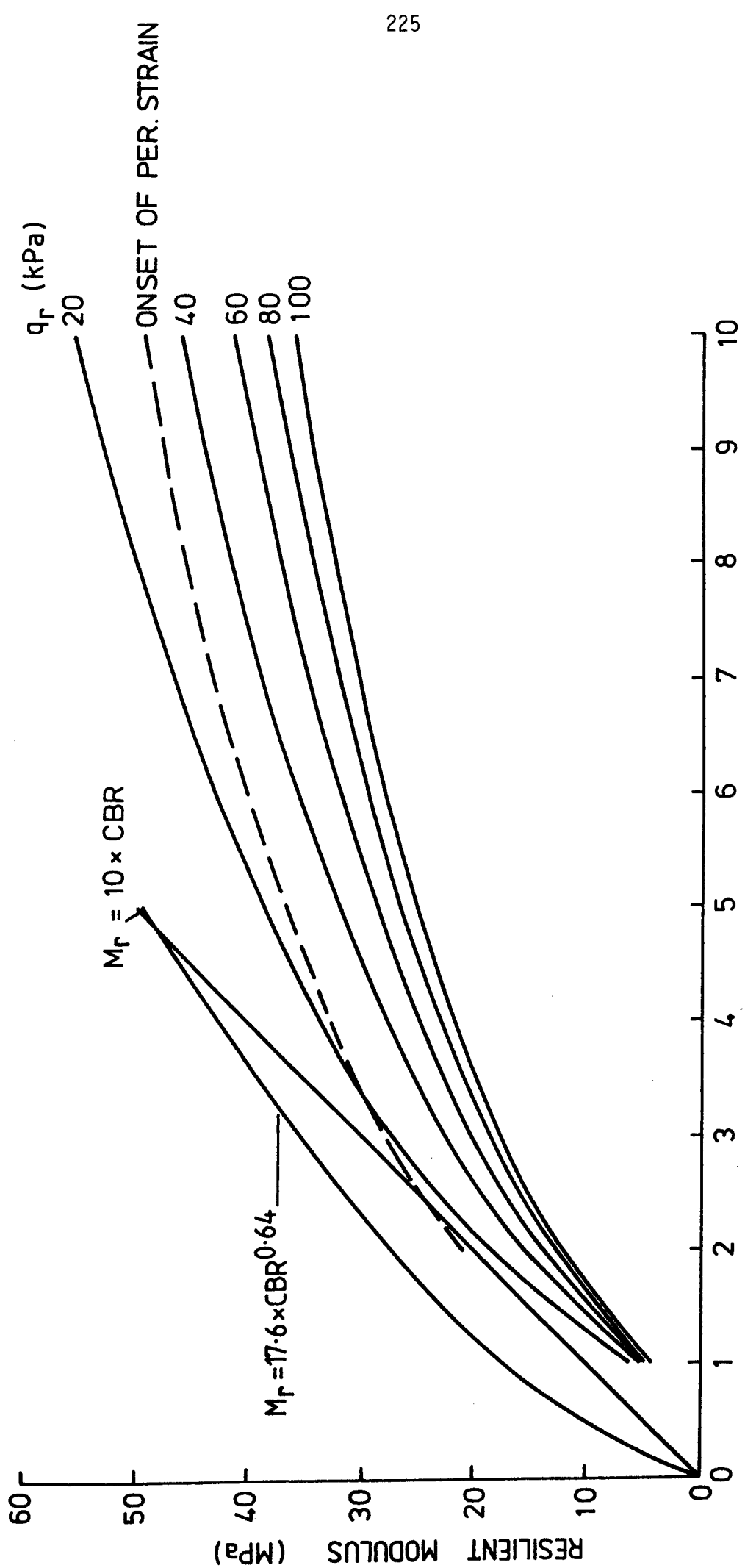

FIGURE 11.6 THE RELATIONSHIP BETWEEN STIFFNESS AND CBR FOR COMPACTED SAMPLES OF LONDON CLAY FOR A RANGE OF STRESS PULSE AMPLITUDES

plasticity indices between 14 and 20. These compare more with the Keuper Marl rather than the London or Gault clays used in this research.

The relationship between the suction and the magnitude of the deviator stress pulse required to cause the onset of permanent strain developed in Chapter 7 is also shown plotted on Figures 11.4, 11.5 and 11.6. The relationship is only approximate as discussed in Chapter 7, but indicates that there will be some permanent strain development for deviator stress pulses of 40 kPa on the Gault and London clays even with a CBR of 10%. The marl is shown to be able to support much higher repeated deviator stresses at particular values of CBR without any permanent strain developing than either of the other more plastic clays.

The suction moisture content relationship for the three clays was shown to be unique in Chapter 7 if the results were plotted in terms of liquidity index, and this result was used to plot the variation in stiffness and CBR with liquidity index. Figure 11.7 shows the variations in stiffness with liquidity index for the three clays, and Figure 11.8 shows the variations in CBR with liquidity index.

The stiffness curves for the London and Gault clays appear coincident, and the CBR curves for these two clays are parallel, though not coincident. The curves for the Keuper Marl do not fit those of the other two clays either in gradient or intercept, and therefore if there is a normalising factor to be incorporated into a single model then it would appear to depend on other parameters rather than just the plasticity index.

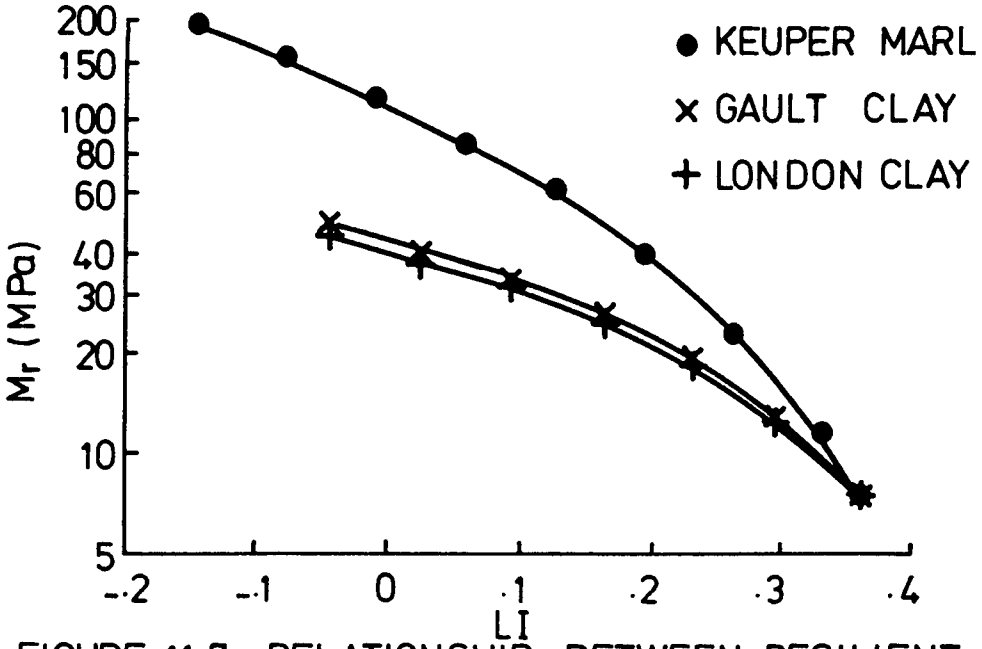

FIGURE 11.7 RELATIONSHIP BETWEEN RESILIENT MODULUS AND LIQUIDITY INDEX FOR THE COMPACTED SAMPLES

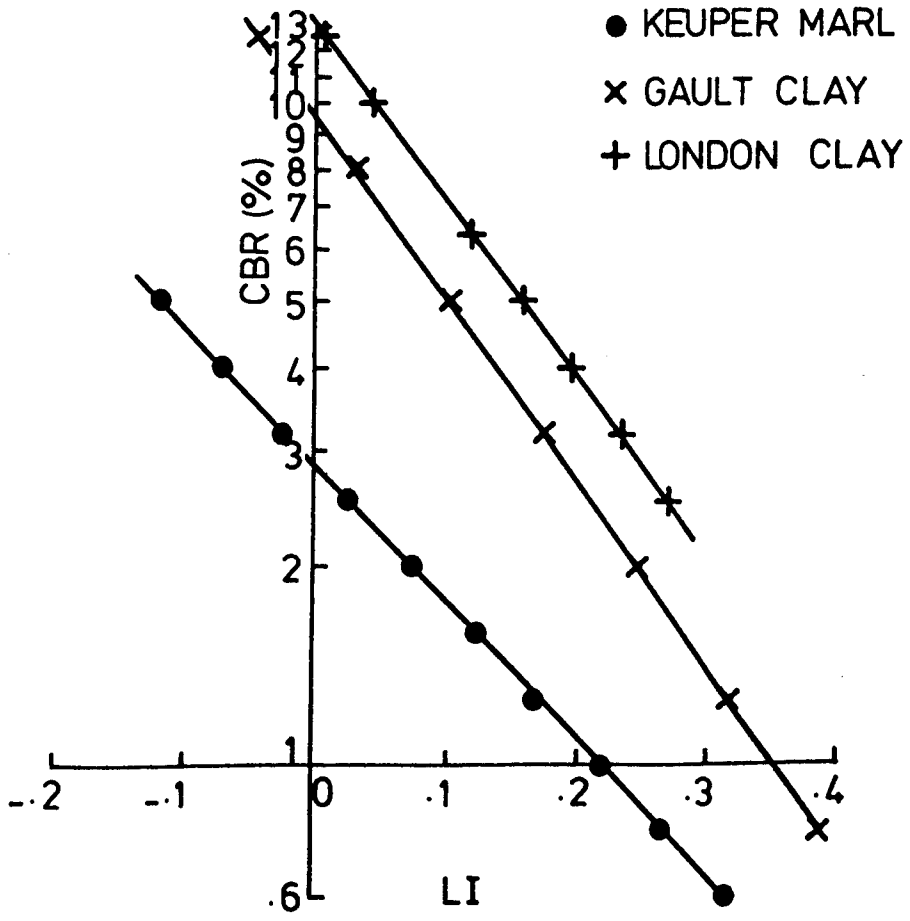

FIGURE 11.8 RELATIONSHIP BETWEEN CBR AND LIQUIDITY INDEX FOR THE COMPACTED SAMPLES

CHAPTER TWELVE

CONCLUSIONS

12.1 CONSOLIDATED TRIAXIAL SAMPLES

12.1.1 Consolidation

(a) The consolidation results show a unique curve, within experimental scatter, in v-lnp' space with gradient $\lambda = 0.1$.

(b) The swell-back curves in v-lnp' space were parallel and of similar shape with an average gradient κ of 0.035.

(c) The value of K_o was measured as 0.54 for the consolidation phase of each sample.

(d) The results from the swell-back phase in q-p' space showed a scatter around the curve proposed by Mayne and Kilharney (1982) where $K_o = (1 - \sin\Phi')\ OCR^{\sin\Phi'}$

(e) The rate of loading during consolidation was sufficiently slow to avoid any significant variation in moisture content with radius at the end of consolidation.

12.1.2 Resilient Response

(a) The repeated deviator stress pulse tests of one second and one tenth second duration showed a significant stress softening effect. These tests with a repeated stress pulse magnitude of twenty seconds did not show any stress softening, however the stress pulse magnitudes were much smaller and covered a smaller range.

(b) The mean normal effective stress was shown to remain constant for the tests with stress pulses of one second and 20 second duration indicating

isotropic elastic behaviour.

(c) Transient pore pressures could be measured under applied loadings of one tenth of a second duration.

(d) The resilient axial strain resulting from a repeated deviator stress pulse depended on the mean normal stress and the magnitude of the deviator stress pulse according to the equation:

$$\varepsilon_a{}^r = A\left[\frac{q_r}{p_o'}\right]^B$$

where A and B are material constants, both of which increased as the stress pulse duration decreased, indicating that the material effectively became stiffer.

(e) For the stress conditions covered by the test programme, the resilient response was independent of the preconsolidation pressure and the ambient deviator stress.

(f) The samples exhibited thixotropic behaviour in that the measured stiffness at a particular deviator stress was lower if the preceeding deviator stress pulses were of greater magnitude. The samples regained their original stiffness if they were left to rest.

12.1.3 **Permanent Strain Response**

(a) The test specimens exhibited a threshold stress which was not well defined but could be represented by a straight line on a normalised q_r - p_o' stress plot. Stress paths crossing that line are likely to cause failure, and those approaching it to cause large permanent deformations under repeated loading.

(b) Stress paths well below this threshold level caused negligible permanent deformation or pore pressure development even after 400,000 applications of stress.

12.1.4 Undrained Strength

(a) The deviator stress-axial strain plots exhibited three distinct regions; an initial stiff section, followed by a linear, less stiff, region, followed by failure, with large deformations for little change in stress. It is thought that this shows the initial yield as the stress path reaches the Hvorslev surface and then failure as the sample reaches the Critical State.

12.2 SUCTION

(a) Plots of suction (in kPa) against Liquidity Index for the Keuper Marl, Gault Clay and London Clay showed a scatter about a unique linear relationship for the range of suctions, 20kPa to 100kPa, used.

(b) For the soils and conditions of these experiments, suction in partially saturated soils, was found to be equivalent to effective stress in the influence it had on soil behaviour.

12.3 COMPACTED TRIAXIAL SAMPLES

12.3.1 Resilient Response

(a) The samples exhibited significant stress softening.

(b) The samples exhibited thixotropic behaviour in that the measured stiffness at a particular deviator stress was lower if the preceeding deviator stress pulses were of greater magnitude.

(c) The resilient axial strain resulting from a deviator stress pulse depended on the suction of the sample and the magnitude of the deviator stress pulse according to the equation:

$$\epsilon_a^r = A\left[\frac{q_r}{S}\right]^B$$

where A and B are material constants which differed for the three clays which were tested.

12.3.2 Permanent Response

(a) A unique, approximately linear, relationship was found between the magnitude of the deviator stress pulse required to cause some development of permanent strain and soil suction for all three clays which were tested.

12.4 CBR TESTS

(a) The minimum CBR occurred at 2.5mm penetration in all tests.

(b) The consolidated and compacted samples were unloaded and reloaded after 1.0mm, 2.5mm and 5.0mm penetration. The initial slope and the slope of the reload sections reflected, quantitively, the CBR value, with higher CBR values exhibiting steeper slopes.

(c) For the overconsolidated samples of Keuper Marl, the CBR was linearly related to the undrained shear strength, as measured by a shear vane, according to the equation: $c_u = 7.8$ CBR (MPa)

(d) For the compacted samples of Keuper Marl, the CBR and undrained shear strength were related by the expression: $c_u = 20$ CBR (MPa). For the compacted samples of Gault clay the expression was: $c_u = 12.5$ CBR (MPa)

(e) The consolidated and compacted CBR samples exhibited a linear relationship between the moisture content and the logarithm of the undrained shear strength.

12.5 RESILIENT MODULUS AND CBR

12.5.1 Consolidated Samples

(a) For the samples tested, the resilient modulus was found to be independent of the moisture content, while the CBR varied with moisture content.

12.5.2 Compacted Samples

(a) The resilient modulus and the CBR were both found to depend on suction and are related by a relationship of the form:

$$M_r = \frac{q_r}{A} \left[\frac{\log CBR - D}{C \quad q_r} \right]^B$$

The empirical relationships $E = 10 \times CBR$ (MPa) and $E = 17.6 \times CBR^{0.64}$ (MPa) give a reasonable approximation to the stiffness of Keuper Marl under a deviator stress pulse of 50-60 kPa, but over-predict the stiffness of the Gault and London Clays under the same repeated deviator stress.

CHAPTER THIRTEEN

RECOMMENDATIONS FOR FURTHER WORK

13.1 CONSOLIDATION TRIAXIAL SAMPLES

The number of samples was not large due to the time consuming nature of sample preparation and therefore a continuation of the test programme is required to define more accurately the resilient and permanent response to this type of loading. The range of overconsolidation ratios should be extended to investigate whether the resilient strain model is applicable to samples on the wet side of critical. The range of final mean normal effective stresses should also be increased.

Further tests should be carried out to better define the Hvorslev surface for the material, and to investigate whether it acts as a yield surface for monotonic tests, and whether it can be modified to allow for viscous effects and form a yield surface for repeated loading.

Attempts should be made to consolidate samples anisotropically from much wetter slurries of the order of three times the liquid limit or greater to investigate whether these samples exhibit anisotropic behaviour in effective stress space.

The development of permanent strain under long term repeated loading is important, and the possibility of relating the onset of permanent strain to the stress conditions requires further investigation. The stability of the equipment would have to be improved before this type of work was undertaken.

The test programme should be extended to cover other clays to investigate the possibility of developing a model that applies to more than one material.

13.2 CONSOLIDATED CBR SAMPLES

In order to complete the test programme and investigate the effect on the CBR of different initial effective stresses CBR samples should be allowed to swell back to different mean normal effective stresses. This would require further development of the apparatus to allow higher preconsolidation loads to be applied. The gradient of the load deformation curves should be measured more accurately using electrical transducers and further attempts made to relate it to stiffness.

13.3 COMPACTED TRIAXIAL SAMPLES

The test programme should be continued to provide a larger pool of results to more accurately characterise the response of the soils. The programme should also be extended to include samples tested under a confining pressure. The effect of a confining stress on the suction of the samples could therefore be investigated. The development of permanent strain with increasing numbers of cycles should also be investigated to parallel the test programme on the consolidated samples. The magnitude of Poisson's Ratio measured in this research also requires further investigation.

13.4 COMPACTED CBR SAMPLES

The number of tests should be increased to define more accurately the response of the CBR samples, and the additional materials should also be investigated. The gradient of the load deformation curve should be investigated more fully as for the consolidated CBR samples.

13.5 EQUIPMENT DEVELOPMENT

13.5.1 Consolidation Control System

The proximity transducers must be fitted with an external or separate oscillator and further alterations to the power supply and earthing arrangements are required to eliminate crosstalk

between the outputs of the individual transducers.

The consolidation control unit requires redesigning to produce more stable switching of the servo motors, and to provide a much smaller null window.

It is doubtful if the present system will ever produce satisfactory swell back curves and some sort of controller which adjusts the rate of reduction of deviator stress as the cell pressure reduces may be more suitable.

The bellofram loading pistons on the cell top require redesigning to provide sufficient travel during consolidation, and to eliminate the bellofram seal against the cell pressure which caused pulsing of the cell pressure at the higher resilient strains achieved during testing.

13.5.2 Servo Control System

The system is required to be much more stable than at present and to be capable of applying true haversine waveforms with periods as short as 0.1 second at a reasonable amplitude. The load system must be stable to within $\pm$.005kN on both the pulsed and ambient components of axial load, and the cell pressure system must be stable to within $\pm$1kPa. The systems must be capable of loading samples with a large range of different stiffness without resorting to adjusting the gain while actually under load.

A digital system is most likely to be able to meet the above specification, and the author recommends that this type of control system is investigated with a view to fitting it to both the axial load and cell pressure systems.

13.5.3 Data Acquisition

The digital data acquisition system fitted during this research project proved to be accurate and capable of providing far more

information from tests over a wider range of frequencies than other means of data acquisition. The method of measuring volume change should be digitised to enable the complete stress history of the sample to be recorded digitally. Combined digital back pressure and volume change devices are available commercially but could be constructed using a bellofram piston unit with an LVDT or linear potentiometer calibrated to provide a readout of volume change. The pressure could be controlled by a stepper motor connected to the bellofram piston.

REFERENCES

ANDERSON, K.H., BROWN, S.F., FOSS, I., POOL, J.H., and ROSENBRAND, W.F. (1976), 'Effect of cyclic loading on clay behaviour', Proc. Conf. on Design and Construction of Offshore Structures, ICE, London.

ANDERSON K.H., POOL, J.H., BROWN, S.F., ROSENBRAND, W.F. (1980), 'Cyclic and static laboratory tests on Drammen clay', Proc. ASCE, Vol 106, GT5.

ATKINSON, J.H., EVANS, J.S. and HO, E.W.L. (1985), 'Non-uniformity of triaxial samples due to consolidation with radial drainage', Geotechnique Vol 35 No. 3.

AUSTIN, G. (1975), 'A comparison of creep and repeated loading of a silty clay', Progress report, Nottingham University. Unpublished.

AUSTIN, G. (1979), 'The behaviour of Keuper marl under undrained creep and repeated loading', Ph.D. thesis, University of Nottingham.

BALASUBRAMANIAN, A.S. (1976), 'Axial strains and displacement patterns in triaxial specimens of a saturated clay', Soils and Foundations Vol 16, No. 1.

BANERJEE, P.K. and STIPHO, A.S. (1979), 'An elasto-plastic model for undrained behaviour of heavily overconsolidated clays', International Journal for Numerical and Analytical methods in Geomechanics, Vol 3.

BARKSDALE, R.D. (1971), 'Compressive stress pulse times in flexible pavements for use in dynamic testing', Highway Research Board Record No. 345.

BELL, C.A. (1978), 'The prediction of permanent deformation in flexible pavements', Ph.D. thesis, University of Nottingham.

BISHOP, A.W. and GIBSON, R.E. (1963), 'The influence of the provisions for boundary drainage on strength and consolidation characteristics of soil measured in the triaxial apparatus', ASTM Special Technical Publication No. 361.

BLACK, W.P.M. (1979), 'The Strength of clay subgrades : its measurement by a penetrometer', Transport and Road Research Laboratory, Laboratory Report 901.

BLACK, W.P.M., CRONEY, D. and JACOBS, J.C. (1958), 'Field studies of the movement of soil moisture', Road Research Technical Paper No. 41.

BJERRUM, L. (1973), 'Problems of soil mechanics and construction on soft clay', Proc. of 8th Int. Conf. SMFE, Vol 3, Moscow.

BOYCE, J.R. (1976), 'The behaviour of a granular material under repeated loading', Ph.D. thesis, University of Nottingham.

BROWN, S.F. (1974), 'Sample end restraint and pore pressure measurement in cyclic load triaxial tests on Drammen clay', Report to N.G.I.

BROWN, S.F., ANDERSON, K.H., and McELVANEY, J. (1977), 'The effect of drainage on cyclic loading of clay', Proc. of 9th Int. Conf. on Soil Mechanics and Foundation Engineering, Tokyo.

BROWN, S.F., LASHINE, A.K.F. and HYDE, A.F.L. (1975), 'Repeated load triaxial testing of a silty clay', Geotechnique, Vol 25, No. 1.

BROWN, S.F. and PAPPIN, J.W. (1981), 'Analysis of Pavements with granular bases', Transportation Research Record No. 810.

BROWN, S.F. and PAPPIN, J.W. (1982), 'Use of a pavement test facility for the validation of analytical design methods', Proc. of 5th Int. Conf. on structural design of asphalt pavements, Vol 1, Delft.

BROWN, S.F. and PAPPIN, J.W. (1985), 'The modelling of granular materials in pavements', Transportation Research Record 1022.

BROWN, S.F. (1980), 'An introduction to the analytical design of bituminous pavements', University of Nottingham.

BROWN, S.F., BRODRICK, B.V. and PAPPIN, J.W. (1980), 'Permanent deformation of flexible pavements', Final technical report submitted to U.S. Army, University of Nottingham.

BS 1377 (1975), 'Methods for testing soils for civil engineering purposes', British Standards Institute.

CARTER, J.P. (1982), 'Predictions of the non-homogenous behaviour of clays in the triaxial test', Geotechnique Vol 32, No. 1.

CRONEY, D. (1977), 'The design and performance of road pavements', HMSO.

CRONEY, D., COLEMAN, J.D. and BLACK, W.P.M. (1958), 'Movement and distribution of water in soil in relation to highway design and performance', Highway Research Board, Special Report No. 40.

CROOKS, J.H.A. and GRAHAM, J. (1976), 'Geotechnical properties of the Belfast estuarine deposits', Geotechnique Vol 26, No. 2.

CULLINGFORD, G., LASHINE, A.K. and PARR, G.B. (1972), 'Servo controlled equipment for dynamic testing of soils', Geotechnique Vol 22, No. 3.

DEHLEN, G.L. (1969), 'The effect of non-linear material on the behaviour of pavements subjected to traffic loads', Ph.D. thesis, University of California.

DUMBLETON, M.J. and WEST, G. (1968), 'Soil suction by the rapid method: an apparatus with extended range', The Journal of Soil Science Vol 19, No. 1.

EDIL, T.B., MOTAN, S.E. and TOHA, F.X. (1980), 'Mechanical behaviour and testing methods of unsaturated soils', Special Technical Publication No. 740.

EDRISS, E.V. and LYTTON, R.L. (1977), 'Dynamic properties of fine grained soils', Proc. of 9th Int. Conf. on Soil Mechanics and Foundation Engineering, Vol 2, Tokyo.

FINN, F.N., NAIR, K. and MONISMITH, C.L. (1972), 'Application of theory in the design of asphalt pavements', Proc. of 3rd Int. Conf. on the Structural design of asphalt pavements. Vol 1, London.

FOLKES, D.J. and CROOKS, J.H.A. (1985), 'Effective stress paths and yielding in soft clays below embankments', Canadian Geotechnical Journal Vol 22, No. 3.

FRANCE, J.W. and SANGREY, D.A. (1977), 'Effects of drainge in repeated loading of clays', ASCE Vol 103, GT7.

FREDLUND, D.G., BERGAN, A.T. and SAUER, E.K. (1975), 'Deformation characterisation of subgrade soils for highways and runways in northern environments', Canadian Geotechnical Journal Vol 12, No. 2.

GRAHAM, J. and HOULSBY, G.T. (1983), 'Elastic anisotropy of a natural clay', Geotechnique 33, No. 2.

GRAHAM, J., NOONAN, M.L. and LEW, K.V. (1983), 'Yield states and stress-strain relationships in natural plastic clay', Canadian Geotechnical Journal, Vol 20, No. 3.

HEUKELOM, W. and KLOMP, A.J.G. (1962), 'Dynamic testing as a means of controlling pavements during and after construction', Proc. of 1st Int. Conf. on structural design of asphalt pavements, Ann Abor, Michigan.

HIGHT, D.W. (1983), 'A simple piezometer probe for the routine measurement of pore pressure in triaxial tests on saturated soils', Draft report for publication.

HIGHT, D.W. and STEVENS, M.G.H. (1982), 'An analysis of the CBR test in saturated clay', Geotechnique, Vol 32, No. 4.

HOUSTON, W.N. and HERRMAN, H.G. (1980), 'Undrained strength of marine soils', Proc. ASCE, Vol 106, GT6.

HYDE, A.F.L. (1974), 'Repeated load testing of soils', Ph.D. thesis, University of Nottingham.

HYDE, A.F.L. and BROWN, S.F. (1976), 'The plastic deformation of a silty clay under creep and repeated loading', Geotechnique Vol 21, No. 1.

HYDE, A.F.L. and WARD, S.J. (1985), 'A pore pressure and stability model for a silty clay under repeated loading', Geotechnique Vol 35, No. 2.

KIM, T.C. and NOVAK, M. (1981), 'Dynamic properties of some cohesive soils of Ontario', Canadian Geotechnical Journal Vol 18, No. 3.

KIMURA, T. and SAITOH, K. (1983), 'The influence of strain rate on pore pressures in consolidated undrained triaxial tests on cohesive soils', Soils and Foundations Vol 23, No. 1.

KIRWAN, R.W., FARRELL, E.R., HARTFORD, D.N.D. and ORR, T.L.L. (1982), 'The interpretation of repeated load parameters for a glacial subgrade from soil properties', Proc. of 5th Int. Conf. on structural design of asphalt pavements, Vol 1, Delft.

KIRWAN, R.W. and SNAITH, M.S. (1976), 'A simple chart for the prediction of resilient modulus', Geotechnique, Vol 26, No. 1.

KIRWAN, R.W., FARREL, E.R., HARTFORD, D.N.D. and ORR, T.L.L. (1982), 'The interpretation of repeated load parameters for a glacial subgrade from soil properties', Proc. of 5th Int. Conf. on structural design of asphalt pavements, Vol 1, Delft.

KNIGHT, K. and BLIGHT, G.E. (1965), 'Studies of some effects resulting from unloading of soils', Proc. of 6th Int. Conf. Soil Mechanics and Foundation Engineering, Montreal.

KOUTSOFTAS, D.C. (1978), 'Effects of cyclic loads on undrained strength of two marine clays', Proc. ASCE, Vol 104, GT5.

KRAHN, J. and FREDLUND, D.G. (1972), 'On total, matric and osmotic suction, Soil Science, Vol 114, Pt 5.

LADD, C.C., FOOTT, R., ISHIHARA, K., SCHLOSSER, F. and POULOS, H.G. (1977), 'Stress-deformation and strength characteristics', Proc. of 9th Int. Conf. Soil Mechanics and Foundation Engineering, Vol 2, Tokyo.

LAMBE, T.W. and WHITMAN, R.V. (1979), 'Soil mechanics S.I. version', John Wiley and Sons.

LASHINE, A.K.F. (1971), 'Some aspects of the behaviour of Keuper Marl under repeated loading', Ph.D. thesis, University of Nottingham.

LEE, K.L. (1976), 'Influence of end restraint in cyclic triaxial tests', U.S. Army Engineers Waterways Experimental Station, Vicksburg, Contract Report S-76-1.

LO, K.Y. (1969), 'The pore pressure strain relationship of normally consolidated undisturbed clay', Canadian Geotechnical Journal Vol 6.

LOUDON, P.A. (1967), 'Some deformation characterics of kaolin', Ph.D. thesis, University of Cambridge.

MACKY, T.A. and SAADA, A.S. (1984), 'Dynamics of anisotropic clays under large strains', Proc. ASCE Vol 110,GT4.

MATSUI, T. and ABE, N. (1981), 'Behaviour of clay on cyclic stress-strain history', Proc. of 10th Int. Conf. Soil Mechanics and Foundation Engineering, Vol 3, Stockholm.

MATSUI, T., O'HARA H., ITO, T., (1980), 'Cyclic stress-strain history and shear characteristics of clay', Proc. ASCE, Vol 106, GT10.

MAYNE, P.W. and KILHANEY, F.H. (1982), 'K_o-OCR relationships in soil', Proc. ASCE Vol 108, GT6.

MITCHELL, J.K. (1960), 'Fundamental aspects of thixotropy', Proc. ASCE Vol 86, SM3.

MITCHELL, J.K. (1969), 'On the yielding and mechanical strength of London clays', Canadian Geotechnical Journal Vol 7, No. 3.

MITCHELL, R.J. AND KING, R.D. (1977), 'Cyclic loading of an Ottowa area Champlain sea clay', Canadian Geotechnical Journal Vol 14, No. 2.

MOU, C.H and CHU, T.Y. (1981), 'Soil-suction approach for evaluation of swelling potential'. Transport Research Record 790.

OGAWA, S., SHIBAYAMA, T., YAMAGUCHI, H. (1977), 'Dynamic strength of saturated cohesive soil', Proc. of 9th Int. Conf. Soil Mechanics and Foundation Engineering, Vol 2, Tokyo.

OSIPOV, V.I., NIKOLAEVA, S.K. and SOKOLOV, V.N. (1984), 'Microstructural changes associated with thixotropic phenomena in clay soils', Geotechnique 34, No 3.

OVERY, R.F. (1982), 'The behaviour of anisotropically consolidated silty clay under cyclic loading', Ph.D. thesis, University of Nottingham.

PAPPIN, J.W. (1979), 'Characteristics of a granular material for pavement analysis', Ph.D. thesis, University of Nottingham.

PARR, G.B. (1972), 'Some aspects of the behaviour of London clay under repeated loading', Ph.D. thesis, University of Nottingham.

PERLOFF, W.H. and PAMBO, L.E. (1969), 'End restraint effects in the triaxial test', Proc. of 7th Int. Conf. Soil Mechanics and Foundation Engineering, Mexico.

POWELL, W.D., POTTER, J.F., MAYHEW, H.C. and NUNN, M.E. (1984), 'The structural design of bituminous roads', TRRL Laboratory Report 1132.

PUSCH, R. (1982), 'Thixotropic stiffening of clay consolidated in the laboratory', Canadian Geotechnical Journal Vol 19, No. 4.

RICHARDS, B.G. and GORDON, R. (1972), 'Prediction and observation of the performance of a flexible pavement on an expansive clay sub-grade', Proc. of 3rd Int. Conf. on structural design of asphalt pavements, Vol 1, London.

ROAD RESEARCH LABORATORY (1970), 'A guide to the structural design of pavements for new roads', Road Note 29, HMSO.

ROWE, P.W. and BARDEN, L. (1966), 'A new consolidation cell', Geotechnique, Vol 16, No. 2.

RUSSAM, K. (1967), 'Subsoil drainage and the structural design of roads', TRRL, Laboratory Report 110.

RUSSELL, E.R. and MICKLE, J.L. (1970), 'Liquid limit by soil moisture tension', Proc. ASCE, Vol 96, SM3.

SAADA, A.S. and BIANCHINI, G.F. (1975), 'Strength of one dimensionally consolidated soils', Proc. ASCE Vol 101, GT11.

SAADA, A.S., BIANCHINI, G.F. and SHOOK, L.P. (1978), 'The dynamic response of anisotropic clay', ASCE special Conf. Earthquake engineering and soil dynamics, Pasadena, California.

SANCHEZ, J.M. and SAGASETA, C. (1981), 'Undrained behaviour of soft clays in triaxial tests', Proc. of 10th Int. Conf. Soil Mechanics and Foundation Engineering, Stockholm.

SANGREY, D.A., HENKEL, D.J. and ESRIG, M.I. (1969), 'The effective stress response of a saturated clay soil to repeated loading', Canadian Geotechnical Journal Vol 6, No. 3.

SANGREY, D.A., POLLARD, W.S., EGAN, J.A. (1977), 'Errors associated with rate of undrained cyclic testing of clay soils', ASTM special technical publication No 654.

SAUER, E.K. and MONISMITH, C.L. (1968), 'Influence of soil suction on the behaviour of a glacial till subjected to repeated loading', Highway Research Board Record, No.215.

SCHOFIELD, A.N. and WROTH, C.P. (1968), 'Critical state soil mechanics', McGraw-Hill.

SEED, H.B., CHAN, C.K. and LEE, C.E. (1962), 'Resilience characteristics of subgrade soils and their relation to fatigue failures in asphalt pavements', Proc. of the 1st Int. Conf. on structural design to asphalt pavements, Ann Arbor, Michigan.

SHACKEL, B. (1973), 'Changes in soil suction in a sand-clay subjected to repeated triaxial loading', Highway Research Record No. 429.

SHAW, P. (1982), 'Stress-strain relationships for granular materials under repeated loading', Ph.D. thesis, University of Nottingham.

SHERIF, M.A., ISHIBASHI, I. and LING, S.C. (1977), 'Dynamic properties of a marine sediment', Proc of 9th Int Conf Soil Mechanics and Foundation Engineering, Vol 2, Tokyo.

SNETHEN, D.R. and JOHNSON, L.D. (1977), 'Characterisation of expansive soil subgrades using soil suction data', U.S. Army Engineer, Waterways Experiment Station, Vicksburg, Mississippi. Conf of TRB Comm. A2L06.

TAVENAS, F., Des-ROSIERS, J-P., LEROUEIL, S., La ROCHELLE, P. and ROY, M.(1979), 'The use of strain energy as a yield and creep criterion for lightly overconsolidated clays', Geotechnique Vol 29, No. 3.

TAYLOR, P.W. and BACCHUS, D.R. (1969), 'Dynamic cyclic strain tests on a clay', Proc. of 7th Int. Conf. Soil Mechanics and Foundation Engineering, Vol 1, Mexico.

TOGROL, E., OZUDOGRN, K. and GULER, E. (1979), 'On the dynamic behaviour of overconsolidated clays', Proc. of 7th Int. Conf. Soil Mechanics and Foundation Engineering, Vol 2, Brighton.

WILSON, N.E. and GREENWOOD, J.R. (1974), 'Pore pressures and strains after repeated loading of saturated clay', Canadian Geotechnical Journal Vol 11, No. 2.

WOOD, D.M. (1980), Laboratory investigations of the behaviour of soils under cyclic loading: a review', Soil Mechanics - Transient and cyclic loads, edited by G.N. Pande and O.Z. Zienkiewicz, J. Wiley and Sons.

YASHUHARA, K., YAMANOUCHI, T. and HIRAO, K. (1982), 'Cyclic strength and deformation of normally consolidated clay', Soils and Foundations, Vol 22, No. 3.

APPENDIX A

MATERIAL PROPERTIES

A1 SOIL CLASSIFICATION DATA

The grading curves for the Keuper Marl, Gault Clay and London Clay are shown in Figure A1. The curves were obtained by a combination of wet sieving and the pipette method as decribed in BS 1377.

A series of standard tests were performed on each clay to obtain the basic soil classification data given in Table A1.

A2 CRITICAL STATE PARAMETERS

The critical state parameters determined from the test results on the Keuper Marl are given in Table A2.

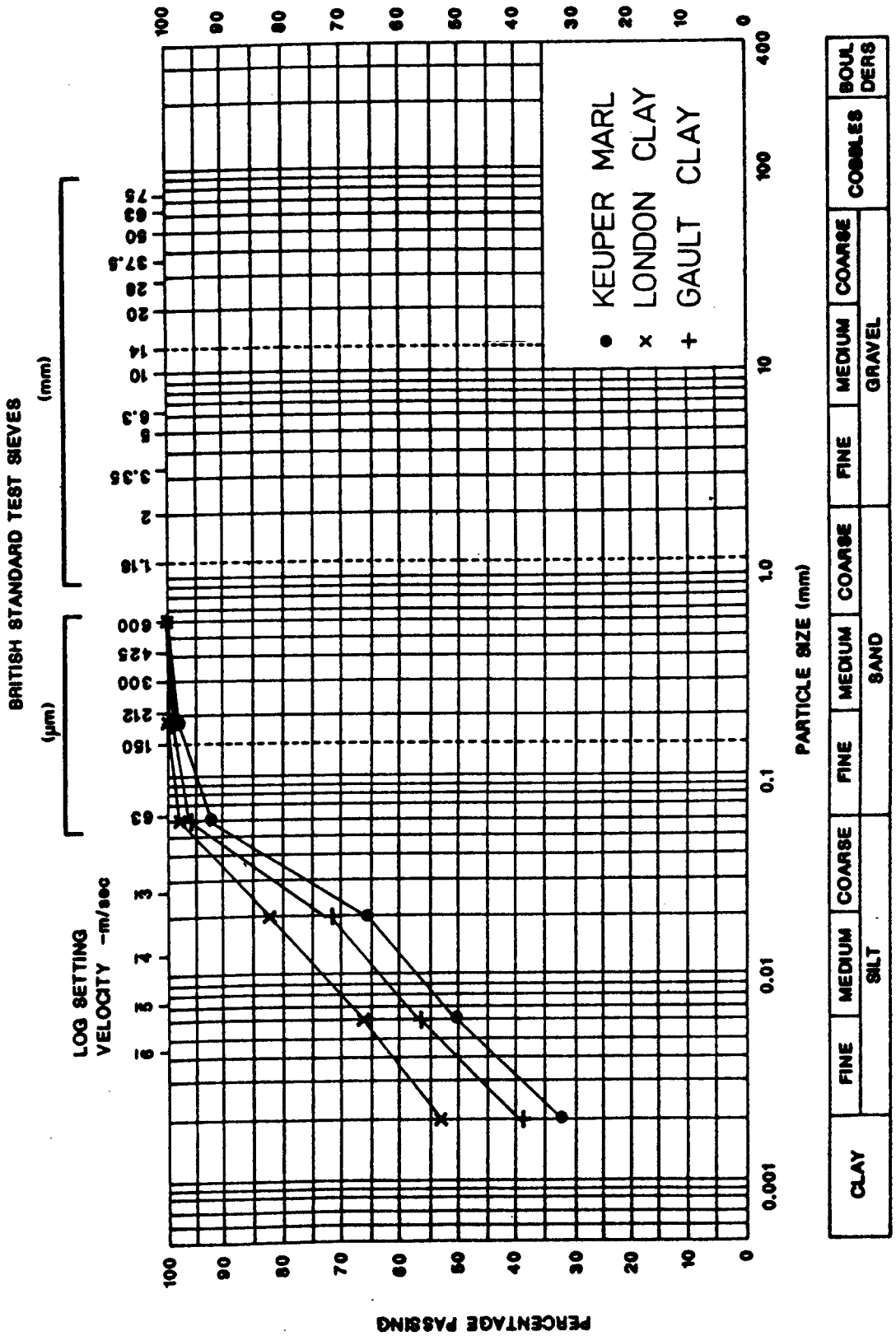

FIGURE A1 PARTICLE SIZE DISTRIBUTION FOR THE KEUPER MARL, GAULT CLAY AND LONDON CLAY

Table A1 Basic Material Properties of Soils used in the Project

Property	Keuper Marl	Gault Clay	London Clay
Specific gravity	2.69	2.69	2.73
% Clay	33	39	54
Plastic limit (%)	18	25	23
Liquid limit (%)	37	61	71
Plasticity Index (%)	19	36	48

Table A2 Critical State Parameters for Keuper Marl

Parameter		Value
Slope of normal compression line	(λ)	0.1
Intercept for anisotropic consolidation	(N_o)	2.105
Mean slope of swell-back lines	(k)	0.035
Angle of shearing resistance	(ϕ')	28.5°
Friction parameter	(M)	1.13
Earth pressure coefficient at rest	(K_o)	0.54

APPENDIX B

B1 PERMEABILITY OF FILTER PAPER SIDE DRAINS

A permeability test on the filter paper side drains was carried out in one of the triaxial cells used in the test programme. The drainage fittings were not modified except that the top cap was fitted with a porous stone and an additional back pressure line. The soil sample was replaced with an impermeable rubber sample, which was installed in the cell in a similar manner to the soil samples.

A pressure difference of 15 kPa was maintained across the filter paper drains and the flow rate was determined for different cell pressures by using the burettes in the back pressure line.

Figure B1 shows the variation in the flow rate through the filter paper with cell pressure. As expected the flow rate decreases as the cell pressure increases because the cell pressure pinches the filter paper against the rubber sample.

A permeability of 1.5×10^{-4} cm/sec was estimated for the filter paper drains at the lowest measured flow rate of 0.8 ml/hr. This compares reasonably well with a permeability of 5.4×10^{-5} cm/sec quoted for filter paper under an effective stress of 690 kPa by Bishop and Gibson (1963). Overy (1982) measured a permeability of 4×10^{-6} cm/sec for a filter paper drain in contact with a sample of Keuper Marl.

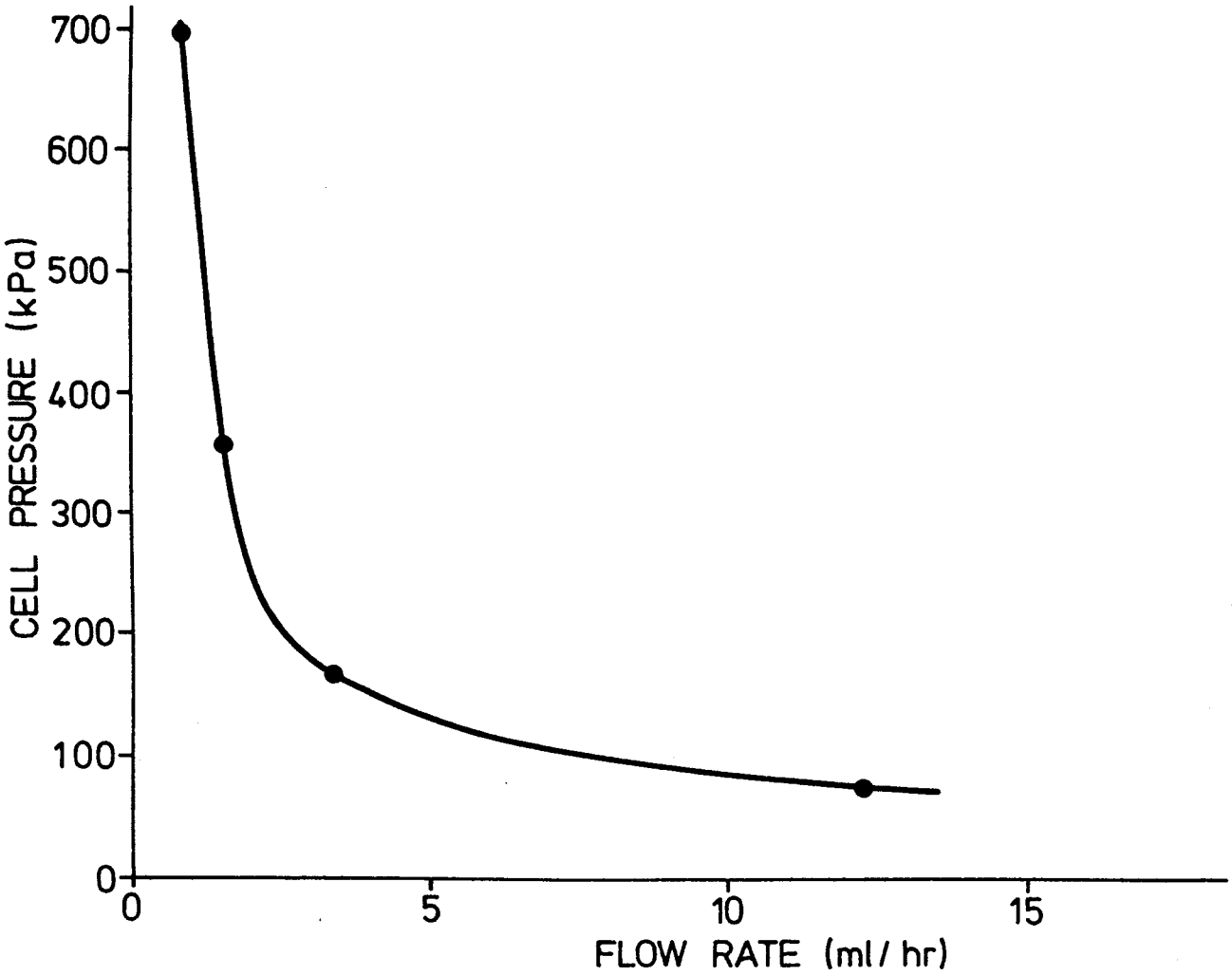

FIGURE B1 FLOW RATE THROUGH FILTER PAPER DRAINS AS A FUNCTION OF CELL PRESSURE

APPENDIX C

SUPPLEMENTARY TESTS

C1 PORE PRESSURE RESPONSE

Each sample was checked for saturation by comparing the change in pore pressure with a change in cell pressure. This was done during the consolidation phase when the cell pressure was controlled by an air regulator acting through an air oil interface, and consequently the rate of increase of cell pressure was quite low compared with the rates of loading during the test periods.

The effect of increased rates of loading on the apparent B value was investigated by pulsing the cell pressure using the servo hydraulic system, and monitoring the base and centre pore pressure pulses. Figure C1 shows a typical plot of the measured B value against the duration of the cell pressure pulse, and shows that centre pore pressure probe showed a value close to 1 for a loading period as low as 0.1 second. The response of the base pore pressure transducer started to drop off above a loading period of approximately 0.5 second.

C2 COMPARISON BETWEEN AN LVDT AND A PROXIMITY TRANSDUCER

A piece of apparatus was constructed which allowed the output of an LVDT and a proximity transducer to be compared with each other over a small range of frequencies at small deflections. The equipment could not be used to calibrate the transducers directly.

The equipment is shown diagrammatically in Figure C2 and consists of an eccentric disc with 0.05mm eccentricity on which rests a lever arm; the other end of which was pivoted on a knife edge. The LVDT core and proximity transducer target were attached to the lever arm, and the transducer bodies to the frame. The eccentric was driven by a variable speed electric motor, which

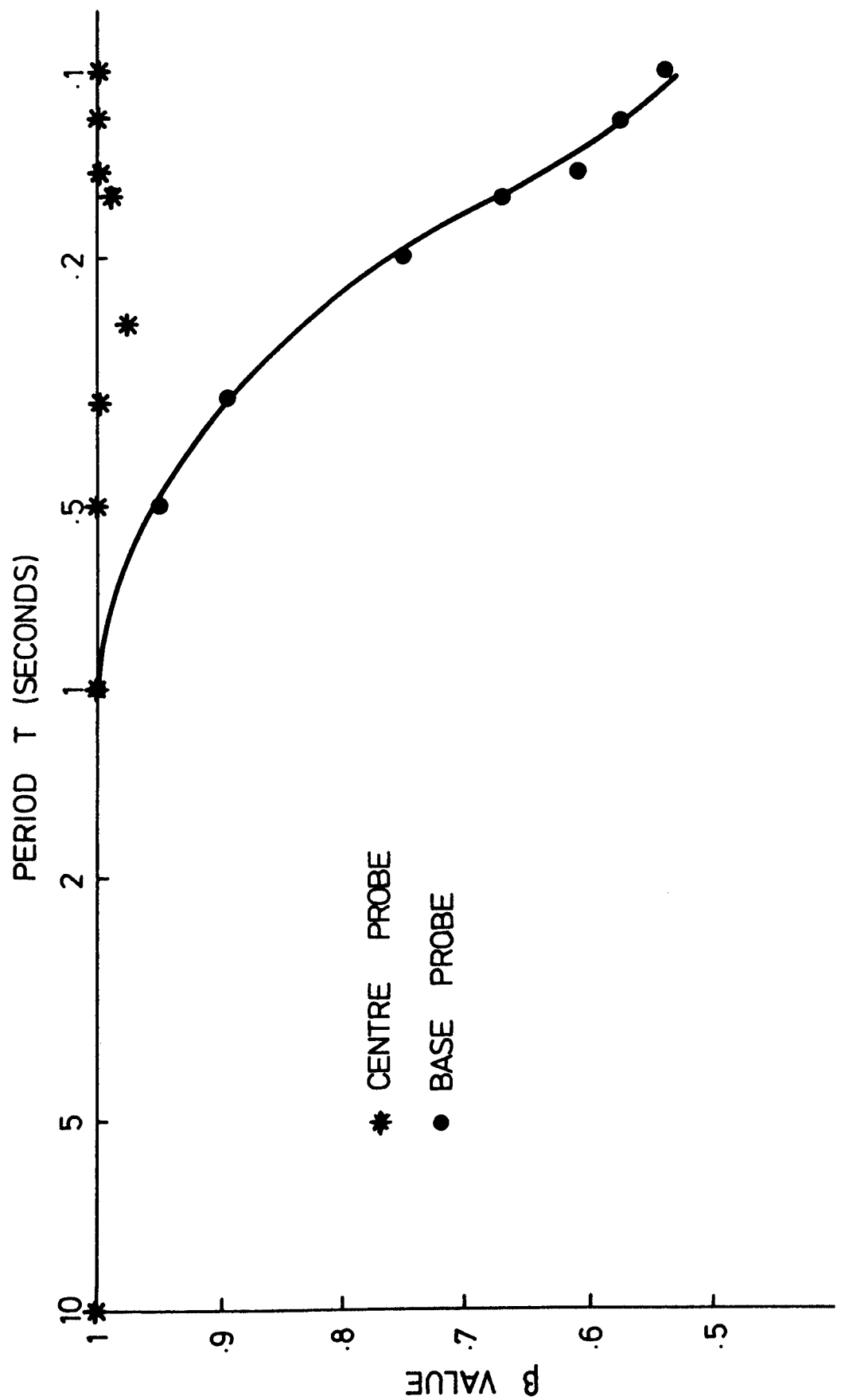

FIGURE C1 PORE PRESSURE RESPONSE TO VARIATIONS IN CONFINING STRESS. SAMPLE 65/12

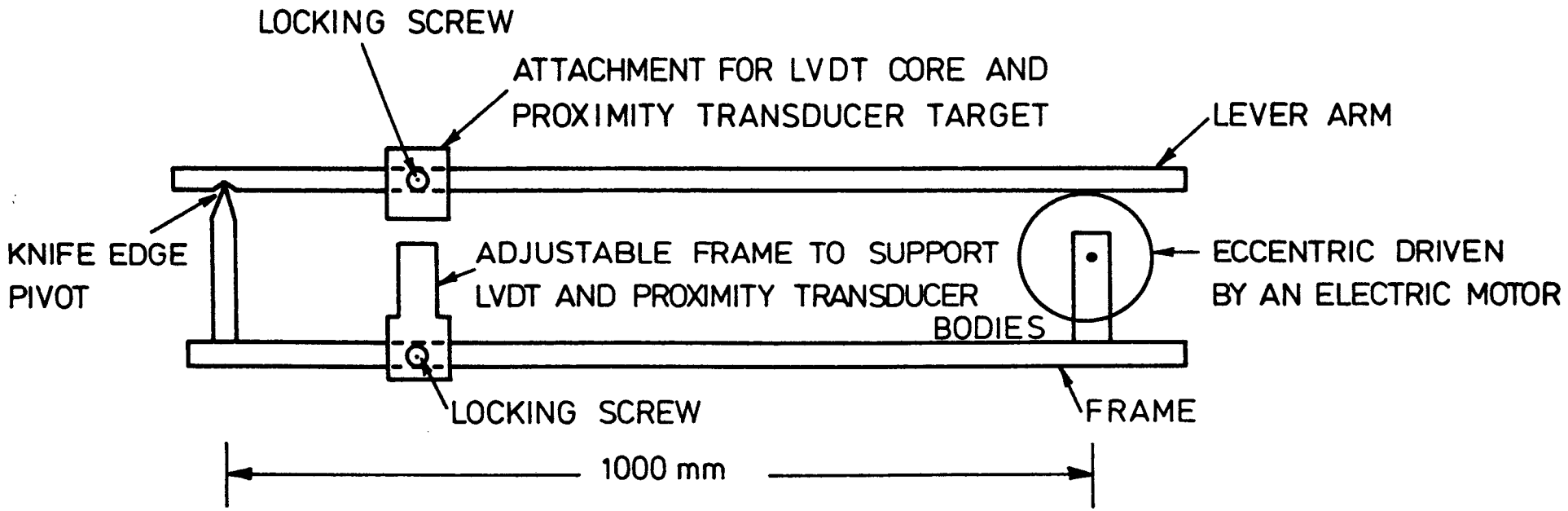

FIGURE C2 DIAGRAMMATIC REPRESENTATION OF APPARATUS TO COMPARE AN LVDT WITH A PROXIMITY TRANSDUCER OVER SMALL DEFLECTIONS

allowed the transducer outputs to be compared over a frequency range from 0.4Hz to 3Hz.

Table C1 contains the results at one amplitude, equivalent to approximately 150 $\mu\epsilon$ on the sample, over the full range of frequencies from the apparatus and demonstrates very good agreement between the two transducers, with little effect over the frequency range for the test. The LVDT output recorded varies by approximately 4%.

Table C1 Comparison between an LVDT and a Proximity Transducer

Frequency Hz	Amplitude recorded (mm)	
	LVDT	Proximity Transducer
0.4	0.00717	0.00732
1	0.00725	0.00734
3	0.00748	0.00732

APPENDIX D

CALIBRATIONS

D1 SERVO HYDRAULIC RIG

The calibrations given for the load cells and pressure transducers are the most recent. The transducers were calibrated regularly and found to vary by up to 2% at the most.

Volts/kN or volts/kPa refer to a monitor point.
Divs/kN or divs/kPa refer to the ultra violet chart recorder where 1 div = 2mm

Cell No	Load Cells		Cell Pressure Transducer		Base Pore Pressure Transducer	
	Volts/kN	Divs/kN	Volts/kPa	Divs/kPa	Volts/kPa	Divs/kPa
1	0.8673	10.915	0.0132	0.130	0.0182	0.177
2	0.9017	11.34	0.0120	0.118	0.0178	0.173
3	0.8636	10.869	0.00233	0.0227	0.0178	0.173

The above calibrations are given with a gain of X1. The gain and hence the sensitivity could be increased by X2, X4 or X8.

	Centre pore pressure transducer number					
	2006	2015	2286	2402	2405	2475
Volts/kPa	0.0141	0.0139	0.0147	0.0129	0.0139	0.0139
Divs/kPa	0.0746	0.0739	0.0780	0.0686	0.0739	0.0736

The above calibrations are given with a gain of X1. The gain could be increased by X2, X4, X8 or X16.

As the axial and radial deformations recorded were an average of the signals from the LVDTs and proximity Transducers respectively, each type of transducer in each cell was adjusted to give the same calibration.

Transducer	Calibrations		
	Monitor Point Volts/mm	U.V. Recorder (Plastic) Div/mm	U.V. Recorder (Elastic) Div/mm
LVDT	0.7874	4.697	12.391
P.T.	3.937	25.394	67.129

The above calibrations are given for gains of X1. There were two outputs to the UV recorder, one was used to record the permanent deformation, and the second was amplified further through an offset generator and was used to measure the resilient response.

The gain of the main amplifier could be increased by X2, X4, X8 or X16 and increased the sensitivity of all the signals including the offset generator. The gain of the offset generator could also be increased by X2, X4, X8, X16 or X32.

D2 PNEUMATIC RIG

	Monitor Point	U.V.Recorder (Plastic)	U.V.Recorder (Elastic)
Load cell	1.623 mV/kN	251 Div/kN	-
LVDT	0.157 volts/mm	10.121 Div/mm	97.09 Div/mm
Strain Loop	0.251 volts/mm	226.3 Div/mm	226.3 Div/mm

The above calibrations are quoted for a gain of X1 in each case.

The definition of the Plastic and Elastic terms is as given for the servo hydraulic rig, and the connection between the main gain and offset generator gain is also as for the servo hydraulic rig.

	Monitor Point	U.V. Recorder (Plastic)	U.V. Recorder (Elastic)
Load cell	X1,X2,X5,X10	X1,X2,X5,X10	-
LVDT	X1,X2,X5,X10	X1,X2,X5,X10	X1,X2,X5,X10,X20,X50,X100
Strain Loop	X1,X2,X4,X8	X1,X2,X4,X8	X1,X2,X5,X10,X20,X50,X100

The resolution of the A-D convertor was 0.000305 v/bit.

The drift of the stress and pressure transducers was found to be approximately ± 2kPa over the longest tests. The calibration of the LVDT's varied by up to ± 2% over the longest tests. The proximity transducers were less stable and were found to vary by as much as ± 5%.

he Author considers that the overall accuracy of the stress and strain measurements was of the order of 5%.